Radioresistance and radiosensitization in high-risk Group 3 pediatric medulloblastoma

Eleanor Hawkins

PSL UNIVERSITÉ PARIS

THÈSE DE DOCTORAT
DE L'UNIVERSITÉ PSL

Préparée à l'Institut Curie, Equipe Pouponnot (Unité : Signalisation, radiobiologie et cancer [UMR3347 / U1021])

Radioresistance and radiosensitization in high-risk Group 3 pediatric medulloblastoma.

Radioresistance et radiosensibilisation du médulloblastome de haut risque de groupe 3.

Soutenue par

Eleanor HAWKINS

Le 13/12/2023

Ecole doctorale n° 561

HOB – Hématologie, Oncogenèse et Biothérapies

Spécialité

Oncogenèse

Composition du jury:

Elizabeth COHEN-JONATHAN MOYAL Professeur, Université Toulouse III - Paul Sabatier	*Président*
Silvia MARINO Professor, Queen Mary University of London	*Rapporteur*
Samuel MEIGNAN Directeur de Recherche, Centre Oscar Lambret	*Rapporteur*
Claire ALAPETITE Docteur en médecine, Institut Curie	*Examinateur*
Eddy PASQUIER Professeur, Aix-Marseille Université	*Examinateur*
François RADVANYI, Directeur de Recherche, Université PSL; Institut Curie	*Examinateur*
Celio POUPONNOT Directeur de Recherche, Université PSL; Institut Curie	*Directeur de thèse*

institutCurie | PSL

Acknowledgements

The thesis is a long and arduous project which I would certainly not have been able to complete without the collaboration of a number of people. I would therefore like to thank all those who have contributed to this thesis in any way.

Firstly, I would like to take this opportunity to thank Professor Elizabeth Cohen-Jonathan Moyal for agreeing to act as the jury president. Further, I would like to thank Prof Silvia Marino and Dr Samuel Meignan for acting as rapporteurs. My thanks also go to Drs Claire Alapetite, Francois Radvanyi and Eddy Pasquier for their role as examiners.

I would also like to thank the members from Merck, including Joachim Albers, Florian Lenz and Poulami Sengupta, without whom this work would have been difficult to complete.

To the lab…I would like to thank everyone for their support and aid throughout the last four years. Firstly, I would like to thank Celio, whose supervision was of course instrumental in the completion of this thesis, and Sabine whose aid throughout this project was key to its success. I would further like to thank Mag, Sara, and Lily for teaching me everything I need to know about handling mice – I think I can safely say that under your instruction I have become an expert. To Dave, Laurence, Bertrand, Tafa, and Celine I would like to extend my sincere thanks for your help with experiments, especially as I am sure there will be more work needed at the revision stage! Boris and Sandra of course I would like to thank for your help with writing this manuscript – your help at this panicked stage was highly appreciated. Finally, I would like to thank Morgane for continuing on some of this work – I hope you have more luck with the CRISPR screen than I did!

To my family… I would like to thank my parents for supporting me this far, I would never have made it without their support. And of course Alex and Frances who have already promised to never call me doctor

To my friends… I would like to thank you all for always being there when I needed a break. Special thanks go to Anouk and Alexandre who were always there to laugh whenever my experiments failed. To Anicia, who was always there forcing me to go out, you were correct, I did need to complain less. And finally, I would like to thank Anna, Claudia, and Max – even through you live countries away, you were always there to call and tell me to pull myself together.

And to Lucas…who has put up with a lot of complaining and a host of breakdowns throughout the last four years. It is not an exaggeration to say I couldn't have done this without your support.

Table of Contents

Figure and Table Index:

List of Abbreviations:

- 3d-CRT - 3 dimensional conformal radiation therapy
- ANOVA - Analysis of Variance
- ATM - Ataxia-telangiectasia mutated
- ATP - Adenosine triphosphate
- ATR - Ataxia telangiectasia and Rad3-related protein
- CAR T cells - Chimeric antigen receptor T cells
- CDK - Cyclin dependant kinase
- CHK - Checkpoint kinase
- CRISPR - Clustered regularly interspersed short palindromic repeats
- CSC - Cancer stem cell
- CSF - Cerebrospinal fluid
- CSI - Craniospinal irradiation
- DDR - DNA damage repair
- D/N - Desmoplastic/nodular
- DNA - Deoxyribonucleic acid
- DSB - Double strand break
- FACS - fluorescence activated cell sorting
- FBS - Foetal bovine serum
- G3 - Group 3
- G4 - Group 4
- GNP - Granule neuron precursor
- GSEA - Gene set enrichment analysis
- GTR - Gross total resection
- HR - Homologous recombination
- IMRT - Intensity Modulated RadioTherapy
- IR - Irradiation
- KEGG - Kyoto Encyclopaedia of Genes and Genomes
- LC/A - Large cell/anaplastic
- MB - Medulloblastoma
- MBEN: MB with extensive nodularity
- MRI - Magnetic resonance imaging
- MRN - MRE11-RAD50-NBS1
- NI - No irradiation
- NHEJ - Non-homologous end joining
- PBS - Phosphate buffered saline
- PDX - Patient derived xenograft
- RNA - Ribonucleic acid
- ROS - Reactive oxygen species
- RT - Radiotherapy
- SCID - Severe combined immunodeficiency
- sh - short hairpin
- SHH - Sonic Hedgehog
- STR - Sub-total resection
- WNT - Wingless and Int-1

1. Medulloblastoma:

1.1 Overview:

Medulloblastoma (MB) is a tumor of the cerebellum which most commonly presents in pediatric patients, but is also diagnosed less frequently in adulthood. MB is the most common form of paediatric malignant brain tumour, and has been shown to arise from various populations of the neural progenitor cells active during early development of the hindbrain[1–5]. This disease has an overall survival rate of approximately 70-80%[6]; however the aggressive nature of treatment (surgical resection followed by radio- and chemotherapy) can induce debilitating side effects, including cognitive impairment and endocrine disorders[2,7–10].

Advances in genomics over the last few decades have allowed the categorization of MB into four distinct molecular groups; the WNT group, SHH group, Group 3, and Group 4, each of which have more recently been further classified into distinct subtypes. These groups were initially stratified based on transcriptomic features, but patients are currently most commonly distinguished based on methylomic data, which has been shown to be a more robust classifier[1–3,11–13]. This specific classification of patients has allowed the identification of potentially actionable targets which may be specific to only a subset of each MB group, which has increased interest into these subtype classifications. Furthermore, classification of patients into a subtype could provide clinicians with valuable information regarding prognosis, and potentially treatment, in the future. No precise consensus on an exact classification for each subtype has been reached, but in this work we use the definitions outlined by Cavalli et al in 2017[14]. Later in this section, I will provide a brief overview of the WNT, SHH, and Group 4 subgroups, as well as Group 3, the subgroup with the worst prognosis which provides the focus of this thesis.

1.2 Subgroups of Medulloblastoma:

WNT Group:

Overview:

Tumours in the WNT group of Medulloblastoma are characterised by activation of the WNT cell signalling pathway, caused predominantly by mutations in *CTNNB1*[15,16], encoding the protein β-catenin. The WNT signal transduction pathway regulates numerous processes, including cell fate determination, cell proliferation, cell migration, polarity, and neural development[17]. MBs of the WNT group account for approximately 10% of all MB diagnoses. These cases are generally found in adults and older children/adolescents, not infants, and exhibit

a balanced gender ratio. Of the four groups, the WNT group has by far the best prognosis, with total survival of over 90%, and a low rate of metastasis of only 10% at diagnosis[2,3]. This favourable prognosis is potentially due to these tumours' increased accessibility to chemotherapeutics, caused by the development of aberrant brain vasculature and a lack of the normal surrounding blood-brain barrier (caused by the overexpression of WNT agonists by neighbouring endothelial cells)[2,18]. WNT-driven tumours are believed to originate from cells in the lower rhombic lip, which migrate and develop into tumours localised to the midline and brain stem or the cerebellar peduncle and cerebellopontine angle cistern[3].

Molecular Basis of Disease:

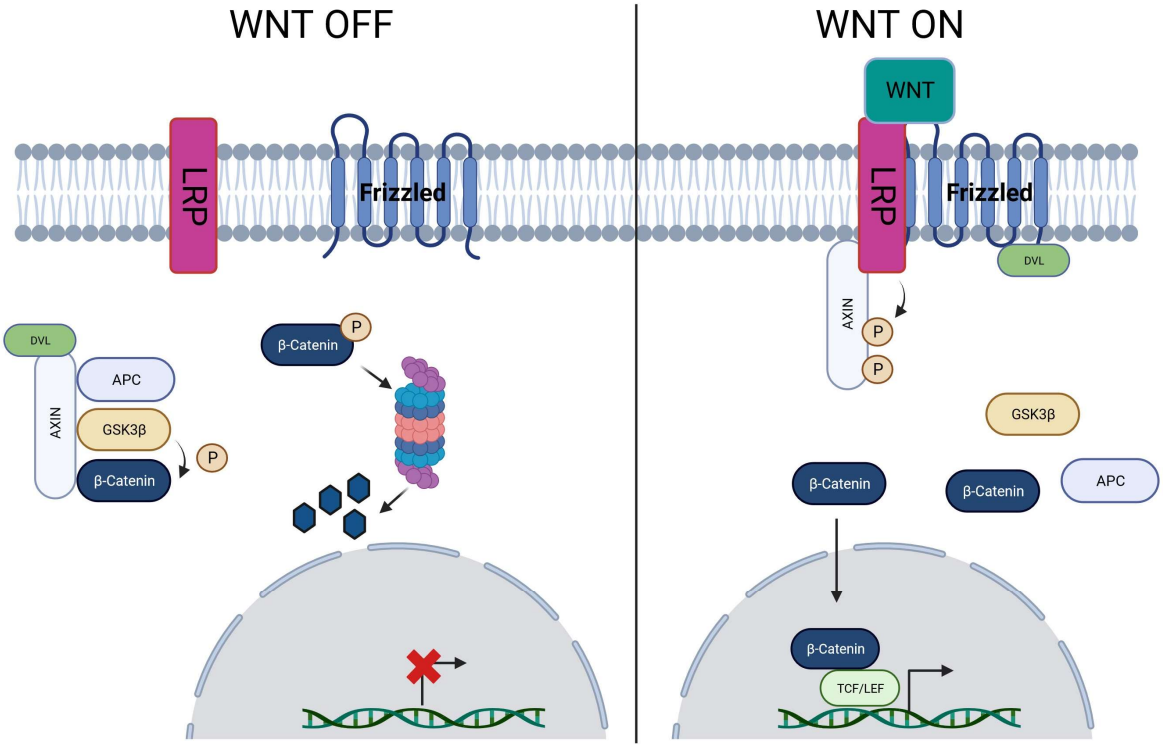

FIGURE 1 OVERVIEW OF THE WNT SIGNALLING PATHWAY.

Left: In the WNT inactive state, β-Catenin is targeted for proteasomal degradation; this process is mediated by protein complexes, including Axin, APC, and GSK3β. Right: WNT binds to the receptor Frizzled, which induces the binding of the membrane lipoprotein receptor-related protein (LRP) to Axin. This prevents degradation of β-Catenin, allowing its stabilization. In the nucleus, β-catenin binds to TCF/LEF transcription factors to regulate the transcription of target genes. Adapted from: Liu et al[19].

Numerous mutations of components in the WNT pathway (Figure 1) have been implicated in oncogenesis. The most commonly mutated gene in WNT MB, with aberrations in 85% of cases, is the *CTNNB1* gene (encoding the key WNT signalling element β-catenin). These mutations

stabilise β-catenin, leading to accumulation in the nucleus, and resulting in increased transcription of target genes, and thereby constitutive activation of WNT signalling[16,20]. *CTNNB1* mutations often co-occur with monosomy 6, a hallmark feature of WNT MB[15], with these aberrations being so common that they are commonly used to identify WNT MB tumours[21]. In the absence of *CTNNB1* mutations, patients often exhibit loss-of-function mutations in the gene encoding APC, which normally helps mediate β-catenin degradation. This also causes accumulation of β-catenin in the nucleus, with the same results[15,22]. Activating mutations in the kinase CKII (a positive regulator of the WNT pathway) have also been implicated, while mutations outside the WNT pathway, such as in the RNA helicase encoding the *DDX3X* gene, which has been shown to drive proliferation of tumor cells of origin, have also been identified[23]. *Tp53* mutations are also common, but remarkably do not appear to affect prognosis[15,20,24–26].

Subgroups:

Tumours in the WNT group have been stratified into two molecular subgroups[14];

- WNTα – Composed primarily of children; at the genetic level this subgroup is characterised by Monosomy 6.
- WNTβ – Patients tend to be older, are diploid for chromosome 6, and exhibit a worse prognosis than subgroup α.

SHH Group

Overview:

The SHH Group of medulloblastoma is characterised by tumours driven by activation of the SHH signalling pathway[1–3]. This pathway is key to cell fate determination and migration during embryonic development. It controls neural progenitor cell patterning, and during adulthood is necessary for organ homeostasis[27]. Aberrant SHH signalling has previously been implicated in a variety of cancers, most notably in basal cell carcinoma, where it is seen in the majority of cases[28]. This MB group also has an even gender ratio, is found in patients of all age ranges (infants, children, and adults), and represents approximately 30% of all patients diagnosed with MB. SHH Medulloblastoma exhibits an intermediate prognosis, with survival rates of 75-90%, and these tumours have a relatively low rate of metastasis at diagnosis, at approximately 15-20%[1–3]. SHH tumours originate from Granule Neuron Precursors (GNPs), and are generally localised to the cerebellar hemispheres[5].

Molecular Basis of disease:

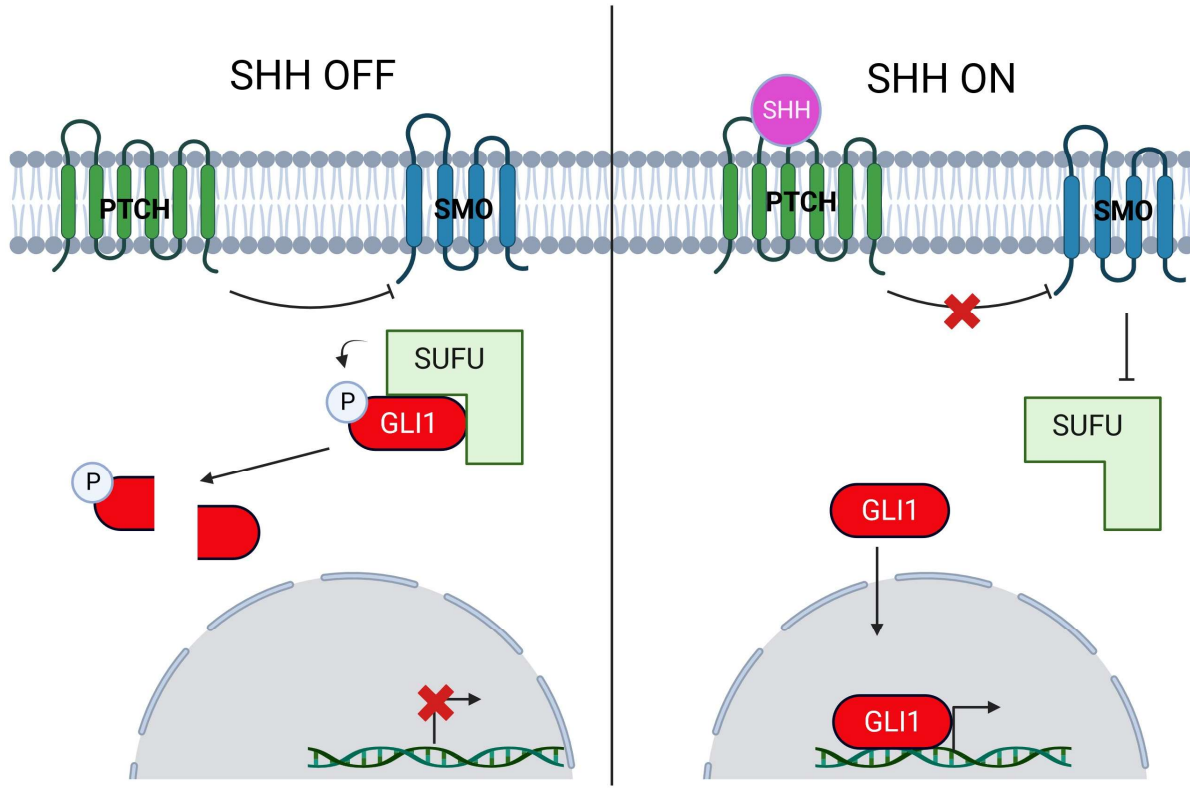

FIGURE 2 OVERVIEW OF THE SHH SIGNALLING PATHWAY.

Left: When the SHH pathway is inactive, PTCH inhibits the action of SMO, resulting in the sequestration of the transcription factor GLI1 in the nucleus. Right: To activate the SHH signalling pathway, SHH binds to PTCH, preventing the inhibition of SMO. Active SMO inhibits the action of SUFU, thereby allowing GLI1 to translocate to the nucleus, resulting in the expression of target genes. Adapted from: Lee et al[29].

Drivers behind SHH MB include many somatic or germline mutations in multiple components of the SHH signalling pathway (Figure 2). Common examples include loss of function mutations in PTCH1 or SUFU, activating mutations in SMO, and amplification of Gli transcription factors[30]. Any of these mutations can lead to ligand-independent activation of the SHH pathway, causing upregulated expression of target genes, ultimately driving cell growth and proliferation, resulting in oncogenesis[24,31]. Mutations outside of the SHH pathway have also been identified: P53 pathway mutations resulting in the deregulation of DNA damage repair can cause defective cell cycle regulation, apoptosis, and DNA damage repair[26]. PI3K cell signalling defects can promote cell survival, growth, and proliferation. Mutations in TERT (telomere maintenance) promoter regions are also commonly identified, with a predominance for this mutation in adult patients[1,24,31]. Other identified mutations have been shown to drive activity of *GLI2*, a member of the SHH pathway, and promote stability of the oncoprotein

MYCN, a target gene of SHH[1]. Further, one recent study has shown a link between the activity of the AHR pathway and prognosis, finding that high expression of the AHR repressor was linked to poor prognosis in patients[32]

Subgroups:

Cavalli *et al* classified SHH MB into 4 subgroups; α, β, γ, and δ. Infant cases of SHH MB are confined to the β and γ subgroups, which are sometimes referred to as i-SHHI and i-SHHII, respectively[14].

- SHHα: This subgroup is characterised by *MYCN* and *GLI2* amplifications, numerous genomic rearrangements, and *TP53* loss or loss of function. An enrichment of genes involved in DNA repair and cell cycling have also been observed. This subgroup has particularly poor prognosis, especially in patients with loss of P53 activity. Patients are generally children aged 3-16 years.
- SHHβ / i-SHHI: Found in infants >3 years; at the genetic level this subgroup is characterised by *PTEN* deletions, focal amplifications, and high levels of metastasis. Patients of this subgroup exhibit poor prognosis.
- SHHγ / i-SHHII: Localised to infants >3 years, these tumours exhibit a quieter copy number profile, no recurrent amplifications, only one common deletion, and relatively few arm level changes. Enrichment of receptor tyrosine kinase signalling and developmental pathways is also observed. The prognosis of this group is good compared to SHHβ.
- SHHδ: Found in adults, with a reasonably favourable prognosis[33], tumours are characterised by high incidence of *TERT* promoter mutations, and telomere maintenance is enriched.[14]

Group 3:

Overview:

Compared to the WNT and SHH Groups, Group 3 tumours are relatively poorly understood and less well-characterized[1–3], although recent studies in MB have tended to focus on this particular group due to the availability of models. Group 3 tumours have the highest levels of metastasis at diagnosis (40-45%), which is a contributing factor to their poor prognosis. Of the four groups, Group 3 has the worst survival rate, at only 60% after 5 years, and is found almost exclusively in infants and young children, with a skewed male to female gender ratio of 2:1[1–3]. These tumours are localised to the midline, sometimes invading the fourth ventricle near the brainstem[2]. Importantly, a recent publication showing similarities in cell signatures with the

early rhombic lip have indicated that both group 3 and 4 MB tumours arise from cells in the antero-inferior cerebellar vermis during development[4]. A more detailed discussion of the origins of group 3 and 4 MB is provided below in the 'Group 3 and Group 4: Blurred lines' section below.

Molecular Basis of Disease:

Group 3 is significantly heterogeneous, but can generally be characterized by MYC overexpression, with *MYC* amplifications occurring in ~20% of G3 patients[24]. These *MYC* amplified tumours are of very poor prognosis. High MYC expression is associated with increased abundance of many proteins related to mRNA processing, transcription, and translation[24,34]. Amplifications of *OTX2* are also believed to be driver mutations in G3, but are only found in 3-5% of cases[35]. Ectopic expression of the transcription factors GFI1 and GFI1B due to enhancer highjacking are also found in 15-20% of cases, and have been demonstrated to contribute to tumorigenesis[36]. Cytogenetic arrangements are also common, the most common being isochromosome 17q, which is found in 40-50% of group 3 cases, but is even more common in group 4[24]. Prior work in our laboratory has also shown that OTX2-driven expression of the photoreceptor-specific transcriptional activators NRL and CRX induces ectopic expression of retinal photoreceptor-specific genes in G3 tumours. NRL and CRX also stimulate tumorigenesis by promoting cell cycle progression and protecting against apoptosis, by increasing the expression of Cyclin D2 and BCL-XL respectively[37]. Concurrent research also showed that activation of the TGFβ pathway caused by increased expression of Activin B promotes tumorigenesis through promotion of cell cycle progression in some group 3 cases[38].

Subgroups:

Group 3 medulloblastomas are divided into three subtypes based on molecular characteristics and associated driver mutations, as follows:

- Group 3α: Comprised primarily of infants >3 years old, with frequent loss of chromosome 8q. These cells often exhibit transcriptional signatures correlated with photoreceptor cells (including NRL and CRX[37]) and muscle contraction[14]. This group has higher levels of metastasis than Group 3β, comparable to Group 3γ.
- Group 3β: Patients tend to be older and to exhibit increased GFI1/1B expression and OTX2 amplification. Losses on chromosomes 1 and 9 are also enriched in this subgroup.

- Group 3γ: This subgroup has a higher level of metastasis, often exhibit *MYC* amplifications and have by far the worst prognosis. Gain of chromosome 8q is more frequent. Similarly to Group 3β, genes involved in protein synthesis are upregulated.[14]

Group 4:

Overview:

Despite being the most prevalent form of the disease (accounting for 35-40% of cases), group 4 medulloblastoma remains the most poorly understood group, due in part to the lack of animal models[1–3]. The cell of origin of these tumours remained unproven until recently, when an extensive multi-omics study confirmed that group 4 tumours arise from a specific subset of cells in the rhombic lip during cerebellar development, maintaining the cellular signatures of these progenitor cells throughout tumor progression[4] (this is discussed in more detail below). Group 4 tumours often invade the fourth ventricle, proximal to the brain stem. This group is confined to children >3, and has a skewed M:F gender ratio of 3:1[2]. Group 4 MB has a high rate of metastasis at diagnosis, at 35-40%, and an intermediate prognosis[1–3].

Molecular Basis of disease:

Group 4 tumours are extremely heterogeneous, and, as mentioned above, driver pathways have only recently begun to be characterized. However, aberrant ERBB4-SRC signalling has been postulated as a hallmark feature of this group[39]. Group 4 tumours can further often be characterised by the presence of large-scale chromosomal aberrations[12]. The most commonly recurrent alteration is enhancer hijacking, resulting in increased activation of PRDM6[24]. Loss of function mutations in chromosome modifying genes (including *KDM6A*, *ZMYM3,* and *KMT2C*) are also common, but mutually exclusive, and amplification of *MYCN* and the cell cycle driver *CDK6* have also been implicated in tumorigenesis[24,40,41]. Group 4 cells can also often be characterised by an expression phenotype resembling glutamatergic neurons[2]. Overexpression of the polycomb group repressor complex gene BMI1 is also commonly observed in group 4 medulloblastoma, where it is linked to migration and invasion[42], as well as mTOR pathway activation and metabolic alterations[43]

Subgroups:

Group 4 medulloblastoma can be divided into 3 subgroups – α, β, and γ – which display similar survival rates and rates of metastasis at diagnosis, with only slight differences in the median age of diagnosis.

- Group 4α: This groups exhibits *CDK6* and *MYCN* amplifications, as well as loss of chromosome 8p and gain of chromosome 7q.
- Group 4β: This group exhibits SNCAIP duplications, leading to PRDM6 overexpression caused by enhancer hijacking.
- Group 4γ: This groups exhibits a similar profile to Group 4α, but lacks *MYCN* amplifications.[14]

Group 3 and Group 4: Blurred lines

Group 3 and group 4 MB are both relatively poorly understood compared to the WNT and SHH subgroups. Indeed, some previous studies have made no distinction between the two, sometimes collectively referring to these tumours as the non-WNT/non-SHH group, due to their similarity[44]. Further, as mentioned above, a recent seminal paper showed that both group 3 and group 4 tumours arise from the same region in the developing brain, the antero-inferior cerebellar vermis in the early rhombic lip[4]. Other key papers have supported this finding, showing that groups 3 and 4 exist along a continuum, with exemplary/archetypal group 3 and 4 tumours at each end, and indeterminate/overlapping tumours in the centre[45,46]. Furthermore, another recent paper showed that group 3 and 4 tumours can be divided across a transcriptional spectrum[45]. Essentially, what this intensive study showed is that group 3 and 4 tumours both arise from a single cell population in the early rhombic lip, but at different developmental stages, with archetypal group 3 tumours showing the strongest affinity with rhombic lip precursors, and classical group 4 tumours showing the highest similarity with excitatory cerebellar nuclei/unipolar brush cells. Furthermore, the position on this transcriptional continuum is strongly correlated with many of the biological features of these tumours, including age at presentation and mutational features, in addition to patient prognosis.

Summary

Overall, medulloblastoma is a diverse disease, with a significant heterogeneity both in and between groups. Table 1 summarizes the characteristics of the four molecular groups of Medulloblastoma, while Figure 3 presents Kaplan-Meier curves showing the prognosis of patients in all of these groups and their subtypes.

TABLE 1 CHARACTERISTICS OF THE FOUR MOLECULAR GROUPS OF MEDULLOBLASTOMA.

	WNT	**SHH**	**Group 3**	**Group 4**
Incidence:	~10%	~25%	~25%	~40%
Survival rate:	~90%	~60%	~50%	~60%
Age at Diagnosis:	Older children and adolescents	Infants and adults	Infants and young children	Young Children (<3)
Rate of metastasis at diagnosis:	5-10%	15-20%	40-45%	30-40%
Relapse:	Local or Metastatic	Local	Metastatic	Metastatic
Male:Female ratio:	1:1	1:1	2:1	3:1
Hallmark genetic features:	Mutations in *CTNNB1, SMARCA4, TP53,* and *DDX3X*	Mutations in *PTCH1, SUFU,* and *SMO.* Amplifications of *GLI2* or *MYCN*	Amplifications of *MYC* or *OTX-2.* Mutations of *SMARCA4.* Activation of *GLI1/GLI1B*	Amplifications of *MYCN* and *CKD6. PRMD6* overactivation.

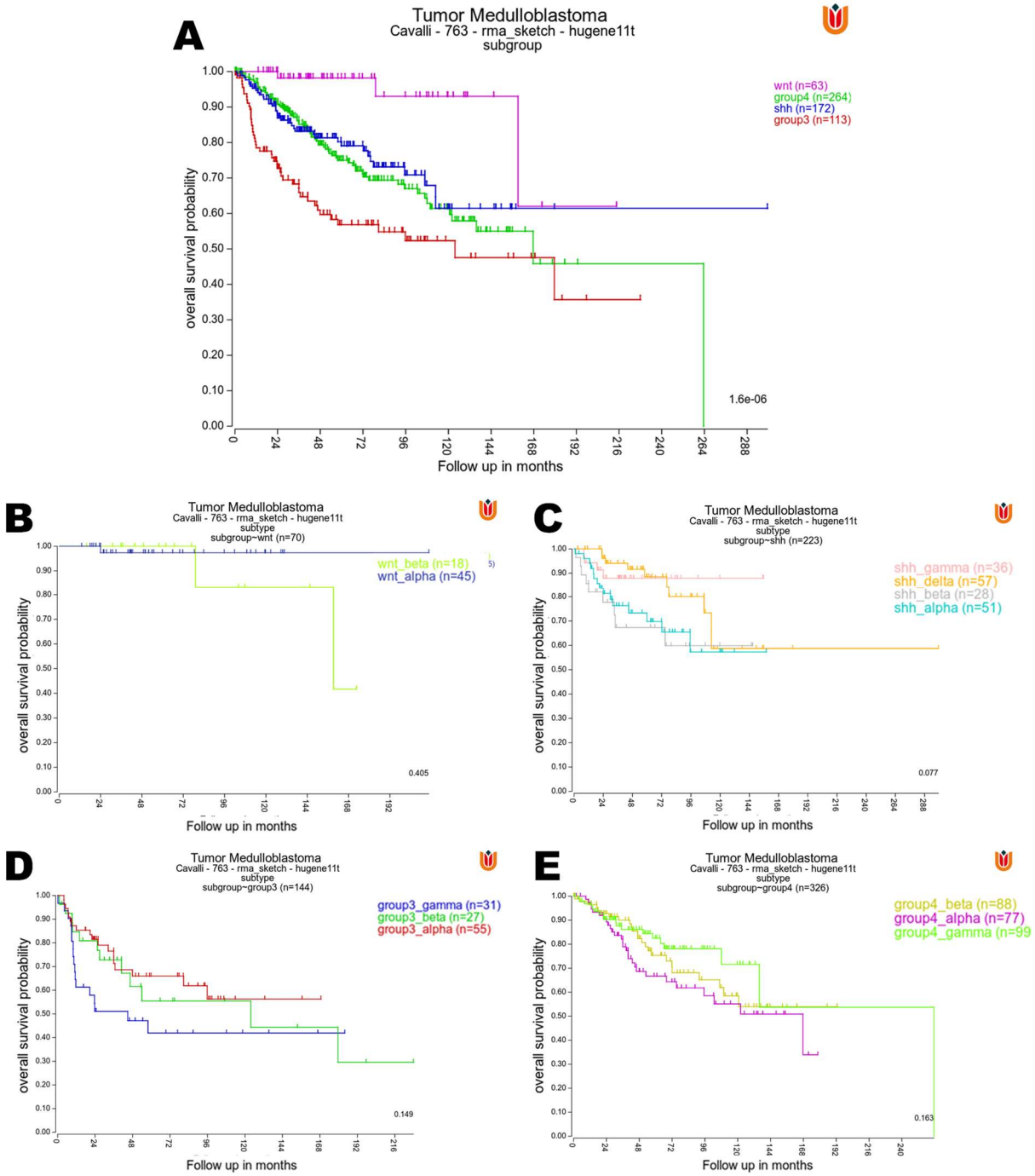

FIGURE 3 SURVIVAL ACROSS THE DIFFERENT SUBGROUPS OF MEDULLOBLASTOMA

Kaplan Meier curves of: (A) The four primary MB groups (Wnt, SHH, Group 3, and Group 4). (B) The two subgroups of the WNT Group (WNTα and WNTβ). (C) The four subgroups of the SHH Group (SHHα, SHHβ, SHHγ, and SHHδ). (D) The three subgroups of Group 3 (Group 3α, Group 3β, and Group 3γ). (E) The three subgroups of Group 4 (Group 4α, Group 4β, and Group 4γ). The x-axis shows the follow-up time in months. The y-axis shows the survival probability. All figures were made using the R2: Genomics analysis and visualization platform (Available at: https://hgserver1.amc.nl/cgi-bin/r2/main.cgi?dscope=MB500&option=about_dscope) to analyse the previously published/public patient dataset (GEO accession number: GSE85218).

1.3 Clinical Management of Medulloblastoma

Diagnosis

Symptoms of MB are common to many neurological conditions, and initially include headaches, clumsiness, nausea, and fatigue, which are commonly followed by ataxia, motor problems, and vision problems[47]. Diagnosis therefore requires MRI scanning of the brain and spinal cord to identify the primary and any potential metastatic tumours. Imaging is followed by analysis of cerebrospinal fluid (CSF) cytology, and together these two techniques allow for grouping of patients based on disease stage[1–3], as outlined in the Chang classification system[48]. However, due to similarities in positioning and appearance with other brain tumours, histopathological analysis is vital to achieve accurate diagnosis of Medulloblastoma. A total of four MB morphological/histological types have been identified; classic, desmoplastic/nodular (DN), MB with extensive nodularity (MBEN) and large cell/anaplastic (LC/A)[1,49]. However, molecular analyses must be completed to stratify patients into one of the aforementioned molecular subgroups. Currently, DNA methylation profiling is the method of choice to classify patients into subgroups, having largely superseded gene expression analyis[1,13].

Treatment:

Treatment of Medulloblastoma is multimodal and non-targeted. The first stage involves maximal surgical resection, which is followed by craniospinal irradiation (CSI) and adjuvant chemotherapy[1–3]. Each stage of this treatment is important, as the efficacy of each is highly linked to survival. Surgical resection reduces tumour mass to increase the efficacy of later radio/chemotherapy[1]. It is generally believed that the extent of tumour cytoreduction is heavily linked to prognosis; with research showing that patients who had undergone Gross Total Resection (GTR) or Near Total Resection (NTR) have significantly higher survival rates than those with only Sub-Total Resection (STR)[50]. This has led to a heavy emphasis being placed on achieving maximal surgical resection, sometimes with adverse outcomes. In opposition to this, one study showed that patients with GTR showed no overall survival benefit compared to those with NTR, suggesting that although extended resection has distinct prognostic value, the exact extent of this benefit is still a subject of debate[50]. Radiotherapy encompasses the entirety of the craniospinal region, to account for metastasis, with boosted therapy targeted at the primary tumour site[1,2]. Radiotherapy is a key stage of treatment[7], and reduction in the therapeutic radiation dose has been strongly linked to a deterioration in prognosis[51]. Although chemotherapy is used as an adjunct to surgical resection and radiotherapy, it is nevertheless an important stage in multimodal treatment, and its usage is strongly linked to increased survival[52].

Treatment varies slightly depending on the risk stratification of the patient. Patients over age 3 can be described as either standard or high risk according to tumour characteristics. Patients lacking metastasis, in whom complete/near complete tumour resection can be achieved are classified as standard risk, whereas patients who exhibit metastases or residual tumour after surgery are deemed high risk. In addition, an anaplastic or large-cell histology is also categorised as high risk, while other morphologies are considered standard[53,54]. Patients can further be stratified based on their risk level according to their molecular subgroup, genetic features, and presence of metastases. Low risk patients (>90% survival possibility) include patients with WNT group tumours, and some non-metastatic group 4 patients with loss of chromosome 11, while standard risk (75-90% survival) patients include those with *TP53* wild type, non-*MYCN* amplified, non-metastatic SHH tumours, as well as non-*MYC* amplified, non-metastatic group 3 and 4 tumours. The high risk group (50-75% survival rate) includes *MYCN*-amplified SHH patients, metastatic *TP53* wild type SHH, and metastatic group 4 patients. The very high risk group (survival rate <50%) include *TP53* mutated SHH tumours, as well as patients with metastatic or MYC-amplified group 3 tumours[54].

The standard radiotherapy treatment course for eligible, standard-risk patients consists of 23.4 Gy (13 fractions of 1.8 Gy) CSI, with an additional boost to the primary tumour to reach 54.0 Gy. Chemotherapeutic treatment is much more variable, with differences in the combination of chemotherapeutic drugs used, the timing of administration, and the number of cycles[55]. However, as several previous long-term studies have shown that post-radiotherapy 'maintenance' chemotherapy has superior outcomes to neoadjuvant chemotherapy, the former is most commonly used[56,57]. In such maintenance chemotherapy regimens, CSI is often followed by 4-9 chemotherapeutic cycles with one or more of the chemotherapeutic drugs vincristine (a mitotic spindle poison), cisplatin, cyclophosphamide (DNA replication inhibitors), or lomustine (a DNA/RNA alkylator)[58]. The prognosis of patients on this treatment course is highly favourable (with an average 5-year survival rate of 80%). Patients who are classified as higher risk receive a higher CSI radiation dose of 36 Gy (20 fractions of 1.8) and the same additional boost to reach 54 Gy at the primary tumour site, followed by a similar chemotherapeutic course[52]. Here prognosis is inferior, with an approximate 5 year survival rate of only 60%[52].

Although the general standard of care for Medulloblastoma patients is similar the world over, some regional differences do exist. For example, chemotherapy is generally administered both adjuvantly and post-radiotherapy (RT) in America, while in Europe pre-RT chemotherapy

is also administered in some cases[9]. Further, depending on the profile of the patient, this standard treatment course may be modified. For example, infants under the age of three are generally ineligible for radiotherapy, and CSI treatment is therefore deferred until the patients reach an appropriate age[59,60]. This can be compensated for by increases in post-operative chemotherapy combined with autologous stem cell transplantation[60,61].

Although efficacious, the aforementioned treatment modality unfortunately causes numerous debilitating side effects in patients, primarily triggered by the trauma caused by CSI[62,63]. The immediate treatment complications caused by surgery and irradiation of the brain include post-operative mutism and the development of hydrocephalus and meningitis, with motor deficits and cranial nerve deficits also often developing[64]. This treatment is also linked to decreased social and intellectual capacity later in life. Survivors of medulloblastoma treatment are less likely to graduate high school, get married, or gain employment, and generally exhibit lower IQ, with high rates of memory and attention deficits[9,62,65]. Indirect effects on the endocrine system (caused by irradiation of the pituitary gland and hypothalamus) are also commonly observed[9], and include hypothyroidism[66], early puberty[10], and growth hormone deficiency[8]. Decreased height is also observed in patients treated for MB as children. This is believed to be caused by the aforementioned growth hormone deficiency, as well as by direct radiation toxicity of the growing spine, and can be treated with growth hormone therapy[9,67]. Ototoxicity and resulting deafness are also common side effects of chemoradiotherapy[68].

Because of the severe side effects of this treatment modality, several attempts have been made to reduce the dose of CSI without compromising treatment effect; however, many of these have encountered serious problems. One study in the late 80s/early 90s attempted to study the potential of deescalating the CSI dose from 36 to 23.4 Gy in lower risk patients with small residual tumours after therapy, without other alterations in treatment. This trial was halted prematurely due to an increase in metastatic relapse in the low-dose radiation group[51]. Another trial in the early 90s attempted to allow delay of radiotherapy by 5/7 weeks after surgical resection by substituting with an intense chemotherapy regimen. Further, once radiotherapy was started, it was targeted only to the spine and posterior fossa, rather than the entire craniospinal region. This study had similarly poor results, with patients experiencing significantly worse survival than usual[69]. Another trial in the late 80s sought to achieve a similar goal. Here children <3 years with malignant brain tumours were treated with chemotherapy *in lieu* of radiotherapy until they either reached the appropriate age or experienced disease progression. Unfortunately, progression occurred early (within 6-8 months) in many of the infants with medulloblastoma[70],

and a high rate of secondary malignancies was observed during follow up[71]. Another trial performed at a similar time showed that the concurrent use of chemotherapy enhanced the efficacy of radiotherapy in patients with advanced stage medulloblastoma[72]. Another, earlier study also showed that adjuvant chemotherapy was beneficial in some subsets of patients, including those with partial/subtotal resection[73]. In the last few decades, many trials have attempted to outline chemotherapeutic regimens which would allow for a decrease in radiotherapy dose[73–76], and over the years it was these studies that established that the use of chemotherapy allowed for a reduction in radiation dose to 23.4 Gy in lower risk patients.

More recent studies have also been conducted with the aim of decreasing radiation dose in medulloblastoma patients. For example, one study (NCT02212574) investigated the use of chemotherapy and surgery only (without radiotherapy) in WNT patients deemed standard risk; however, this trial was halted due to early failure[77]. Another, more promising, trial investigating the potential of a further reduction of the radiotherapy dose to 18 Gy for newly diagnosed WNT MB patients deemed very low risk, with a boost to the primary tumor reaching 36 Gy (NCT02724579), is currently ongoing[55]. Conversely, other studies have used the opposite route, opting to increase the radiotherapy regimen and exclude chemotherapy to reduce side effects. For example, several clinical trials in France (MSFOP98 and MSFOP07)[78,79] previously investigated the potential of implementing a hyperfractionated radiation therapy regimen with a reduced boost volume for MB patients deemed to be standard-risk: in these trials, patients were administered 36 Gy CSI irradiation in 36 fractions (twice a day) with a boost to the tumor bed (+ a 1.5 cm safety margin) of 68 Gy administered over 68 fractions (twice a day), with no subsequent chemotherapy. These studies found 5-year survival rates equivalent to those with standard therapy modalities, with an improved intelligence quotient[78,79].

Although radiotherapy is an integral part of medulloblastoma treatment, and is generally necessary for complete cure, the many side effects induced by this treatment make its use extremely debilitating. The development of treatment modalities which would allow for further decreases in radiation dose, while maintaining the high survival rate of the current medulloblastoma treatment regimen, is therefore a highly attractive goal.

1.4 Medulloblastoma Radioresistance and Recurrence:

Mechanisms of Medulloblastoma Recurrence

Although the primary course of treatment for medulloblastoma is generally effective, recurrent tumours can arise in some patients. These tumours tend to be extremely resistant to the original therapy modality, and are therefore incredibly difficult to treat and are almost invariably fatal. Indeed, treatment of patients with recurrent tumours tends to focus on improving the quality of life remaining, rather than attempting to cure disease[80].

The mechanism by which medulloblastoma escapes treatment, and in particular radiotherapy, to allow for recurrence is currently poorly characterized. Escape from therapy in general occurs through two main mechanisms, classified as genetic and non-genetic. Genetic resistance arises from mutations which decrease the ability of a targeted drug to be effective through different mechanisms[81,82]. In this case, tumoral resistance can arise either from selection of clones with pre-existing resistance mutations, or de novo mutations during treatment[82]. Non-genetic resistance relies on the presence of so-called 'persister cells' which may exhibit therapy tolerance due to slow growth and cell cycle progression[83]. The plasticity of cancer cells allows them to reversibly switch between different growth states by altering their expression profiles depending on the tumoral environment, possibly via an epigenetic mechanism[82]. Such cells become enriched during drug treatment, and can cause tumour recurrence if therapy is stopped.

The importance of these two mechanisms of resistance is not well established for MB. Biopsy is rarely performed on recurrent tumours, as surgical resection is rarely performed at this stage. Consequently, although medulloblastoma is well characterised in its initial form, comparatively little is known about recurrent disease. Nevertheless, a few studies have established the characteristics of recurrent MB. For example, the group classification appears to be stable over the course of the disease, with the majority of tumours maintaining the same group before and after recurrence[80,84], although some exceptions have been found[85].

Further, one study using matched primary and recurrent patient biopsies showed that recurrent tumours are enriched in loss of p53 pathway and *MYC/MYCN* amplification, which was not seen in the initial disease. Indeed, these two aberrations – loss of p53 activity and *MYC* amplification – were associated, and together represented highly aggressive, but potentially therapeutically targetable, tumors[80]. Another study which compared the whole genome sequences of patient-matched initial and recurrent tumours showed high genetic divergence following recurrence, suggesting that recurrent tumours arose from a minor clone present at

initial diagnosis[86], and indicating that a genetic mechanism may be at play in recurrent MB. Concerning non-genetic escape, there is little available data, although some scRNAseq data have revealed high levels of intratumoral heterogeneity in MB[87]. A further study using a mouse tumour model capable of forming recurrent tumours identified several genes upregulated in recurrent tumours, including BPIFB4[88]. Furthermore, one study showed that the transcription factor OLIG2 played an important role in the recurrence of MYC-driven MB tumours, finding that MB cells expressing high levels of OLIG2 were much more resistant to radiotherapy and were more likely to form recurrent tumours in vivo[89].

Concerning in particular resistance to radiotherapy (RT), in general, recurrent tumours grow from radioresistant cells in the original tumour. These cells are able to escape death induced by radiotherapy through the activation of survival pathways, including DNA damage repair[90], and organelle rescue pathways such as autophagy[91]. These cells decrease the efficacy of radiotherapy by promoting tumour regrowth and facilitating tumour recurrence after therapy, which often results in more aggressive, treatment resistant tumours, due to the selection for novel aggressive cells[91].

Another important consideration in tumor escape from irradiation is the persistence of cancer stem cells (CSCs), defined as highly plastic cells with stem-like properties, including the ability to self-renew and differentiate into heterogeneous cancer cell populations which comprise the majority of the tumor volume[92]. Indeed, although CSCs make up only a very small proportion of tumor cells, they have been postulated the source of the majority of tumor cells, differentiating into multi-lineage cells which are less proliferative[92]. These CSCs are generally resistant to therapy modalities, including chemotherapy and radiotherapy, and are widely believed to be the primary source of therapy resistance and recurrence in many cancers[93]. Regarding radiotherapy in particular, numerous studies have shown a link between CSCs and radioresistance/recurrence. Studies have alternately suggested that tumour irradiation drives the generation of CSCs from non-stem like radiosensitive cells in some instances[94], while in other circumstances, radiation selects for radioresistant CSCs[95,96].

In the field of MB, recent studies have identified the presence and importance of CSCs, implicating them in therapy escape and relapse, with a few further identifying these cells as potential targets for treatment. Indeed, one study showed that stem-like CD133+ DAOY cells were more radioresistant than CD133- cells[97]. In addition, one study showed that recurrent tumours biopsied from patients showed enrichment in cells expressing SOX9 (a stem cell/glial fate marker) compared with the corresponding tumours at original resection. Subsequent

experimental analyses revealed that SOX9 played a key role in relapse, in a manner dependent on suppression of MYC[98]. Another study showed that quiescent cells expressing SOX2, a marker of multipotent neural stem cells, promoted relapse following anti-mitotic chemotherapy of a murine model of SHH MB[99].

Regarding therapeutic targeting, one study found that the receptor NRP1 stimulated the differentiation of MB stem cells, while inhibition of this receptor sensitized MB cells to radiation both in vitro and in vivo, thereby promoting the targeting of MB CSCs as a novel mechanism of therapy[100]. Importantly for group 3 MB, studies have implicated MYC as important for CSC-related signalling and stemness in several cancers[101,102], while another study showed that MYC is required for the proliferation and survival of CSCs in glioma[103]. In support of the potential role of MYC in MB CSCs, one study showed that inhibition of the bromodomain protein BRD4, which restricts cell pathways associated with MYC, suppressed stem-cell associated signalling pathways in MYC-driven MB, thereby promoting such treatment as a potential therapeutic approach[104]. Other research has suggested targeting of the PI3K pathway in CSCs as an option to improve MB treatment. One study using multiple mouse models of MB showed that Nestin+ stem like-tumor cells were more resistant to irradiation than bulk tumor cells, in a manner dependent on the PI3K/Akt pathway[105]. A subsequent study by another group showed that treatment of MB cells with the PI3K pathway inhibitor LY294002 triggered cell death, with CSCs (Nestin+ CD133+ cells) being especially sensitive to this treatment[106]. Other pathways implicated in the action of CSCs in MB include the Notch signalling pathway[107] and the SHH pathway[108].

Together, these varied studies indicate the important role of CSCs in MB survival and relapse. While work specifically on their role in escaping irradiation in MB is less well characterized, considering the considerable evidence supporting the role of CSCs in escape from radiotherapy in other cancers, it is likely that a similar effect occurs in MB.

In order to prevent the recurrence of tumours following radiotherapy, it is necessary to eliminate radioresistant cells and CSCs wherever possible. The use of pharmacological agents or chemotherapy to promote tumour cell susceptibility to irradiation - a process termed radiosensitisation - is the best method to achieve this. In order to be effective, radiosensitisers must improve the therapeutic index, i.e., they must selectively sensitise tumour cells to radiotherapy more efficiently than the surrounding normal tissue, resulting in a decrease of the necessary effective does. Failure to do this would result in unacceptable levels of toxicity which

would not improve treatment efficacy. A more detailed description of radiosensitisers and their clinical potential is provided later in this introduction.

Treatment of Recurrent Medulloblastoma:

Unfortunately, due to the poor treatment response and high fatality rate, treatment of recurrent tumours tends to focus on improving patient quality of life remaining, rather than attempting to cure the disease[80]. Unlike primary medulloblastoma, there is no defined treatment course for patients with recurrence[109]. There are, however, several options, the use of which depends on factors related to both the tumour and patient. Administration of second-line chemotherapeutics is the most common treatment choice[110], with drugs such as topotecan, etoposide, temozolomide, bevacizumab, or their various combinations being commonly used[111]. Re-resection can also be performed if suitable. However, this is rare and has an indeterminate value on prognosis[109]. Re-irradiation is also an option, although its use is also very rare. In such cases, re-irradiation is performed concurrently with chemotherapy after re-resection, and is most efficacious in patients with minimal disease remaining after second surgery[112]. Unfortunately, re-irradiation is associated with high levels of toxicity[113,114], and is therefore rarely used, with application generally limited to patients who received a low initial dose of irradiation, as the maximum tolerated total dose to the CSI is 50 Gy[115]. Although the efficacy of re-irradiation has been the subject of debate, a relatively recent retrospective study indicated that such treatment did prolong overall survival. This benefit was most obvious in patients who were categorised as standard risk at diagnosis[116]. Another treatment option is high dose chemotherapy with stem cell rescue[110,111]. Nevertheless, despite these different treatment options, recurrent medulloblastoma remains almost entirely treatment resistant and represents a major cause of mortality among pediatric cancer patients, with survival rates lower than 10%[117,118]. This raises the importance of the development of new therapies to increase the response to initial therapy to prevent the development of recurrence in the first place.

2. Radiation and Radiosensitization in Cancer

2.1 Radiotherapy and Cancer

Cancer is a group of heterogonous diseases characterised by uncontrolled cellular proliferation and loss of cell death pathways. One of the leading causes of death worldwide, cancer is becoming even more prevalent in the increasingly aging populations of the developed world. Current treatment for cancer depends on the type, location, and stage of the tumour, but generally consists of some combination of maximal surgical resection (when possible, in the case of solid tumours), chemotherapy, radiotherapy, targeted therapies and, more recently, immunotherapy. Although advances are constantly being made in cancer therapy, many cases remain incurable, and the risk of tumour recurrence following treatment is high.

Radiotherapy is one of the main curative strategies used to treat solid tumour cancers, which primarily works by inducing lethal DNA damage, and can be either curative or palliative. Approximately half of the 15 million cancer sufferers diagnosed each year benefit from radiotherapy, with almost half of these presenting the potential for curative treatment[119]. The classic view of radiotherapy posits that cancer cell death is primarily mediated by the induction of DNA damage in target cells, either directly, or indirectly via the production of free radicals produced by the radiolysis of water. Cancer cells, which tend to have deficiencies in DNA repair pathways, are more susceptible to this DNA damage than the normal tissue[90,120,121]. However, other cellular effects of radiotherapy, such as direct organelle damage (of the mitochondria, endoplasmic reticulum, lysosomes etc.) and lipid peroxidation also play a role in the response of cancer cells to radiotherapy[121]. In addition, radiotherapy has been shown to alter the immune response through modulation of the tumour microenvironment[122]. For example, post-irradiation, dying cells release inflammatory mediators which attract immune cells to the surrounding environment, resulting in an increased immune response in the tumor. Indeed, it has been shown that in some cases, radiotherapy can turn ‘cold’ tumours lacking a strong immune infiltrate into ‘hot’ tumours. Furthermore, recognition of antigens presented on irradiated cells by circulating T cells can result in a stronger immune response even to un-irradiated tumor cells, resulting in shrinkage of un-irradiated tumours, a phenomenon known as the abscopal effect[123].

Radiotherapy is almost always applied in conjunction with other treatment modalities. Combination with surgical resection is common, in which case radiotherapy can be either pre-operative, to shrink tumour volume[124,125], or post-operative to clear remaining cancer cells[50].

Both modalities have been shown to significantly improve treatment efficacy. Combinations of radiotherapy with chemotherapy (termed 'chemoradiotherapy') are also commonly used to improve treatment efficacy. The timing of chemotherapy treatment depends largely on the aim of the treatment. Neoadjuvant chemotherapy is used to shrink tumour volume and eliminate micrometastases[126,127]; however, the efficacy of this approach remains controversial[126]. Although this treatment modality has shown no significant survival benefit, it is still used as it has been shown to spare normal tissues from radiation-induced damage in some cases[128]. Concurrent chemotherapy is used to increase control of local solid tumours; as both chemo- and radiotherapy target proliferating cells, their coordinated use can increase levels of acute tumour toxicity[126]. Adjuvant use of chemotherapy (i.e. treatment post-irradiation) can increase the efficacy of chemotherapy by reducing the initial tumour burden[126]. Although the combined use of chemo- and radio-therapy inevitably induces detrimental effects on the normal tissue, provided that the combined effect is greater on tumor tissue, such side effects are considered acceptable[129].

Although radiotherapy is effective at killing cancer cells, it is, in essence, a victim of its own success. The primary limitation of radiation therapy is its toxicity towards the normal tissue, as this damage can result in severe treatment side effects. Clinicians must therefore select treatment modalities which allow maximal irradiation dose deposition to the tumour cells, while limiting to the greatest possible extent the effect on vulnerable surrounding tissue[130]. This idea is encapsulated in one metric, termed the therapeutic index. The therapeutic index is a measurement of the safety of a treatment, calculated as a ratio of the toxic and effective treatment doses (see formula 1). Improvements in radiotherapy efficacy can be achieved by enhancing the therapeutic index (TI), by either increasing the toxic dose (TD), or decreasing the effective dose (ED)[131].

Formula 1: $TI = \frac{TD_{50}}{ED_{50}}$

Historically, conventional X-ray radiotherapy uses several 2 dimensional external radiation beams to target a localised tumour from multiple angles – in this method, the normal tissues lying between the tumour and the radiation source receive high radiation doses. However, in recent years, advancements in the mechanics of radiotherapy delivery have ameliorated this problem, by allowing the delivery of increased radiation doses to tumour tissues, while limiting normal tissue exposure. The most obvious example of this is 3 dimensional Conformal Radiation Therapy (3d-CRT), which uses 3D models of patient

tumours, produced using advanced imaging techniques, to shape the multiple radiation beams to match the tumour's 3D shape. This allows maximal tumour targeting with minimal radiation of the surrounding normal tissue[132]. Recently, more advanced forms of 3D-CRT have been developed; these include Intensity Modulated RadioTherapy (IMRT), which alters radiation intensity to more accurately match tumour shape[133] and volumetric modulated arc therapy, which makes use of a rotating beam undergoing shape modulation[134]. Beyond this, 4-dimensional CRT, which is able to monitor positional movements in tumours and adjust the radiation focus accordingly, has also been developed to treat tumours in regions such as the lungs, which undergo constant movement[135]. More recently developed techniques include proton minibeam radiation therapy, which uses spatially fractionated proton beams to target tumours while limiting the targeting of surrounding tissues[136], and FLASH radiotherapy, which utilises ultra-fast delivery of high dose irradiation to spare normal tissue[137–139]. Other novel treatment options include CyberKnife, a radiation platform capable of stereotaxic radioresection of tumours using multi-directional radiation beams to target small tumours, while largely sparing surrounding tissue[140]. All of these methods are able to improve the therapeutic index by increasing radiation doses to tumours, while sparing normal tissues to the greatest extent possible, which results in an increase in the toxic dose.

The second major challenge to the efficacy of radiotherapy is the existence of radioresistant cells. These cells are able to escape death induced by radiotherapy through the activation of survival pathways such as DNA damage repair[90] and organelle rescue pathways or autophagy[91]. Such cells decrease the efficacy of radiotherapy by promoting tumour regrowth and facilitating tumour recurrence after therapy, which often results in more aggressive, treatment resistant tumours, due to the selection of novel, aggressive cells[91]. The mechanisms of radioresistance are varied and complex, involving both intrinsic cellular pathways, and interplay with the tumour microenvironment. Such strategies generally involve avoidance or 'escape' from the damaging effects of IR. Well known examples include the maintenance of a hypoxic tumour environment, which reduces the formation of DNA-damaging ROS, and upregulation of DNA repair pathways. Considerable research has gone into evaluating these mechanisms of resistance, and targeted radiosensitisation methods using pharmacological intervention has subsequently gained traction as a potential strategy to increase the efficacy of radiotherapy, and to thereby increase prognosis of cancer sufferers. Here we will provide an overview of the current knowledge regarding the tumour cell mechanisms underlying radiation

damage and radioresistance in cancer, and explore the novel radiosensitisation targets and methods that have arisen from this knowledge.

2.2 Radiosensitization, a concept:

In essence, the primary pitfall of radiotherapy is that the dose required to achieve tumor control or cure is often too high to feasibly be applied, due to unacceptable toxicity to the surrounding normal tissue. Thus, methods are required to promote the tumor-killing ability of irradiation. The use of pharmacological intervention to promote tumour cell susceptibility to irradiation - a process termed radiosensitisation - is the best method to achieve this. In order to be effective, radiosensitisers must improve the therapeutic index, i.e. they must selectively sensitise tumour cells to radiotherapy more efficiently than they sensitise the surrounding normal tissue, resulting in a decrease of the necessary effective dose. Failure to do this can result in unacceptable levels of toxicity which would not improve treatment efficacy.

There are many different classes of drugs which can promote radiosensitization, including targeted therapies, chemotherapeutics, and immune-modulating therapies. Among these, chemotherapeutics have been used for the longest, due to their long-standing use in the clinic. Some common chemotherapeutics used to induce radiosensitization include gemcitabine[141,142], which targets cells in the S phase, triggering disrepair of DNA damage[143], and platinum-based chemotherapeutics such as cisplatin, which functions as a radiosensitizer by inhibiting non-homologous end joining repair[144]. Indeed, the platinum-based antineoplastic carboplatin has previously been investigated as a radiosensitizer in clinical trials of medulloblastoma patients, yielding positive results[145,146]. In addition to these, due to the well-established immune-modulating effects of radiotherapy, the possible combination of immunotherapy with radiotherapy has recently received significant interest[147]. While immunotherapeutics have been widely applied in recent years, their use in brain cancer, including medulloblastoma, remains comparatively underdeveloped[148,149], in part due to the low (but subgroup specific) immune infiltration of MB tumours[150], as well as the physical barriers that prevent the entry of drugs to the central nervous system. Further, to the best of my knowledge, although several studies have started to investigate immunotherapy alone in medulloblastoma, no studies have yet investigated combined immunotherapy with radiation in medulloblastoma. Cellular immunotherapy (involving the administration of primed living immune cells) has begun to be investigated in MB, with CAR T cells being the best characterized[149]. Checkpoint inhibitors are less well understood in medulloblastoma; however, recent research in other brain tumours may indicate that this is a topic of future research. For

example, one study showed that administration of brain irradiation with the anti-PD-L1 checkpoint inhibitor durvalumab was well-tolerated by patients[151]. Another phase II trial investigating the anti-PD1 immunotherapeutic nivolumab in the treatment of recurrent IDH-mutant high-grade gliomas also found a strong safety profile, with long-lasting responses in some patients[152]. Thus, immunotherapeutic radiosensitization may be an avenue for future research in MB.

Despite the promise of chemo- and immune-radiosensitization, as the present work focuses on targeted therapies to promote radiosensitization, this is discussed in more depth below. Although the use of targeted treatments to induce radiosensitisation in cancer shows great promise, one important factor that must be considered is the proper targeting of these treatments based on tumour molecular signatures, as the efficacy of an inhibitor is largely dependent on cell context. For example, the efficacy of inhibiting DNA repair pathways would depend on the existing status of these pathways in tumour cells. For example, PARP inhibition is most efficacious in HR-deficient cancers[153]. Conversely, the conservation of non-homologous end joining (NHEJ) in most cancer cells, combined with the knowledge that defects in NHEJ increase radiosensitivity[154] indicates that targeting of this pathway may provide a more ubiquitous approach.

Another important factor to consider is the effect of the drug on the surrounding normal tissue. As previously mentioned, the primary aim of a radiosensitising drug would be to improve the therapeutic index of the radiotherapy treatment[131]. It is therefore important that any drug would have a greater radiosensitising effect on cancerous cells than normal tissue, as otherwise the level of normal tissue toxicity may be unacceptable. Over the last few years, knowledge regarding the effects of radiation on cancer cells, and the cell pathways which are modulated to escape its cytotoxicity, has increased dramatically. With this knowledge, many targets have been proposed to induce tumoural radiosensitivity; with the DNA damage repair and response pathways being the most obvious targets. Although much work and clinical investigation is still required to translate this knowledge more widely to patient treatment, the direct targeting of cellular processes to promote radiosensitisation has great potential to increase the efficacy of radiotherapy in the future.

2.3 DNA Damage Repair as a Radiosensitization Target

Radiation lethality is primarily (although certainly not exclusively) dependent on the production of irreversible DNA damage leading to cell cycle arrest and ultimately cell death. Double strand breaks (DSBs) are the most lethal form of damage, and the ability of cells to sense and repair DSBs is therefore vital[90,155]. DSBs can be classified into two main types: simple and complex DSBs. Simple DSBs are caused directly by radiation, are localized to euchromatic regions (uncoiled, active DNA), and can be rapidly repaired. Complex DSBs generally occur within the heterochromatin (tightly coiled, inactive DNA regions), which must be repaired more slowly.

There are two main pathways by which DSBs can be repaired: non homologous end joining (NHEJ) and homologous recombination (HR). NHEJ is a process in which the two ends of the broken DNA are directly ligated. This process is quick and can occur at any point in the cell cycle. However, as no homologous template is used, repair is error prone. This process has been extensively reviewed by Davis and Chen[156]. The second repair method, HR (reviewed by Li and Heyer[157]) uses homologous DNA sequences to facilitate faithful repair. This process is much more accurate than NHEJ, but is also much more time consuming due to its relative complexity, and can only occur during the S and G2 phases because of the need for sister chromatids. Prior research has shown that approximately 80% of DSBs induced by ionizing irradiation are repaired by NHEJ[158]. Irradiation also results in the formation of Single Strand Breaks (SSBs). Although SSBs are much less deleterious than DSBs, their repair is nevertheless necessary, as unrepaired SSBs can lead to collapsed replication forks, leading to double-strand breaks which must subsequently be repaired by homologous recombination. This effect is especially important in cancer cells, which replicate at a high rate.

The mechanisms of both DNA damage sensing and the subsequent cellular consequences depend both on the type of damage and the phase of the cell cycle in which the damage occurs. DNA damage repair is especially critical in cancer cells, which divide and multiply rapidly, as DNA lesions can prevent mitotic division by leading to the activation of cell cycle checkpoints (discussed in more detail later). As the primary function of radiotherapy is the production of fatal DNA lesions, these pathways are attractive targets for the radiosensitisation of cancer cells. These different pathways have been targeted at multiple levels, with several DNA-repair inhibiting drugs having already been approved for clinical use in combination with radiotherapy, and many others currently being studied pre-clinically and in clinical trial. These are discussed below.

Single Strand Break Repair

The repair of single strand breaks (SSBs) (Figure 4) is mediated by the DNA damage sensor PARP1. Contact with SSBs triggers the activation of PARP1, resulting in activatory auto-PARylation. This further activates PARP, which subsequently PARylates target proteins such as XRCC1 to recruit them to the site of damage. The DNA is finally repaired by Polymerase β and ligase 1/3[159,160].

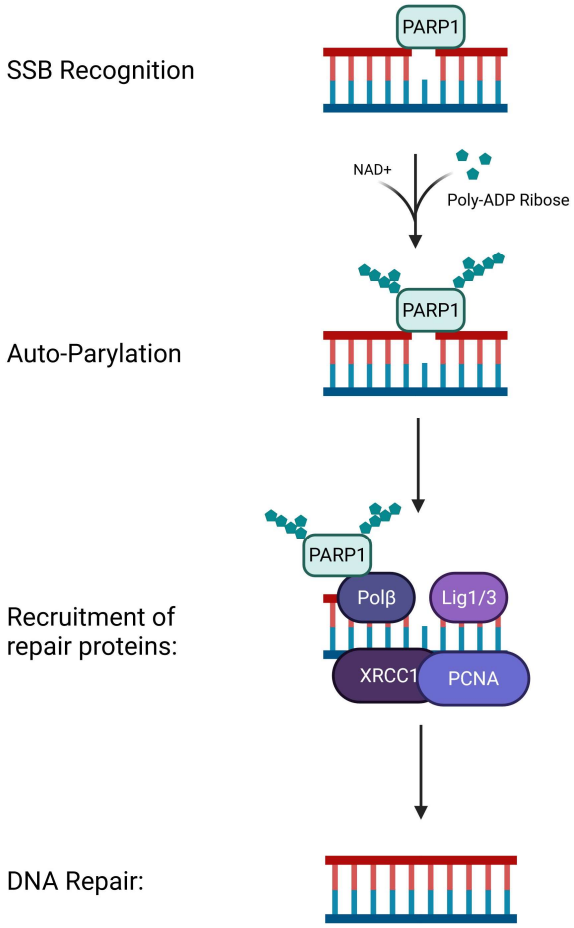

FIGURE 4 A SIMPLIFIED OVERVIEW OF SINGLE STRAND BREAK REPAIR

PARP1 binds to sites of single strand breaks, resulting in its auto-PARylation, and subsequent PARylation of other repair effectors to recruit them to the sites of damage. PARP1 dissociates, allowing repair factors including the polymerase Polβ, the ligases LIg1/3, and the repair factors XRCC1 and PCNA to drive DNA repair. Figure is modified from Biau et al.[161]

Lig1/3, Ligase 1/3; Polβ, Polymerase β

Of the multiple factors involved in SSB repair, PARP1 has arisen as a promising treatment target in cancers. Indeed, PARP1 has been shown to be overexpressed in a variety of cancers, including breast and prostate cancers[162]. The rationale for the use of PARP-inhibiting

therapies in cancer is based on the concept of synthetic lethality. In this concept, two separate molecular pathways which are dispensable individually cause cell lethality when inhibited concurrently[159]. In the normal cellular context, the SSB repair pathway is dispensable, as unrepaired SSBs result in the production of DSBs during DNA replication, which can be repaired via the HR pathway. As such, PARP inhibitors have shown great efficacy in tumours deficient in HR (e.g. BRCA-mutated cancers), and are currently used in the clinical treatment of ovarian, fallopian tube, and peritoneal cancers[163,164].

While the primary mechanism underlying lethality of irradiation involves DSBs, SSB repair is nevertheless important to allow DNA replication and cell division. It is therefore logical to assume that this pathway may affect radiosensitivity, and that PARP1 may therefore be an effective target for radiosensitisation. As such, several studies have investigated the use of PARP1 inhibitors as radiosensitisers in several cancers. In nasopharyngeal carcinoma, it was shown that PARP1 was upregulated, and that concurrent treatment with ionizing radiation and the PARP1 inhibitor olaparib increased cell cycle arrest and apoptosis *in vitro* and promoted the anti-tumor effects *in vivo*[165]. A similar study in mouse models of glioblastoma showed equally promising results[166]. Another study using the more recently developed PARP1 inhibitor BMN673 also showed effective radiosensitising effects, and demonstrated that this was due to increased accumulation of SSBs and failure in their repair[167]. Another pre-clinical study showed that inhibition of PARP1 sensitized models of inflammatory breast cancer to irradiation, due to the delayed repair of DNA damage[168]. Despite this preclinical research, and the fact that PARP inhibitors are currently applied in the clinic, their potential as radiosensitizers remains relatively unclear, with the majority of work being pre-clinical. Overall, despite some promise, more work is needed before PARP inhibitors can be brought to the clinic as radiosensitizers[160,169].

Recognition of Double Strand Breaks

Recognition of both simple and complex double-ended double strand breaks is mediated by the serine/threonine kinase Ataxia telangiectasia mutated (ATM), in concert with the protein trimer MRE11-RAD50-NBS1 (MRN). This activation results in cell cycle arrest or apoptosis, and triggers repair by either NHEJ or HR, depending on the cell context. Recognition of single-ended DSBs (generally arising from collapse of the DNA replication fork) is mediated by the serine/threonine kinase ATM and Rad3-related (ATR) protein. Recognition results in cell cycle arrest and repair by homologous recombination. The role of these kinases in DNA recognition and repair has been extensively reviewed by Maréchal and Zou[170]. Both of these kinases play key roles in the mechanisms of DNA repair in response to radiation-induced DSBs, and their

function is therefore key to maintaining radioresistance. Inhibitors of both of these molecules have been investigated for their efficacy as radiosensitisers.

ATM was initially proposed as a target for radiosensitisation, as it is known that people with ataxia-telangiectasia, a heritable disease caused by ATM mutations, are hypersensitive to radiotherapy[171]. Although no ATM inhibitors have yet been approved for clinical use, several have shown promise in studies, and have progressed to the early stages of clinical trial. One early study showed that treatment of a variety of cancer cells with the ATM inhibitor KU-55933 in combination with radiotherapy resulted in decreased cell cycle arrest and increased cell death[172]. Taking this further, another study showed that KU-55933 effectively radiosensitised previously radio-resistant glioblastoma stem-like cells, primarily by abrogating the previous upregulation of DNA damage response pathways and inhibiting activation of cell cycle arrest[173]. Other ATM specific inhibitors, such as KU59403[174] and AZ32[175] have shown similar promise for radiosensitisation. Although effective in all cell lines studied, AZ32 was shown to be particularly effective in cells with mutations in *TP53*, a downstream effector of ATM and global mediator of DNA repair and cell cycle arrest (discussed in more detail below)[175]. Although promising, due to their relative novelty, very few of these molecules have progressed to clinical trial. One Phase I trial investigating the ATM inhibitor M3541 with irradiation was abandoned due to a lack of efficacy[176].

Inhibitors of the DNA damage sensor ATR have been less well studied as radiosensitisers, although some initial work has shown promise. For example, the efficacy of the DNA damage sensor ATR inhibitor AZD6738 as a radiosensitiser has also been shown[177], and this drug is currently in phase I clinical trial.

Overall, while it is still believed that inhibitors of these DNA damage sensors may have significant promise as radiosensitizers, particularly in patients with cancers deficient in other DNA-damage sensing pathways[178], further clinical and preclinical research is required to validate their use.

Homologous Recombination:

Homologous recombination (Figure 5) is a form of DNA repair which uses a homologous DNA strand as a template for repair of damaged DNA. This pathway is therefore only activated in the S and G2 phases of the cell cycle, prior to mitosis, when homologous sister chromatids are available. In the context of radiation-induced DNA damage, HR is necessary to repair both directly-induced double strand breaks, and stalled/broken replication forks, commonly caused

by unrepaired single strand breaks. It is this latter function which underlies the synthetic lethality with the SSB repair pathway mentioned above.

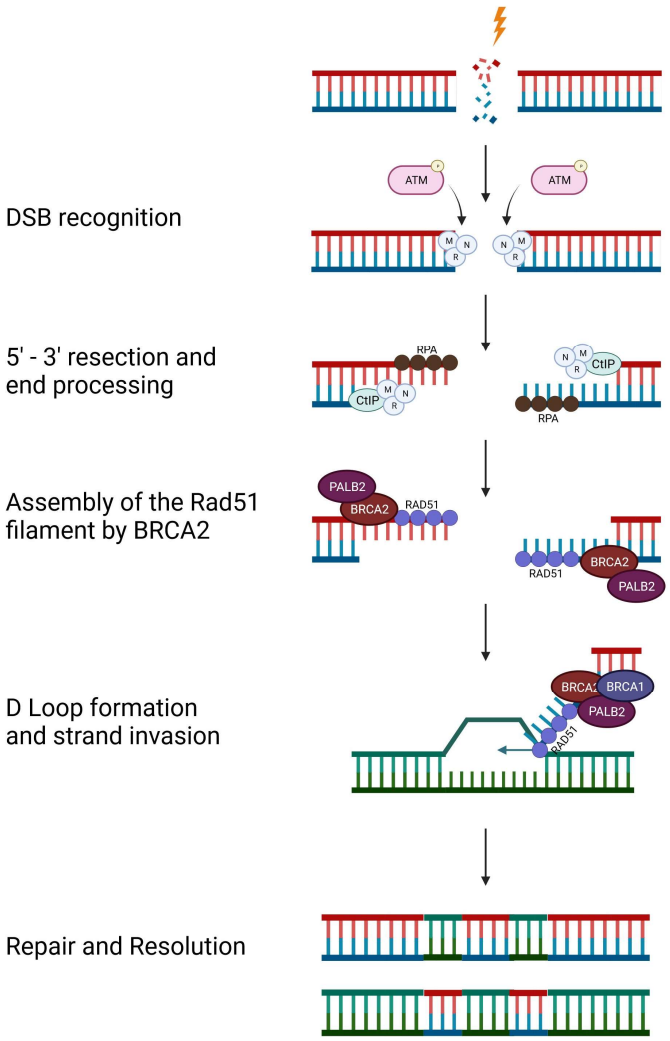

FIGURE 5 A SIMPLIFIED OVERVIEW OF THE REPAIR OF DOUBLE STRAND BREAKS BY HOMOLOGOUS RECOMBINATION

The MRN complex senses and processes the region of double strand break, subsequently recruiting ATM, which phosphorylates its down-stream substrates. CtIP promotes 5'-3' end-resection of the DNA, allowing loading of RPA on the subsequent single stranded DNA. PALB2 recruits BRCA2, which mediates the replacement of RPA by Rad51. Homology search, D-Loop formation, and strand invasion occur, and strand repair and resolution is processed (details not shown). This figure is a modification of that by Hosoya & Miyagawa[179].
ATM: Ataxia telangiectasia mutated; MRN: Mre11, Rad50, and Nbs1.

Here we will provide a very brief overview of the HR repair pathway[157]. As mentioned above, DNA double strand breaks are detected by the action of ATM/ATR/MRN. DNA end resection (5'-3') is subsequently triggered by the MRN complex and the CtIP 5' strand flap endonuclease, resulting in the creation of 3' ssDNA overhangs, which are protected by binding

of RPA proteins. BRCA1 facilitates the recruitment of PALB2, which promotes the activity of BRCA2. BRCA2 subsequently recruits its binding partner the Rad51 recombinase to the dsDNA-ssDNA junction. Rad51 subsequently displaces RPA to form the Rad51-loaded ssDNA filament, which invades the created D-loop of the homologous DNA template, allowing repair.

Direct inhibition of HR has been relatively poorly studied due to the lack of specific inhibitors[180]. However, a few direct inhibitors of HR components are being studied pre-clinically, including the Rad51 inhibitors[181] RI-1[182] and B02[183,184], and the RPA inhibitor HAMNO[185], all of which prevent induction of HR repair. Inhibition of BRCA1/2 has also been investigated as a potential treatment. However, development of drugs targeting these factors have been complicated due to their large size and domain structure[186]. Overall, inhibitors of the HR repair pathways remain poorly characterized, with very little research into their radiosensitization potential thus far.

Non-Homologous End Joining

Non-homologous end joining (NHEJ), as the name suggests, is a DDR repair pathway in which DSBs are repaired without the need for a homologous template. This process involves the joining of two broken DNA ends in close proximity, and carries the risk of introducing errors, such as insertions and deletions, as well as chromosomal aberrations caused by joining of non-partner DNA strands. NHEJ is a more error prone pathway than HR, which is active throughout the cell cycle. In healthy cells, NHEJ is most important in the G1 phase, where HR repair is impossible as no homologous template is available. To provide a very brief and simplistic summary of the process, NHEJ (Figure 6) proceeds in the following order of operations [187]:

1. *DSB recognition:* The Ku heterodimer (Ku70/80) recognizes and binds to sites of DNA damage, triggering the recruitment of other components of the DNA-PK complex, including DNA-PKcs (the catalytic kinase subunit of DNA-PK). Activation of the DNA-PKcs kinase results in its autophosphorylation, as well as the phosphorylation of other target proteins involved in the NHEJ process[188]. Activated DNA-PK tethers the broken DNA strands, thereby inhibiting their degradation[189]. Autophosphorylation of DNA-PKcs triggers the activation of DNA repair via NHEJ[190], in a manner dependent on γH2AX, which recruits the necessary factors and drives related phosphorylation cascades[191].
2. *Processing of broken DNA ends:* Most DSBs cannot be directly ligated due to incompatibility caused by the DNA damage. As such, processing of the DNA ends is

required. In NHEJ, this processing is predominantly mediated by the Artemis nuclease, activated following phosphorylation by DNA-PKcs. When complexed with DNA-PK, Artemis exerts both 5' and 3' endonuclease activity[192]. Other potential nucleases which may function to process DSBs include the MRN complex and APLF.

3. *Polymerization/ligation of DNA ends:* after processing of the DNA ends, the broken DNA is repaired through polymerization and ligation. Polymerization, or 'gap filling' is predominantly performed by the DNA polymerases Pol μ and Pol λ[193]. These polymerases incorporate nucleotides in a template-independent manner until regions of microhomology are formed. Finally, the two DNA ends are ligated by Ligase 4[194], whose activity is promoted by the XRCC4-XLF complex, which has been hypothesized to stabilise the DNA strands during ligation[195].

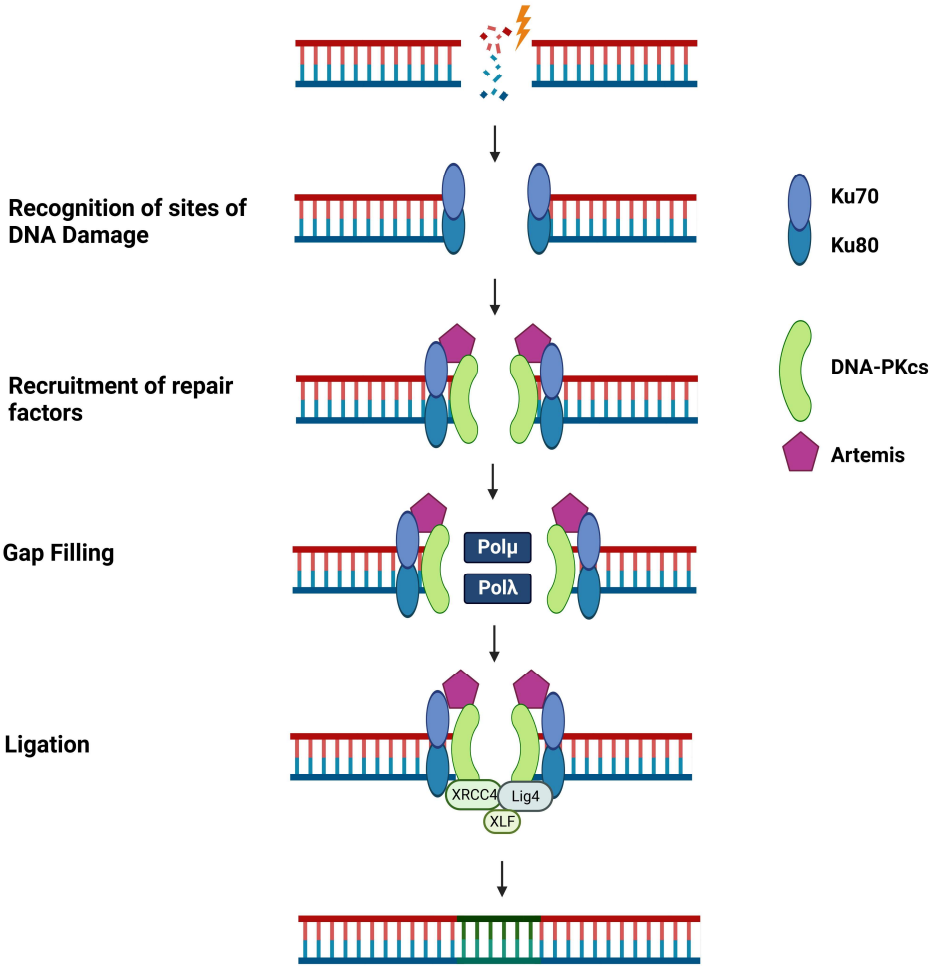

FIGURE 6 A SIMPLIFIED OVERVIEW OF THE NON-HOMOLOGOUS END JOINING REPAIR PATHWAY

Sites of DNA damage are recognized by the Ku70/80 complex, which binds to the DNA ends and subsequently recruits other repair factors, including DNA-PKcs and the nuclease artemis. When complexed with DNA-PKcs,

artemis exerts 5' and 3' endonuclease activity, preparing the DNA ends for subsequent polymerization. Polμ and Polλ mediate gap filling: nucleotides are incorporated in a template-independent manner to form regions of microhomology. Subsequently, ligation factors, including Ligase4, XRCC4, and XLF, ligate the DNA ends. This figure was adapted from Sishc & Davis[154].

The overwhelming majority of research into inhibiting the NHEJ pathway to radiosensitize cells has focused on inhibiting the DNA-PK complex, in particular the kinase activity of DNA-PKcs. As the inhibition of DNA-PKcs forms the primary focus of this research, this topic is discussed in much greater detail later in the text (Section 4.3 Targeting DNA-PK as a cancer treatment). However, in addition to DNA-PKcs, several studies have investigated the inhibition NHEJ through other targets. For example, one study suggested that inhibiting the action of the endothelial growth factor receptor (EGFR) may be an effective radiosensitization strategy, as EGFR or its downstream effectors can activate NHEJ[196]. Other studies have looked at targeting other key proteins in the NHEJ network. For example, one study showed that inhibition of Ligase 4 with the drug SCR7 resulted in a strong decrease in tumor growth in mouse in vivo cancer models when combined with irradiation[197], while another study using SCR7 showed a similar radiosensitization effect against cancer cells in vitro[198]. However, it should be noted that further research has shown that SCR7 is a poor inhibitor of Ligase 4, with low specificity and potency[199]. Another study showed that treatment of cells with a peptide blocking the interaction between Artemis and Ligase 4 radiosensitised cancer cells in vitro[200], and yet another study showed that expression of a non-functional form of Artemis radiosensitised cancer cells in vitro by inhibiting the proper activity of Artemis, thereby preventing NHEJ[201]. Other studies have shown the potential of inhibiting XRCC4 activity to promote radiosensitization: one study showed that RNAi silencing of XRCC4 radiosensitized breast cancer cells[202], while another showed that overexpression of a non-functional fragment of XRCC4 induced radiosensitivity in breast cancer cells[203]. Nevertheless, only inhibitors of DNA-PKcs have progressed to clinical trial, and this remains the most promising target for inhibiting NHEJ to promote radiosensitization.

Cell cycle checkpoints:

In healthy cells, the repair of DNA lesions is heavily dependent on the activation of cell cycle checkpoints (Figure 7), which provide more time for repair prior to progression to DNA replication and mitosis. In the case of irreparable damage, the cell undergoes apoptosis. These pathways help to prevent the passage of mutations to daughter cells. Cancer cells, however, are often defective in these mechanisms, which prevents apoptosis and allows the accumulation of

chromosomal aberrations, thereby driving cancer progression[204]. Due to the intrinsic link between the two pathways, the same signalling molecules which sense DNA damage and promote repair also promote activation of cell cycle checkpoints and apoptosis, and these pathways are intertwined at multiple levels; together this response is termed the DNA Damage Response (DDR) pathway[90]. Promotion of cell cycle checkpoints has recently gained favour as a potential target for novel cancer drugs and radiosensitisers[90,204].

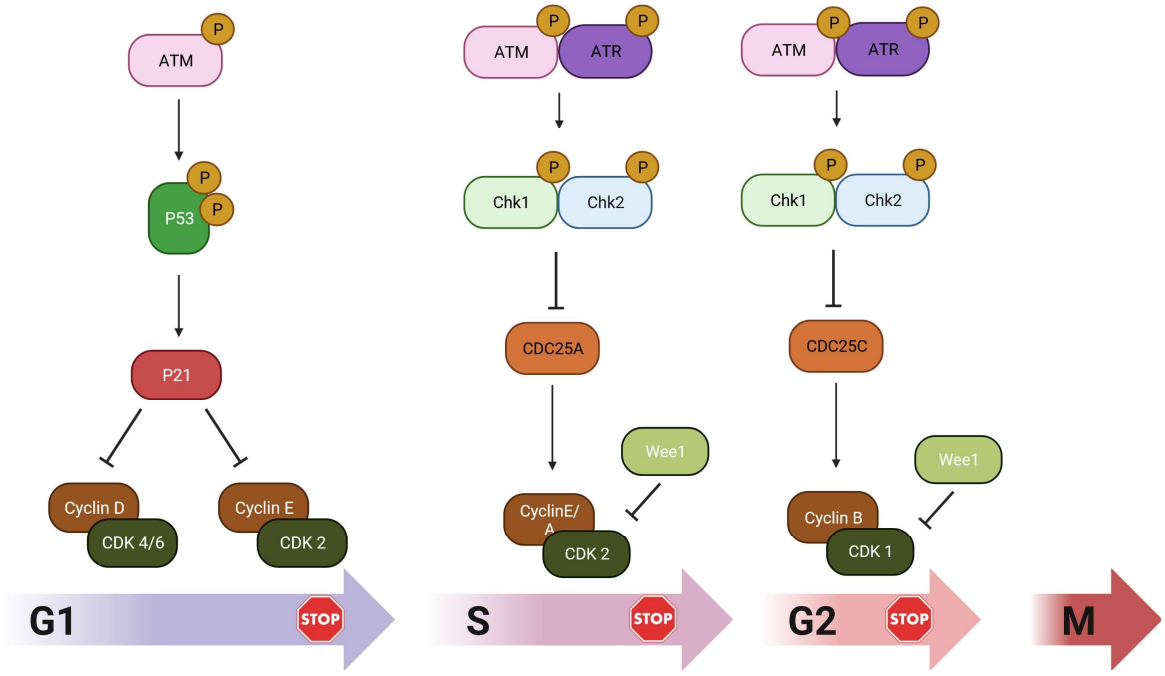

FIGURE 7 AN OVERVIEW OF THE DIFFERENT CELL CYCLE CHECKPOINTS.

A summary of these pathways is provided in the text. The figure was adapted from figures in the paper by Donzelli and Draetta[205].

M, Mitosis

As cell cycle checkpoints are activated in response to DNA damage, the first players in the signalling pathway are the DNA damage sensors (ATM, ATR, and MRN)[170,204]. The ATM and ATR kinases, in addition to triggering DNA repair pathways, also activate signalling pathways leading to activation of cell cycle checkpoints. There are three cell cycle checkpoints, which can be activated at the G1 phase, in the S phase, and at the G2/M transition. Each of these cell cycle checkpoint pathways ultimately leads to activation of a specific Cyclin Dependent Kinase (CDK) by phosphatase-mediated activation of the relevant cyclin. These Cyclin-CDK

complexes promote entry into the next phase of the cell cycle by mediating transcription of the necessary genes. more detailed accounts of this process have previously been published[206].

In cells undergoing the G1-S transition, the phosphatase Cdc25A removes inhibitory phosphorylation from CDK4/6 or CDK2, which interact with Cyclin D and E, respectively, to promote progression to the S phase. To activate the G1 checkpoint, activated ATM phosphorylates the downstream kinase Checkpoint Kinase (CHK) 2, which phosphorylates Cdc25A to inhibit its activity. In addition, ATM-CHK-mediated activation of the global DNA damage regulator, P53, activates P21, which directly inhibits CDK/cyclin action. Through a different pathway (discussed later) continually active P53 also promotes apoptosis. This process has been reviewed in detail by Bertoli and Skotheim et al[207].

Transition from the S to the G2 phase is similarly regulated. In healthy cells undergoing this transition, Cdc25A promotes the interaction between Cyclin E/A and CDK2. In the G2-M transition the similar phosphatase Cdc25A/C promotes the activation of the CDK1/Cyclin B complex. During both of these transitions, activated ATM/ATR kinases phosphorylate the downstream kinases CHK2 and 1, respectively, which inhibit Cdc25A/C phosphatase activity, thereby preventing the Cyclin/CDK-mediated transcription necessary for transition. The kinase WEE1 can also promote cell cycle checkpoint activation by phosphorylating the relevant CDKs These pathways have been thoroughly reviewed by Barnum and O'Connell[206].

Failure of cells to repair DNA damage prior to entering mitosis generally results in cell death due to the induction of mitotic catastrophe[208]. One potential method of radiosensitisation which is coming under increasing focus is the inhibition of cell cycle checkpoints to prevent cancer cells from repairing radiation-induced DNA damage, eventually resulting in mitotic catastrophe and cell death[209]. So far, the most commonly research players in these pathways are CHK1, CHK2, and WEE1, which are discussed below.

CHK1 has multiple functions throughout the cell cycle. In the S phase, CHK1 can stall replication to repair damage to the DNA[210]. CHK1 is also a key regulator of the G2/M transition, with this kinase functioning to stall cell cycling until the cell is ready to enter mitosis[211]. Research has also indicated a role of CHK1 in the M phase, although the knowledge of this role is less clear[212]. So far, there is significant pre-clinical evidence to suggest the potential of targeting CHK1 to promote radiosensitization in a variety of cancers. For example, one study showed that the CHK1 inhibitor SAR-020106 exerted potent radiosensitising capabilities in a variety of P53-deficient cancer models by suppressing radiation-induced G2/M arrest[213].

Another showed that CHK1 inhibition strongly sensitized head and neck squamous cell carcinoma to chemoradiotherapy, again by preventing therapy-induced G2 arrest[214]. A further study showed that radiosensitization induced by CHK1 inhibition functioned by inhibiting repair by homologous recombination, and preventing the normal radiation-induced G2 arrest[215].

Similar to CHK1, CHK2 is a multifunctional kinase active throughout many phases of the cell cycle, modulating DNA repair, cell cycle checkpoints, and activation of apoptosis[216]. Compared to CHK1, CHK2 has been relatively poorly studied as a target for cancer therapy. However, there is still some evidence to suggests its potential as a target for radiosensitization. For example, one study of malignant meningioma showed that knockdown of players in the CHK2 pathway radiosensitized cells[217], while the novel CHK2 inhibitor PV1019 has also shown to have radiosensitisation potential[218]. Regarding the clinical applications of these inhibitors, the dual CHK1/2 inhibitor Prexasertib is currently under phase 2 clinical trial as a targeted therapy[219]. Meanwhile, several studies have shown its efficacy as a radiosensitiser in cancers including radioresistant medulloblastoma[220] and head and neck squamous cell carcinoma[221].

The kinase WEE1 is also an important player in the control of the cell cycle, which functions primarily to control the G2/M transition, thereby playing a role in the regulation of mitosis[222]. A variety of pre-clinical studies have shown the radiosensitising effects of WEE1 inhibitors in a variety of cancers, including cervical cancer[223], pontine gliomas[224], osteosarcoma[225], and hepatocellular carcinoma[226]. Furthermore, the in vitro/in vivo efficacy of the WEE1 inhibitor adavosertib as a radiosensitiser has been shown[227], and its potential as a clinical radiosensitiser is being evaluated in a phase 2 clinical trial. In response to this promise, numerous early stage clinical trials have investigated the treatment efficacy WEE1 inhibition, with several showing promise[228].

Direct inhibition of CDKs, which function downstream of the CHK kinases in the cell cycle checkpoints, has also been successfully used as a combination therapy concurrent with or following chemotherapy to increase treatment efficacy. Inhibitors of CDK 4/6, which control G1 arrest, such as abemaciclib, palbociclib, and ribociclib, have shown efficacy in treating several cancers, most notably breast cancer[229]. However, recent studies have indicated that use of these inhibitors either prior to or concurrent with cytotoxic chemotherapy may actually inhibit treatment efficacy as the resulting G1 arrest may affect their mechanisms of action in the later stages of the cell cycle[230]. The use of such agents in combination with radiotherapy is also advancing, with CDK4/6 inhibitors so far showing the most promise[231]. One preclinical

study showed that combination of radiotherapy with the CDK4/6 inhibitor palbociclib increased anti-tumor activity in atypical teratoid/rhabdoid and glioblastoma tumor xenografts[232]. Other studies have evaluated the safety of concurrent radiotherapy and CDK4/6 inhibitor treatment with positive results[233,234], and a recent study showed a strong radiosensitising effect of CDK4/6 inhibition in retinoblastoma protein positive Meningiomas[235].

Targeting of P53 – A global regulator

P53 is a crucial tumour suppressor gene, responsible for the control of cell cycle arrest and apoptosis in dividing cells. Through its action as a transcription factor, P53 also acts as a crucial mediator of the cell stress response, being activated in response to a wide variety of signals, including DNA damage, oxidative stress, and nutrient depletion. The activity of p53 at the protein level is controlled by post-translational modifications, including phosphorylation, acetylation, and ubiquitination. P53 is expressed constitutively in cells; however, it is generally maintained in an inactive form through binding to the repressor MDM2. Phosphorylation of this repressor along with concurrent phosphorylation of P53 (such as by activated ATM) results in dissociation of the two, allowing the release of active P53. Active P53 triggers a wide range of responses, most notably cell cycle arrest, DNA repair and, ultimately, apoptosis. The role of P53 in numerous cell processes has been reviewed by Farnebo et al[236]. P53 is mutated in approximately 50% of cancers, and the P53-null phenotype is associated with aggressive cancer and poor overall survival in many cancer types[237], while it has long been known that P53 mutations are correlated with radioresistance[238,239].

Because of its integral role as a tumor suppressor, promotion of p53 activity has been considered a potential, although underdeveloped, target for both cancer therapy and radiosensitisation. The most common pathway to achieve this is through inhibition of the p53 repressor MDM2, with several such drugs under clinical or preclinical evaluation[240]. One such example is idasanutlin (RG7388), which inhibits the MDM2-P53 interaction. This drug showed significant preclinical promise in combination with chemotherapy, progressing to several clinical trials as a targeted therapy. While some of these trials have been abandoned due to a lack of benefit, others continue[241]. Nevertheless a few pre-clinical studies have indicated the potential utility of idasanutlin as a radiosensitizer for atypical teratoid rhabdoid tumors[242] and childhood sarcoma[243]. However, its radiosensitization benefits have yet to be tested clinically.

Reactivation of mutant p53 is also a topic of considerable interest, and screening of chemical libraries have identified several relevant compounds[236]. The most advanced of these

is the small molecule PRIMA-1 which can bind to mutant P53 to stabilize and reactivate it[244]. Both PRIMA-1 and its derivative PRIMA-1Met/APR-246 have shown promising anti-tumor activity in pre-clinical studies[245–247], with the latter already progressing to Phase I clinical trial Although this has not yet been investigated as a radiosensitiser, it may warrant investigation as such.

Indeed, the ubiquity of P53 in the DNA Damage response pathway makes P53 status an important prognostic factor in many therapies, as loss of P53 activity makes activation of cell cycle checkpoints much less likely[236]. The efficacy of many of the targeted therapies acting on members of the DDR pathway therefore relies on the P53 status of the cell – with cells with un-mutated, active P53 much more susceptible in most cases. This therefore raises the possibility of a treatment strategy combining the use of the above-mentioned P53 activators with drugs targeting the DDR pathways to increase treatment efficacy. However, this remains under-investigated in the field of radiosensitization.

2.4 Radiosensitisers in the Clinic: Future perspectives

Despite the wealth of preclinical research into radiosensitisers, relatively few of these drugs have progressed to clinical trial, and even fewer have been successful. Nevertheless, there have been some instances of relative success. For example, a phase III trial in the late 90s showed that nimorazole (a drug which reduces tumoral hypoxia) effectively radiosensitised supraglottic larynx and pharynx carcinoma tumors[248]. However, this drug has not been applied outside of the host country of Denmark. Furthermore, other similar radiosensitising drugs targeting hypoxia tested in clinical trial have failed due to inconsistent results, high toxicity, or difficulty applying the treatment regimen[249]. Regarding in particular inhibitors of the DNA damage response pathways, PARP inhibitors have progressed the furthest, although their application as radiosensitisers remains relatively poorly developed. One phase 1 trial investigating olaparib as a radiosensitiser for triple negative breast cancer found that this combination was safe and could have potential in the clinic; however, this has not yet translated to patient management[250]. Another trial investigating the PARP inhibitor veliparib with radiotherapy in patients with inflammatory or locoregionally-recurrent breast cancer showed unacceptable toxicity of the drug, with 30% of patients showing severe acute toxicity at the highest dose, and, more importantly, ~50% of surviving patients showing grade 3 adverse events by 3 years post-treatment[251]. Although less well investigated so far, Wee1 inhibitors, such as adavosertib, have also shown promise as radiosensitisers in the clinic. For example, one recent study investigating the utility of adavosertib in combination with radiation, while the drug gemcitabine showed

acceptable toxicity and promising survival in patients with locally advanced pancreatic cancer[252]. Drugs targeting other components of the DNA damage repair pathways, including ATM, ATR, and DNA-PK (discussed in more detail towards the end of this introduction) are less well-developed, but have nevertheless garnered significant interest[253].

Unfortunately, despite a wealth of pre-clinical studies, the majority of radiosensitisers moved forward to clinical trials have failed to progress further, and as of January 2023, the only targeted treatment approved for clinical use as a radiosensitiser by the FDA is the EGFR inhibitor cetuximab, which is administered in some head and neck cancers[254,255]. Furthermore, efforts to apply the same drug as a radiosensitiser in other EGFR-driven cancers showed no added benefit[253,256,257]. These innumerate failed radiosensitisers were generally discarded due to either unacceptable toxicity (both short term or long term), or a lack of efficacy.

Altogether, the body of evidence and results regarding the clinical use of radiosensitisers suggests several important points, including that pre-clinical success does not necessarily guarantee clinical success, toxicity is an important issue that must be better investigated in pre-clinical studies, and that radiosensitisers must be targeted to specific cancers, taking into account the molecular context.

3. Radiosensitization and Medulloblastoma:

As discussed in detail at the start of this introduction, radiation is a key component of medulloblastoma therapy. As such, it is applied in all patients in whom such treatment is possible, and is necessary to achieve cure. Radiotherapy in the treatment of medulloblastoma has two primary pitfalls: the imposition of severely debilitating side effects in patients, especially infants and young children, and the potential of residual cells to develop resistance and lead to recurrence. An understanding of the mechanisms of resistance to irradiation in medulloblastoma, especially group 3 medulloblastoma, which has the worst prognosis, is therefore important, as it would allow the potential identification or development of radiosensitisers. As outlined in detail earlier, radiosensitisers enhance the susceptibility of cancer cells to irradiation, thereby enhancing the therapeutic index[258], by either increasing the toxic dose, or decreasing the effective dose[131]. Effective radiosensitisation of medulloblastoma could therefore serve several purposes. First, it could decrease the effective dose of radiotherapy required to achieve tumour regression in primary patients, thereby decreasing the incidence and severity of treatment side effects. Second, the use of radiosensitisers in the initial treatment of primary tumours could improve the response to therapy, and thereby reduce the rate of recurrence after therapy.

In the past, several clinical trials have investigated the use of chemotherapies to induce radiosensitization in medulloblastoma[259]. For example, one study investigated the use of metronomic temozolomide concomitant with re-irradiation of MB focal recurrence, identifying a radiosensitising effect of this drug[260]. Further, several other studies have investigated carboplatin as a radiosensitiser: one trial in high risk medulloblastoma patients found that the addition of carboplatin to the radiotherapy regimen improved event-free survival[145], while another similarly showed that concomitant carboplatin improved patient outcome[146]. Other clinical trials are currently ongoing to assess the efficacy of concomitant radiotherapy and chemotherapeutics (NCT00276666, NCT00003573, NCT00392327, NCT00003309, and NCT00002875).

In addition to this, numerous pre-clinical studies have investigated targeted drugs as radiosensitisers, with significant variations in target and approach. Several of the more promising trials focused on targeting different DNA damage repair pathways. One such study found that the PARP-inhibitor veliparib successfully radiosensitised G3 MB cells both in vitro and in an in vivo orthotopic implant model[261]. Another investigated the potential of the base

excision repair inhibitor methoxyamine, finding that in vitro treatment of cells with this drug sensitized them to both ionizing radiation, and chemotherapy (cisplatin, temozolomide, and thiotepa) by decreasing cell proliferation and driving apoptosis[262]. Of note, this study further suggested that this effect was subtype-dependent. Finally, one study investigating the efficacy of treatment with asiDNA, an oligonucleotide mimicking double strand breaks which sequesters DNA-PK and PARP, thereby acting as an agonist to repair of the actual genome, found that asiDNA treatment sensitized orthotopic mouse models of medulloblastoma to irradiation in a manner independent of *TP53* status[263]. Importantly, this study found that treatment of pup mice with this drug induced no toxic side effects on growth or behaviour, indicating its potential as a safe drug for future work[263]. Finally, another study found that upregulation of the expression of SPARC, a known radioresistance-reversal gene, sensitized cells to irradiation by reducing SOX4-driven DNA damage repair[264].

The majority of studies validating drugs/targets for radiosensitization in medulloblastoma have focused on the targeting of kinases and signal transduction proteins important in cell cycling or functioning. For example, one study showed that treatment of MB cells with the CDK6 inhibitor PD0332991 decreases MB cell proliferation and triggers a G0/G1 cell cycle arrest, thereby radiosensitising cells[265]. In order to assess the potential toxicity of this targeting in patients, the authors also assessed the effect of short hairpin (sh) RNA knockdown on the proliferation of mouse neural stem cells, interestingly observing an increase in proliferation with knockdown[265]. Another study showed that treatment with the PLK1 inhibitor onvansertib combined with irradiation increased DNA damage and apoptosis in G3 MB cells in vitro, in addition to promoting tumor regression in vivo[266]. Interestingly, this study is one of the only studies mentioned here to propose a potential stratification method for patients, showing the efficacy of the drug specifically in MYC-driven tumours[266]. Further, one study investigating the NF-κB-targeting drug DHMEQ found that treatment with this drug decreased cell viability and increased levels of apoptosis in response to irradiation[267]. Another found that treatment with M443, an inhibitor of the MRK/ZAK protein kinase, radiosensitised MB cell lines and patient-derived primary cells in vitro, and had a synergistic effect with irradiation on orthotopically-grafted tumours in vivo[268]. Another study found that up-regulation of the pro-apoptotic protein caspase-8, induced by treatment with IFN-γ, sensitized MB cell lines to both radiotherapy and chemotherapy in vitro[269]. Another study found that inhibition of the Hedgehog pathway with the drug Gant61 radiosensitised the MB cell line DAOY to proton and carbon ion irradiation, but not traditional X-ray irradiation[270]. Finally, one study showed that knockdown

of the ephrin receptor, EphB1, radiosensitized MB cells in vitro, and delayed tumor recurrence post-irradiation in a genetically engineered mouse model[271].

Other investigations have looked at targeting pathways associated with DNA maintenance or more general cellular pathways. For example, one study showed that targeting of the histone chaperone FACT complex with the drug CBL0137 inhibited DNA repair, thereby radiosensitising MB cells both in vitro, and in in vivo xenografts[272]. Another study showed that pharmacological inhibition of histone deacetylases sensitized cells to both radiation and chemotherapy (etoposide) by promoting apoptosis[273]. Another study showed that inhibition of MMP9, a matrixin, and upregulation of Gadd45a, a factor whose expression is induced by DNA damage, reduced both cell viability and metastatic potential in MB cells when combined with irradiation[274]. In addition, treatment with patupilone, an inhibitor of microtubule stabilization, radiosensitized MB cells in vitro, and was shown to inhibit tumor growth in combination with fractionated irradiation in in vivo xenograft models[275]. Another found that inhibition of the proteasome with the drug NPI-0052 synergized with γ-radiation to increase apoptosis in MB cells[276]. Finally, one study showed that treatment with arsenic trioxide, which alters the mitochondrial membrane potential, radiosensitised *TP53*-mutated SHH MB cells[276]. Finally, one study found that the administration of β-blockers could increase the effects of radiation on medulloblastoma models by triggering metabolic catastrophe, subsequently resulting in an increase in the production of superoxide radicals, thereby potentiating the cellular effects of radiation[277].

While the majority of the studies investigating radiosensitivity in group 3 medulloblastoma have looked only at cell lines, some have specifically focused on targeting stem-like MB cells, with the rationale that stem-like cancer cells have a greater adaptability and are therefore more likely to escape from radiation. One study looked specifically at CD133+ MB cells, showing that treatment of these stem-like MB cells with Cucurbitacin I, an inhibitor of phospho-STAT3, decreased stemness markers, and sensitised the cells to both chemo- and radio-therapy in vitro; this effect carried over in vivo, where treatment promoted radiation-induced shrinkage of in vivo-grafted tumors[278]. A similar study investigating CD133/Nestin double positive stem-like MB cells, found that inhibition of these cells with celecoxib, a COX2 inhibitor, suppresses STAT3 activation, thereby driving apoptosis and sensitizing the cells to irradiation[279].

It is also interesting to note that several other studies have investigated the use of inhibitors of different targets of the DNA damage repair pathways either alone or in

combination with chemotherapy rather than radiotherapy. For example, several studies have shown the potential of targeting CHK1 and 2 with or without chemotherapy[280–282], while another showed a potential therapeutic benefit of combining PARP and CHK1 inhibition[283]. Other studies have indicated the potential of inhibiting WEE1 as a therapeutic possibility[284–286]. Interestingly, the WEE1 inhibitor adavosertib has progressed to clinical trial as a combination drug with irinotecan in pediatric patients with relapsed neuroblastoma, medulloblastoma, and rhabdomyosarcoma; however, no benefit was observed in the medulloblastoma patients[287]. These drugs/targets, particularly WEE1 and CHK1, which have previously validated as targets for radiosensitization in other cancers, may be promising candidates for further research into the radiosensitization of group 3 medulloblastoma. However, significant pre-clinical work is needed to validate this.

Unfortunately, most of the aforementioned preclinical studies are subject to many of the same limitations as in other cancers. Firstly, stratification beyond the group level was rarely performed, meaning that it is unclear which patients would actually benefit from these treatments in the clinic. Secondly, only a few of these studies discussed the potential toxicities of the drug. While this may not have been so necessary in the studies investigating more well-characterized drugs (e.g. veliparib, which has been assessed in many clinical trials, or asiDNA, a known normal tissue protector), such work is key when promoting the possibility of using drugs which have not yet been thoroughly investigated. As such, more work is needed before any of the above-mentioned drugs may progress to clinical trial or usage. Nevertheless, this body of work strongly suggests the potential of radiosensitization in the future treatment of medulloblastoma.

4. DNA-PK

DNA-dependent protein kinase (DNA-PK) is a protein complex abundantly expressed in all mammalian cells and comprising multiple protein subunits, including a catalytic subunit (DNA-PKcs, encoded by the gene *PRKDC*), and a Ku heterodimer. DNA-PK was first discovered by accident in 1985 when researchers discovered that contamination of a diverse range of eukaryotic cells with dsDNA resulted in the phosphorylation of a common protein[288]. In the decades since this discovery, extensive research has been conducted to characterize the structure, function, and interaction networks of DNA-PK. In this section, we will discuss what is known about the canonical roles of DNA-PK in healthy cells, its role in cancer development and progression, and its potential as a target for cancer treatment.

4.1 Cellular Functions of DNA-PK

DNA-PK in DNA damage sensing and repair

As outlined in the section on NHEJ above, DNA-PK is a DNA damage sensor which drives the NHEJ DNA repair pathway. Thus, canonically, the DNA-PK complex, and by extension, the DNA-PK catalytic subunit, is best known as the key driver of NHEJ to repair DNA damage. More recently, however, knowledge regarding the role of DNA-PK in DDR has expanded beyond the NHEJ pathway, with significant evidence showing that DNA-PKcs also functions in the control of HR, a longer, more accurate DNA damage repair network. Numerous studies have shown that DNA-PK plays a crucial role in driving the cell decision to activate either NHEJ or HR to repair dsDNA breaks[289–292]. Although the exact pathways underlying this decision remain relatively poorly understood, here we will quickly summarize what is known about the role of DNA-PK in this section. DNA-PKcs is a large protein, with over 40 phosphorylatable residues[190]. As mentioned earlier, phosphorylation of DNA-PKcs at some sites drives the activation of the NHEJ pathway[190]. However, some studies have further shown that phosphorylation at other sites inhibits NHEJ, driving activation of the HR pathway instead[291], thereby indicating that alternative DNA-PKcs phosphorylation is a key step in this decision pathway. Other studies have postulated that the occurrence of the resection of DNA damage sites is a key deciding factor; if resection occurs, HR progresses, while NHEJ (which involves the repair of blunt-ended DNA) is repressed[292–294]. These same studies have shown that DNA-PK and DNA end-resection complexes compete with each other to bind to sites of DNA damage. Thus, the binding of active DNA-PK to sites of DNA damage represses HR. In support of this, another study showed that BRCA1-mediated repression of DNA-PKcs

autophosphorylation increased HR activity[295]. The restriction of HR in the G1 phase has also been indicated to be modulated by the inhibitory phosphorylation of the DNA damage sensor ATM by DNA-PKcs[296].

DNA-PK in Apoptosis

Apoptosis is a programmed cell death pathway, which in healthy cells is activated in response to DNA damage, among other insults[297]. Many studies have shown that DNA-PK plays a role in the regulation of apoptosis activation in both healthy and cancer cells[298]. For example, one study showed that inhibitory phosphorylation of ATM by DNA-PKcs reduced apoptosis in response to DNA damage[296]. Another study showed that DNA-PK acted as a strong suppressor of P53-independent apoptotic pathways[299]. Other studies have shown that numerous downstream effectors of DNA-PK may function to inhibit apoptosis[300,301].

DNA-PK in the response to replication stress

Replication stress is a cellular state in which insults to the DNA result in slowing or stalling of DNA replication forks[302]. Replication stress is sensed by the DNA damage sensor ATR, which subsequently phosphorylates DNA-PKcs, initiating a transcriptional cascade which results in activation of the S phase checkpoint by CHK1[303,304]. Several studies have shown that the activity of DNA-PK can abrogate the deleterious effects of replication stress in cancer cells. For example, one study using breast cancer models showed that DNA-PK (which is known to locate to replication forks, although with an indeterminate activity) promoted fork reversal, thereby stabilizing stressed replication forks to prevent genome instability, reducing cell sensitivity of chemotherapy[305]. Another study showed that DNA-PKcs acted in concert with endonuclease 1 to stabilize stressed replication forks in glioma, thereby reducing the potential cytotoxic effects of replication stress[306]. Another study showed that DNA-PKcs-mediated phosphorylation of RPA32 was required for replication stress checkpoint activation to prevent mitotic catastrophe[307].

DNA-PK as a transcriptional activator:

In addition to its numerous direct roles in the activation, modulation, and repression of different DNA damage repair pathways, there is also abundant evidence to suggest diverse roles of DNA-PKcs in modulating transcription. Indeed, the kinase activity of the DNA-PK complex plays an integral role in regulating overall transcription, by phosphorylating TATA-binding protein (TBP) and transcription factor IIB (TFIIB) to allow complexing with RNA polymerase II[308]. In

healthy cells, the kinase activity of DNA-PK also functions in the modulation of more specific transcription factors[309]. In the context of cancer, one study showed that DNA-PK phosphorylated oestrogen receptor alpha, resulting in transcriptional activation, in certain breast cancer models[310]. Another study showed that transcriptional landscapes driven by DNA-PK activity promoted metastasis in prostate cancer[311]. In addition, one study showed that DNA-PK was one of many kinases which could phosphorylate c-MYC[312], which is well known to be linked to replication stress

DNA-PK in the immune system

In addition to its diverse roles stemming from its action in DNA repair, DNA-PK also plays a role in the functioning of the immune system, due to its importance in lymphocyte development. During the development B and T cells, NHEJ drives a specific form of somatic recombination, termed V(D)J recombination, which is required to ensure the diversity in the range of antibodies and T cell receptors produced by B and T cells, respectively[313]. During V(D)J recombination, specific enzymes (including VDJ recombinase, RAG, TdT, and the artemis nuclease) bind to recombination signal sequences, defined as specific sequences flanking the variable (V), diversity (D), and joining (J) segments of target antibody and receptor genes. This triggers cutting of the DNA, resulting in the formation of blunt ends, which are processed to form recombinant genes in a DNA-PK dependant manner[313]. More recently, DNA-PK has also been shown to function in class switch recombination, which is essential for B cell functioning[314]. These pathways are crucial in the immune system, and as such, inhibition of DNA-PK may have immune consequences. For example, one study showed that administration of a DNA-PK inhibitor decreased both the activity and cytotoxicity of CD4+ and CD8+ effector T cells[315].

Other studies have shown more diverse roles of DNA-PK in the immune system. For example, one transcriptomic study revealed that DNA-PK played a key role in cytokine expression in T cells by promoting the expression of the transcription factor Egr1, which promotes T cell stimulation[316]. Another showed that DNA-PK played a role in the pathogenesis of rheumatoid arthritis, an autoimmune disease, by triggering apoptosis of T cells[317].

DNA-PK in Neurogenesis

Neurogenesis is the cellular process by which neurons are formed in the brain; although this process is most important during foetal development, it continues throughout life, with higher levels observed in early childhood, and an age-related decline observed thereafter[318,319]. Recent studies have indicated that the DNA damage sensors DNA-PK, ATM, and ATR play diverse

and complementary roles in neurogenesis, as cellular DNA is exposed to a significant number of threats. One recent extensive study[320] showed that DNA-PK protects non-replicating cellular subpopulations in the developing neocortex from DNA damage by activating NHEJ repair. Specifically, this study showed that cerebellar progenitor cells lacking DNA-PK accumulated DNA damage, promoting apoptosis. In contrast, ATM controlled apoptosis in immature progenitor cells, while ATR controlled cell cycle checkpoints in proliferative neuroprogenitor populations. Another study has shown the importance of DNA-PK in protecting developing neurons in the mouse retina from apoptosis[321].

Together, these studies have well-established the role of DNA-PK and NHEJ in the protection of developing neural cells from cell death. However, the role of DNA-PK in this process is not crucial, as it has been well-established that mouse models deficient in DNA-PK, including severe combined immunodeficiency (*SCID)* mice can produce viable young[322]. However, while DNA-PK loss is not deleterious, *SCID* mice exhibit increased levels of DNA damage and apoptosis in the developing brain[323,324], further supporting the important role of DNA-PK in preventing this. The importance of the NHEJ pathway, in particular in neuronal protection, has further been highlighted by studies of mouse models deficient in other components of this pathway. For example, loss of Lig4 has been shown to result in embryonic lethality stemming from massive neuronal apoptosis and loss of neurogenesis[325], and deficiency of XRCC4 has also been shown to result in late embryonic lethality[326].

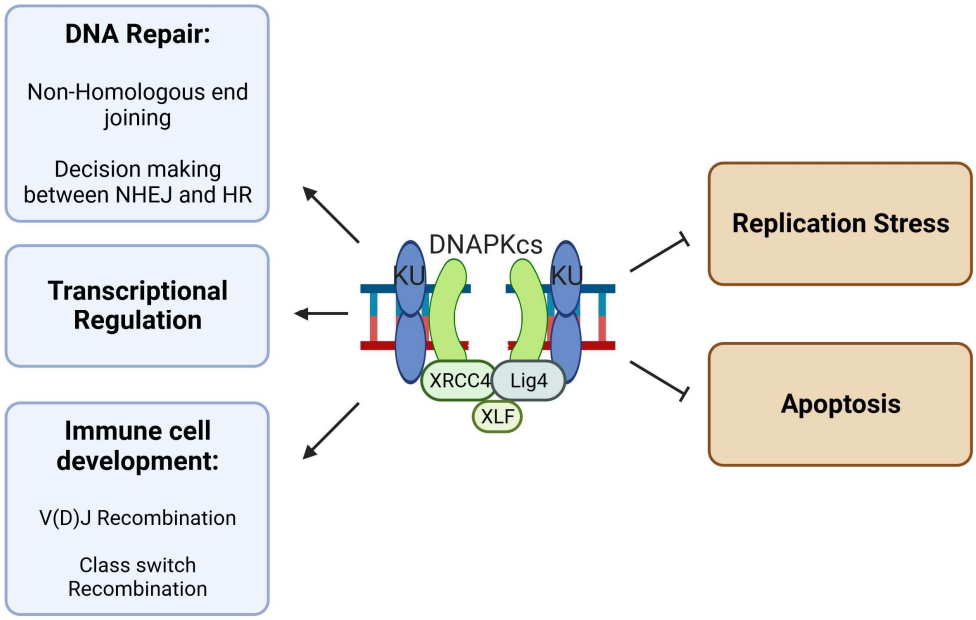

FIGURE 8 CELLULAR ROLES OF THE DNA-PK COMPLEX

4.2 The role of DNA-PK in cancer development, progression, and response to treatment

Despite its role in ensuring genetic stability, numerous studies have identified high expression of DNA-PK in a multitude of human malignancies, including melanoma, where it drives angiogenesis and metastasis[327], and prostate cancer, where it is associated with aggressive phenotypes[328]. Furthermore, a recent analysis of *PRKDC* mutations across different cancers in the TCGA database showed high mutation rates in a number of cancers, including colorectal, gastric, and endometrial cancer[329]. In addition, many studies have shown a link between high *PRKDC* expression and poor prognosis in a variety of cancers, including non-small cell lung cancer[330], gastric cancer[331], and breast cancer[332].

Previous studies have shown that expression of PRKDC/DNA-PKcs is highly correlated with a number of tumor characteristics, including initiation[333], development[327,332], invasion, and metastasis[327]. Numerous prior researchers have posited that in cancers with mutated DNA-PK, this association in some cases stems from an increase in the number of mutations which develop following the loss of DNA damage repair capacity induced by loss of DNA-PK activity[334]. Conversely, there are numerous pathways through which high expression/activity of DNA-PK may be implicated in tumorigenesis. For example, one study in renal cell carcinoma showed that DNA-PKcs overexpression promoted cell growth by driving mTORC2 activation[335], while another study showed that DNA-PK promoted cell proliferation by suppressing apoptosis[336]. Other studies have shown that DNA-PK may modulate the tumor microenvironment, thereby driving tumorigenesis[337]. DNA-PK may also be associated with poor outcomes due to its link with metastasis. Indeed, several prior studies have shown that high expression of DNA-PK induces a transcriptional landscape which promotes metastasis[311,327,338,339]. Together, all of these results promote DNA-PK as a potential target for tumor therapy.

4.3 Targeting DNA-PK as a cancer treatment

Given the commonality of DNA-PK dysregulation in cancer, its prognostic implications, its targetability, and its key role in DNA damage repair, significant interest has arisen in the targeting of DNA-PK as a cancer treatment. The majority of research into targeting DNA-PK have looked at its effect on the response of cancer cells to genotoxic insult, such as chemotherapy and radiotherapy. Indeed, many studies have previously shown that high expression of DNA-PK is associated with both chemo-[305,334] and radioresistance[340–342]. Thus, reducing the activity of DNA-PK through pharmacological inhibition will reduce the ability of

cancer cells to respond to genotoxic insult, resulting in increased chemo- or radiosensitivity. A number of selective DNA-PK inhibitors have been pre-clinically validated as radiosensitisers in a number of different cancer models, including breast cancer[343], gliomablastoma[344,345], pancreatic cancer[346], and non-small cell lung cancer[347], to name only a few.

The majority of available DNA-PK inhibitors are classified as type I inhibitors, meaning they target the ATP binding site of the kinase domain of DNA-PKcs[348]. The first DNA-PK inhibitor (LY294002) to be identified was in fact a repurposed PI3K inhibitor[349]. Since the discovery of this compound, numerous other DNA-PK inhibitors with higher selectivity and improved pharmacokinetics have been developed, although some of the inhibitors which have progressed to clinical trial are considered dual inhibitors of other PIKKs, such as mTOR[348]. The most widely known newer, more selective DNA-PK inhibitors include AZD7648, VX-984, and peposertib[348], the latter of which is discussed in more detail in section 4.5.

4.4 DNA-PK in Medulloblastoma

Despite increasing research being performed into the roles of DNA-PK in cancer, only a few studies have yet investigated its role in MB. One study investigated dual inhibition of DNA-PKcs and telomerase in brain tumour cells as a potential treatment mechanism for MB, showing a promising cytotoxic effect in the human MB cell line ONS-76[350]. Another paper showed that further knockout of DNA-PKcs in Ptch1 heterozygous knockout mice (a mouse model which develops MB) increased DNA damage and apoptosis in neural precursors of the developing cerebellum, suppressing MB tumorigenesis. Further in vitro testing revealed that inhibition of DNA-PK with the drug NU7441 sensitized MB cells to radiation[351]. Most interestingly, a recent paper investigating the proteomic profiles of the different MB subgroups showed that levels of phosphorylated DNA-PK in medulloblastoma was linked to levels of phosphorylated MYC (the main driver of G3 MB), and that inhibition of DNA-PK strongly sensitized MYC-driven MB cells to irradiation in vitro [352]. Although the evidence is relatively sparse, all of these papers suggest that DNA-PK may be a target for sensitization in MB, particular in G3 MB, which is characterized by increased MYC expression.

4.5 Peposertib: A specific inhibitor of DNA-PK

DNA-PK has been investigated as a potential treatment target for cancer for a long time; however, initial research into this potential was limited by the low selectivity of first-line drugs, many of which also inhibited PI3K or members of the PIKK family, such as mTor[353]. However, more recent drug screening studies have identified more specific inhibitors of DNA-PK. The

drug peposertib, previously known as M3814 or MSC2490484A, is one such specific DNA-PK inhibiting drug, which is currently under both preclinical (Table 2) and clinical (Table 3) investigation as a radiosensitising drug in a variety of cancers. Although this drug has not yet been translated to routine use in the clinic, a previous clinical trial showed good tolerability in adult cancer patients[354]. Another clinical trial investigating the use of peposertib in patients with solid tumours showed that treatment induced some low-grade side effects, including fatigue, constipation, decreased appetite, dry mouth, dysphagia, headache, oral pain, radiation skin injury, and mucositis, which were generally considered as acceptable[355].

Furthermore, a recent study showed that the concentrations of peposertib in treated mice are much lower in the central nervous system than other peripheral organs, because of the active efflux across the blood brain barrier by ABC transporters; however, peposertib was concentrated in the core of brain tumours (in this case metastatic melanoma tumours)[356]. This heterogeneity in drug distribution (with high concentrations in the tumor core and low concentrations in the healthy brain) would help to reduce any normal tissue toxicities associated with dual irradiation and DNA-PK inhibition. As such, this drug appears to be a promising candidate for targeted radiosensitization of brain tumours susceptible to DNA-PK inhibition. In this context, several prior studies have shown very preliminary results to indicate DNA-PK as a potential therapeutic target in medulloblastoma in combination with irradiation[351] or other promoters of DNA damage[350]. Further, a recent paper investigating the proteomic profiles associated with the different subgroups of MB presented preliminary results indicating a possible association between the activities of DNA-PK and MYC (the main driver of G3 MB), finding that DNA-PK inhibition radiosensitized MYC-driven D458MED group MB cells[34]. Thus, peposertib could be considered an excellent drug candidate for MYC-driven G3 MB.

TABLE 2 PRE-CLINICAL STUDIES INVESTIGATING PEPOSERTIB/M3814 AS A RADIOSENSITISER (PUBLISHED UP TO MAY, 2023)

Author, Year	Title	Target Cancer	Results
Wang et al., 2022[346]	DNA-PK Inhibition and Radiation Promote Antitumoral Immunity through RNA Polymerase III in Pancreatic Cancer	Pancreatic cancer	DNA-PK inhibition with peposertib in conjunction with irradiation promotes PD-L1 expression, and anti-PD-L1 treatment combined with radiation and peposertib potentiates antitumor immunity in models of pancreatic cancer.
Smithson et al., 2022[357]	Inhibition of DNA-PK may improve response to neoadjuvant chemoradiotherapy in rectal cancer	Rectal Cancer	The addition of peposertib to the standard of care treatment improved the clinical response rate of murine rectal cancer models.
Gordhandas et al., 2022[358]	Pre-clinical activity of the oral DNA-PK inhibitor, peposertib (M3814), combined with radiation in xenograft models of cervical cancer	Cervical Cancer	Peposertib significantly increased the irradiation response of HPV-associated cervical cancer xenograft models.
Carr et al., 2022[359]	DNA-PK Inhibitor Peposertib Amplifies Radiation-Induced Inflammatory Micronucleation and Enhances TGFβ/PD-L1 Targeted Cancer Immunotherapy	Locally advanced solid tumors	Inhibition of radiation-induced DNA damage repair with peposertib both increased cancer cell toxicity and modulated the immune system to increase tumoral response to bifunctional TGFβ "trap"/anti-PD-L1 cancer immunotherapy.
Wang et al., 2021[347]	DNA-PK inhibition by M3814 enhances chemosensitivity in non-small cell lung cancer	Non-small cell lung cancer	Peposertib increased the chemosensitivity of NSCLC models and induced P53-dependent accelerated senescence when administered in combination with paclitaxel/etoposide.

Haines et al., 2021[360]	DNA-PK inhibitor peposertib enhances p53-dependent cytotoxicity of DNA double-strand break inducing therapy in acute leukemia	Leukemia	Peposertib-mediated inhibition of DNA-PK sensitized P53-wild type Leukaemia models to DNA-damaging agents by inducing apoptosis. This effect was not seen in P53-mutated models.
Zenke et al., 2020[361]	Pharmacologic Inhibitor of DNA-PK, M3814, Potentiates Radiotherapy and Regresses Human Tumors in Mouse Models	Multiple cancer models	Treatment with peposertib sensitizes cancer cell lines and xenograft tumours to radiation in vitro and in vivo, respectively.
Sun et al., 2019[362]	Therapeutic Implications of p53 Status on Cancer Cell Fate Following Exposure to Ionizing Radiation and the DNA-PK Inhibitor M3814	Multiple cancer models	The action of peposertib is dependent on P53 activity; as such, P53 activity may be a biomarker for response to DNA-PK inhibition.
Klein et al., 2017[363]	Overcoming hypoxia-induced tumor radioresistance in non-small cell lung cancer by targeting DNA-dependent protein kinase in combination with carbon ion irradiation	Non-small cell lung cancer	Inhibition of DNA-PK preferentially sensitizes hypoxic cells to irradiation.
Notes: Peposertib may also be known by the names MSC2490484A, M3814, or Nedisertib			

TABLE 3 CLINICAL TRIALS INVESTIGATING PEPOSERTIB IN COMBINATION WITH RADIOTHERAPY TO TREAT CANCER UP TO MAY, 2023

ClinicalTrials.gov Identifier	Phase	Combined Therapies	Targeted cancer	Year	Status	Notes
NCT02516813	I	Fractionated Radiotherapy, Cisplatin	Advanced Solid Tumours	2015-2022	Completed	-
NCT04068194	I/II	Radiotherapy, Avelumab	Advanced/Metastatic Solid Tumors and Hepatobiliary Malignancies	2019-Present	Recruiting	-
NCT04533750	I	Radiotherapy	Advanced Head and Neck Cancer	2018-2022	Suspended	Suspended as met accrual for Dose Level -1
NCT03770689	I	Radiotherapy, Capecitabine	Rectal Cancer	2018-2022	Completed	-
NCT04555577	I	Radiotherapy, Temozolomide	Newly Diagnosed MGMT Unmethylated Glioblastoma or Gliosarcoma	2020-2022	Recruiting	-
NCT04750954	I	Radiation-Based Treatment (Lutetium Lu 177 Dotatate)	Neuroendocrine tumors	2021-2022	Recruiting	-
NCT04172532	I/II	Radiotherapy	Localized pancreatic cancer	2019-2022	Suspended	

Notes: Peposertib may also be known by the names MSC2490484A, M3814, or Nedisertib

5. Aims and Summary of the Current Work

Despite the comparatively good prognosis of medulloblastoma with current treatment regimens, cases of recurrent and refractory medulloblastoma remain an important cause of pediatric mortality worldwide, accounting for ~10% of cancer-related deaths in children. Although significant research has been conducted to optimize medulloblastoma treatment strategies, approximately 30% of patients relapse[117], with 90% of these succumbing to disease[117,118]. This outlook is particularly bleak for patients with group 3 medulloblastoma (MB), with these patients showing the shortest time to relapse, and a high rate of distant relapse[117].

The abysmal prognosis of relapsed medulloblastoma patients is due primarily to the lack of treatment options, with most patients treated only palliatively to maintain quality of life to the greatest extent possible[80]. While re-resection has been associated with a longer survival time, it is not curative, and is not commonly performed[117]. Furthermore, re-irradiation is almost universally avoided due to the unacceptable toxicity[113,114], as the maximum radiation dose tolerated by the CSI is 50 Gy[115], although recent research has indicated that re-irradiation may also prolong survival[364]. As such, administration of second-line chemotherapeutics is the most common treatment choice for relapsed medulloblastoma, but prognosis is again poor[110].

Overall, considering the dire prognosis and lack of effective treatment strategies for relapsed medulloblastoma, the identification of novel therapies which can be applied in the first-line treatment of primary disease remains a significant unmet need. It was this field that formed the basis of my thesis project, which focused primarily on identifying methods to improve the efficacy of radiation as a key treatment strategy for medulloblastoma. The importance of radiotherapy in the treatment of medulloblastoma has been extensively established in recent decades. However, the mechanisms by which medulloblastoma escapes radiotherapy to relapse have thus far remained relatively poorly characterized. Further, although several studies have investigated the use of chemotherapeutics (specifically carboplatin[145,146]) as radiosensitisers in group 3 MB, as yet, there have been no clinical trials assessing targeted drugs as potential radiosensitizers to improve the efficacy of therapy in MB.

The overarching aim of my project was to improve the efficacy of radiotherapy in group 3 medulloblastoma, this was achieved through two primary strategies: 1. A targeted approach testing different components of the DNA damage repair pathway which can effectively

radiosensitize G3 MB; and 2. An unbiased approach to identify the mechanisms underlying relapse in G3 MB, analysis of which could identify potential novel therapeutic targets.

In this thesis, these aforementioned strategies have been separated into distinct chapters, which can be summarized as follows:

1. **Results Chapter 1 (article in preparation):** "The DNA-PK inhibitor peposertib as a radiosensitizer in high-risk Group 3 pediatric medulloblastoma." In this branch of the research, we identified DNA-PK as a target for radiosensitization in group 3 medulloblastoma from a screen of inhibitors of different components of the DNA damage repair pathway (ATM, ATR, DNA-PK, CHK1, CHK2, WEE1, PARP1, & RAD51). Due to its well-studied nature and the large number of clinical trials underway, we selected peposertib as the target drug for validation of this therapeutic strategy. Mechanistic analysis revealed that peposertib sensitized group 3 MB cells to irradiation in vitro, triggering apoptosis and a G2/M arrest caused by increased DNA damage due to decreased activation of the NHEJ pathway. We further validated peposertib as an effective radiosensitizer in vivo, finding that it prolonged survival in a number of tumour-bearing mouse models when combined with irradiation compared to fractionated irradiation alone. Finally, using long-term, non-tumour bearing pediatric models, we assessed the toxicity of the peposertib and irradiation combination, finding an acceptable toxicity profile. Overall, this work begins to validate peposertib as a potential novel therapeutic which could be used in combination with irradiation to improve the efficacy of radiotherapy and thereby reduce the rates of recurrence in group 3 medulloblastoma.
2. **Results Chapter 2**: "Modelling Relapse after Radiotherapy in Group 3 Medulloblastoma." In this chapter, I used a variety of in vitro and in vivo models to replicate the conditions of medulloblastoma relapse following irradiation. Herein, we performed a combination of bulk RNAseq, single cell RNAseq and phosphoarray in vivo, as well as CRISPR Cas9 screening in vitro, in an attempt to understand the mechanisms by which group 3 MB escapes irradiation to form relapse. Unfortunately, this work remains unfinished. Once completed, this project should allow an improved understanding of the tumour biology of relapsed MB, and should identify the pathways by which group 3 MB forms relapse. This work would have two primary applications: Firstly, we aimed to gain a better understanding of the pathways by which group 3 MB escapes radiotherapy and forms relapse. Secondly, we aimed to achieve an improved

understanding of the biology of relapsed tumours compared with primary tumours (the knowledge of which remains relatively limited due to the lack of biopsy at relapse). Together, this could help to identify more therapeutic strategies to prolong survival in patients with relapsed tumours.

6. Results Chapter 1:

The DNA-PK inhibitor peposertib as a radiosensitizer in high-risk Group 3 pediatric medulloblastoma [Article in Preparation]

Contribution Statement:

The work conducted throughout this paper was conducted by me, with the aid of several collaborators, as follows:

- Behavioural testing was performed by Charlotte Lamirault, under the direction of Frédéric Pouzolet (Institut Curie, Université PSL, Département de Recherche Translationnelle, CurieCoreTech-Experimental Radiotherapy (RadeXp), Paris, France).
- Analyses of neural stem cells were performed by Alexandra Chicheportiche, under the direction of François D. Boussin (Université Paris Cité, Inserm, CEA, Stabilité Génétique Cellules Souches et Radiations, LRP/iRCM/IBFJ, F-92265, Fontenay-aux-Roses, France).
- Analysis of blood parameters on the Sysmex analyser were performed by L'école nationale vétérinaire d'Alfort.
- Mass spectrometry analysis of peposertib concentrations was performed by Merck KgaA, under the direction of Joachim Albers (Research Unit Oncology, the healthcare business of Merck KGaA, Darmstadt, Germany).

All in vitro analyses (survival analyses, cell cycle analyses, apoptosis analyses, western blotting, immunofluorescence) were performed by me. In vivo analyses (mouse grafting, management, treatment, bioluminescent imaging, sacrifice, dissection, and preparation of blood/tissue samples for analysis) were performed by me, with the assistance of other members of the lab (Magalie Larcher, Celine Roulle, and Sara Chabi, CRCN, INSERM in the lab), as required.

The DNA-PK inhibitor peposertib as a radiosensitizer in high-risk Group 3 pediatric medulloblastoma.

Eleanor Hawkins[1-6], Sabine Druillennec[1-6], Magalie Larcher[1-6], Celine Roulle[1-6], Laurence Mery[1-6], Alexandra Chicheportiche[7], Charlotte Lamirault[8], Alain Eychene[1-6], Frédéric Pouzoulet[8], Joachim Albers[9], François D. Boussin[7], Celio Pouponnot[1-6].

[1]Department of Signaling, Radiobiology and Cancer, Institut Curie, Orsay, France

[2]INSERM U1021, Centre Universitaire, Orsay, France

[3]CNRS UMR 3347, Centre Universitaire, Orsay, France

[4]Université Paris-Saclay, Orsay, France

[5]PSL Research University, Paris, France

[6]Equipe Labellisée Ligue Contre le Cancer

[7]Université Paris Cité, Inserm, CEA, Stabilité Génétique Cellules Souches et Radiations, LRP/iRCM/IBFJ, F-92265, Fontenay-aux-Roses, France.

[8]Institut Curie, Université PSL, Département de Recherche Translationnelle, CurieCoreTech-Experimental Radiotherapy (RadeXp), Paris, France

[9]Research Unit Oncology, the healthcare business of Merck KGaA, Darmstadt, Germany.

Disclosures: This study was supported by Merck (CrossRef Funder ID: 10.13039/100009945), who provided peposertib and the vehicle for in vivo experimentation. Merck reviewed this manuscript for medical accuracy only before submission. The authors are fully responsible for the content of this manuscript, and the views and opinions described in the publication reflect solely those of the authors. We thank Felix Neumann, Stefan Leicht, and Julia Doerr, all employees of Merck KGaA Darmstadt, Germany, for support with peposertib PK analysis.

Abstract

Medulloblastoma, the most common pediatric brain tumor, is treated with a multimodal treatment regimen of surgical resection, radiotherapy, and chemotherapy. However, relapse, which is almost invariably fatal, occurs in ~30% of patients, and is a particular problem in the high-risk, MYC-driven group 3 subset of medulloblastomas (G3 MB). As such, new therapies are needed to increase initial treatment efficacy. Herein, we provide significant *in vitro* and *in vivo* evidence to support the use of the selective DNA-PK inhibitor peposertib as a radiosensitizer in G3 MB. DNA-PK was identified as a target for radiosensitization in a targeted screen of different components of DNA damage repair pathways. This radiosenizitisation effect was subsequently validated in vitro and in vivo with sh-knockdown models. Peposertib was subsequently chosen as a model drug due to its high selectivity and potency. *In vitro*, peposertib treatment increased DNA damage accumulation due to a decrease in non-homologous end joining repair compared to irradiation alone. In vivo, peposertib treatment combined with irradiation prolonged survival in orthotopically-grafted mouse models of G3 MB. Toxicity analyses in murine pediatric models revealed a slight acute effect on immune cell populations, which resolved over time. Analyses of neural stem cell populations revealed a decrease in cell populations in mice treated with peposertib and irradiation compared to those treated with irradiation alone; however, these mice showed no difference on behavioral testing, indicating a minimal influence of this decrease. Overall, these results show peposertib as an effective radiosensitizer with good tolerability in G3 MB.

1. INTRODUCTION

Medulloblastoma (MB) is the most common malignant brain tumor in children, accounting for nearly 20% of all pediatric tumors globally[1]. MB arises in the cerebellum, but high heterogeneity is observed between patients. In recent years, advances in tumour profiling and OMICS technology have allowed the classification of these tumours into distinct groups: sonic hedgehog (SHH), WNT, group 3, and group 4[2]. Due to their similarity and shared lack of a specific driver pathway, the latter two are sometimes grouped together under the umbrella term non-WNT/non-SHH groups[3]. Patients are generally diagnosed between 6-9 years of age, although this can vary depending on the group[1]. Treatment for MB is multimodal, comprising maximal surgical resection, chemotherapy, and radiotherapy whenever possible[4,5]. This treatment regimen can achieve a five-year survival rate of approximately 70-80% across subgroups[1]. However, it is associated with significant secondary effects which severely impact patient quality of life. Furthermore, this survival rate decreases in certain patient groups deemed high risk, including those classified as group 3.

Of all the subgroups of MB, group 3 is poorly understood and has the worse prognosis, with a survival rate of only 60% after 5 years, driven by a high rate of metastasis at diagnosis (40-45%[6]), a relatively poor response to treatment, and a higher rate of relapse[1,6,7]. Unlike the WNT and SHH groups, group 3 is not associated with the deregulation of a specific pathway, although several associated signatures have been identified, including expression of a photoreceptor program[8], and MYC overexpression[9]. High MYC expression is commonly seen in cancer, and is uniformly associated with an increased abundance of many proteins related to mRNA processing, transcription, and translation, leading to replication stress[9–11]. *MYC* amplifications are found in ~15-20% of group 3 patients, and this subset of group 3 displays the worst prognosis[9,12].

Treatment for MB patients is largely uniform, comprising maximal surgical resection, followed by chemotherapy (generally comprising vincristine, cisplatin, cyclophosphamide, or lomustine), and radiotherapy[1,13]. However, radiotherapy is avoided for children under 3 years[14]. This treatment regimen can achieve a five-year survival rate of approximately 70-80%. However, it is associated with significant secondary effects which severely impact patient quality of life. Furthermore, this survival rate decreases in certain patient groups deemed high risk, including those classified as group 3. The exact treatment course varies depending on the risk classification of the patient, which is determined by the extent of surgical resection, presence of metastases, and tumour histology[15]. Treatment for standard-risk patients comprises 23.4 Gy (13 fractions of 1.8 Gy) cranio-spinal irradiation (CSI), with a boost to the primary tumour to reach 54.0 Gy, followed by chemotherapy. Clinical trials for WNT MB, which is classified as low risk, are underway to investigate dose de-escalation is CSI radiotherapy to decrease toxic effects (ClinicalTrials.gov Identifier: NCT02724579)[16]. Conversely, in high-risk groups, the CSI dose can be increased to 36 Gy[17]. Although radiotherapy has been widely proven to be an important aspect of medulloblastoma therapy, as in all cancers, its application is limited by an age-, dose-, and volume-dependent toxicity against the normal tissue surrounding the tumor. Indeed, CSI irradiation has been shown to induce significant side effects in patients who survive MB treatment, including neurocognitive impairment, endocrine disorders, and a risk of secondary cancers[18]. However, beyond the aforementioned patient risk stratification and modulation of radiotherapy dose, treatment for MB has not changed in recent decades.

In recent decades, preclinical research has focused on targeted therapeutic drugs, due to their specificity and improved toxicity profiles compared with standard chemotherapy, with some of these drugs subsequently being approved for use in the clinic[19]. As a consequence, many researchers have investigated the possibility of applying targeted therapy to increase the

efficacy of radiotherapy on cancer cells – a process termed radiosensitization. However, while many preclinical studies have identified promising radiosensitising drugs for a wide array of cancers, very few have been translated into the clinic. This trend also holds true for medulloblastoma. Significant pre-clinical research has been conducted to identify potential radiosensitising targets and drugs in MB, examples of which include the β-blockers propranolol/carvedilol/nebivolol[20]; PD0332991/palbociclib, a CDK6 inhibitor[21]; methoxyamine, an inhibitor of base excision repair[22]; DHMEQ, an inhibitor of NF-κB[23]; the PARP inhibitor veliparib[24]; and onvansertib, an inhibitor of PLK1[25], the latter two of which are in clinical trial for other cancers. However, compared with other cancers, this field remains relatively underdeveloped in the study of medulloblastoma. While many of the aforementioned studies presented promising preclinical data, the majority of the work was conducted *in vitro*, and further investigation of the efficacy and tolerability of these drugs *in vivo* is required before these drugs can progress to clinical trial as radiosensitisers in MB.

Due to the action of radiation as an inducer of DNA damage, many studies investigating potential radiosensitising drugs have focused on inhibitors of different components of the DNA damage repair pathways. DNA-dependent protein kinase (DNA-PK) is a protein complex abundantly expressed in mammalian cells which is involved in a wide variety of cellular processes. Although it plays a diverse role in a number of cellular pathways, DNA-PK primarily functions as the driver of the non-homologous end joining (NHEJ) pathway of DNA repair. NHEJ is the primary pathway by which DNA double strand breaks induced by irradiation are repaired[26]. As such, DNA-PK plays an important role in the cellular response to DNA damage inflicted by irradiation. High DNA-PK expression has also been linked to poor prognosis in a number of cancers, including non-small cell lung cancer[27], gastric cancer[28], and breast cancer[29], and several studies have associated high DNA-PK activity with radioresistance[30–32]. Together,

these results indicate the strong potential of targeting DNA-PK to induce radiosensitivity in cancers, and indeed many researchers have previously investigated this potential.

Peposertib (formerly known as M3814, or MSC2490484A) is a highly selective inhibitor of DNA-PK which is currently being investigated both clinically and preclinically as a radiosensitizer in various cancer indications. Prior investigation of this drug has shown that it is a highly specific ATP-competitive inhibitor. Although some cross-reactivity with other members of the phosphoinositide 3 kinase (PI3K) family has been observed, its potency in DNA-PK was orders of magnitude higher. Indeed, one study showed that peposertib had IC50 values of 0.6, 10,000, and 2,800 nmol/L against DNA-PK and the PI3k family members ATM and ATR, respectively[33]. Preclinical research has shown a strong radiosensitising effect of DNA-PK inhibition by peposertib in numerous cancers, including pancreatic cancer[34], rectal cancer[35], cervical cancer[36], non-small cell lung cancer[37,38], and leukemia[39]. Although not yet approved for routine clinical application, numerous clinical trials have been conducted, including one which showed good drug tolerability as a monotherapy in adult cancer patients[40]. Further, this drug is under clinical evaluation in clinical trials for the treatment of several cancers, including pancreatic cancer (NCT04172532), glioblastoma (NCT04555577), and neuroendocrine tumours (NCT04750954).

In the present study, we identified inhibition of DNA-PK as a potential method of radiosensitization in group 3 MB. Subsequently, we validated the selective inhibitor peposertib as a potential therapeutic for the clinical treatment of group 3 medulloblastoma.

2. MATERIALS AND METHODS

Cell Culture:

All cell lines used in this study were purchased from ATCC. The group 3 medulloblastoma cell lines HDMB03 and D425MED were used as the primary models, with the group 3 cell lines

D458MED and D283MED and the non-group 3 lines DAOY and ONS-76 also used in some experiments. HDMB03 and ONS-76 were cultured as a monolayer, passaged 1 in 2 or 3, three times a week in RPMI 1640 media supplemented with 10% FBS, Sodium Pyruvate (1 mM), Non-Essential Amino acids (1%), Penicillin Streptomycin (100 µg/ml) and Fungizone (2.5 µg/ml). Non-adherent D425MED and D458MED cells were passaged 1 in 3 twice a week, and cultured in suspension in Improved MEM media, supplemented with 10% FBS, Penicillin Streptomycin (100 µg/ml) and 0.5% Fungizone (2.5 µg/ml). D283MED and DAOY were cultured in MEM media supplemented with 10% FBS, Sodium Pyruvate (1mM), Non-Essential Amino acids (1%), Penicillin Streptomycin (100 µg/ml) and Fungizone (2.5 µg/ml). All cell culture reagents were purchased from Gibco (USA), unless otherwise stated.

Cells were cultured at 37 °C under a humidified atmosphere with 5% CO_2. Mycoplasma detection was performed at regular intervals.

Drug Treatment:

All compounds were solubilized in DMSO, and stored at -80°C for long-term storage and -20°C for short-term storage. The drugs used, their target, source, and working concentration are shown in Table 1.

Table 1: Drugs used in experimental analyses.

Drug Name	Cellular Target	Working Concentration	Source
Adavosertib	Wee1	10-100 nM	CliniSciences
AZD1390	ATM	100-500 nM	CliniSciences
AZD7762	Chk1/2	10-100 nM	CliniSciences
CC115	DNA-PKcs, mTOR	100-500 nM	CliniSciences
Ceralasertib	ATR	100-500 nM	CliniSciences

Niraparib	Parp1/2	100-500 nM	CliniSciences
Peposertib	DNA-PKcs	100-500 nM	Merck
RI-1	Rad51	250-1000 nM	CliniSciences
SCH900776	Chk1	10-100 nM	CliniSciences
VX984	DNA-PKcs	100-500 nM	CliniSciences

Antibodies

A variety of antibodies were used for western blot and immunofluorescence assay. Their target, working concentration, and molecular weight of the target molecule are shown in Table 2. All antibodies were purchased from Cell Signaling Technologies (USA), unless otherwise stated.

Table 2: Antibodies used in all Experiments.

Application	Target	Working Concentration	Isotype	Molecular weight (kDa)
WB	α-β Actin [Sigma-Aldrich]	1:5000	Mouse IgG	42
	α-ATM	1:1000	Rabbit IgG	350
	α-Phospho-ATM (Ser1981)	1:1000	Rabbit IgG	350
	α-ATR	1:1000	Rabbit IgG	300
	α-Phospho-ATR (Ser428)	1:1000	Rabbit IgG	300
	α-Phospho-Chk1 (Ser345)	1:1000	Rabbit IgG	56
	α-Phospho-Chk2 (Thr68)	1:1000	Rabbit IgG	62
	α-DNA-PKcs	1:1000	Rabbit IgG	450
	α-Phospho-DNA-PKcs (Ser2056)	1:1000	Rabbit IgG	450
	α-Phospho-Histone H2A.X (Ser 139)	1:1000	Rabbit IgG	15
	α-Phospho Kap1 Ser824	1:1000	Rabbit IgG	100

	α- p53	1:500	Rabbit IgG	53
	α-Phospho-p53 (Ser15)	1:1000	Mouse IgG	53
	α-Phospho-p53 (Ser20)	1:1000	Rabbit IgG	53
	α-Phospho-p21	1:500	Rabbit IgG	21
IF	α-53BP1	1:500	Rabbit IgG	
	α-Phospho-Histone γH2AX (Ser139) [Millipore]	1:200	Mouse IgG	

***In vitro* irradiation:**

Cells were irradiated at different doses using the Xrad320 X-ray irradiator (Precision X-ray, USA). For all experiments involving drug treatment, cells were treated with drugs 24 hours after seeding, 1 hour prior to irradiation. Control samples were simultaneously treated with DMSO vehicle.

Assessment of *in vitro* cell viability:

Cell viability was assessed at specific time points using the CellTiter-Glo® Luminescent Cell Viability Assay (Promega, USA), following the manufacturers instruction. Cells were seeded at densities of 10,000 cells/well (HDMB03) or 7,500 cells/well (D425MED) in 96 well plates, 24 hours prior to irradiation.

Western Blot:

For protein extraction, cells were seeded at densities of 150,000 cells/ml 24 hrs prior to irradiation. Cells were collected at different timepoints post-irradiation, and lysed.

Proteins were separated in 7.5/10/15% SDS-PAGE gels (Bio-Rad), and transferred to PVDF membranes. Membranes were blocked in 5% milk solution in phosphate buffered saline + 0.1% TWEEN-20 (PBS-T), and probed with the required primary antibody (see Table 2) overnight

at 4 °C. Membranes were washed three times in PBS-T, and then probed with the relevant horseradish peroxidase-conjugated secondary antibody, washed three times in PBS-T, and visualized by ECL (ThermoFisher, USA) on the Fusion FX Spectra system (Vilber, Germany).

Apoptosis Assay

Cellular apoptosis was determined using the phycoerythrin (PE) Active Caspase-3 Apoptosis Kit (BD Pharmingen, USA), following the manufacturer's instructions. Cells were seeded in 6 well plates (300,000 cells/well) 24 hrs prior to drug treatment/irradiation, and were collected 24/48 hours post-irradiation. Fluorescently-labelled cells were quantified on the BD LSRFortessa™ Cell Analyzer (BD Biosciences, USA), and analysis was performed using FlowJo software (V10).

Cell cycle Analysis:

Evaluation of cell cycle profiles was performed using the FITC BrdU flow kit (BD Pharmingen) following the manufacturer's instructions. Cells were seeded in 6 well plates (300,000 cells/well) 24 hrs prior to irradiation, and were collected 24/48 hours post-irradiation. BrdU and 7AAD positive cells were analyzed on the BD LSRFortessa™ Cell Analyzer (BD Biosciences), and analysis was performed using FlowJo software (V10).

Generation of shKnockdown cell lines

All shRNAs (SMARTvector Lentiviral shRNA) were purchased from Horizon Discovery. The shRNAs used in this study are as follows: shCtrl, SHC002; shDNA-PK#1, TRCN0000194985; shDNA-PK#2, TRCN0000195491. All were inserted into the lentiviral pLKO vector for infection.

Construction of Lentiviruses expressing shRNAs

Lentiviral pLKO vectors encoding shRNAs were prepared by co-transfecting HEK 293T cells with the pLKO vector and the packaging vectors pMD2/VSVG (gag/pol) and psPAX2 (env). The lipofectamine 2000 (Invitrogen) reagent was used for transfection, following the manufacturer's instructions. Supernatants were collected 36/48/60 hours after transfection, pooled, and filtered.

Infection of cells to stably express shRNAs

Cells were plated at low confluency in T25 flasks in 5 ml media. The next morning, 1 ml of virus supernatant was added to the culture. After 48 hours, cells were passaged in complete media containing 1 μg/ml puromycin for selection. After 2 days, the media was changed and cells were harvested for lysis and protein collection. Western blotting was performed to confirm knockdown.

Immunofluorescence

Cells were seeded on Millicell® EZ SLIDES (Merck) coated with 100 μg/ml poly-lysine, at densities of 20,000 cells/well, and incubated overnight. Cells were fixed at different timepoints post-irradiation in 4% PFA in water for 15 minutes, and permeabilized with 0.5% Triton X-100 for 10 minutes. Slides were blocked in 2% BSA for 1h, then incubated in the primary antibody (Table 2) for 1 h, followed by washing and incubation in the relevant Alexa-488 conjugated secondary antibody for 30 mins, all at room temperature. Slides were mounted in Fluoroshield mounting media with DAPI (Abcam, UK). Slides were visualized with the SP5 confocal laser scanning microscope (Leica, Germany), and foci were counted with the Mic-Mac pipeline in ImageJ (Java Ver 8).

Preparation of cells for Grafting *in vivo*:

Modified HDMB03 and D425MED cell lines stably expressing a GFP-Luciferase construct, and dissociated patient derived xenograft (PDX) cells infected with a GFP-Luciferase construct,

were used for all *in vivo* experiments to allow monitoring of tumor growth. Cells were cultured until the day of injection, at which point they were collected, washed and suspended in ice-cold PBS at a concentration of 20 million cells/ml (cell lines) or 60 million cells/ml (PDX).

Culture and dissociation of PDX models:

PDXs were maintained by serial passage in the fat pad of NMRI nude mice. This allowed the growth and maintenance of large tumours which could later be dissociated for orthotopic injection.

For culture *in vitro*, PDX tumours were dissected from the fat pad and necrotic tissue was removed. Tumours were dissociated in an enzymatic dissociation buffer, and cultured in a bespoke media in low adhesion flasks (Sigma-Aldrich), as previously described[8]. PDX1 and PDX2 in the current manuscript correspond to ICN-MB-PDX-3 and ICN-MB-PDX-7 in the literature, respectively[8].

PDX models were dissociated 3 to 4 days before grafting; 48 hours before grafting, ~40 million cells were infected with a VSV-G lentivirus carrying the pMIGR GFP-Luc construct, to allow monitoring of tumors grown *in vivo*. These cells were cultured without passaging until the day of injection, at which point they were collected, the virus was washed, and cells were suspended in ice-cold PBS at a concentration of 60 million cells/ml.

Animal experimentation:

All tumor-bearing experiments were performed in 7-8 week old female NMRI-nude immunodeficient mice after a 1 or 2-week acclimation period; for these experiments, six-week-old mice were obtained from Janvier Laboratory. All experiments to assess tolerability in a pediatric setting were performed in male Rj:Orl Swiss mice; mice were obtained at 10 days old from Janvier Laboratory, and experiments were initiated at postnatal day (P) 14, after a 4 day acclimation period. Pups were weaned at P21. All mice were housed in social groups at a

controlled temperature of 20-24 °C, with food and water provided *ad libitum.* Animal care and use for this study were performed in accordance with the European and the French National Regulation for the Protection of Vertebrate Animals used for Experimental and other Scientific Purposes (Directive 2010/63; French Decree 2013-118).

Orthotopic transplantation:

Mice were anaesthetized with continuous administration of 2.5-3% isoflurane. The head was then fixed using ear bars in stereotaxic frame (Kopf Instruments), and bupivacaine local anaesthesia was administered to the skull region. The scalp was disinfected with betadine, and a small incision was made into the scalp to reveal the skull. The skull was punctured 2 mm lateral and 2 mm anterior to the lambda using a 25G needle. Cells ($1x10^5$ cultured cells or $3x10^5$ dissociated PDX cells in 5 µl PBS) were then injected at a depth of 2.5 mm into the right cerebellum, at an injection rate of 1 µl/min using Hamilton syringe and an injection system. Mice were removed from the apparatus, the incision was sutured, and buprenorphine was provided as an analgesic. Mice were monitored for any signs of distress.

Bioluminescent assay:

Tumor growth was monitored by Bioluminescent assay. Mice were administered 50 mg/kg D-Luciferin (Caliper Life Sciences) by intraperitoneal injection, and anaesthetized with 2.5% isoflurane. Fifteen minutes after injection, bioluminescence was measured on the Xenogen Ivis Spectrum Imaging System (Perkin-Elmer), and Living Image software (Perkin-Elmer) was used to quantify the bioluminescent signal.

Sacrifice:

Mice were sacrificed by cervical dislocation when they began to show signs of distress (loss of 20% of body weight, difficulty walking, etc.), or at pre-determined experimental timepoints.

Irradiation:

Irradiation targeted only to the brain was administered using the Small Animal Radiation Research Platform (SARRP) irradiator (Xstrahl). Three doses of 3 Gy were administered, with 24 hours between each dose

Peposertib treatment

Peposertib was suspended in a vehicle comprising 0.5% Methocel / 0.25% Tween-20 in 300 mM Na-Citrate pH 2.5. The drug was administered via oral gavage at doses of 75 or 125 mg/kg, in 200 µl volume for adult mice, and 100 µl volume for pup mice. Control mice were treated with a corresponding volume of the vehicle, following the same schedule. Peposertib and the vehicle for *in vivo* experimentation were provided by Merck.

In Vivo Tumor Spatial Distribution Studies of Peposertib

NMRI Nude mice grafted with GFP+ D425MED tumours as previously described were used as the model for peposertib pharmacokinetic analysis, performed 16 days after grafting. Mice were treated with 125 mg/kg peposertib, and sample collections were performed at 1, 2, 4, and 8 hours after treatment in irradiated (3 Gy, 45 min after treatment) and non-irradiated mice. In brief, 200 µl of blood was collected from the orbital sinus in EDTA-soaked capillary tubes (Fisher Scientific) and transferred to EDTA K2 microvette tubes (Sarstedt) for short-term storage. Blood samples were stored for 1-2 hours at room temperature before centrifugation (10 min 500g) to collect plasma. Immediately after blood collection, mice were sacrificed by cervical dislocation and the brain was dissected. Tumour tissue was separated from the healthy cerebellum by macrodissection for GFP signal under a Stereo Microscope Fluorescence Adapter (Nightsea, USA). For each mouse, 20-50 mg of tumour and healthy cerebellum were separately collected and flash frozen. Serum and tissue samples were stored at -20 °C and -80

°C until processing, respectively. Pharmacokinetic analysis was performed by liquid chromatography with tandem mass spectrometry (LC-MS-MS), as previously described[41].

Assessment of drug tolerability in pup mice:

The tolerability of the drug peposertib was assessed in male Rj:Orl pup mice. Drugs were administered (5 doses of 125 mg/kg) and irradiation (3 doses of 3 Gy) was performed as described above, starting at P14.

Blood testing

Systemic tolerability was assessed by measurement of blood parameters. In brief, 40 µl of blood was collected from the orbital sinus of pup mice (age 20 and 34 days) in EDTA-soaked capillary tubes (Fisher Scientific) and transferred to EDTA K2 microvette tubes (Sarstedt) for short-term storage. Samples were diluted 1:5 in CELLPACK buffer (Sysmex Corporation, Kobe, Japan) for analysis on the Sysmex XT-2000iV machine and associated software (Sysmex Corporation, Kobe, Japan). All blood analyses were conducted by the École nationale vétérinaire d'Alfort (the National veterinary school of Alfort), following a previously outlined protocol[42].

Behavioral testing

The Open Field and Morris Water Maze test were performed following standard protocols in mice at the age of 5.5-6 months (~5-5.5 months after irradiation/treatment). All behavioral tests were conducted by the RadExp platform at the Curie Institute, following standard protocols[43,44].

Analysis of subventricular zone cell populations

FACS analysis to assess cell populations in the subventricular zone (SVZ) was conducted according to previously published protocols[45] in mice at the age of 6 months (~5.5 months after irradiation/treatment). All analyses were conducted by the Boussin team at the Institut de biologie François Jacob. In brief, the lateral ventricle walls of mouse brains (containing SVZ

cells) were microdissected and the tissue was enzymatically dissociated. Dissociated cells were then labelled with antibodies against LeX (a stem/progenitor marker), CD24 (a marker of neuroblasts), and EGFR (a marker of proliferation). Please refer to the figure in the Annex for an overview of the gating strategy and identification of cell populations.

Statistical analysis

All statistical analyses were conducted using GraphPad Prism (Ver 10), except for analyses of publicly available patient datasets (R2), which were performed using R software (Ver 4.0.3). Statistical differences in data extracted from R2 were analyzed using the Wilcoxon test. For survival curves, P-values were calculated using the log-rank (Mantel-cox) test. All other normally-distributed variables were analyzed using a one-way or two-way ANOVA. Non-normally distributed variables were assessed using a Kruskal Wallis test. P-values ≤ 0.05 were considered statistically significant.

3. RESULTS

3.1 A screen of inhibitors of the DNA damage repair pathways reveals DNA-PK as a promising target for radiosensitization in group 3 MB.

To identify potential targets for irradiation, we performed a targeted screen of drugs targeting different components of the DNA damage signaling pathways, including the DNA damage sensors ATM (AZD1390), ATR (ceralasertib), DNA-PK (AZD7648), and PARP1 (niraparib); the downstream kinases CHK1 (SCH900776), CHK2 (AZD7768), and WEE1 (adavosertib); and the repair protein RAD51 (RI-1). Cells were treated with these inhibitors at a range of concentrations either with (red) or without (green) 6 Gy irradiation (IR). A dose of 6 Gy of irradiation was chosen as this was found to have a strong effect without inducing total cell death in all of the cell lines under investigation (Supp Fig 1A). Cell viability was assessed at 5 days (dashed lines) post-IR (6 Gy) in four group 3 (HDMB03, D425MED, D458MED, and

D283MED, Fig 1) and two non-group 3 MB cell lines (DAOY and ONS76, Supp Fig 1B). No major effect was observed following treatment with ATM, PARP1, and RAD51 inhibitors with (red lines) or without (green lines) IR. Inhibition of CHK1/2, WEE1, and ATR all induced a notable decrease in cell viability, both with and without irradiation, at both of the assessed timepoints. These results are in line with prior studies which have shown that WEE1[46] and CHK1[47] are both promising targets for treatment of MYC-driven MB independent of IR. Most notably, treatment with the DNA-PK inhibitor AZD7648 alone had minimal effect (green lines). However, when combined with 6 Gy of irradiation (red lines), inhibition of DNA-PK induced a strong, dose-dependent decrease in cell viability. Thus, this screen indicated DNA-PK as a strong target for radiosensitization in group 3 MB. The same assay in non-group 3 cell lines showed a relatively weaker effect of DNA-PK inhibition (Supp Fig 1B), indicating a higher sensitivity of the group 3 MB cell lines to DNA-PK inhibition.

To confirm this result, we further investigated the radiosensitization effect of other non-structurally related pharmacologic inhibitors of DNA-PK in the cell lines HDMB03 and D425MED (Fig 2A), which were chosen as representative radiation sensitive and resistant models, respectively (Supp Fig 1A). This analysis validated our initial findings: when treated with the selective DNA-PK inhibitors VX984 and peposertib, both cell lines showed a similar phenotype, with almost no change in cell viability under control conditions (green lines), but a strong radiosensitization effect (red lines). Conversely, the drug CC115 (a dual inhibitor of DNA-PK and mTOR) induced a strong decrease in cell viability without irradiation, in addition to a radiosensitising effect, likely due to the known dependency of group 3 MB on mTOR[48].

Analysis of previously published/public patient datasets[49] (GEO accession number: GSE85218) revealed a high expression of *PRKDC* (the gene encoding the catalytic subunit of the DNA-PK) and *MYC* in the group 3 and WNT MB groups (Fig 2B). Interestingly, the expression of *PRKDC* was highest in the group 3γ subtype, which is characterized by *MYC* amplification

(resulting in the highest MYC expression, Fig 2C) and is of particular poor prognosis. A strong correlation (R=0.725) was also identified between the expression of *MYC* and *PRKDC* in group 3 MB (Fig 2D). Together, these results validate DNA-PK as a promising target for radiosensitization in group 3 MB. This association between the expression of *PRKDC* (encoding the catalytic subunit of DNAPK) and *MYC* highlights the radiosensitization potential of group 3 cells by DNA-PK inhibition.

3.2 shKnockdown of DNA-PK sensitizes group 3 MB models to irradiation *in vitro* and *in vivo*.

To definitively validate the radiosentization potential of DNA-PK inhibition, we genetically knocked-down DNA-PKcs expression using shRNA. We identified two shRNAs (sh#1 and sh#2) which could effectively reduce DNA-PKcs expression in the group 3 cell lines HDMB03 and D425MED (Fig 3A). We evaluated the effects of this knockdown (KD) together with irradiation on cell viability. Overall, we found that shRNA-mediated knockdown of DNA-PKcs (shDNA-PK) increased sensitivity to irradiation (Fig 3B) by increasing apoptosis (Fig 3C) in both cell lines *in vitro*. Importantly, we further validated these results *in vivo* in both cell lines. Mice were orthopically grafted into the cerebellum with control (shCtrl) or DNA-PK-KD (sh#1 and sh#2) cells expressing the luciferase gene. Mice were left untreated or were irradiated with 3 doses of a daily fraction of 3 Gy (3x3 Gy) over 3 consecutive days, once the tumors had reached the exponential growth phase (day 16 and 14 after grafting in HDMB03 and D425MED, respectively). Although this dose scheduling does not fully recapitulate the patient schedule (13 or 20 fractions of 1.8Gy), the 3x3 Gy procedure was chosen as it was validated in pilot experiments as an experimentally plausible fractionated regimen which could achieve a transient therapeutic benefit in all of the tumour models selected (data not shown). Tumor growth was monitored by bioluminescence (Fig 3D) and mouse survival was assessed by Kaplan Meier analysis (Fig 3E). Overall, we found that knockdown of DNA-PK increased the

radiosensitivity of orthotopically grafted D425MED and HDMB03 cerebellar tumors, resulting in a significant survival benefit compared to irradiated shCtrl tumors. Conversely, shDNA-PK induced minimal differences without irradiation (Fig 3D,E). Together, these results validate that inhibition of DNA-PK radiosensitizes group 3 MB.

3.3 The selective DNA-PK inhibitor peposertib is a strong radiosensitizer in group 3 MB, promoting apoptosis and inducing a strong G2/M arrest.

Peposertib is a promising and well-studied inhibitor of DNA-PK currently under clinical and preclinical investigation in a variety of cancers[34–39]. We therefore investigated this drug for further validation as a potential radiosensitization treatment for group 3 MB. Western blotting showed that treatment with peposertib significantly abrogated the increase in DNA-PK activation induced by irradiation both in HDMB03 and D425MED, as monitored by autophosphorylation on the Ser2056 residue (Fig 4A). Furthermore, treatment with peposertib synergized with irradiation to decrease cell viability (Fig 4B). FACS analysis for cleaved caspase 3 showed that peposertib treatment alone had little effect on apoptosis, but induced a significant increase in apoptosis in both cell lines when combined with irradiation (Fig 4C). Further, cell cycle analysis revealed a strong increase in G2/M arrest concomitant to a decrease in S Phase at 48 hours following combined treatment with irradiation and peposertib (Fig 5A).

Western blotting of extracts collected from cells treated with peposertib or vehicle following 6 Gy of irradiation (Fig 5B) confirmed the decrease in DNA-PK activity in cells treated with peposertib, with no apparent compensation by ATR or ATM in the immediate response to irradiation.

3.4 Peposertib inhibits IR-induced NHEJ and increases DNA damage.

To understand the mechanism by which peposertib radiosensitizes group 3 cells, we performed foci formation analysis for γH2AX (a marker of DNA double strand breaks) and 53BP1 (a

marker of NHEJ) at 0, 0.5, 1, 2, 6, 18, and 24h hours post-irradiation by immunofluorescence. This analysis revealed that peposertib treatment induced an increase in γH2AX foci in irradiated cells at short timepoints (0.5 to 6 hours), as well as at 24 hours post irradiation, indicating a significant increase in DNA damage (Fig 6A). In contrast, 53BP1 foci analysis revealed a decrease in foci number with peposertib treatment at short timepoints post-irradiation, likely indicating a decrease in activity of the NHEJ repair pathway (Fig 6B), which could explain the aforementioned increase in unrepaired sites of DNA damage.

3.5 Peposertib is an effective radiosensitizer in *in vivo* orthotopic grafted models of group 3 MB

To further assess the potential of Peposertib as a treatment for group 3 MB, we assessed the radiosensitizing effect of this drug *in vivo* in different orthotopic grafted models in NMRI nude mice. In this model, group 3 cells expressing luciferase were grafted and allowed to grow until they reached the beginning of the exponential growth phase, as assessed by bioluminescence. At this stage (14 days for D425MED, 17 days for HDMB03, 18 days for PDX1, and 28 days for PDX2), mice were irradiated with a total of 9 Gy, comprising 1 daily dose of 3 Gy administered over 3 consecutive days (3x3Gy). Irradiation was targeted to the brain, sparing the olfactory bulb and throat, using the SARRP platform. Peposertib (75 or 125 mg/kg in 200 µl vehicle) or an equivalent volume of vehicle was administered via oral gavage 40-45 minutes before irradiation on the three irradiation days, and for the two additional days after the last irradiation fraction (5 daily doses total, Fig 7A). Control mice were administered 5 doses of peposertib/vehicle without irradiation. As an initial experiment, we assessed the effect of peposertib treatment at two concentrations (75 or 125 mg/kg) in tumours grafted from D425MED cells. In the absence of irradiation, neither of the two doses showed any effect on tumor growth (bioluminescence signal) or mouse survival compared to vehicle treatment alone. In contrast, both showed a significant benefit when combined with irradiation (Fig 7B and Supp

Fig 2A). Although this difference did not reach statistical significance, treatment with 125 mg/kg peposertib resulted in a greater tumor shrinkage effect, and improved survival compared to 75 mg/kg (Fig 7B, Supp Fig 2A), while neither dose triggered any noticeable adverse health effects or difference in weight (Supp Fig 2A). Therefore, 125 mg/kg was used for subsequent experiments.

Subsequent analyses showed a similar survival benefit and decrease in tumor growth following treatment with peposertib combined with irradiation in mice grafted with tumors derived from the HDMB03 cell line (Fig 7C and Supp Fig 2B). Importantly, we further validated this observation using two group 3 MB PDX models. These experiments were important, as numerous studies have shown PDX models to be molecularly more similar to original human tumours, and to show greater tumoural heterogeneity. Indeed, several studies have shown this high fidelity in MB PDXs[50,51], indicating that these models better recapitulate the patient phenotype than cell-line models. We observed no decrease in weight, while a clear radiosensitization effect was observed, with a statistically significant survival benefit in PDX1 (Fig 7D, Supp Fig 2C), and a trend towards a survival benefit in PDX2 (Fig 7E, Supp Fig 2D).

We subsequently performed LC-MS-MS analysis to determine the pharmacokinetics of peposertib in mice during treatment. We assessed the concentrations of peposertib in the blood plasma, tumour tissue, and surrounding healthy cerebellum in mice treated with and without 3 Gy irradiation (Fig 8). Analysis of plasma concentrations revealed a gradual decrease in concentration from 1-8 hours after treatment, confirming the validity of the treatment regimen (Fig 8A). Further, although no statistical significance was observed due to the small sample size, the pharmacokinetic analysis nevertheless revealed higher peposertib concentrations in tumours compared to matched cerebellum samples in both irradiated and unirradiated mice, indicating increased accumulation in the tumour compared to the cerebellum (Fig 8B). No differences were observed between irradiated and non-irradiated mice. Importantly, this

increased accumulation would indicate a greater radiosensitization of the tumour compared to the surrounding normal tissue.

3.6 Peposertib is overall well-tolerated in pediatric models.

After validating peposertib as a promising treatment for group 3-MB, with no notable toxicity in tumor-bearing adult mice, we sought to assess the potential toxicity of the drug alone and in combination with irradiation on a more relevant pediatric model. Therefore, we performed several tolerability investigations in mouse pups. For these experiments, we used immunocompetent male Rj:Orl Swiss mice, treated and irradiated at 3x3 Gy, with 5 doses of 125 mg/kg starting at 14 days of age (Fig 9A). We initially assessed systemic tolerability by monitoring mouse weight during the growth phase, from day 14 (start of drug treatment/irradiation) to 5.5 months of age. Although not reaching statistical significance, this analysis revealed a slight effect of both irradiation and peposertib treatment alone and in combination on the growth of these mice (Fig 9B).

Subsequently, we analyzed blood parameters in pups treated with/without peposertib, with/without irradiation at three ages: 18 days (fifth and final day of peposertib treatment), 1 month (two weeks post-treatment), and 3.5 months. Most notably, at 18 days, we observed a significant decrease in the population of total white blood cells in mice treated with peposertib, but with no additive effect of brain-targeted irradiation (Fig 9C). This effect appears to be only transient, as this decrease was not observed at the two subsequent analyses at age 1 and 3.5 months. Specifically, neutrophils, lymphocytes, eosinophils, and monocytes all trended towards a decrease in mice treated with peposertib compared to vehicle; however, none of these differences reached statistical significance alone (Fig 9C). Mice recovered from this transient depletion by the final analysis at 3.5 months, indicating that peposertib only has a transient effect on blood cell populations. The results of other blood parameters are shown in Supplemental Fig 3, and definitions for these parameters are shown in Supplemental Table 1.

Regarding the ratios of different white blood cell types, the percentage population of lymphocytes tended to decrease, while those of neutrophils, eosinophils, and monocytes tended to increase at 18 days, with the latter showing statistical significance in irradiated mice (Supp Fig 3A, Supp Table 1). These differences had corrected by the final analysis at age 3.5 months. Peposertib treatment induced no differences in platelet parameters (Supp Fig 3B, Supp Table 1) or mature red blood cells (Supp Fig 3C, Supp Table 1). However, peposertib treatment induced a slight decrease in reticulocytes in the acute phase post-treatment, which normalized at later analyses (Supp Fig 3D, Supp Table 1). Thus, overall, only minor systemic effects were observed in pup mice treated with peposertib and/or irradiation; further, this effect was transient, with cell populations all rapidly normalizing once the treatment was stopped.

As the majority of the side effects associated with radiotherapy for MB are neurological, we further aimed to investigate the potential neurological effects of peposertib in combination with fractionated irradiation through analyses of neural stem cell populations and behavioral testing. To assess the long-term neurological toxicity of the peposertib together with the aforementioned irradiation treatment regimen, we performed FACS analysis of immune populations (Fig 10A), and different cell populations in the subventricular zone (SVZ) (Fig 10B) of mice at 6 months old. Overall, neither peposertib treatment, fractionated irradiation, or their combination resulted in any difference in the number of microglia, macrophages, or lymphocytes (Fig 10A). Regarding SVZ cell populations (Fig 10B), neither irradiation nor peposertib combined with irradiation resulted in any difference in quiescent neural stem cell populations (qNSCs). Conversely, while irradiation alone had no significant effect on the number of active neural stem cells (aNSCs), combined treatment resulted in a slight decrease in this population compared to irradiation alone. In addition, irradiation alone resulted in a decrease in the transit amplifying progenitors (TAP) and immature neuroblast (iNB) populations compared to control mice, while combined treatment tended to cause a further decrease in these populations,

although these differences did not reach statistical significance (Fig 10B). Peposertib treatment also tended to trigger an increase in mature neuroblasts (mNB) compared to irradiation alone, although again this difference was not significant. Taken together, these results indicate that peposertib together with irradiation seems to spare quiescent neural stem cells at the top of the hierarchy, but may decrease their mobilization.

We next assessed if this added toxicity of peposertib to irradiation may alter the behavior of these mice. Mice were subjected to behavioral testing involving the open field test to assess general locomotor activity, anxiety, and willingness to explore, and the Morris water maze test, to assess spatial learning and memory at six months of age. In the open field test, no significant differences were found in the total distance travelled (Fig 11A); these results indicate that the irradiation and peposertib treatment regimen induced no impairments in locomotor activity. Conversely, a trend towards a decrease in the number of center entries and the distance travelled in the center in irradiated compared to non-irradiated mice indicated an increase in anxiety-related behavior in mice who underwent 3x3 Gy irradiation. However, importantly, there was no additive effect of peposertib treatment (Fig 11A). Regarding the water maze test, although no significant differences were found between groups in terms of the total distance travelled over the 6 habituation days, irradiated mice showed a slight trend towards a longer distance travelled, potentially indicating poorer memory function (Fig 11B). However, no significant differences or trends towards differences were observed in the time or distance travelled in each of the quadrants on the final test day when the platform was removed (Fig 11B). Importantly, mice treated with the combination of peposertib and irradiation showed no difference compared with mice treated with irradiation alone in any of the tests.

Together, the results of the NSC analysis and behavioral testing importantly show that while we observed a decreased in active stem cells at the cellular level, peposertib in combination

with irradiation did not modify the behavior of the mice, suggesting that this treatment combination has acceptable toxicity.

4. DISCUSSION

Despite improvement in the prognosis of medulloblastoma patients in recent decades, certain subsets, especially MYC-driven group 3 medulloblastoma, remain more difficult to treat, with significantly worse prognosis. Relapse, driven by radio- and chemo-resistance of the original primary/metastatic tumors, remains an important concern in group 3 MB, with almost all patients who develop recurrent tumors succumbing to the disease. As such, novel treatment modalities to sensitize group 3 MB tumors to radio- and chemo-therapy will be of great significance to reduce relapse, and therefore mortality, in these patients.

Although the roles of DNA-PK in tumorigenesis have recently gained attention, only very few studies have investigated the roles of DNA-PK in MB. For example, one study showed that simultaneous inhibition of DNA-PK and telomerase exerted a cytotoxic effect in the MB cell line ONS-76[52]. Of note, in our study, we found that inhibition of DNA-PK alone combined with irradiation exerted little effect on viability in ONS-76 (Supp Fig 1B). Furthermore, another study showed that inhibition of DNA-PK with NU7441 radiosensitized the MB cell lines DAOY and D283MED[53]. This effect of DNA-PK inhibition was also observed in these cell lines in our screen (Supp Fig 1B). Further, a recent paper investigating the proteomic profiles of the different MB subgroups presented preliminary results indicating a possible association between the expression of phosphorylated MYC and phosphorylated DNA-PK, finding that inhibition of DNA-PK sensitized D458MED group MB cells, but not the non-group 3 DAOY cell line to irradiation *in vitro*[10]. This result was confirmed by the results of our initial screen (Supp Fig 1B). Although this topic remains relatively underdeveloped, the *in vitro* data in these papers suggest DNA-PK as a potential radiosensitization target in MB. In the present study, we

firmly established DNA-PK as strong target for radiosensitization in group 3 MB, and demonstrated that the DNA-PK inhibitor peposertib is of therapeutic interest with acceptable toxicity in *in vivo* models of group 3 MB.

In the present study, we identified DNA-PK as a promising target for radiosensitization in an unbiased screen of drugs targeting different components of the DNA damage repair pathways in numerous group 3 and non-group 3 cell lines. The validity of this screen was confirmed by our observation of a potent effect of WEE1 and CHK1 inhibition, even without irradiation. This confirms the results of prior studies, which have shown the efficacy of these inhibitors alone[46,47]. Further, our observation of a strong effect of ATR inhibition agrees with prior research, which has shown a strong sensitivity of MYC-driven medulloblastoma to ATR inhibition due to the high level of replication stress[54]. Although not investigated in this study, these preliminary results suggest that CHK1/2 and ATR may also be promising targets for radiosensitisation in addition to monotherapies in group 3 MB.

Interestingly, we observed a stronger effect of DNA-PK inhibition in group 3 cell lines than in non-group 3 cell lines, indicating a possible group specificity of this treatment. This difference may be due to the relatively high expression of *PRKDC* observed in group 3 (Fig 2B). Further, in line with the study by Archer et al.[10], a correlation was observed between the expression of *MYC* and *PRKDC* in group 3 tumor samples (Fig 2D). We subsequently validated DNA-PK as a target by showing that radiosensitization was observed with treatment with a panel of structurally-unrelated DNA-PK inhibitors, as well as by shKnockdown. Furthermore, at the functional level, we demonstrated that combined treatment with peposertib and irradiation increased DNA damage in both the short- and long-term response to irradiation, resulting in both an increase in apoptosis, and a significant G2/M arrest. Finally, our foci analyses indicated that the observed increase in DNA damage was due to a decrease in the activity of the NHEJ repair pathway.

As a widely-investigated DNA-PK inhibitor, we selected peposertib as the model drug to validate for potential clinical use. We used a variety of group 3 MYC-amplified medulloblastoma models orthotopically grafted into the cerebellum of nude mice to assess the efficacy of peposertib treatment in combination with irradiation. Of these, we used two cell lines, both a radiation-sensitive P53-competent (HDMB03) and a radiation-resistant P53-mutated (D425MED) model, and observed a significant survival benefit in both models. More importantly, we used two group 3-PDX models which show high homology with patient tumours, and again observed a survival benefit with peposertib combined with irradiation compared to fractionated irradiation alone. These experiments firmly established a significant survival benefit of peposertib when combined with fractionated irradiation compared to irradiation alone in many group 3 MB models. Finally, we conducted pharmacokinetic analysis to assess the uptake of peposertib into tumours and healthy cerebellar tissue of our model mice undergoing peposertib treatment. This analysis confirmed the results of a previous study[41], which showed that the concentration of peposertib in brain tumors was significantly higher than in surrounding normal brain tissue. Unfortunately, a mechanistic analysis of the processes underlying this concentration difference was outside the scope of this work. However, this prior study investigating peposertib CNS distribution showed that peposertib accumulation in the normal CNS was severely restricted by the active efflux of the drug across the blood brain barrier (BBB); however, accumulation in tumors (melanoma metastases) was possible due to disruption of the BBB[41]. It is probable that a similar mechanism would be at play in our MB model. Importantly, these results show a greater accumulation in tumour tissue, indicating that a greater radiosensitization effect would be seen in tumour than healthy tissue cells, which should help to increase the therapeutic window.

Despite these results, to determine the potential clinical utility of this treatment combination, we deeply investigated the potential toxicity of this treatment in a pediatric setting, as the

primary concern with treatments which target molecules important to normal tissue cells is the potential toxicity. Firstly, due to the diverse roles of DNA-PK in a number of cellular processes throughout the body, particularly the immune system, we investigated the potential systemic toxicity of peposertib administration, with or without targeted brain irradiation. To achieve this, we monitored the weight analyzed the blood parameters of pup mice treated with and without peposertib and fractionated irradiation to determine any potential toxicity of this combination. Overall, we observed no major toxicities, although we did note a transient decrease in several immune cell populations in mice treated with 5 doses of peposertib. This is in line with clinical trials which showed an acceptable toxicity of the drug, with only relatively minor side effects (nausea, vomiting, fatigue, pyrexia, and rash) in adult participants[40].

Furthermore, it has been well-established that even when used alone, the CNS-targeted irradiation applied in the treatment of medulloblastoma patients is known to induce significant toxicity, with the most important side effects being neurocognitive impairment, endocrine disorders, and risk of secondary cancers[18]. As such, it is important to ensure that any radiosensitizer applied in such patients would not greatly exacerbate the radiation-induced insult to the neurons. This is especially true for the targeting of DNA-PK, which has been previously shown to play a protective role in neurogenesis by activating NHEJ-mediated DNA repair in non-replicating cell populations in the neocortex[55], as well as protecting cells from apoptosis[56]. In this context, in the present study, we investigated the long-term effect of the peposertib/irradiation combination by investigating the neural stem cell populations in adult mice 6 months after peposertib treatment and irradiation starting on P14. We found an effect of irradiation alone, which was slightly exacerbated by peposertib treatment, but not reaching statistical significance. The only significant difference identified between irradiated mice treated with vehicle and peposertib was a decrease in aNSCs. However, it should be noted that the lack of any difference in qNSCs (which are at the top of the stem cell hierarchy) suggests

that the total population of NSCs was not strongly affected. Notably, all irradiated mice showed a decrease in immature neuroblasts, which agrees with the results of a prior study which showed that irradiation of the SVZ resulted in a decrease in migrating neuroblasts[57]. In our analysis, mice treated with the combination of peposertib and irradiation showed a trend towards a decrease in immature neuroblasts, but an increase in mature neuroblasts, compared to mice treated with irradiation alone, suggesting a possible increase in neuroblast maturation. Furthermore, all irradiated mice showed a decrease in transit amplifying progenitors, which agrees with the general consensus that irradiation of the SVZ stem cell niche results in a decrease in proliferation of local cells[58]. This population decrease was somewhat exacerbated by peposertib treatment; however, this did not reach significance compared to irradiation alone. Despite these differences, it should be noted that none of the mice showed any developmental effects of this treatment combination. There were no cases of mortality or the development of secondary tumours, and no major difference in growth or weight between any of the groups. Importantly, and despite the aforementioned differences in SVZ stem cell populations, behavioral analysis revealed no differences in locomotor activity, spatial learning, or memory between mice treated with irradiation and peposertib compared to those treated with peposertib alone. Together, these results suggest that the same combination of 3x3 Gy irradiation with 125 mg/kg peposertib which exerted an excellent tumor control on different group 3 models including PDXs, showed a limited and acceptable neural toxicity in a pediatric model. This highlights a potential therapeutic window for this combination. However, it should be noted that the immunocompetent mouse model used for the experiments assessing tolerability was not tumour-bearing, and as such did not fully recapitulate the patient phenotype. While this situation was unavoidable, as it would be impossible to maintain tumour-bearing mice long enough to assess long-term toxicity, it remains a limitation of the model that should be considered.

Overall, the present study introduces and validates peposertib as a novel radiosensitizer in group 3 MB, which is known to be primarily MYC-driven. When considering the clinical application of radiosensitizers, it is important to consider a possible mechanism of patient stratification, to determine which patients are most likely to benefit from treatment, as the primary drawback of many targeted treatments is a lack of ability to determine which patients may benefit. Based on our preliminary results regarding the correlation between the expression of *PRKDC* and *MYC* (the primary driver of group 3 medulloblastoma), we suggest that the proposed treatment with peposertib would be effective in a large subsection of group 3 patients, due to the reliance of this tumor on MYC. Further, it may be most effective in the group 3γ subtype, which is characterized by MYC overexpression and associated with a particular poor prognosis. However, this must be clarified in further analyses.

5. CONCLUSION

Overall, the present study validates the specific DNA-PK inhibitor peposertib as an effective radiosensitizer in combination with a fractionated irradiation regimen for group 3 medulloblastoma, with acceptable toxicity in a pediatric setting. Although more work is needed before this drug can progress to clinical application, our results provide a valid basis for the delivery of peposertib as a drug for combination with radiotherapy in the treatment of high risk group 3 medulloblastoma.

REFERENCES

1. Northcott PA, Robinson GW, Kratz CP, et al. Medulloblastoma. *Nat Rev Dis Prim*. 2019;5(1). doi:10.1038/s41572-019-0063-6

2. Taylor MD, Northcott PA, Korshunov A, et al. Molecular subgroups of medulloblastoma: the current consensus. *Acta Neuropathol*. 2012;123:465-472. doi:10.1007/s00401-011-0922-z

3. Orr BA. Pathology, diagnostics, and classification of medulloblastoma. *Brain Pathol*. 2020;30(3):664-678. doi:10.1111/bpa.12837

4. PDQ_Pediatric_Treatment_Editorial_Board. Childhood Medulloblastoma and Other Central Nervous System Embryonal Tumors Treatment (PDQ®): Patient Version. In: *PDQ Cancer Information Summaries*. Bethesda (MD); 2002.

5. Franceschi E, Hofer S, Brandes AA, et al. EANO–EURACAN clinical practice guideline for diagnosis, treatment, and follow-up of post-pubertal and adult patients with medulloblastoma. *Lancet Oncol*. 2019;20(12):e715-e728. doi:10.1016/S1470-2045(19)30669-2

6. Wang J, Garancher A, Ramaswamy V, Wechsler-Reya RJ. Medulloblastoma: From Molecular Subgroups to Molecular Targeted Therapies. *Annu Rev Neurosci*. 2018;41(1):207-232. doi:10.1146/annurev-neuro-070815-013838

7. Juraschka K, Taylor MD. Medulloblastoma in the age of molecular subgroups: A review: JNSPG 75th Anniversary invited review article. *J Neurosurg Pediatr*. 2019;24(4):353-363. doi:10.3171/2019.5.PEDS18381

8. Garancher A, Lin CY, Morabito M, et al. NRL and CRX Define Photoreceptor Identity and Reveal Subgroup-Specific Dependencies in Medulloblastoma. *Cancer Cell*. 2018;33(3):435-449.e6. doi:10.1016/j.ccell.2018.02.006

9. Northcott PA, Buchhalter I, Morrissy AS, et al. The whole-genome landscape of medulloblastoma subtypes. *Nature*. 2017;547(7663):311-317. doi:10.1038/nature22973

10. Archer TC, Ehrenberger T, Mundt F, et al. Proteomics, Post-translational Modifications, and Integrative Analyses Reveal Molecular Heterogeneity within Medulloblastoma Subgroups. *Cancer Cell*. 2018;34(3):396-410.e8. doi:10.1016/j.ccell.2018.08.004

11. Roussel MF, Robinson GW. Role of MYC in Medulloblastoma. *Cold Spring Harb Perspect Med*. 2013;3(11). doi:10.1101/cshperspect.a014308

12. De Haas T, Hasselt N, Troost D, et al. Molecular risk stratification of medulloblastoma patients

based on immunohistochemical analysis of MYC, LDHB, and CCNB1 expression. *Clin Cancer Res*. 2008;14(13):4154-4160. doi:10.1158/1078-0432.CCR-07-4159

13. Ray S, Chaturvedi NK, Bhakat KK, Rizzino A, Mahapatra S. Subgroup-Specific Diagnostic, Prognostic, and Predictive Markers Influencing Pediatric Medulloblastoma Treatment. *Diagnostics (Basel, Switzerland)*. 2021;12(1). doi:10.3390/diagnostics12010061

14. Deutsch M, Thomas PRM, Krischer J, et al. Results of a prospective randomized trial comparing standard dose neuraxis irradiation (3,600 cgy/20) with reduced neuraxis irradiation (2,340 cgy/13) in patients with low-stage medulloblastoma. *Pediatr Neurosurg*. 1996;24(4):167-177. doi:10.1159/000121042

15. Gerber NU, Mynarek M, von Hoff K, Friedrich C, Resch A, Rutkowski S. Recent developments and current concepts in Medulloblastoma. *Cancer Treat Rev*. 2014;40(3):356-365. doi:10.1016/j.ctrv.2013.11.010

16. Michalski JM, Janss AJ, Vezina LG, et al. Children's Oncology Group Phase III Trial of Reduced-Dose and Reduced-Volume Radiotherapy With Chemotherapy for Newly Diagnosed Average-Risk Medulloblastoma. *J Clin Oncol*. 2021;39(24):2685-2697. doi:10.1200/JCO.20.02730

17. Ramaswamy V, Remke M, Bouffet E, et al. Risk stratification of childhood medulloblastoma in the molecular era: the current consensus. *Acta Neuropathol*. 2016;131(6):821-831. doi:10.1007/s00401-016-1569-6

18. Bernier V, Klein O. Late effects of craniospinal irradiation for medulloblastomas in paediatric patients. *Neurochirurgie*. 2021;67(1):83-86. doi:10.1016/J.NEUCHI.2018.01.006

19. Zhong L, Li Y, Xiong L, et al. Small molecules in targeted cancer therapy: advances, challenges, and future perspectives. *Signal Transduct Target Ther*. 2021;6(1). doi:10.1038/s41392-021-00572-w

20. Rossi M, Talbot J, Piris P, et al. Beta-blockers disrupt mitochondrial bioenergetics and increase

radiotherapy efficacy independently of beta-adrenergic receptors in medulloblastoma. *eBioMedicine*. 2022;82:104149. doi:https://doi.org/10.1016/j.ebiom.2022.104149

21. Whiteway SL, Harris PS, Venkataraman S, et al. Inhibition of cyclin-dependent kinase 6 suppresses cell proliferation and enhances radiation sensitivity in medulloblastoma cells. *J Neurooncol*. 2013;111(2):113-121. doi:10.1007/s11060-012-1000-7

22. Pezuk J, Valera E, Delsin L, Scrideli C, Tone L, Brassesco M. The Antiproliferative and Pro-apoptotic Effects of Methoxyamine on Pediatric Medulloblastoma Cell Lines Exposed to Ionizing Radiation and Chemotherapy. *Cent Nerv Syst Agents Med Chem*. 2015;16(1):67-72. doi:10.2174/1871524915666150817112946

23. Ramos PMM, Pezuk JA, Castro-Gamero AM, et al. Antineoplastic Effects of NF-κB Inhibition by DHMEQ (Dehydroxymethylepoxyquinomicin) Alone and in Co-treatment with Radio-and Chemotherapy in Medulloblastoma Cell Lines. *Anticancer Agents Med Chem*. 2018;18(4):541-549. doi:10.2174/1871520617666171113151335

24. Buck J, Dyer PJC, Hii H, et al. Veliparib Is an Effective Radiosensitizing Agent in a Preclinical Model of Medulloblastoma. *Front Mol Biosci*. 2021;8:1-11. doi:10.3389/fmolb.2021.633344

25. Wang D, Veo B, Pierce A, et al. A novel PLK1 inhibitor onvansertib effectively sensitizes MYC-driven medulloblastoma to radiotherapy. *Neuro Oncol*. 2022;24(3):414-426. doi:10.1093/neuonc/noab207

26. Kakarougkas A, Jeggo PA. DNA DSB repair pathway choice: an orchestrated handover mechanism. *Br J Radiol*. 2014;87(1035):20130685. doi:10.1259/bjr.20130685

27. Xing J, Wu X, Vaporciyan AA, Spitz MR, Gu J. Prognostic significance of ataxia-telangiectasia mutated, DNA-dependent protein kinase catalytic subunit, and Ku heterodimeric regulatory complex 86-kD subunit expression in patients with nonsmall cell lung cancer. *Cancer*. 2008;112(12):2756-2764. doi:10.1002/cncr.23533

28. Zhang Y, Wen G-M, Wu C-A, et al. PRKDC is a prognostic marker for poor survival in gastric

cancer patients and regulates DNA damage response. *Pathol Res Pract*. 2019;215(8):152509. doi:10.1016/j.prp.2019.152509

29. Zhang Y, Yang W-K, Wen G-M, et al. High expression of PRKDC promotes breast cancer cell growth via p38 MAPK signaling and is associated with poor survival. *Mol Genet Genomic Med*. 2019;7(11):e908. doi:10.1002/mgg3.908

30. Shimura T, Kakuda S, Ochiai Y, et al. Acquired radioresistance of human tumor cells by DNA-PK/AKT/GSK3b-mediated cyclin D1 overexpression. *Oncogene*. 2010;29:4826-4837. doi:10.1038/onc.2010.238

31. Yu Y, Liu T, Yu G, et al. PRDM15 interacts with DNA-PK-Ku complex to promote radioresistance in rectal cancer by facilitating DNA damage repair. *Cell Death Dis*. 2022;13(11). doi:10.1038/s41419-022-05402-7

32. Kienker LJ, Shin EK, Meek K. Both V(D)J recombination and radioresistance require DNA-PK kinase activity, though minimal levels suffice for V(D)J recombination. *Nucleic Acids Res*. 2000;28(14):2752-2761. doi:10.1093/nar/28.14.2752

33. Zenke FT, Zimmermann A, Sirrenberg C, et al. Pharmacologic Inhibitor of DNA-PK, M3814, Potentiates Radiotherapy and Regresses Human Tumors in Mouse Models. *Mol Cancer Ther*. 2020;19(5):1091-1101. doi:10.1158/1535-7163.MCT-19-0734

34. Wang W, McMillan MT, Zhao X, et al. DNA-PK Inhibition and Radiation Promote Antitumoral Immunity through RNA Polymerase III in Pancreatic Cancer. *Mol Cancer Res*. 2022;20(7):1137-1150. doi:10.1158/1541-7786.MCR-21-0725

35. Smithson M, Irwin RK, Williams G, et al. Inhibition of DNA-PK may improve response to neoadjuvant chemoradiotherapy in rectal cancer. *Neoplasia*. 2022;25:53-61. doi:10.1016/J.NEO.2022.01.004

36. Gordhandas SB, Manning-Geist B, Henson C, et al. Pre-clinical activity of the oral DNA-PK inhibitor, peposertib (M3814), combined with radiation in xenograft models of cervical cancer.

Sci Rep. 2022;12(1). doi:10.1038/s41598-021-04618-5

37. Wang M, Chen S, Wei Y, Wei X. DNA-PK inhibition by M3814 enhances chemosensitivity in non-small cell lung cancer. *Acta Pharm Sin B*. 2021;11(12):3935-3949. doi:10.1016/j.apsb.2021.07.029

38. Klein C, Dokic I, Mairani A, et al. Overcoming hypoxia-induced tumor radioresistance in non-small cell lung cancer by targeting DNA-dependent protein kinase in combination with carbon ion irradiation. *Radiat Oncol*. 2017;12(1). doi:10.1186/s13014-017-0939-0

39. Haines E, Nishida Y, Carr MI, et al. DNA-PK inhibitor peposertib enhances p53-dependent cytotoxicity of DNA double-strand break inducing therapy in acute leukemia. *Sci Rep*. 2021;11(1):12148. doi:10.1038/s41598-021-90500-3

40. van Bussel MTJ, Awada A, de Jonge MJA, et al. A first-in-man phase 1 study of the DNA-dependent protein kinase inhibitor peposertib (formerly M3814) in patients with advanced solid tumours. *Br J Cancer*. 2021;124(4):728-735. doi:10.1038/s41416-020-01151-6

41. Talele S, Zhang W, Oh JH, et al. Central Nervous System Delivery of the Catalytic Subunit of DNA-Dependent Protein Kinase Inhibitor Peposertib as Radiosensitizer for Brain Metastases. *J Pharmacol Exp Ther*. 2022;381(3):217-228. doi:10.1124/jpet.121.001069

42. Layssol-Lamour CJ, Sarry J-E, Braun J-PD, Trumel C, Bourgès-Abella NH. Reference Values for Hematology, Plasma Biochemistry, Bone Marrow Cytology and Bone Histology of NOD.Cg-Prkdc(scid) Il2rg(tm1Wjl)/ SzJ Immunodeficient Mice. *J Am Assoc Lab Anim Sci*. 2021;60(1):4-17. doi:10.30802/AALAS-JAALAS-20-000020

43. Vorhees C V, Williams MT. Morris water maze: procedures for assessing spatial and related forms of learning and memory. *Nat Protoc*. 2006;1(2):848-858. doi:10.1038/nprot.2006.116

44. Seibenhener ML, Wooten MC. Use of the Open Field Maze to measure locomotor and anxiety-like behavior in mice. *J Vis Exp*. 2015;(96):e52434. doi:10.3791/52434

45. Daynac M, Chicheportiche A, Pineda JR, Gauthier LR, Boussin FD, Mouthon M-A. Quiescent

neural stem cells exit dormancy upon alteration of GABAAR signaling following radiation damage. *Stem Cell Res*. 2013;11(1):516-528. doi:https://doi.org/10.1016/j.scr.2013.02.008

46. Moreira DC, Venkataraman S, Subramanian A, et al. Targeting MYC-driven replication stress in medulloblastoma with AZD1775 and gemcitabine. *J Neurooncol*. 2020;147(3):531-545. doi:10.1007/s11060-020-03457-0

47. Prince EW, Balakrishnan I, Shah M, et al. Checkpoint kinase 1 expression is an adverse prognostic marker and therapeutic target in MYC-driven medulloblastoma. *Oncotarget*. 2016;7(33):53881-53894. doi:10.18632/oncotarget.10692

48. Aldaregia J, Odriozola A, Matheu A, Garcia I. Targeting mTOR as a Therapeutic Approach in Medulloblastoma. *Int J Mol Sci*. 2018;19(7). doi:10.3390/ijms19071838

49. Cavalli FMG, Remke M, Rampasek L et al. Intertumoral Heterogeneity within Medulloblastoma Subgroups. *Cancer Cell*. 2017;31(6):737-754. doi:10.1016/j.ccell.2017.05.005

50. Sandén E, Dyberg C, Krona C, et al. Establishment and characterization of an orthotopic patient-derived Group 3 medulloblastoma model for preclinical drug evaluation OPEN. 2017. doi:10.1038/srep46366

51. Zhao X, Liu Z, Yu L, et al. Global gene expression profiling confirms the molecular fidelity of primary tumor-based orthotopic xenograft mouse models of medulloblastoma. *Neuro Oncol*. 2012;14(5):574-583. doi:10.1093/neuonc/nos061

52. Gurung RL, Lim HK, Venkatesan S, Lee PSW, Hande MP. Targeting DNA-PKcs and telomerase in brain tumour cells. *Mol Cancer*. 2014;13:232. doi:10.1186/1476-4598-13-232

53. Tanori M, Pannicelli A, Pasquali E, et al. Cancer risk from low dose radiation in Ptch1(+)(/)(-) mice with inactive DNA repair systems: Therapeutic implications for medulloblastoma. *DNA Repair (Amst)*. 2019;74:70-79. doi:10.1016/j.dnarep.2018.12.003

54. Krüger K, Geist K, Stuhldreier F, et al. Multiple DNA damage-dependent and DNA damage-

independent stress responses define the outcome of ATR/Chk1 targeting in medulloblastoma cells. *Cancer Lett*. 2018;430:34-46. doi:10.1016/j.canlet.2018.05.011

55. Enriquez-Rios V, Dumitrache LC, Downing SM, et al. DNA-PKcs, ATM, and ATR Interplay Maintains Genome Integrity during Neurogenesis. *J Neurosci*. 2017;37(4):893-905. doi:10.1523/JNEUROSCI.4213-15.2016

56. Baleriola J, Suárez T, De La Rosa EJ. DNA-PK promotes the survival of young neurons in the embryonic mouse retina. *Cell Death Differ*. 2010;17(11):1697-1706. doi:10.1038/cdd.2010.46

57. Achanta P, Capilla-Gonzalez V, Purger D, et al. Subventricular zone localized irradiation affects the generation of proliferating neural precursor cells and the migration of neuroblasts. *Stem Cells*. 2012;30(11):2548-2560. doi:10.1002/stem.1214

58. Capilla-Gonzalez V, Bonsu JM, Redmond KJ, Garcia-Verdugo JM, Quiñones-Hinojosa A. Implications of irradiating the subventricular zone stem cell niche. *Stem Cell Res*. 2016;16(2):387-396. doi:10.1016/j.scr.2016.02.031

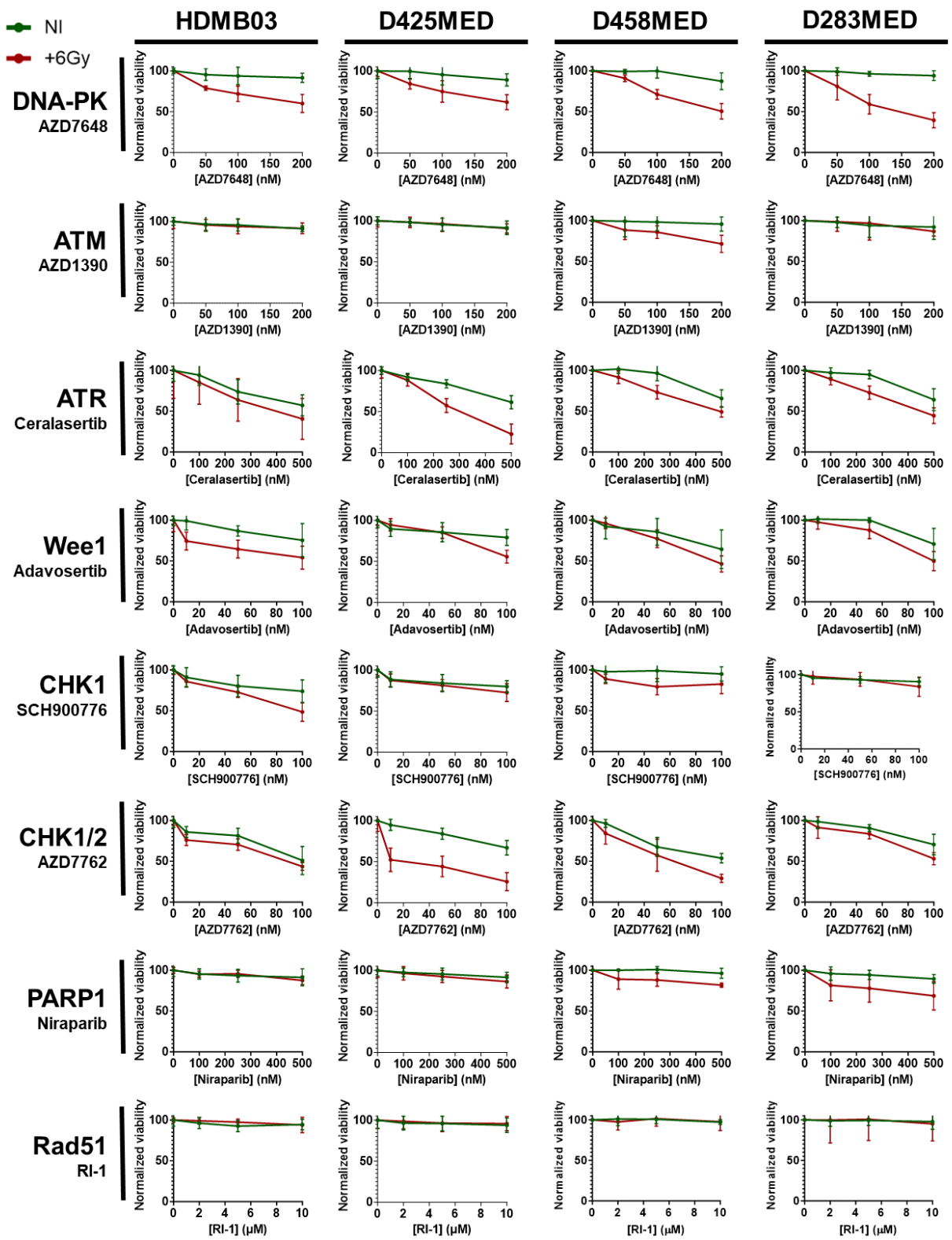

Fig 1. A screen of DNA-damage repair inhibitors reveals DNA-PK as a target for radiosensitization. A targeted screen was performed to assess the effect of drugs targeting different components of the DNA damage repair pathway on cell viability with (red lines) and without (green lines) 6 Gy of irradiation. Drugs targeting the DNA damage sensors DNA-PK (AZD7648), ATM (AZD1390), and ATR (ceralasertib); the downstream effectors WEE1 (adabosertib), CHK1 (SCH900776), CHK1/2 (AZD7762), the single-strand break repair sensor PARP1 (Niraparib), and the homologous recombination mediator RAD51 (RI-1) were tested at three concentrations. Viability was assessed using the ATP-based cell-titer glo assay 5 days post-irradiation in the group 3 medulloblastoma cell lines HDMB03, D425MED, D458MED, and D283MED. Each line is normalized to the DMSO control for the related condition, the effect of irradiation alone therefore cannot be seen. Results shown are the mean ± SEM of four biological replicates, and are representative of three experimental replicates.

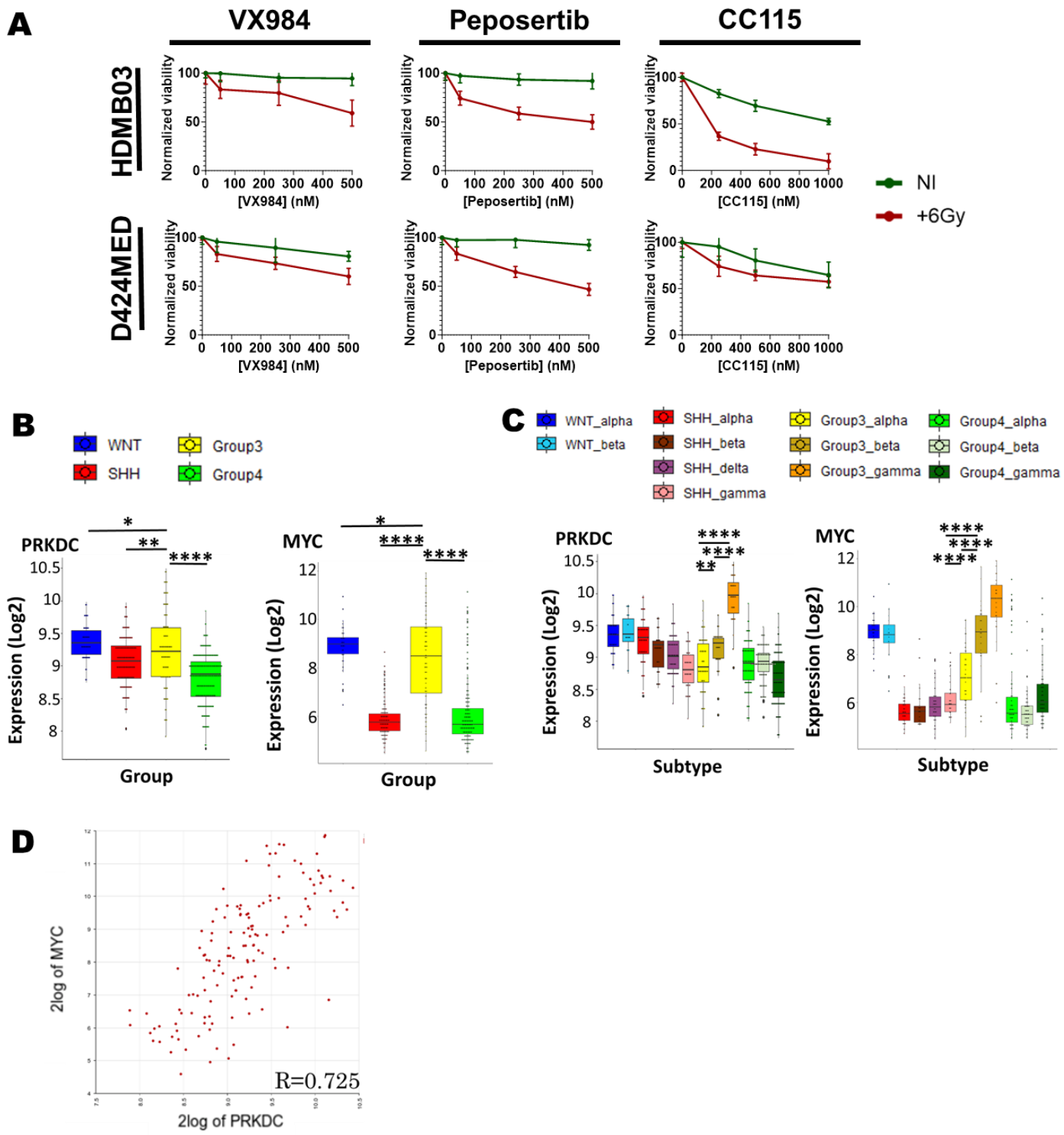

Fig 2. Validation of DNA-PK as a target for radiosensitization in Group 3 Medulloblastoma. (A) The effects of two specific DNA-PK inhibitors (VX984 and Peposertib) and a dual DNA-PK and mTOR inhibitor (CC115) on cell viability were assessed with (red lines) and without (green lines) 6 Gy of irradiation. Viability was assessed using the ATP-based cell-titer glo assay 5 days post-irradiation in the cell lines D425MED and HDMB03. Each line is normalized to the DMSO control for the related condition, the effect of irradiation alone therefore cannot be seen. Results are shown as the mean ± SEM of four biological replicates, and are representative of three experimental replicates. (B) Expression analysis of the publicly available Cavalli dataset showing the expression of *PRKDC* and *MYC* in the four medulloblastoma groups (SHH, WNT, Group 3, and Group 4). Statistical differences were analyzed using the Wilcoxon test. (C) Further analysis of *PRKDC* and *MYC* expression in different medulloblastoma subtypes (WNT α and β; SHH α, β, δ, and γ; Group 3 α, β, and γ; and Group 4 α, β, and γ). Statistical differences were analyzed using the Wilcoxon test. (D) Correlation analysis between the expressions of *MYC* and *PRKDC* across patients in the group 3 subgroup. Analysis was performed using the R2 Genomics Analysis and Visualization platform.
NI, Non-irradiated. *p<0.05; **p<0.01; ****p<0.0001

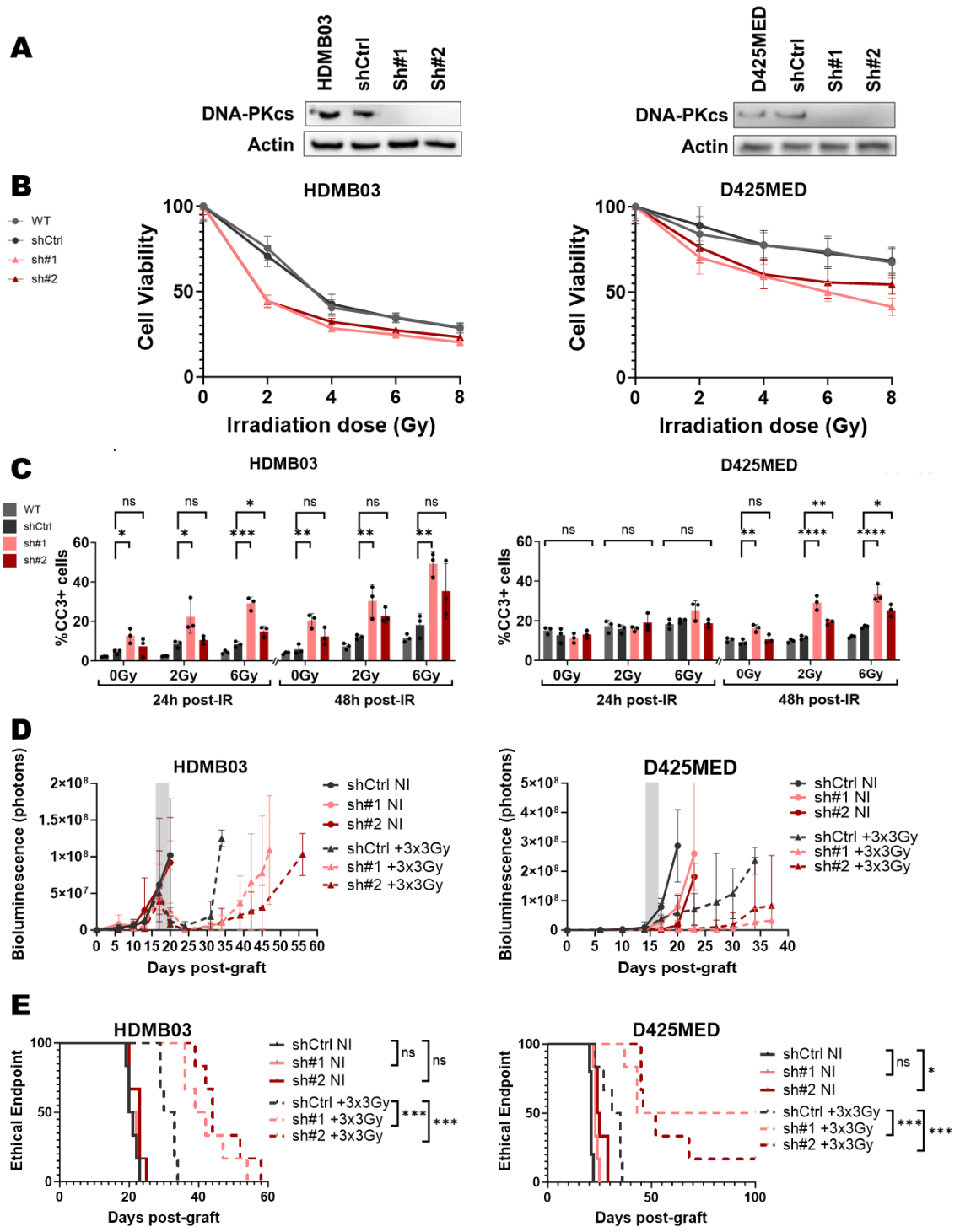

Fig 3. Sh-mediated knockdown of DNA-PK sensitizes medulloblastoma to irradiation both in vitro and in vivo. (A) Knockdown of DNA-PK in the cell lines HDMB03 and D425MED was confirmed by western blot. (B) Graphs showing the response of HDMB03 and D425MED cells knocked down for DNA-PK to irradiation compared to shCtrl cells, as assessed by cell-titre Glo assays at 3 and 5 days post-irradiation, respectively. Lines are normalized to the 0 Gy control. Results shown are the mean ± SEM of four biological replicates, and are representative of three experimental replicates. (C) FACS analysis of the apoptosis marker cleaved caspase 3 in shCtrl and shKnockdown HDMB03 and D425MED cells treated with 0, 2, and 6 Gy irradiation. Statistical differences were assessed by one-way ANOVA. (D&E) Orthotopic tumors were grafted from shKnockdown and shCtrl HDMB03 and D425MED cells. Mice in each tumor group were divided into a non-irradiated and an irradiated group (n=6 each) Tumor growth (D) was monitored by bioluminescent assay, with results shown as the mean ± SD. Grey shading indicates the timing of irradiation (3 doses of 3 Gy). Mouse survival was assessed by Kaplan Meier curves (E). Statistical differences in survival were assessed with the log-rank Mantel-Cox test.

SD, standard deviation; SEM, standard error of the mean; sh, short hairpin; NI, non-irradiated; WT, wild type. * p <0.05, ** p>0.01, ***p<0.001.

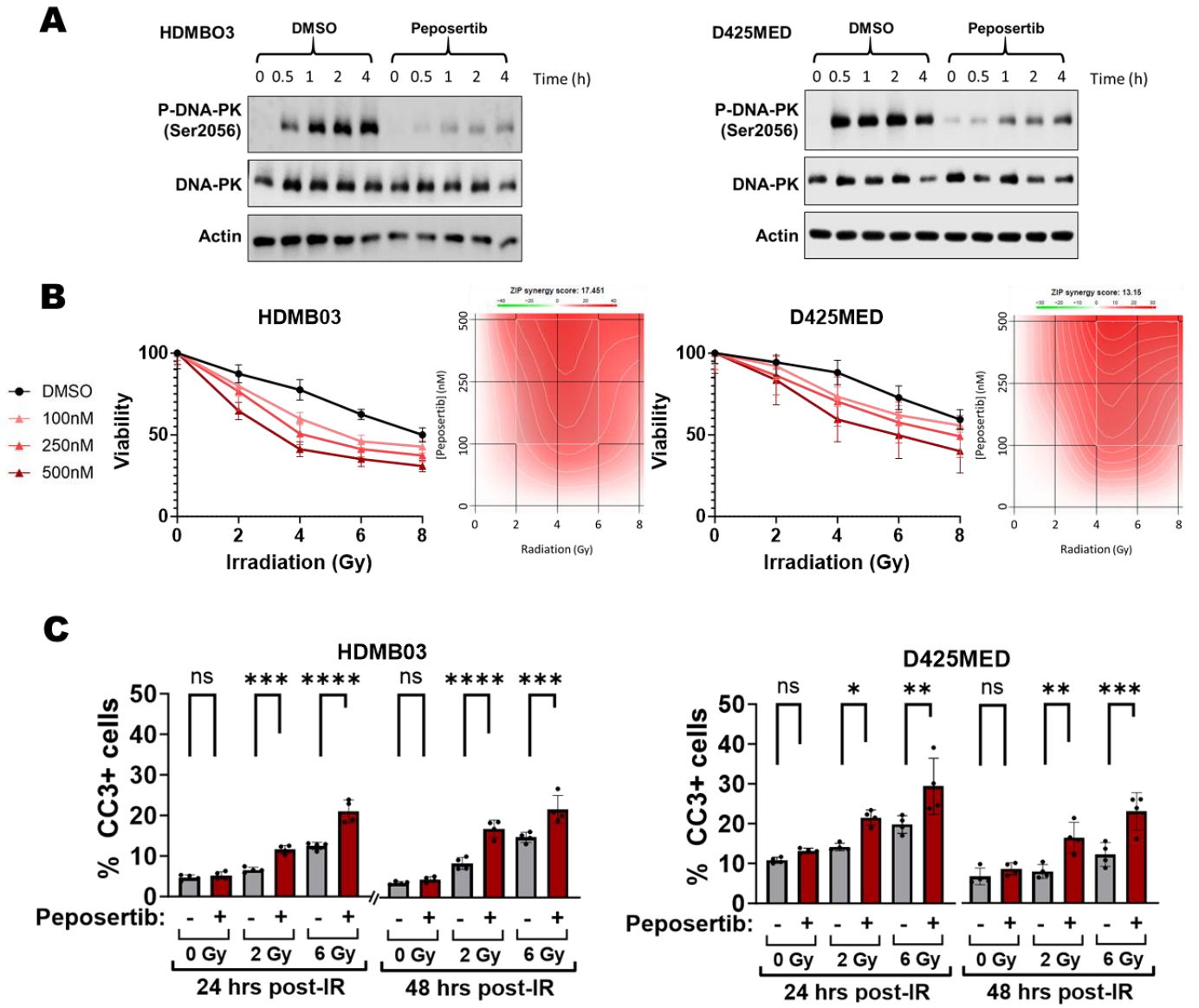

Fig 4. Peposertib is a strong radiosensitizer in vitro. (A) Western blots of HDMB03 and D425MED cells treated with 500 nM peposertib or vehicle (DMSO) showing levels of autophosphorylated (Ser 2056) DNA-PK, total DNA-PK, and Actin at different timepoints post-6 Gy irradiation. (B) Analysis of cell viability (y-axis) of HDMB03 (left, 3 days post-IR) and D425MED (right, 5 days post-IR) cells treated with peposertib (0-500 nM) and irradiation (x-axis, 0-8 Gy). The synergy between peposertib and irradiation was assessed by analysis of the Zero Interaction Potency (ZIP) synergy score. (C) FACS analysis of cleaved caspase 3 showing the levels of apoptosis in G3 MB cells treated with and without peposertib following 0, 2, and 6 Gy irradiation. All statistical differences were assessed by one-way ANOVA.
CC3, Cleaved Caspase 3; Gy, Grey. ns, non-significant; * P <0.05; **P>0.01; ***P<0.001.

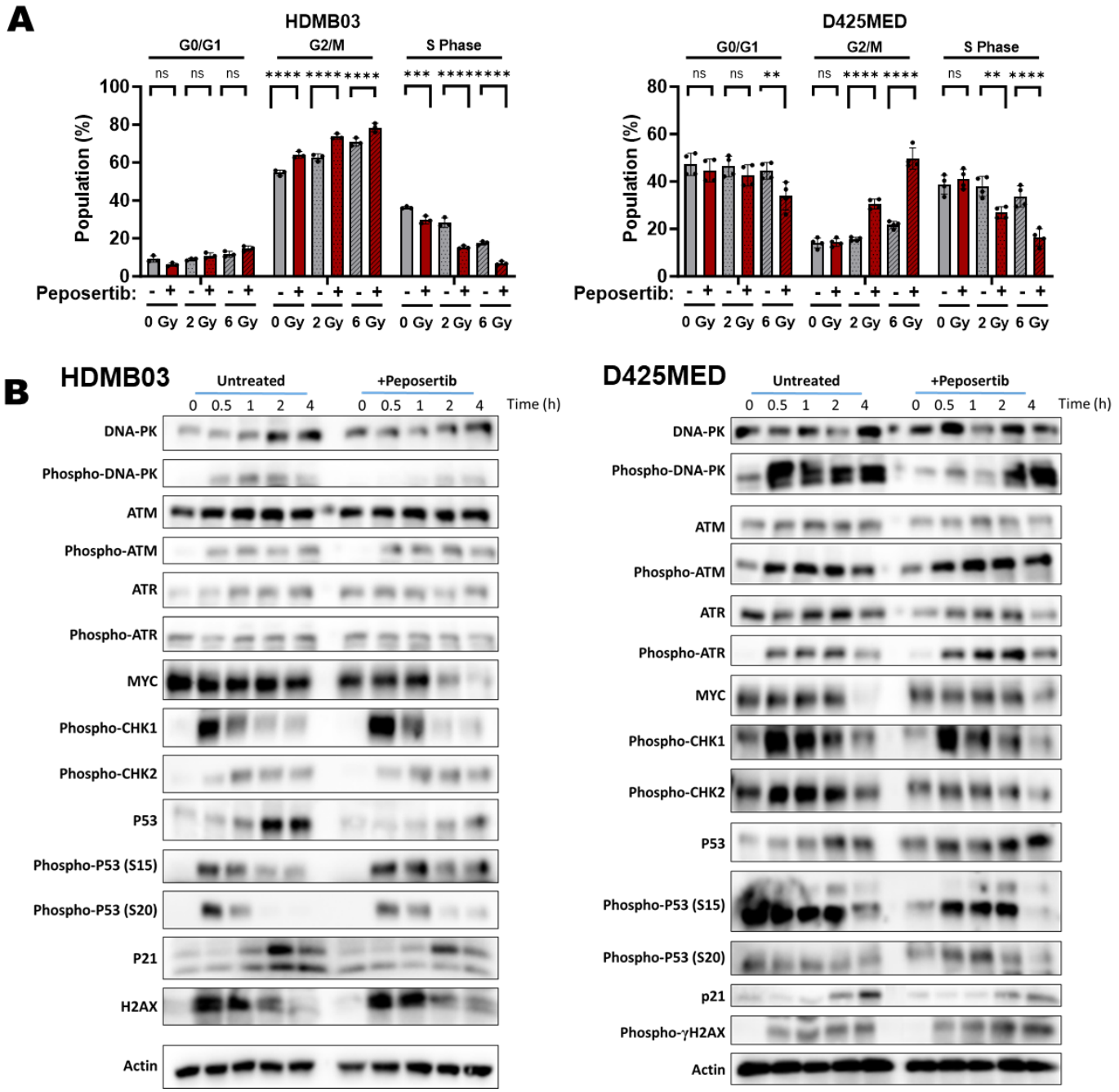

Fig 5. Peposertib treatment induces a G2/M arrest when combined with irradiation. (A) Cell cycle analysis was performed using FACS to assess BrdU and 7AAD incorporation in cells treated with 0, 2, or 6 Gy irradiation with or without pre-treatment with 500 nM peposertib. FACS analyses were performed 48 hrs post-irradiation in the group 3 medulloblastoma cell lines HDMB03 (left) and D425MED (right). Statistical differences were assessed by one-way ANOVA. (B) Western blotting of protein extracts of cells treated with vehicle or 500 nM peposertib collected 0.5, 1, 2, and 4 hours post-6 Gy irradiation was performed to assess the activity of DNA-PK and other DNA damage-related pathways in the group 3 medulloblastoma cell lines HDMB03 (left) and D425MED (right).
FACS, fluorescence activated cell sorting; ns, non-significant; *p <0.05; **p>0.01; ***p<0.001; ****p<0.0001.

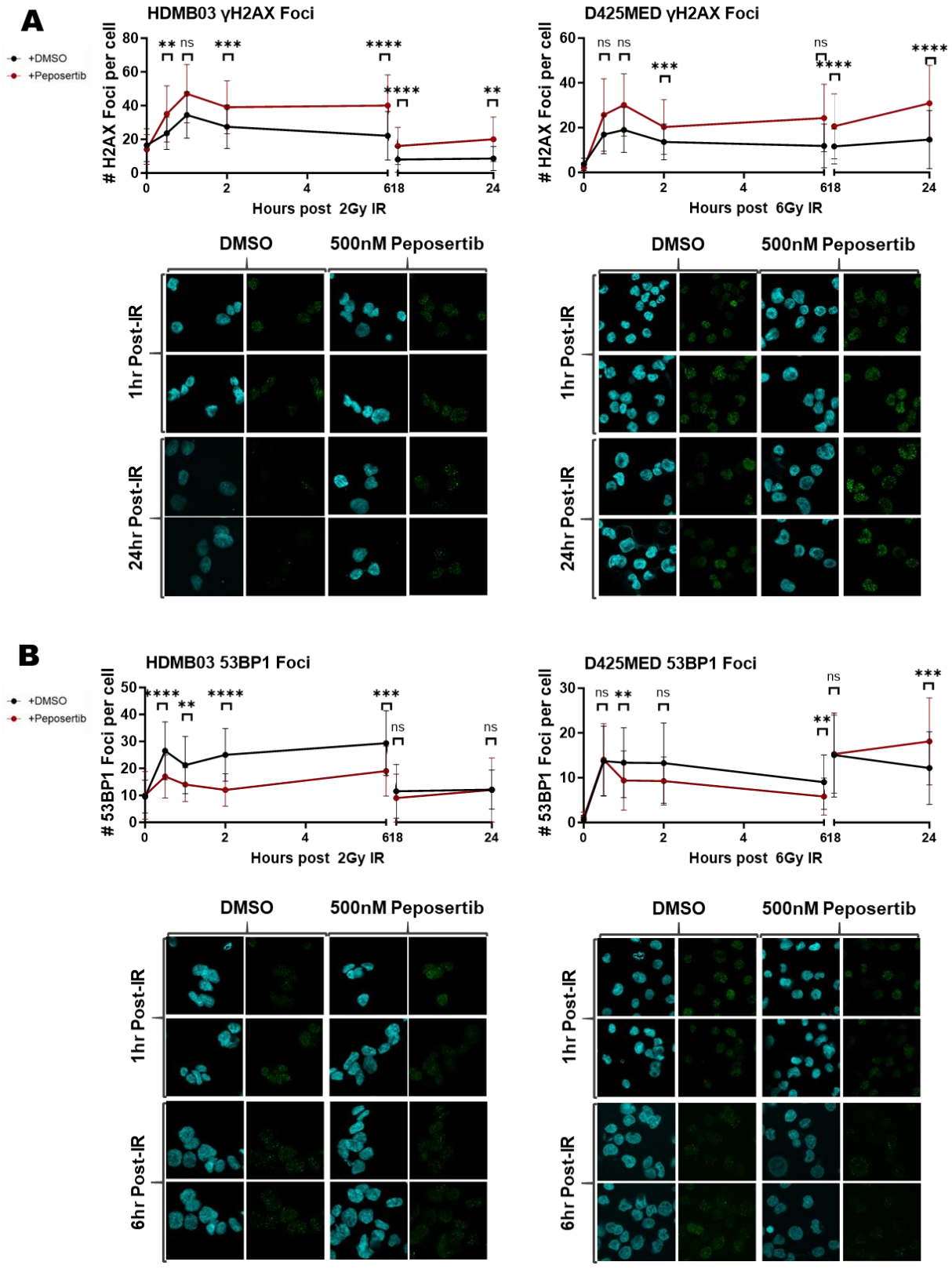

Fig 6. Peposertib and irradiation increases DNA damage and decreases NHEJ activity compared to irradiation alone. (A) Immunofluorescence analysis of the number of γH2AX foci per cell following treatment with 500 nM peposertib and irradiation in HDMB03 (2 Gy, left) and D425MED (6 Gy, right) cell lines compared with irradiation alone. Representative images at 1 and 24-hrs post irradiation are shown. (B) Immunofluorescence analysis of the number of 53BP1 foci per cell following treatment with 500 nM peposertib and irradiation in HDMB03 (2 Gy, left) and D425MED (6 Gy, right) cell lines compared with irradiation alone. Representative images at 1 and 6-hrs post irradiation are shown. Statistical differences at each timepoint were assessed with the Kruskal Wallis test. All graphs shown are representative of three replicates.
IR, irradiation; ns, non-significant; *p <0.05; **p>0.01; ***p<0.001; ****p<0.0001.

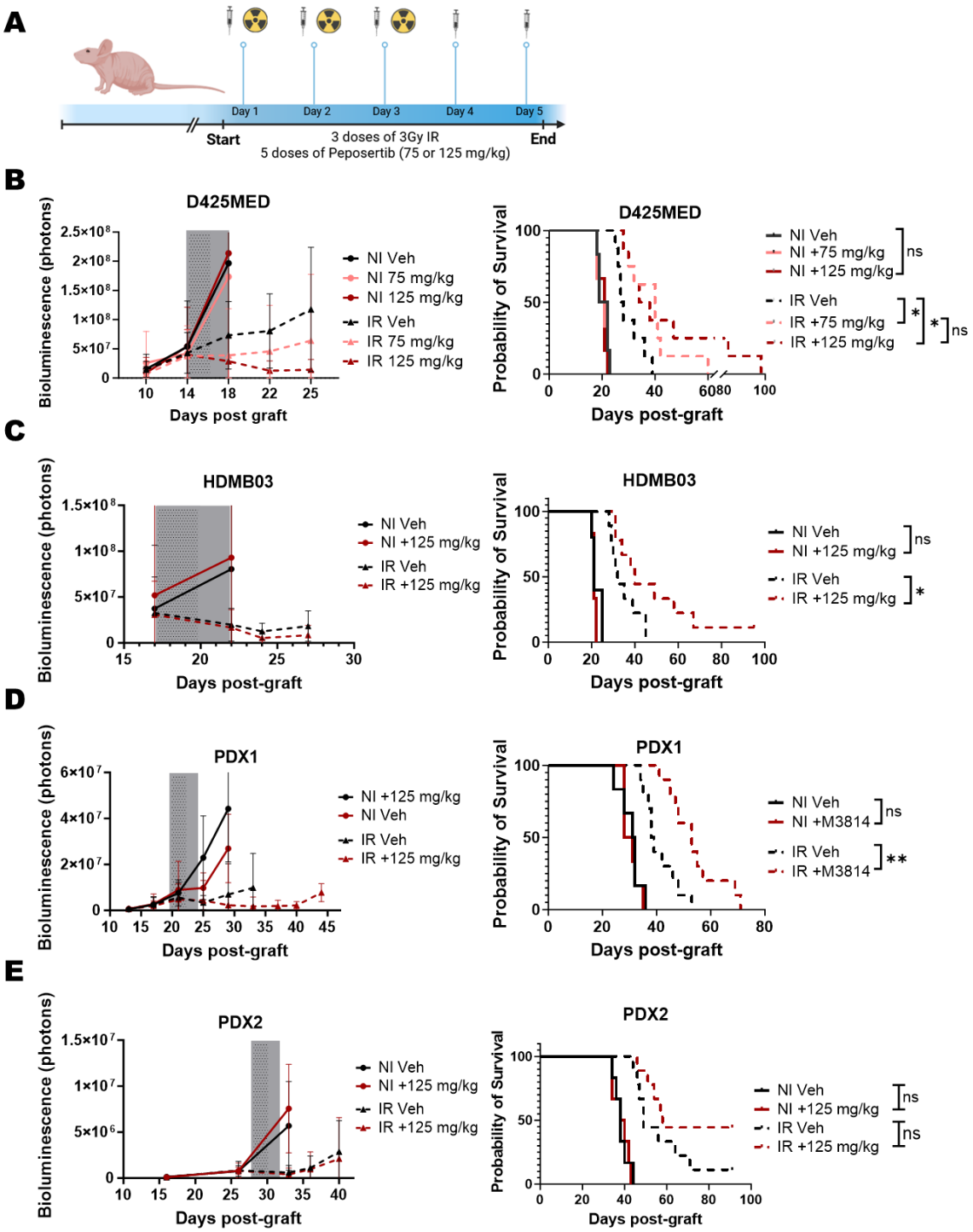

Fig 7. Treatment with peposertib induces a significant survival benefit in orthotopic grafted models of G3 MB when combined with irradiation. (A) Overview of the treatment schedule: tumours were grafted orthotopically into the right hemisphere of the cerebellum, and allowed to grow to the exponential phase. Mice were irradiated on the SARRP irradiator with 3 doses of 3 Gy IR (spaced 24 hrs apart), 45 min after treatment with either vehicle or 75/125 mg/kg peposertib. Treatment with vehicle/peposertib was continued for 2 days following IR (5 doses total). Bioluminescence (left panel) and Kaplan Meier (right panel) curves showing the effect of peposertib treatment on orthotopic grafted tumors with (B) D425MED, (C) HDMB03, (D) PDX1, and (E) PDX2. Bioluminescent graphs (left panel) show the mean ± SD of the bioluminescent signals of all mice in each group. Means are shown until the first mouse in each group was sacrificed. Grey shading indicates the timing of peposertib treatment, and black hashing indicates irradiation. For the Kaplan-Meier curves, statistical differences between groups were assessed with the log-rank Mantel-Cox test. For graphs showing the individual bioluminescent signals of all irradiated mice until sacrifice, please refer to supplementary Figure 2.

IR, irradiated; NI, Non-Irradiated; PDX, Patient derived xenograft; SD, standard deviation. ns, non-significant; * P <0.05; **P>0.01.

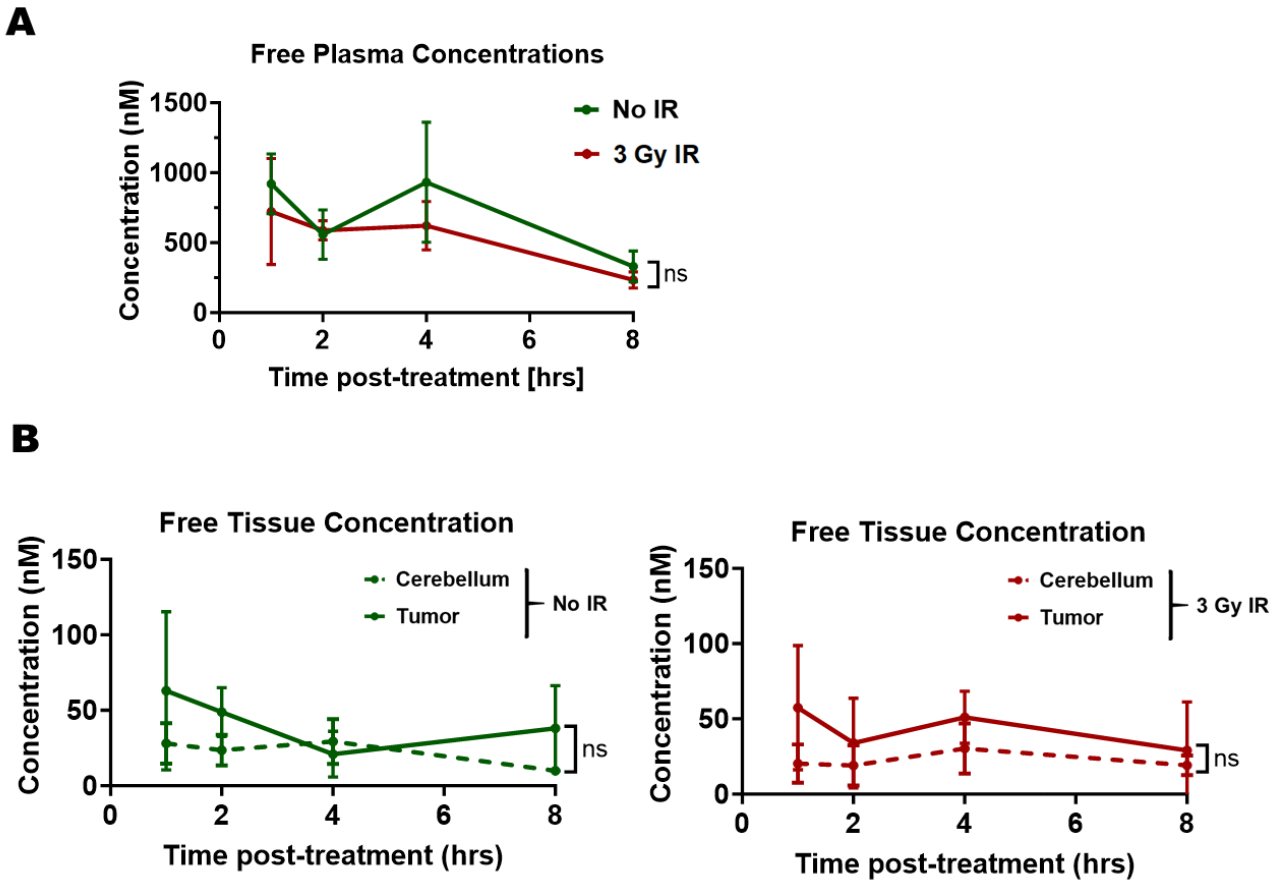

Fig 8. Peposertib shows increased accumulation in medulloblastoma tumours compared to the normal cerebellum. NMRI Nude mice bearing D425MED tumours grafted into the cerebellum were treated with 125 mg/kg peposertib. Half of the mice were irradiated with 3 Gy brain-targeted irradiation 45 mins post-treatment. Blood, tumour, and cerebellum samples were collected from irradiated and un-irradiated mice at 1, 2, 4, and 8 hours post-treatment. Peposertib concentrations were assessed by LC-MS/MS analysis. (A) Concentration of peposertib in plasma samples of mice treated with (red) and without (green) 3 Gy of irradiation to the brain. (B) Concentrations of peposertib in tumours (solid lines) and matched cerebellum samples (dashed lines) in irradiated (red) and unirradiated (green) mice. Results shown indicate the free (unbound and active) drug concentrations, calculated as 5% of the total drug concentrations, in accordance with prior analyses. Statistical differences were assessed by Two-way ANOVA. hrs, hours; ns, non-significant; LC-MS/MS, liquid chromatography with tandem mass spectrometry.

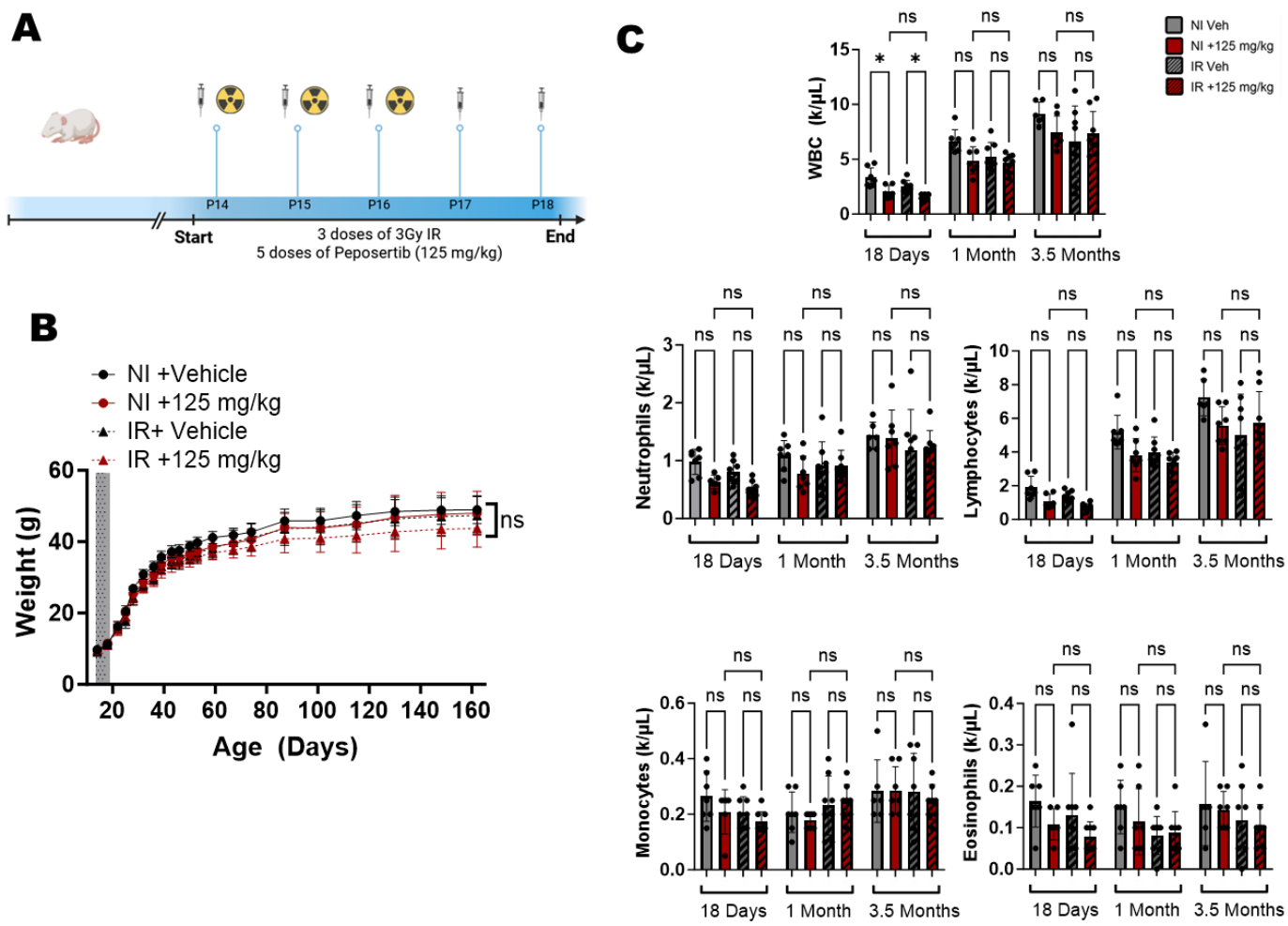

Fig 9. Peposertib with irradiation is well-tolerated in an immune-competent pediatric mouse model. (A) Schema showing the treatment of pup mice for toxicity experiments: Male RjOrl:SWISS mice were used as the model for all toxicity experiments. Using the SARRP irradiator, 3 doses of 3 Gy (spaced 24 hours apart) were administered to the brain, starting on postnatal day 14. Mice were treated with vehicle or 125 mg/kg peposertib 45 minutes prior to irradiation on the three irradiation days, and for the two following days (5 doses in total). Control mice were administered 5 doses of peposertib or vehicle without irradiation (B) The weight of mice in the four groups was monitored from P14 (start of treatment) to age 5.5 months. Statistical differences were assessed by two-way ANOVA. (C) To assess the systemic toxicity of peposertib combined with targeted irradiation of the brain, blood parameters were measured using the Sysmex XP300 system at three ages (18 days [final day of treatment], 1 month [2 weeks post-treatment], and 3.5 months). The number of total white blood cells, neutrophils, lymphocytes, monocytes, and eosinophils in mice in each group over the three timepoints are shown. Statistical differences were assessed by one-way ANOVA. IR, irradiated; NI, non-irradiated; P, postnatal day; k/µL, Thousand of cells per µL ns, non-significant; * $p < 0.05$.

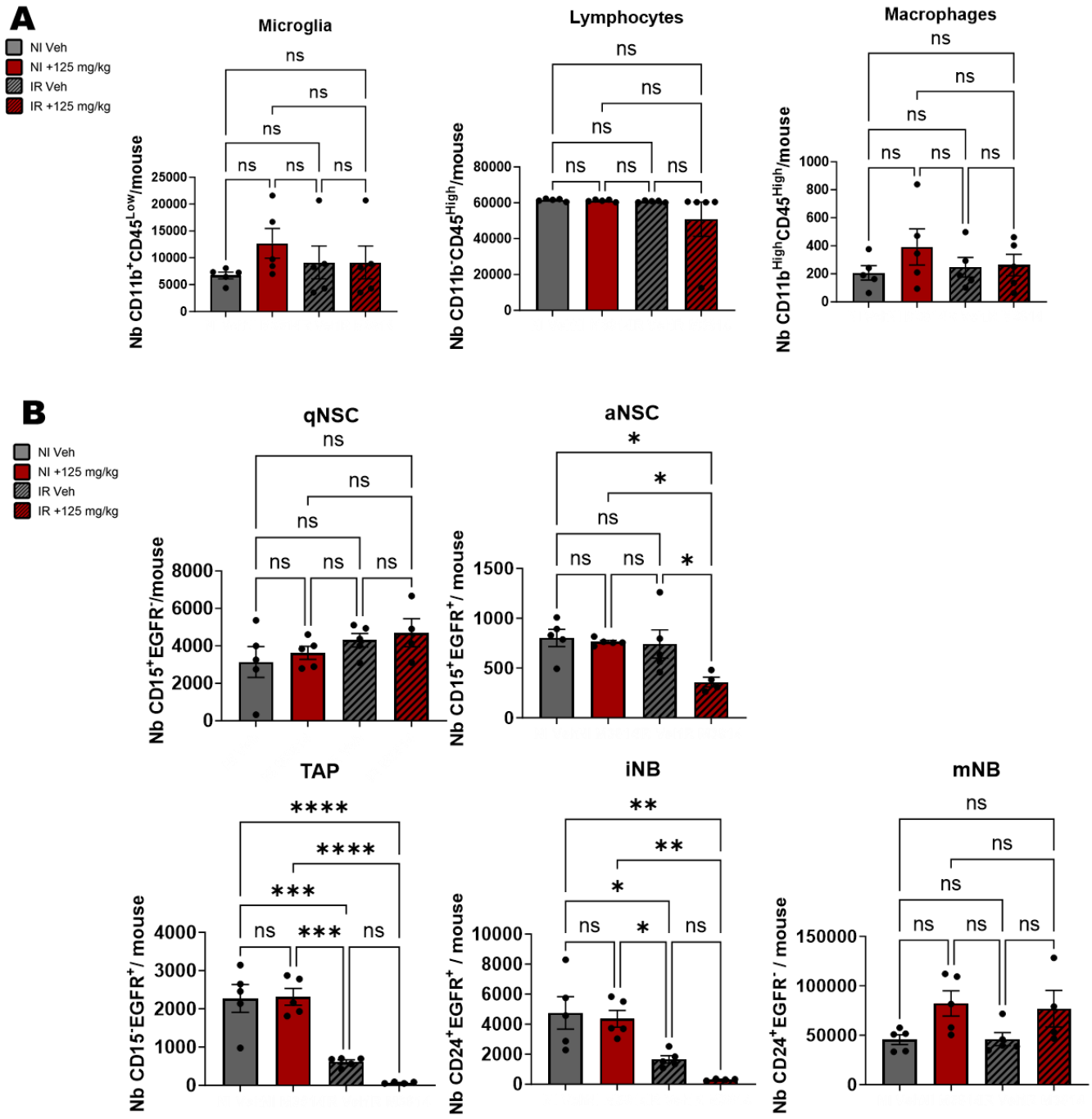

Fig 10 Irradiation and peposertib exert minor toxic effects on the brain of immunocompetent mice. Using the SARRP irradiator, 3 doses of 3 Gy were administered to the brain of male RjOrl:SWISS mice, starting on postnatal day 14. Mice were treated with vehicle or 125 mg/kg peposertib 45 minutes prior to irradiation on the three irradiation days, and for the two following days (5 doses total). Control mice were administered 5 doses of peposertib or vehicle without irradiation. Analyses were performed at 6 months old to assess whether peposertib added toxicity to irradiation. (A) FACS analysis of immune populations, including microglia ($CD11b^{High}/CD45^{Low}$), macrophages ($CD11b^{High}/CD45^{High}$), and lymphocytes ($CD11b^{-}/CD45^{High}$). (B) FACS analysis of cell populations in the subventricular zone, including quiescent neural stem cells (CD15+/EGFR-), TAP (CD15-/EGFR+), iNB (CD24+/EGFR+), and mNB (CD24+/EGFR-). Statistical differences were assessed by one-way ANOVA. All analyses were conducted on mice aged 6 months (5.5 months post IR and treatment).
aNSC, active neural stem cells; iNB, immature neuroblasts; IR, irradiated; mNB, mature neuroblasts; Nb, Number; NI, not irradiated; NSP, Neurospheres, qNSC, quiescent neural stem cells; TAP, transit amplifying progenitors.
ns, non-significant; *p <0.05; **p>0.01; ***p<0.001; ****p<0.0001.

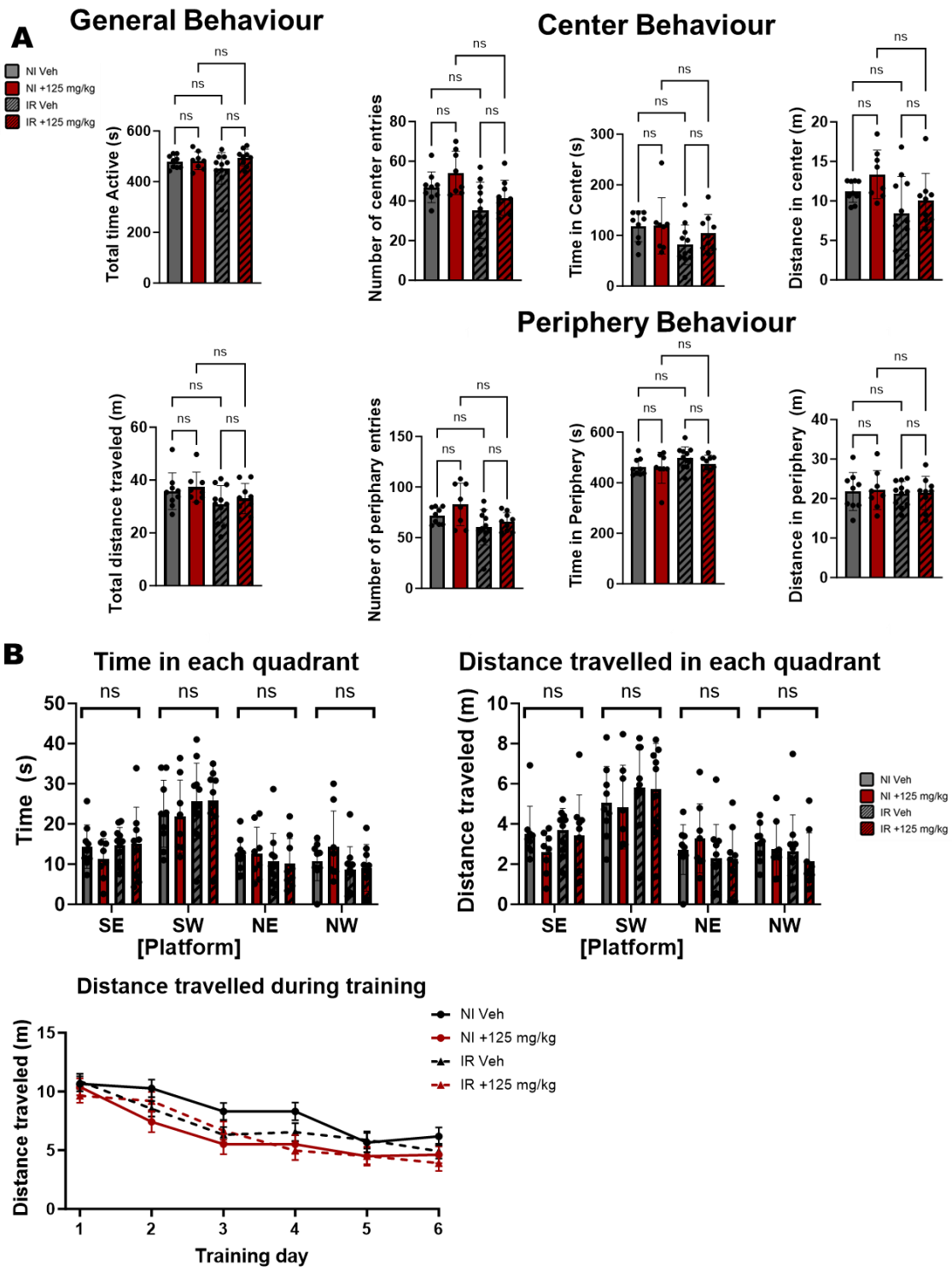

Fig 11 Peposertib and irradiation (3x3 Gy) exert no effects on behavior of mice at 6 months old. Using the SARRP irradiator, 3 doses of 3 Gy were administered to the brain of male RjOrl:SWISS mice, starting on postnatal day 14. Mice were treated with vehicle or 125 mg/kg peposertib 45 minutes prior to irradiation on the three irradiation days, and for the two following days (5 doses total). Control mice were administered 5 doses of peposertib or vehicle without irradiation. Behavioural tests were performed at 6 months old to assess whether peposertib added toxicity to irradiation. (A) Results of the open field test. The total time active and the total distance travelled in the open field are shown in the left panel. The number of region entries, time spent, and distance travelled in the center and periphery of the field are also shown. Statistical differences were assessed by one-way ANOVA. (B) The top panel shows the time and distance travelled in each quadrant on the final test day. The bottom panel shows the total distance travelled by mice before finding the platform in each group over 6 training days. The platform was located in the SW quadrant.

IR, Irradiated; NI, Non-Irradiated; NE, Northeast, NW; Northwest; SE, Southeast; SW, Southwest.
ns, non-significant; *p <0.05; **p>0.01.

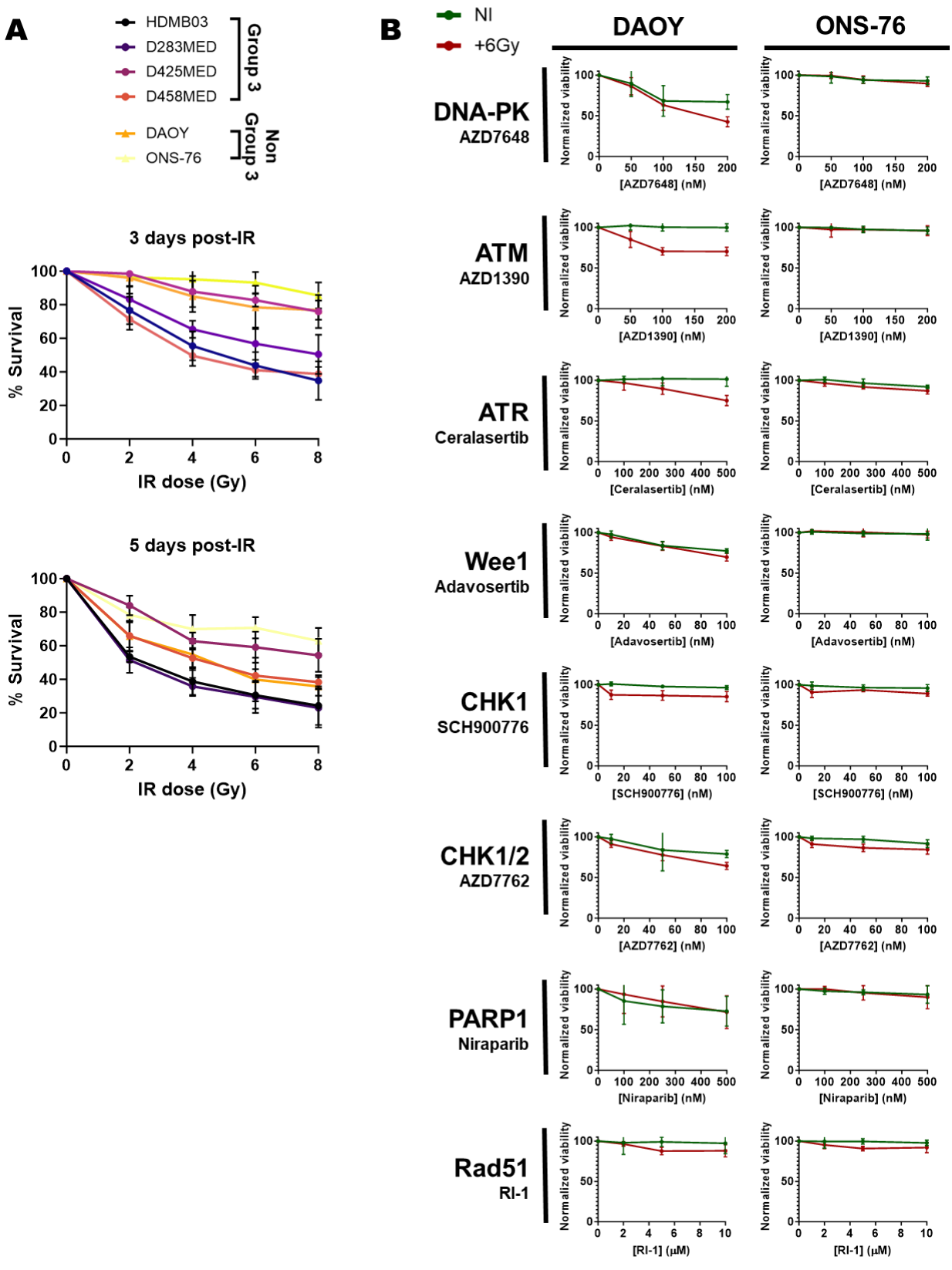

Supplementary Fig 1 (Continuation of Figure 1). (A) A kinetics analysis was performed to assess the relative radiation sensitivities of the group 3 cell lines HDMB03, D283MED, D425MED, and D458MED, and the non-group 3 cell lines DAOY and ONS-76. Viability was assessed using the ATP-based cell-titer glo assay 3 and 5 days post-irradiation with 0, 2, 4, 6, & 8 Gy. Viability at each dose is normalized to 0 Gy. Results are shown as the mean ± SEM of four biological replicates, and are representative of two experimental replicates. (B) The targeted screen outlined in Figure 1 was replicated in the non-group 3 medulloblastoma cell lines DAOY and ONS-76. Results are shown as the mean ± SEM of four biological replicates, and are representative of two experimental replicates.

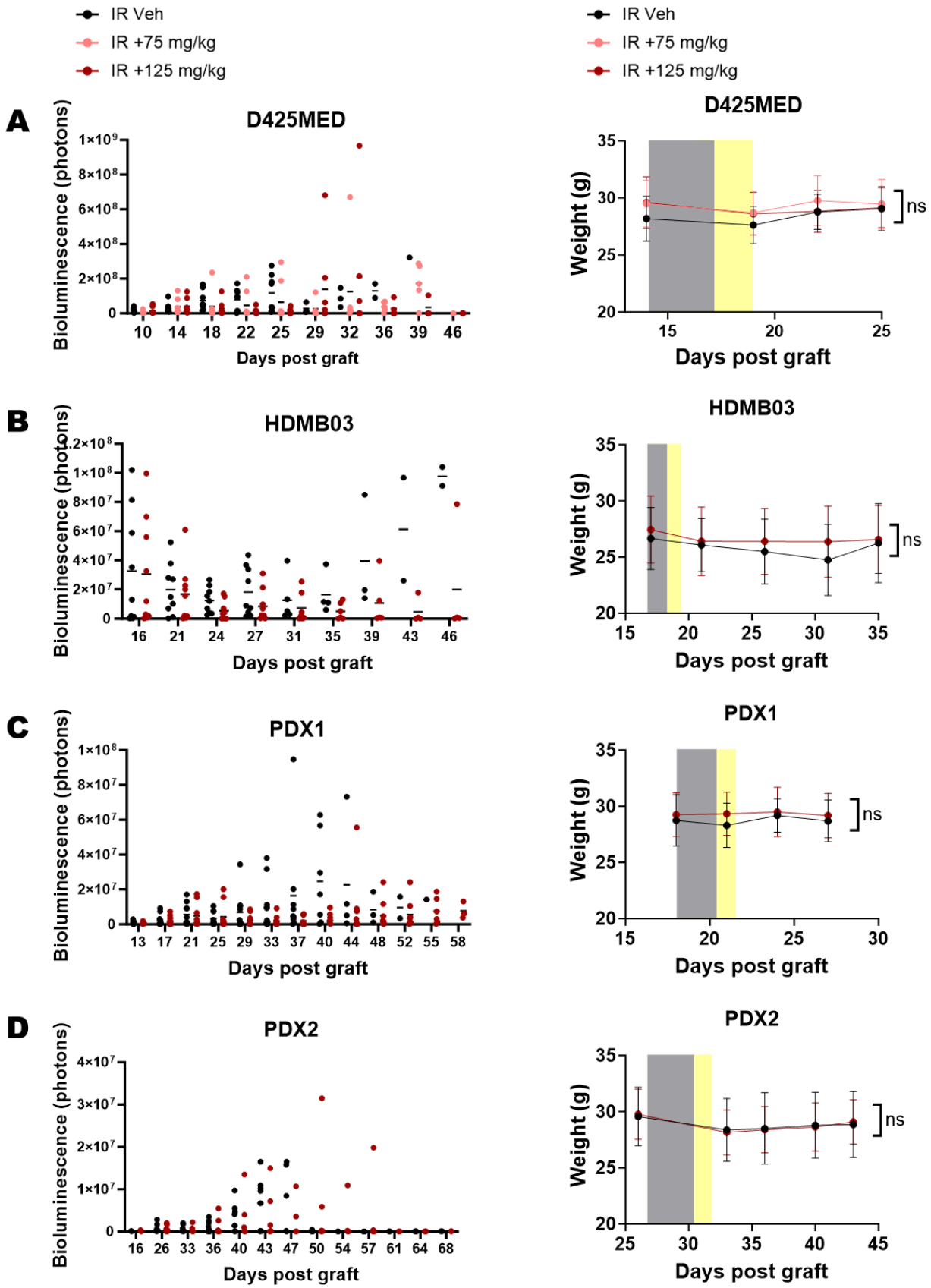

Supplementary Figure 2 (Continuation of Figure 7)**.** The bioluminescent signals and weight of mice grafted with (A) D425MED, (B) HDMB03, (C) PDX1, (D) PDX2 are shown. The left panel shows the bioluminescent signals of individual mice in the irradiated groups (Vehicle in black, peposertib treatment in pink/red). The right panel shows the weight of mice treated with irradiation and peposertib (pink/red) or vehicle (black). Weight was monitored from the start of treatment until the sacrifice of the first mouse in each group. Significant differences in weight were assessed by Two-way ANOVA.

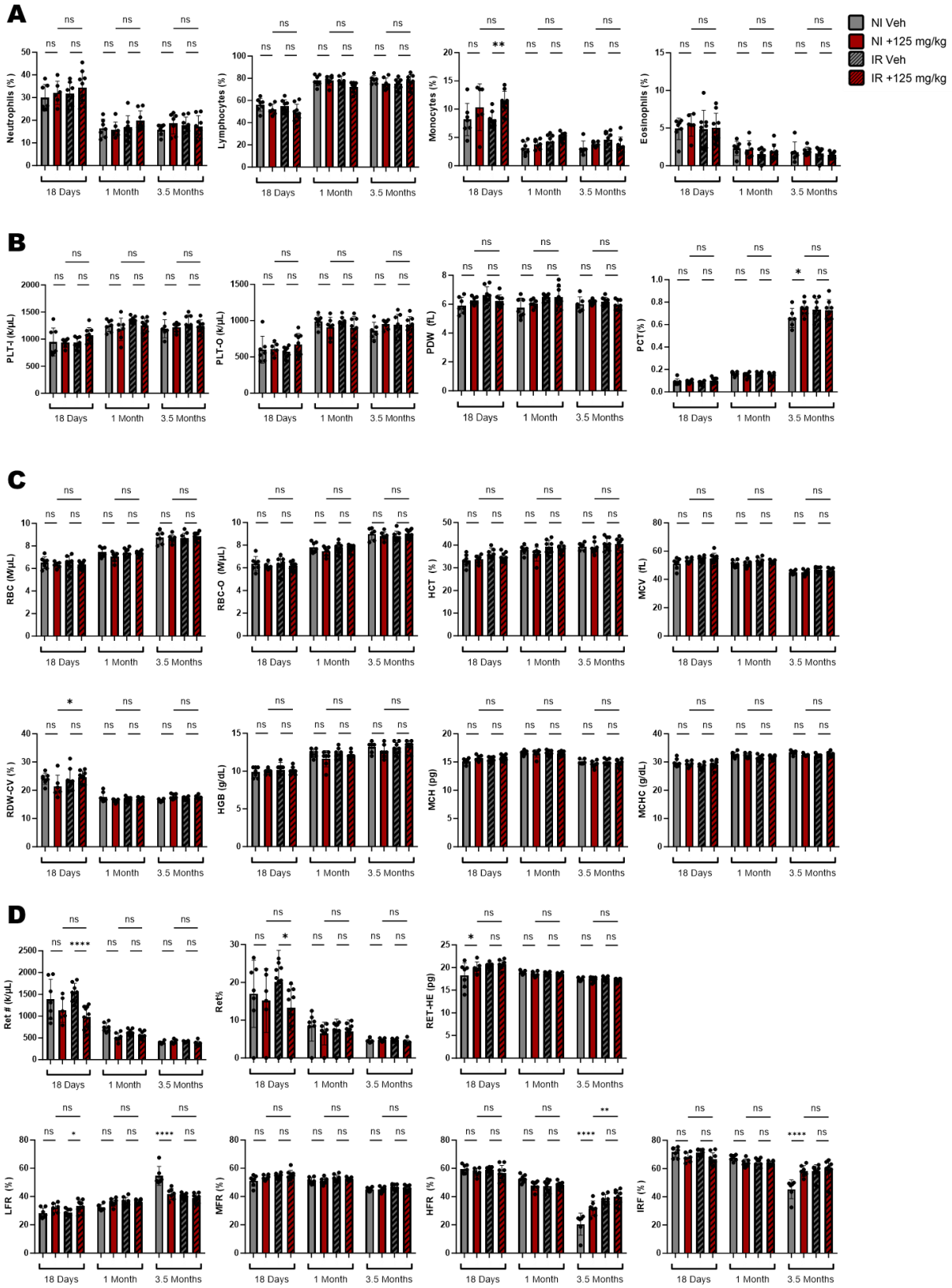

Supplementary Figure 3: Continuation of Figure 8. Results of blood analysis of Rj:Orl male pup mice treated with/without fractionated brain-targeted irradiation (3 doses of 3 Gy), and with and without peposertib (5 doses of 125 mg/kg or vehicle). (A) Populations of immune cells (neutrophils, lymphocytes, monocytes, and eosinophils) as a percentage of all white blood cells. (B) Results of analysis of platelet parameters. (C) Results of analysis of red blood cells parameters. (D) Results of analysis of reticulocyte parameters. All parameters were assessed using the Sysmex XP300 system at three ages (18 days [final day of treatment], 1 month [2 weeks post-treatment], and 3.5 months). For a full description of all of the described parameters, please refer to Supplementary Table 1. Statistical differences were assessed by one-way ANOVA.
K, thousands per unit; M, Millions per unit. ns, non-significant; *p <0.05; **p>0.01; ***p<0.001; ****p<0.0001.

Supplementary Table 1: Overview of the non-immune blood parameters analyzed using the Sysmex XT-2000iV system.

	Parameter (Unit)	Definition of abbreviation	Explanation
Platelet Parameters	PLT-I (K/µl)	Platelet-I	A specific method used to count the number of platelets
	PLT-O (K/µl)	Platelet-O	A specific method used to count the number of platelets
	PDW (fL)	Platelet distribution width	An indicator of the heterogeneity of platelet size
	PCT (%)	Plateletcrit	Volume of the blood occupied by platelets
Red Blood Cell Parameters	RBC (M/µl)	Red blood cells	Number of red blood cells in the blood
	RBC-O (M/µl)	Red blood cell count (optical method)	An optical method used to count the number of red blood cells.
	HCT (%)	Hematocrit	Proportion of red blood cells in the blood
	MCV (fL)	Mean corpuscular volume	Average volume of red blood cells
	RDW-CV (%)	Red cell distribution width	An indicator of the heterogeneity of red blood cell size
	HGB (g/dL)	Hemoglobin	Concentration of hemoglobin in the blood
	MCH (pg)	Mean corpuscular hemoglobin	Average quantity of hemoglobin in a single red blood cell
	MCHC (g/dL)	Mean corpuscular hemoglobin concentration	Quantity of hemoglobin in a single red blood cell relative to the cell size.
Reticulocyte Parameters	RET# (K/µl)	Reticulocyte number	Number of reticulocytes (immature red blood cells) in the blood.
	RET% (%)	Percentage of reticulocytes	Percentage of reticulocytes (immature red blood cells) in the blood.
	RET-He (pg)	Reticulocyte hemoglobin equivalent	Measurement of the hemoglobin content of reticulocytes.
	LFR (%)	Low fluorescence reticulocytes	Percentage of reticulocytes which show low fluorescence, representing a high level of maturity
	MFR (%)	Medium Fluorescence reticulocytes	Percentage of reticulocytes which show medium fluorescence, representing a lower level of maturity
	HFR (%)	High Fluorescence reticulocytes	Percentage of reticulocytes which show high fluorescence, representing a low level of maturity
	IRF (%)	Immature reticulocyte fraction	The combination of the MFR and HFR low maturity reticulocytes, used as an indicator of erythropoiesis

K, Thousands; M, Millions

ANNEX:

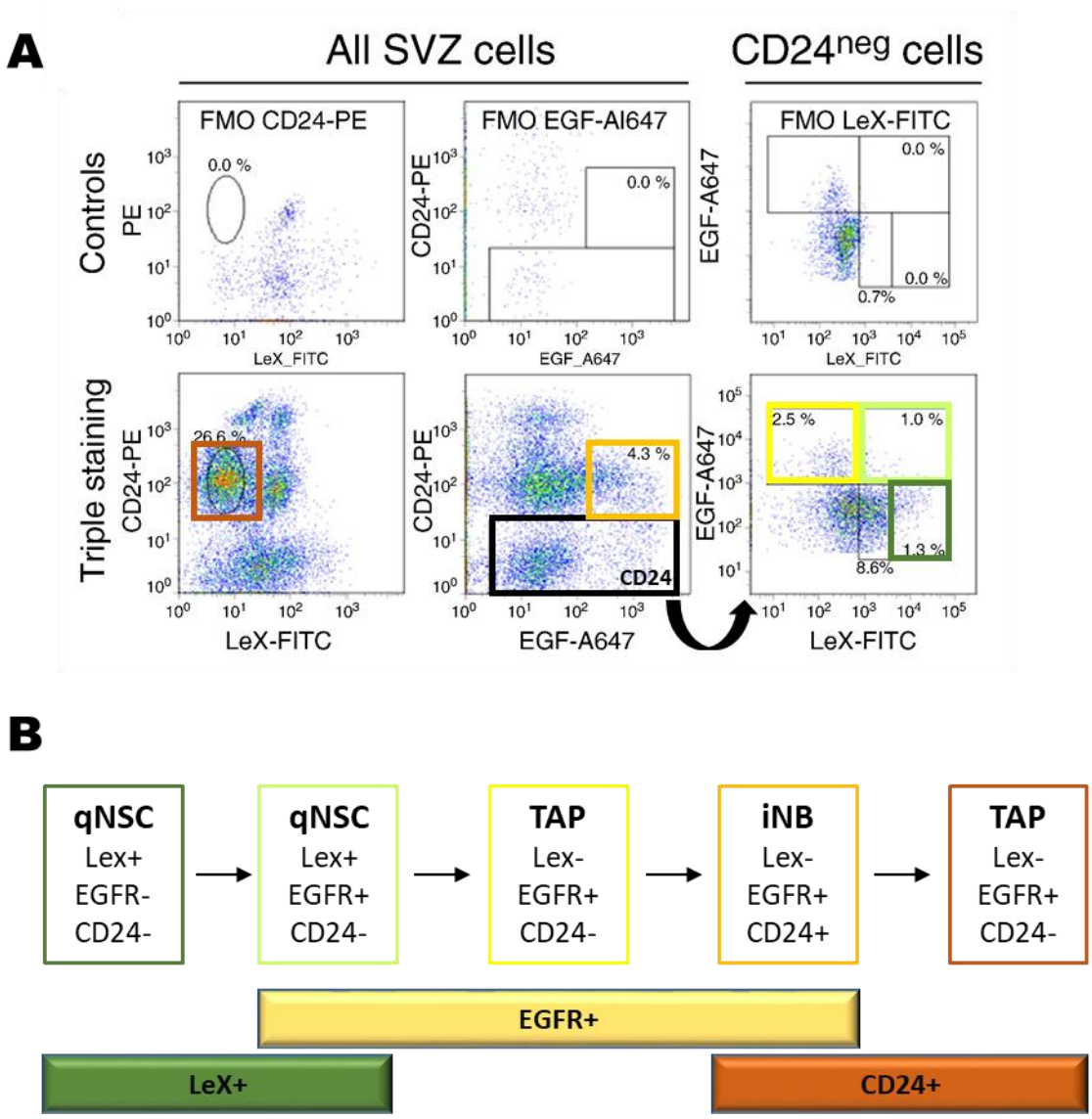

Annex 1: (A) Representative flow cytometry showing standard floz cytometry analysis of dissociated subventricular zone cell populations. (B) Schema showing the identification of the different SVZ cell population based on flow cytometry analysis. LeX+/EGFR-/CD24- cells were classified as quiescent neural stem cells. LeX+/EGFR+/CD24- cells were classified as active neural stem cells. LeX-/EGFR+/CD24- cells were classified as transit amplifying progenitors. LeX-/EGFR+/CD24+ cells were classified as immature neuroblasts. LeX-/EGFR-/CD24+ cells were classified as mature neuroblasts.

aNSC, active neural stem cells; iNB, immature neuroblasts; NB, mature neuroblasts; qNSC, quiescent neural stem cells; TAP, transit amplifying progenitors.

Fig A was taken from Daynac et al, Stem Cell Res, 2013 [45].

7. Results Chapter 2:

Modelling Relapse after Radiotherapy in Group 3 Medulloblastoma.

Contribution Statement:

All in vivo analyses (mouse grafting, management, bioluminescent imaging, sacrifice, dissection, and tissue dissociation) were performed by me, with the assistance of other members of the lab (Magalie Larcher, Celine Roulle, CRCN, INSERM in the lab). The preparation of RNA samples for bulk RNAseq was performed by me. The preparation of samples for scRNAseq was performed by me in collaboration with the Institut Curie platform.

Sequencing of bulk and scRNAseq samples was performed by the CurieCoreTech Next Generation Sequencing (ICGex) platform. All subsequent bioinformatics analyses were performed by Sabine Druillenec (CRCN, INSERM in the lab).

The CRISPR-Cas9 screen was performed as a collaboration with the Institut Curie-SIRIC (Site de Recherche Intégrée en Cancérologie, INCa-DGOS-Inserm_12554; ITMO Cancer AVIESAN), who performed all processing steps following sample collection of the samples, as well as the bioinformatics analysis.

7.1 Abstract:

Medulloblastoma (MB) is the most common form of paediatric malignant brain tumour. MB patients are treated with a stringent multimodal therapy regime comprising maximal surgical resection, radiotherapy, and chemotherapy. This treatment strategy achieves a 5-year survival rate of approximately 70%. However, ~30% of patients experience relapse, with an almost invariably fatal outcome. Although several treatment options have been proposed for relapsed MB (additional chemotherapy, re-resection, and re-irradiation), none have achieved great success. These therapeutic dead ends require the development of alternative therapeutic strategies. One option would be to prevent relapse by understanding and targeting the mechanisms underlying initial treatment escape, and to target minimal residual disease-phase tumours before relapse. In this context, the present study was conducted to better understand how the most aggressive molecular MB subtype, group 3 MB, escapes irradiation to relapse. Herein, we performed in vivo experiments comparing unirradiated tumours with irradiated tumours in the control (minimal residual disease) and aggressive relapse phases using a variety of untargeted techniques (bulk RNAseq, scRNAseq, phosphoarray). Further, we performed in vitro CRISPR-Cas9 screening to identify genes important in the irradiation response. This approach will allow us to understand the mechanisms by which group 3 MB escapes irradiation to form relapse, potentially identifying novel treatment targets to reduce the rate of relapse. We hope that integrating these approaches will allow us to identify the most relevant targets to radiosensitize MB in an unbiased manner. Although the bioinformatic analyses of these experiments remains incomplete, preliminary analyses revealed an upregulation of P53 pathway activation, apoptosis induction, and alterations in cell cycle checkpoint and DNA damage repair pathways.

7.2 Background to The Project:

As discussed extensively in the introduction, the primary treatment course for MB (surgical resection followed by radiotherapy and chemotherapy) achieves a high overall survival rate of approximately 70%. However, recurrent tumours nevertheless arise in ~30% of patients, of whom approximately 90-95% will eventually succumb to disease[118]. Currently, there is no universal consensus on the optimal management of recurrent MB, although further surgical resection[365,366], re-irradiation[112,115,116,367], and further chemotherapy[368] have all been proposed. Unfortunately, none of these treatment modalities greatly improve patient outcome, and the treatment of patients with recurrent tumours is often palliative rather than curative[80]. Further,

biopsy is rarely performed on recurrent tumours, as surgical resection is rarely performed at this stage. Consequently, although medulloblastoma is well characterised in its initial form, comparatively little is known about recurrent disease, although existing research has shown that MB escape from therapy to form relapse in medulloblastoma may occur through both genetic and non-genetic mechanisms (for more detail, please see Introduction, section 1.4 Medulloblastoma Radioresistance and Recurrence [Page 20-24]).

Considering the limitations of clinical research into this area, including the relative lack of matched biopsies and treatment regimens for recurrent medulloblastoma, pre-clinical studies investigating the mechanisms of medulloblastoma relapse are required to fully understand this process. Unfortunately, although many such studies have identified interesting results, the exact landscape of medulloblastoma recurrence remains only incompletely characterized. Thus, the main overarching aim of this branch of my project is to explore the processes underlying the development of radioresistance in group 3 medulloblastoma tumours which drive tumour recurrence following radiotherapy.

To achieve this, we created models which replicate the stages of relapse both in vitro and in vivo. In vivo, we used orthotopic tumour models of cell lines and faithful patient derived xenografts (PDX) grafted into the cerebellum. These orthotopic tumours were irradiated with a fractionated irradiation regimen of 3x3 Gy targeted to the brain using the small animal radiation research platform (SARRP) irradiator. This treatment induced a phenotype similar to that observed in patients after therapy; with tumours shrinking following irradiation and entering a controlled period of low growth, mimicking the minimal residual disease phase seen in patients. These controlled tumours eventually regrew to form aggressive tumours, mimicking the relapse phase observed in patients. A number of non-targeted screening techniques (bulk RNAseq, single-cell [sc]RNAseq, and phosphoarray in vivo, as well as CRISPR-Cas9 screening in vitro) were then applied. The aim of these experiments was to identify genes which could potentially be targeted to both prevent relapse by promoting response to initial treatment by inducing radiosensitisation, and genes in relapsed tumours which could potentially be targeted to improve treatment outcome of relapsed patients.

Overall, the current work has started to show the landscape of relapse in group 3 medulloblastoma. For example, our bulk RNAseq analyses revealed the importance of the P53 response and apoptosis induction in irradiated tumours, while CRISPR-Cas9 screening identified ATM and WDR11 as potential genes involved in irradiation escape. Unfortunately, due to time constraints, this work remains unfinished. However, in the future, the combination

of all of these unbiased approaches should allow a better understanding of the state of cells in different phases of growth and relapse following irradiation, and should reveal the mechanisms underlying the transition to relapse from the controlled stage. These investigations should together identify relevant targets which could form a basis for the development of novel therapeutic strategies to prevent relapse.

7.3. Materials and Methods

For detailed information regarding cell culture, animal management, grafting, and irradiation strategies, as well as ethical considerations, please refer to the methods section of the previous chapter. This chapter only describes methods unique to the results presented herein.

Generation of in vivo models

One of the first aims of my project was to establish models and parameters for in vivo experiments. These pilot experiments were performed using the cell lines HDMB03 and D425MED, and one group 3 PDX (PDX1, corresponding to ICN-MB-PDX-3 in the literature[37]). Cell lines or PDXs expressing luciferase and GFP were stereotactically grafted into the cerebellum of nude mice, as described in the previous chapter. Tumours were allowed to grow, with growth monitored by Luciferase assay. When the tumours had begun to enter the exponential growth phase (Day 16 for HDMB03, Day 14 for D425MED, and Day 18 for PDX1), the mice were subjected to a fractionated irradiation regimen of 3 doses of 3 Gy, administered 24 hours apart (3x3 Gy). Irradiation was targeted to the entire brain, sparing the surrounding tissue, using the image-guided SARRP (small animal radiation research platform) irradiator. Throughout the experiment, tumor growth was monitored by bioluminescent luciferase assay, and survival was assessed by Kaplan Meier analysis.

Bulk RNAseq:

Tissue harvesting and RNA extraction

Mice were sacrificed by cervical dislocation at pre-determined experimental timepoints. Tumours were macrodissected by GFP signal under a Stereo Microscope Fluorescence Adapter (Nightsea, USA), and immediately stored in RNAlater (Thermofisher, USA) for 24 hours at 4 °C. RNA was extracted from tissue samples using the RNeasy mini kit (Qiagen, The Netherlands), following the manufacturer's instructions.

RNA quantification and RIN testing:

RNA quality and concentration were assessed using the Agilent RNA 6000 Nano Kit (Agilent, USA) on the Bioanalyzer 2100 system (Agilent), which provided the RNA concentration and RNA integrity number (RIN). Only samples with RIN > 9 were used for analysis.

RNA Sequencing:

RNA-sequencing libraries were prepared from 1 µg of total RNA following the Illumina stranded mRNA prep Ligation protocol. Sequencing was carried out on a NovaSeq 6000 instrument from Illumina (S1-PE100, paired-end reads). Raw sequencing reads were first checked for quality with Fastqc (ver. 0.11.8), and trimmed for adapter sequences with cutadapt using the TrimGalore (ver. 0.6.2) wrapper. Trimmed reads were subsequently aligned to the complete human ribosomal RNA sequence with bowtie (ver. 1.3.0).

Bioinformatics analysis

The pipeline used xengsort (ver. 1.1.0) to separate Human and Mouse reads in distinct fastq files. Reads that did not align to rRNA were then mapped to the human reference genome hg19 and read counts per gene were generated with STAR mapper (ver. 2.6.1a_08-27). The bioinformatics pipelines used for these tasks are available online (RNAseq ver. 3.1.8 and ver. 4.1.0 for HDMB03 and PDX1, respectively, available at: https://gitlab.curie.fr/data-analysis/RNA-seq). Counts were normalized using TMM normalization from EdgeR (ver. 3.32.1). Differential gene expression was assessed with the Limma voom framework (ver. 3.46.0). Genes with an absolute fold-change ≥1.5 and an adjusted p-value < 0.05 were labeled significant using R (ver. 4.0.3). Gene Ontology analyses were performed using clusterProfiler package (ver. 3.18.1). Gene Sets Enrichment Analyses (GSEA, available at: http://software.broadinstitute.org/gsea) were run using signal-to-noise for the ranking gene metric and 1000 permutations. All bioinformatics analyses were performed by Sabine Druillenec (CRCN, INSERM in the lab).

scRNAseq

Harvesting of tumor cells from tissues:

Grafted GFP+ PDX tumours were harvested and macrodissected under a microscope equipped with a Stereo Microscope Fluorescence Adapter (Nightsea). Tumours were then dissociated in CO_2-Independent Media (Gibco), supplemented with 20,000 U/mL DNase and 0.15 mg/ml Liberase TL (Roche, Switzerland) at 37 °C for 35 mins. Cells were then washed in PBS+5% FBS, and stained for 20 mins in LIVE/Dead™ Fixable Aqua - Dead Cell Stain Kit (405 nm,

ThermoFisher). Live, GFP+ tumor cells were then sorted into 50% serum/PBS on a BD FACSAria III cell sorter (BD Biosciences) before processing.

scRNAseq:

scRNAseq was performed using the 10x Genomics Chromium™, Single-Cell RNA-Seq System using the Chromium Next GEM Single Cell 3′ Reagent Kits v3.1 (Dual Index), following the manufacturer's recommendations and instructions. Each sample was targeted to contain 10,000 single cells (collected by FACS). In cases where the number of cells obtained from a single tumour did not reach this amount, tumours from multiple mice were pooled.

Phosphoarray analysis

PDX cells were grafted into nude mice and tumours were allowed to grow. Tumours were macrodissected at different timepoints, flash frozen in liquid nitrogen, and stored at -80°C until they could be sent for analysis. Tissue lysis and phosphoarray profiling on the Phospho Explorer Antibody Array (PEX100) were performed by Tebu Bio (France). Results were analyzed using the Metascape online resource (Available at: https://metascape.org/gp/index.html).

CRISPR Knockout Screen

Construction of a stable Cas9 expressing clone:

D425MED cells were infected with a lentivirus expressing a Cas9-mCherry vector. Twenty-four hours after infection, mCherry+ cells were sorted on a BD FACSAria III cell sorter (BD Biosciences), with a single clone sorted into each well of a 96-well plate. Single cells were allowed to grow and serially passaged at appropriate intervals to amplify the clones. Lines grown from single clones were tested for mCherry expression by FACS (LSRFortessa X20, BD biosciences), and for Cas9 expression by western blot using the α-Cas9 (*S. pyogenes*) primary antibody (CST, USA).

Cas9 activity testing:

Based on the results of these analyses, clones expressing the highest levels of the Cas9 protein were selected for subsequent testing of Cas9 efficiency. The Cas9 activity of clones verified to stably express Cas9 were assessed using example gRNA expressing viruses. Cells were infected with lentiviruses to deliver the pLenti-sgRNA plasmid carrying a puromycin resistance gene and a test guide (g)RNA targeting a non-essential gene. Genomic DNA was extracted from puromycin-selected cells at set time points post-infection using the Nucleospin DNA RapidLyse kit (Macherey-Nagel, Germany), following the manufacturer's instructions. PCR was

performed using the GoTaq DNA polymerase and Master Mix (Promega). PCR was conducted according to the following procedure: initial denaturation step at 95 °C for 2 mins; 35 cycles of denaturation at 95 °C (30 s), annealing at 64 °C (30 s), extension at 72 °C (30 s). Bespoke primers were used (Fwd: GCCATGCTGAGACGGTTTAG, Rev: AGTTTTGGTGAGGCTGCAAT).

PCR products were sequenced using the TubeSeq service offered by Eurofins Genomics (Germany) with the aforementioned fwd primer. Finally, the knockout score of each sample was determined using the publicly available Inference of CRISPR edits (ICE) analysis pipeline (Synthego, available at: https://ice.synthego.com).

The clone which showed the highest knockout score was moved forwards for further testing. To determine the time post-infection at which the maximal knock-out of the target gene was achieved, the PCR and sequencing analyses were repeated over a time course, and this analysis was repeated twice. Finally, ~10 days post-infection was determined as the time at which optimal knockout of the target gene was achieved.

Knockout Screen:

The final CRISPR-Cas9 knockout screen was performed using a validated stable Cas9-expressing D425MED cell line, and the Brunello gRNA library, which comprises 4 sgRNAs per target gene, as well as 1000 non-targeting sgRNAs, totalling 77,441 sgRNAs.[369]

In brief, 150 million Cas9-expressing D425MED were infected with the Brunello Library, targeting a multiplicity of infection (MOI) of 0.3. After 24 hours, transduced cells were selected by puromycin (1 µg/ml) for 48 hours, after which the media was changed. Cells were serially passaged until 10 days post-infection, at which point they were seeded at 250,000 cells/ml, and split into two groups. Half of the cells were irradiated with a regimen of 3x2Gy (3 doses of 2 Gy each separated 24 hours apart) on the CIXD irradiation cabinet (Xstrahl, USA) on days 11-13 post-infection. Subsequently, irradiated and unirradiated cells were passaged and collected separately at pre-determined timepoints by freezing in 90% FBS with 10% DMSO at each doubling point. In total, 40-50 million irradiated and unirradiated cells were collected at each collection to ensure a minimum 500x coverage of the library.

At the end of the screen, cell samples were lysed, genomic DNA was extracted, and gRNA sequences were sequenced. Genomic DNA extraction was performed using the QIAGEN Blood & Cell Culture DNA Maxi Kit following the manufacturer's instructions (Qiagen, Cat#13362).

The resulting DNA pellet was washed in ethanol and resuspended in 800 µL of ultrapure H_2O. PCR amplification was performed using Herculase II fusion DNA polymerase (Agilent, Cat #600679) following the protocol developed by the Broad Institute (Available at: https://media.addgene.org/cms/filer_public/61/16/611619f4-0926-4a07-b5c7-e286a8ecf7f5/broadgpp-sequencing-protocol.pdf). Twenty-seven reactions with 10 µg DNA were performed and pooled for each sample. PCR purification was performed using AMPure magnetic beads (Beckman, ref A63881), following the manufacturer's instructions. The purity and concentration of the subsequent sample were assessed using the DNA 5000 ScreenTape (Agilent, 5067-5588) following the manufacturer's protocol. Equimolar pools were made for each sample and sent for 50 bp single read sequencing on a NovaSeq 6000 device (Illumina) using 20% PhiX sequencing controls (Illumina, ref 15017872).

The CRISPR-Cas9 screen was performed in collaboration with the Institut Curie-SIRIC (Site de Recherche Intégrée en Cancérologie, INCa-DGOS-Inserm_12554; ITMO Cancer AVIESAN), who performed all processing steps following collection of the samples, as well as the bioinformatics analysis.

7.4. Experimental Strategies and Preliminary Results:

Construction of in vivo models of relapse

In order to investigate the mechanisms underlying relapse in group 3 MB, we first created in vivo tumour models which replicate the stages of relapse observed in patients. To achieve this, we used orthotopic tumour models of cell lines and faithful PDX models grafted into the cerebellum (Figure 9A). These orthotopic tumours were irradiated with a fractionated irradiation regimen of 3x3 Gy targeted to the brain using the small animal radiation research platform (SARRP). In HDMB03 and PDX1 (Figure 9B & D), which are relatively radiation sensitive, tumor shrinkage and a control phase (mimicking the minimal residual disease [MRD] seen in human patients) were readily observed following fractionated irradiation. After a period of ~1-2 weeks of low growth, these control tumours developed into rapidly growing relapsed tumours. Thus, these models mimic the tumor progression observed in patients who develop relapse. Tumours grown from D425MED cells, which is a more radiation resistant model both in vitro and in vivo (potentially due to the loss of TP53 activity), showed a slightly different profile – tumours did not shrink following irradiation, but growth was nevertheless arrested (Figure 9C), and was followed by an exponential growth phase. This irradiation regimen induced a statistically significant survival benefit in all models. These models were used for the

subsequent analyses outlined below.

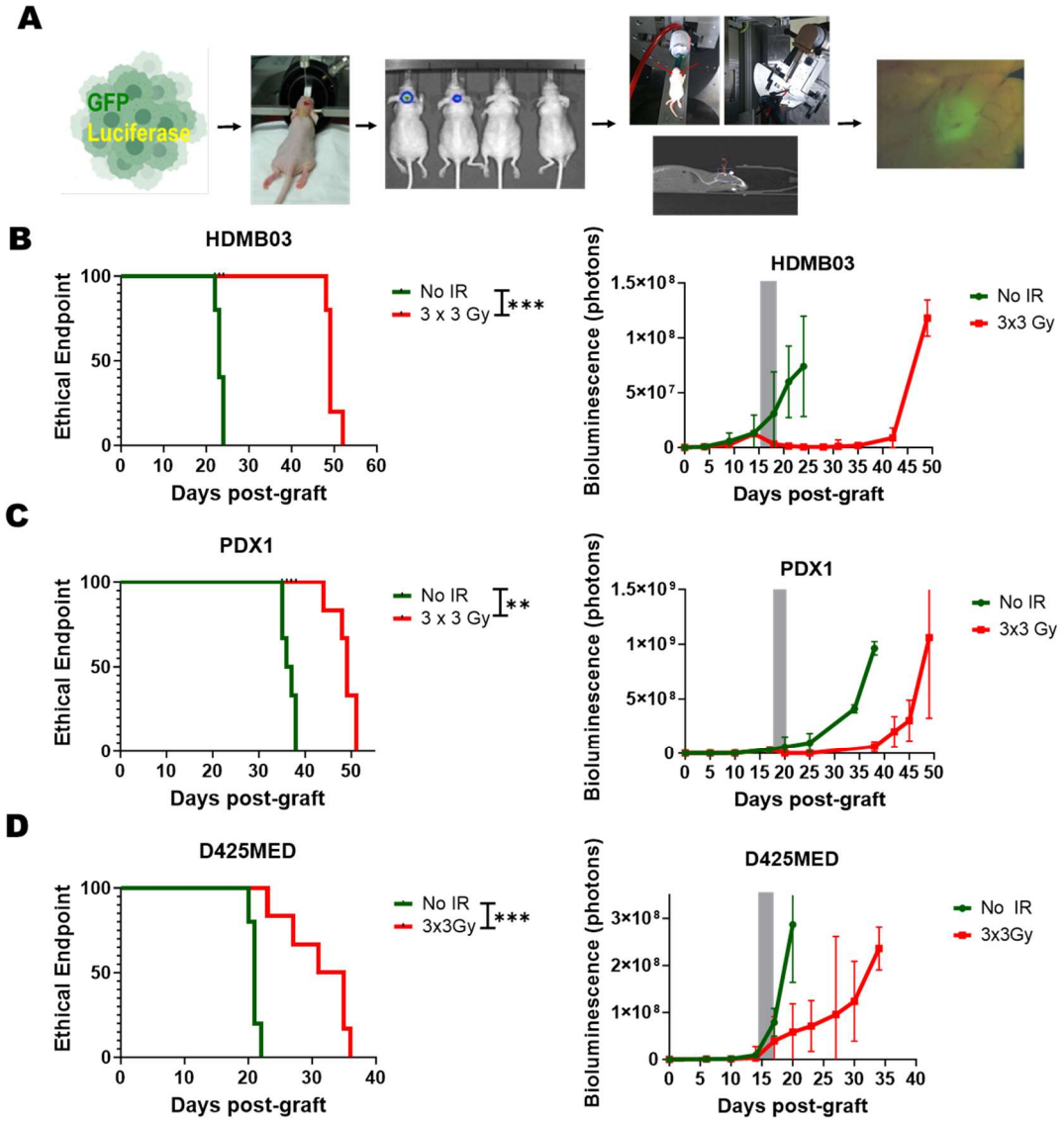

FIGURE 9 ESTABLISHMENT AND CHARACTERIZATION OF IN VIVO MODELS OF GROUP 3 MEDULLOBLASTOMA RELAPSE FOLLOWING IRRADIATION.

(A) Schema showing the setup of the in vivo model: cells expressing Luciferase and GFP were stereotactically grafted into the cerebellum of nude mice. Tumors were allowed to grow, with growth monitored by bioluminescence. Once the tumors reached the exponential growth phase (day 16 for HDMB03, 14 for D425MED, and 18 for PDX1), they were irradiated with the SARRP irradiator (3x3Gy - 3 daily fractions of 3Gy). Tumor growth was followed by bioluminescence, while GFP expression allowed macrodissection. (B/C/D) Left panel: mouse survival was assessed and compared between unirradiated (green) and irradiated (red) mice. Statistical differences were assessed using the log rank (Mantal-Cox) test. Right panel: tumor growth in unirradiated (green) and irradiated (red) mice was assayed by bioluminescence (results are shown as the average ± standard deviation). Results are shown for the HDMB03 (B) and D425MED (C) cell lines and the faithful PDX1 model (D).

Assessment of Transcriptional Adaptation to Irradiation: Bulk RNAseq

As a first approach to understand the global transcriptional adaptations underlying how group 3 MB tumours escape fractionated irradiation, survive in the control phase, and regrow to form recurrent tumours, we performed bulk RNAseq using our in vivo models. Analyses were

conducted on RNA extracted from tumours grafted with the cell line HDMB03, and the PDX model, PDX1. Tumours were collected at different time points of tumor growth in both irradiated and non-irradiated tumours as shown in Fig 10 A&B, and described below:

- 24 hours before the first irradiation (PDX1: Day 17 post-grafting, HDMB03: Day 15): non-irradiated tumours were collected to provide a baseline for subsequent analyses
- 24 hours after the final irradiation dose (PDX1: Day 21, HDMB03: Day 19; this corresponded with the ethical endpoint mentioned below): both irradiated and non-irradiated tumours were collected.
- The minimal residual phase (irradiated mice only): Tumours arrested in growth (5 days post-irradiation/day 25 post-grafting in PDX1, and 7 days post-irradiation/day 25 post-grafting in HDMB03) were collected to assess the tumours in the control phase.
- Endpoint/relapse phase: tumours were collected in both non-irradiated and irradiated mice that had reached ethical endpoints due to tumor growth. The exact timing post-grafting/irradiation differed.
- In the PDX1 model, which shows a high rate of metastasis to the olfactory bulb (Fig 10C), metastatic tumours were also collected at the ethical endpoint.

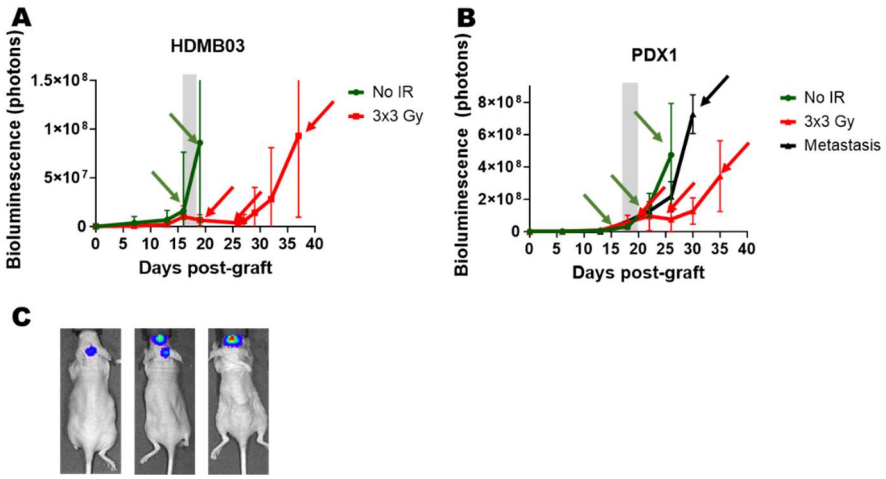

FIGURE 10 OVERVIEW OF THE PLAN FOR BULK RNASEQ EXPERIMENTS.

(A&B) Graphs showing the bioluminescence signals of mice in the bulk RNAseq experiments. Green indicates unirradiated mice, red indicates mice irradiated with 3x3 Gy, and black indicates mice with metastases to the olfactory bulb. Arrows indicate the timepoints for tumor collection. (A) In the HDMB03 model, tumours were collected 24 hours prior to irradiation (control mice), 24 hours after scheduled irradiation (control & irradiated mice – for non-irradiated mice this coincided with 24 hours after irradiation), 7 days after scheduled irradiation (irradiated mice), and at ethical endpoint (control & irradiated mice). (B) In the PDX1 model, tumours were collected 24 hours prior to irradiation (control mice), 24 hours after scheduled irradiation (control & irradiated mice), 5 days after scheduled irradiation (irradiated mice), and at ethical endpoint (control & irradiated mice, and mice with metastases to the olfactory bulb [black arrow]). (D) Example Bioluminescent signals of a mouse with a normal cerebellar tumor (left), both a visible cerebellar tumor and metastasis to the olfactory bulb (center), and a

mouse with a metastasis to the olfactory bulb which exceeds the cerebellar tumor in size to the extent that the signal of the latter is obscured (right).

Preliminary Analysis

The analyses of the bulk RNAseq data remains a work in progress; however, preliminary analysis of the data has begun to reveal some features of the irradiation response. Firstly, principal component analysis of the HDMB03 (Fig 11A) and PDX1 (Fig 12A) data revealed strong clustering of samples between different treatments and timepoints, indicating homogeneity of clustered samples and heterogeneity between different timepoints/treatments. Heatmaps showed similar clustering (Fig 11B and 12B). Together, these results confirm the validity of these experiments. Currently, we have performed targeted analyses to investigate the modulation of pathways of interest in these different samples, as discussed below. Unfortunately, due to low RNA concentrations, some of the timepoints (no irradiation day 0 and +irradiation day 1) in the PDX1 model were excluded from the final analysis.

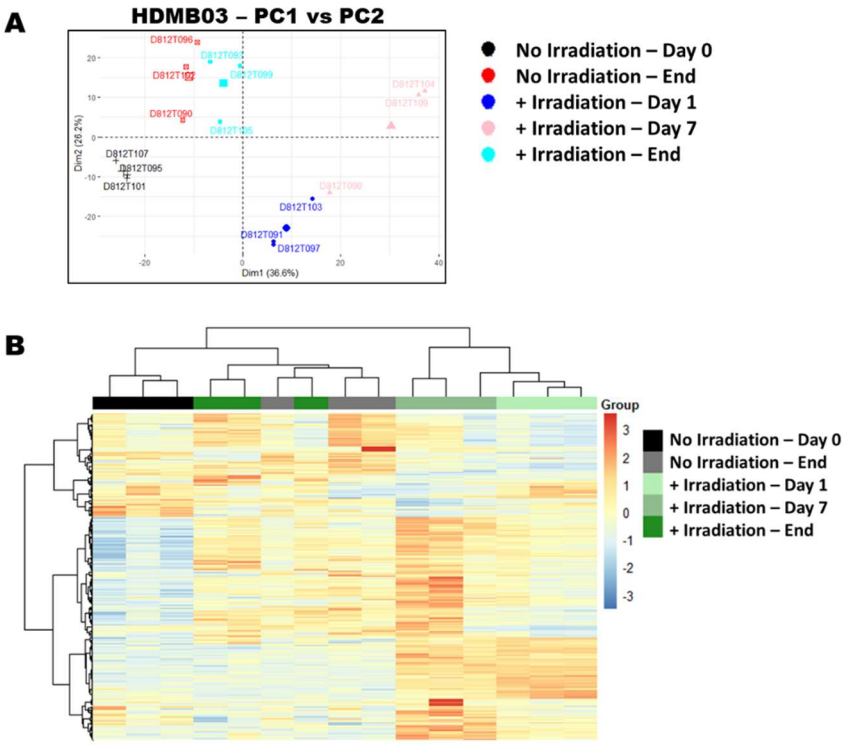

FIGURE 11 PRELIMINARY ANALYSIS OF THE HDMB03 BULK RNASEQ DATA SHOWS STRONG CLUSTERING BETWEEN TREATMENT GROUPS.

(A) Principal component analysis of bulk RNAseq data in the HDMB03 model was performed to identify clustering between different timepoints and treatments (no irradiation vs irradiation). (B) Heatmap showing clustering of the 1000 most variable genes.
Dim, Dimension; IR, Irradiated. PC, Principal component;

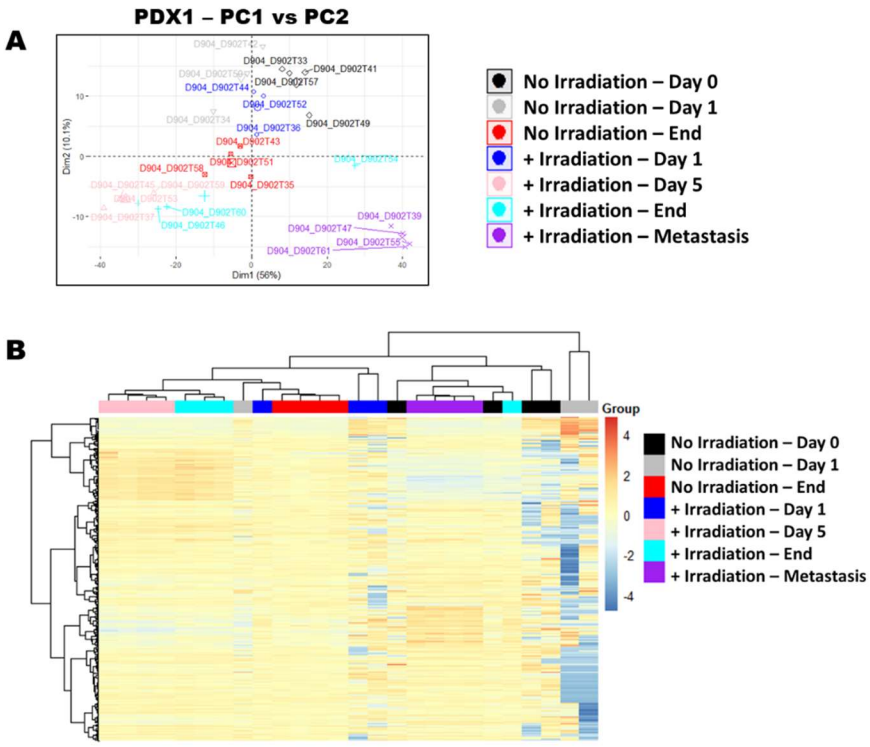

FIGURE 12 PRELIMINARY ANALYSIS OF THE PDX1 BULK RNASEQ DATA SHOWS STRONG CLUSTERING BETWEEN TREATMENT GROUPS.

(A) Principal component analysis of bulk RNAseq data in the PDX1 model was performed to identify clustering between different timepoints and treatments (no irradiation vs irradiation). (B) Heatmap showing clustering of the 1000 most variable genes.
Dim, Dimension; IR, Irradiated. PC, Principal component;

After confirming the validity of our data through PCA and heatmap analyses, we assessed the activity of several target pathways in irradiated and non-irradiated tumours through GSEA and gene expression analyses. As the primary aim of this project was to understand the mechanisms by which MB tumours survived, we initially focused on the control phase of irradiated tumours. Therefore, in all preliminary GSEA analyses, we focused on comparing IR control phase tumours with non-irradiated tumours at the corresponding timepoint (NI end). Further analyses will involve more comparisons. Firstly, we investigated activation of the P53 pathway. GSEA analysis of non-irradiated endpoint vs irradiated control phase tumours revealed an enrichment of genes related to the P53 pathway in irradiated tumours in both the HDMB03 and PDX1 models (Fig 13A). Specific analyses of gene expression revealed no particular trend in TP53 mRNA expression in either model (Fig 13B). We next checked the expression of the well-established P53 target genes CDKN1A (encoding P21) and MDM2. However, in HDMB03, P21 (CDKN1A) was significantly upregulated in tumours immediately post irradiation and in irradiated controlled tumours (Fig 13C); however, this had normalized in irradiated endpoint tumours. Interestingly, the profile of MDM2 expression was quite distinct between the two

models, with an upregulation in irradiated HDMB03 tumours and very little expression in non-irradiated tumours (Fig 13D). Conversely, in PDX1, MDM2 expression showed no correlation with irradiation, but was upregulated in metastases (Fig 13D).

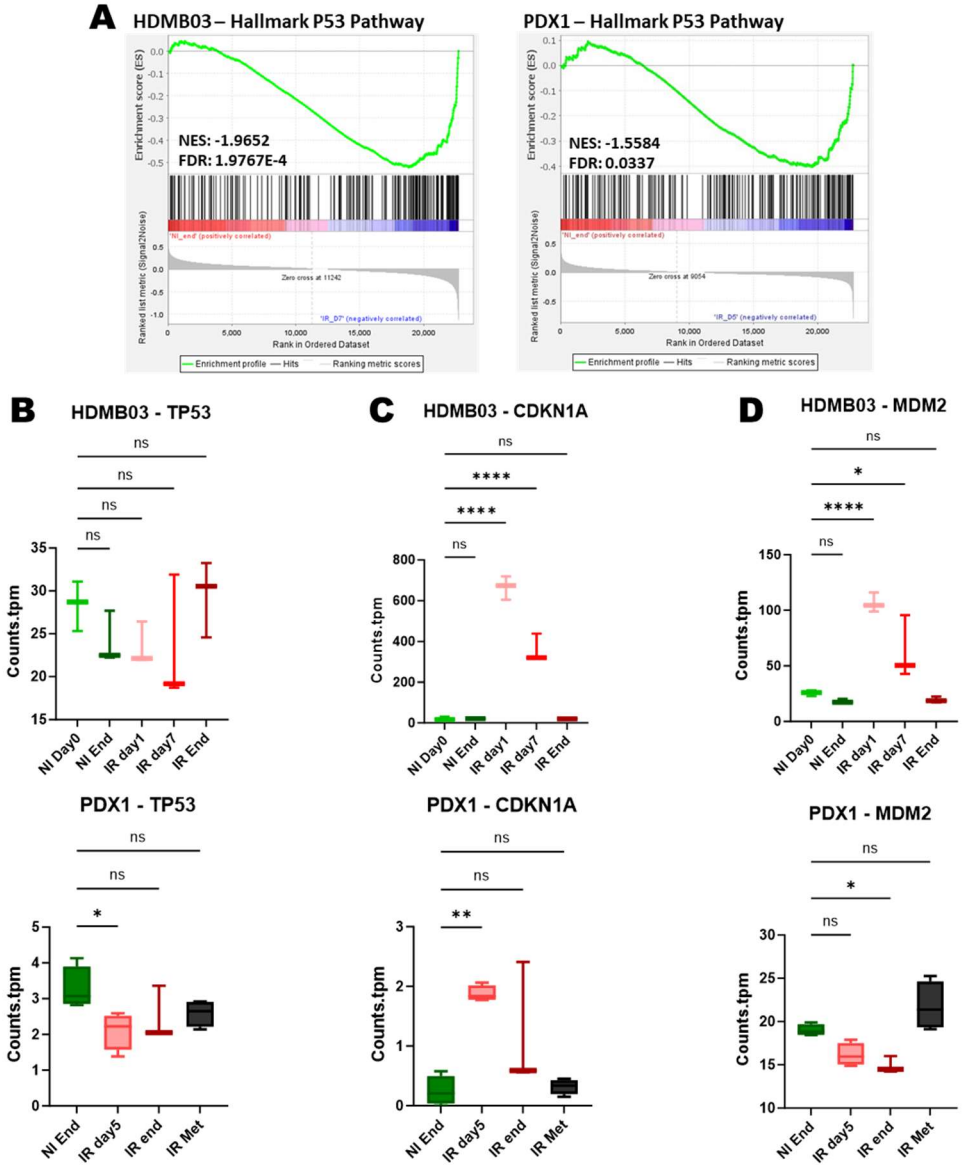

FIGURE 13 THE P53 PATHWAY IS UPREGULATED IN IRRADIATED TUMORS

(A) GSEA analysis of P53 pathway activation in non-irradiated endpoint tumors and irradiated control phase tumors in HDMB03 (left panel) and PDX1 (right panel) grafted tumors. Expression plots of the P53 pathway genes P53 (B), CDKN1A (C), and MDM2 (D) in HDMB03 (top panel) and PDX1 (bottom panel) grafted tumors. All statistical differences were assessed by one-way ANOVA.
GSEA, Gene set enrichment analysis; IR Day 5/7, tumors in the control phase 5 (PDX1) or 7 (HDMB03) days post-irradiation; IR End, Irradiated tumors collected at ethical endpoint; NI day0, non-irradiated tumors collected at the start of the irradiation regimen; NI day1, non-irradiated tumors collected at the end of the irradiation regimen; NI end, non-irradiated tumors collected at ethical endpoint.

Subsequently, we investigated activation of apoptosis in irradiated tumours across our models. Firstly, GSEA analysis of non-irradiated endpoint tumours vs irradiated control-phase tumours

showed that the latter condition was positively correlated with apoptosis signatures (Fig 14A). Further, expression analysis of apoptosis-related genes (Fig 14B-D) revealed an increase in expression of the pro-apoptotic genes BAX and BAK in irradiated HDMB03 tumours, with a trend towards a decrease in expression of the anti-apoptotic BCL2 gene. However, no such profile was observed in PDX1 tumours, indicating an important difference between the models.

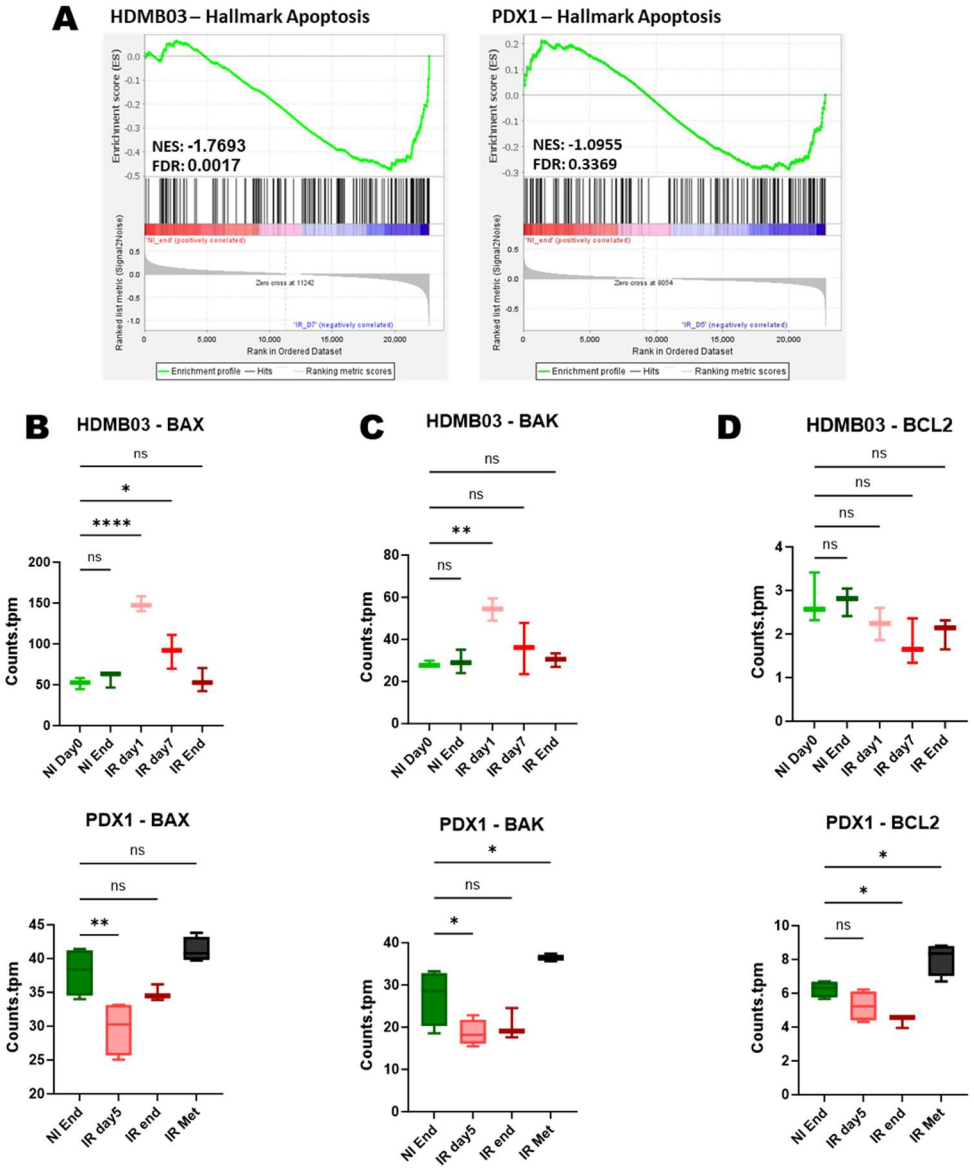

FIGURE 14 THE APOPTOSIS PATHWAY IS STRONGLY UPREGULATED IN IRRADIATED HDMB03 TUMORS, WITH LESS EFFECT IN PDX1

(A) GSEA analysis of apoptosis pathway-related genes in non-irradiated endpoint tumors and irradiated control phase tumors in HDMB03 (left panel) and PDX1 (right panel) grafted tumors. Expression plots of the apoptosis pathway-related genes BAX (B), BAK (C), and BCL2 (D) are shown in HDMB03 (top panel) and PDX1 (bottom panel) grafted tumors. All statistical differences were assessed by one-way ANOVA.
GSEA, Gene set enrichment analysis; IR Day 5/7, tumors in the control phase 5 (PDX1) or 7 (HDMB03) days post-irradiation; IR End, Irradiated tumors collected at ethical endpoint; NI day0, non-irradiated tumors collected at the start of the irradiation regimen; NI day1, non-irradiated tumors collected at the end of the irradiation regimen; NI end, non-irradiated tumors collected at ethical endpoint.

As we have previously noted a G2/M arrest following irradiation in group 3 models in vitro (data not shown), we further investigated activation of the G2/M cell cycle checkpoint. Interestingly, in contrast to our expectations, GSEA analysis revealed a decrease of G2/M arrest-related signatures in control phase tumours compared to non-irradiated tumours (Fig 15A). Subsequent analyses of expression of G2/M-associated genes revealed a trend towards a decrease for the DNA damage sensor ATM (Fig 15B) and a significant decrease in its downstream kinase CHEK2 (Fig 15C) in irradiated tumours in both models. Similarly, mRNA expressions of the DNA damage sensor ATR (Fig 15D) and its downstream kinase CHEK1 (Fig 15E) were decreased in irradiated tumours (although not significantly for ATR).

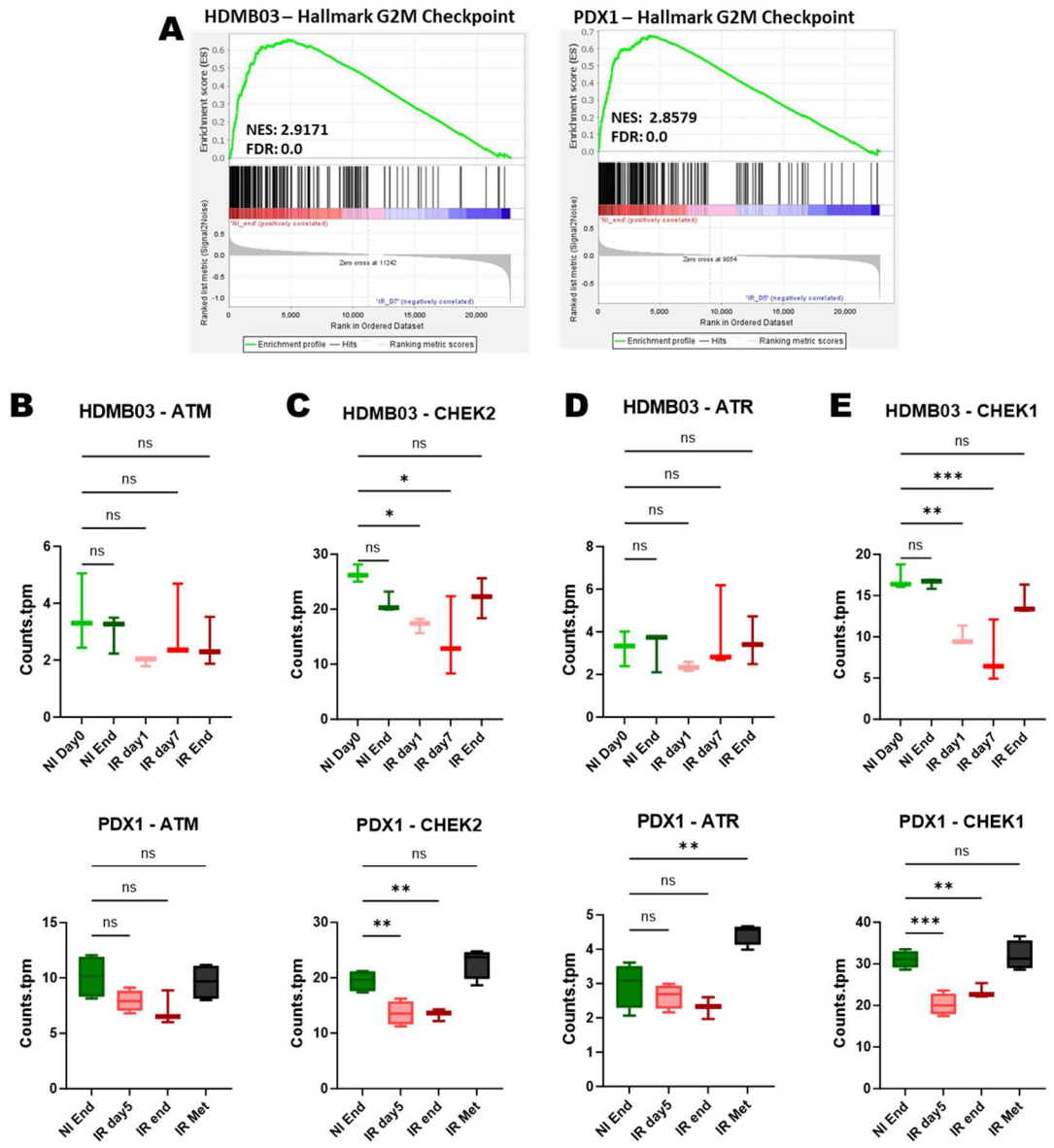

FIGURE 15 THE G2/M PATHWAY IS DOWNREGULATED IN IRRADIATED TUMORS.

(A) GSEA analysis of G2/M arrest pathway activation in non-irradiated endpoint tumors and irradiated control phase tumors in HDMB03 (left panel) and PDX1 (right panel) grafted tumors. Expression plots of the pathway

genes ATM (B), CHEK2 (C), ATR (D), and CHEK1 (E) in HDMB03 (top panel) and PDX1 (bottom panel) grafted tumors. All statistical differences were assessed by one-way ANOVA.
GSEA, Gene set enrichment analysis; IR Day 5/7, tumors in the control phase 5 (PDX1) or 7 (HDMB03) days post-irradiation; IR End, Irradiated tumors collected at ethical endpoint; NI day0, non-irradiated tumors collected at the start of the irradiation regimen; NI day1, non-irradiated tumors collected at the end of the irradiation regimen; NI end, non-irradiated tumors collected at ethical endpoint.

Finally, we performed some initial analyses to investigate the relative importances of the two major pathways of double strand break repair: non-homologous end joining (NHEJ, Fig 16) and homologous recombination (HR, Fig 17). GSEA analysis of NHEJ revealed no significant differences between non-irradiated endpoint and irradiated control phase tumours (Fig 16A). Interestingly, expression analysis of PRKDC, which encodes DNA-PK, revealed a decrease in expression in irradiated tumours in both HDMB03 and PDX1 (although this only reached significance in PDX1). Conversely, expression of LIG4 (Ligase 4) was increased in control-phase PDX1 tumours (Fig 16C). No particular trend was observed in the expression of the NHEJ-player Artemis in HDMB03 tumours, whereas it was decreased in irradiated PDX1 tumours (Fig 16D). GSEA analysis of HR-associated genes revealed a downregulation in irradiated tumours vs non-irradiated tumours in both HDMB03 and PDX1 (Fig 17A). This result was validated by expression analysis of the HR mediators RAD51 (Fig 17B), BRCA1 (Fig 17C), and BRCA2 (Fig 17D), all of which showed at least a trend towards a decreased expression in irradiated tumours. Together, these results indicate that the HR is downregulated in group 3 medulloblastoma tumours exposed to irradiation.

Overall, these preliminary analyses indicate the validity of our models, showing increased apoptosis and P53 activation in irradiated tumours. However, significantly more investigation of these data is required to show the overview of the mechanisms of radiation escape of group 3 MB.

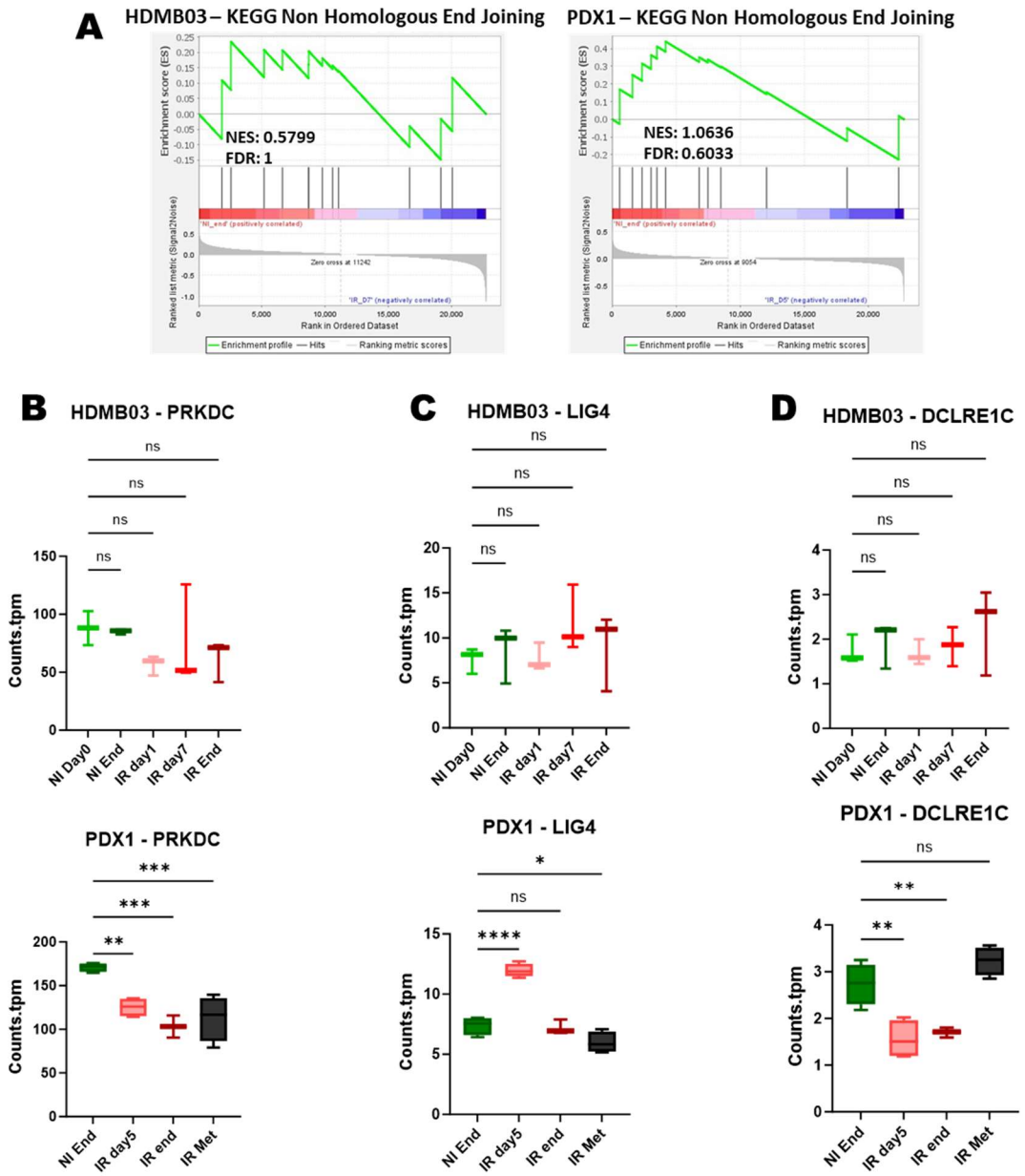

FIGURE 16 THE NON-HOMOLOGOUS END JOINING PATHWAY SHOWS NO SIGNIFICANT ALTERATION WITH IRRADIATION.

(A) GSEA analysis of apoptosis pathway-related genes in non-irradiated endpoint tumors and irradiated control phase tumors in HDMB03 (left panel) and PDX1 (right panel) grafted tumors. Expression plots of the genes PRKDC [encoding DNA-PK] (B), LIG4 [encoding Ligase 4] (C), and DCLRE1C [encoding Artemis] (D) in HDMB03 (top panel) and PDX1 (bottom panel) grafted tumors. All statistical differences were assessed by one-way ANOVA.

GSEA, Gene set enrichment analysis; IR Day 5/7, tumors in the control phase 5 (PDX1) or 7 (HDMB03) days post-irradiation; IR End, Irradiated tumors collected at ethical endpoint; NI day0, non-irradiated tumors collected at the start of the irradiation regimen; NI day1, non-irradiated tumors collected at the end of the irradiation regimen; NI end, non-irradiated tumors collected at ethical endpoint.

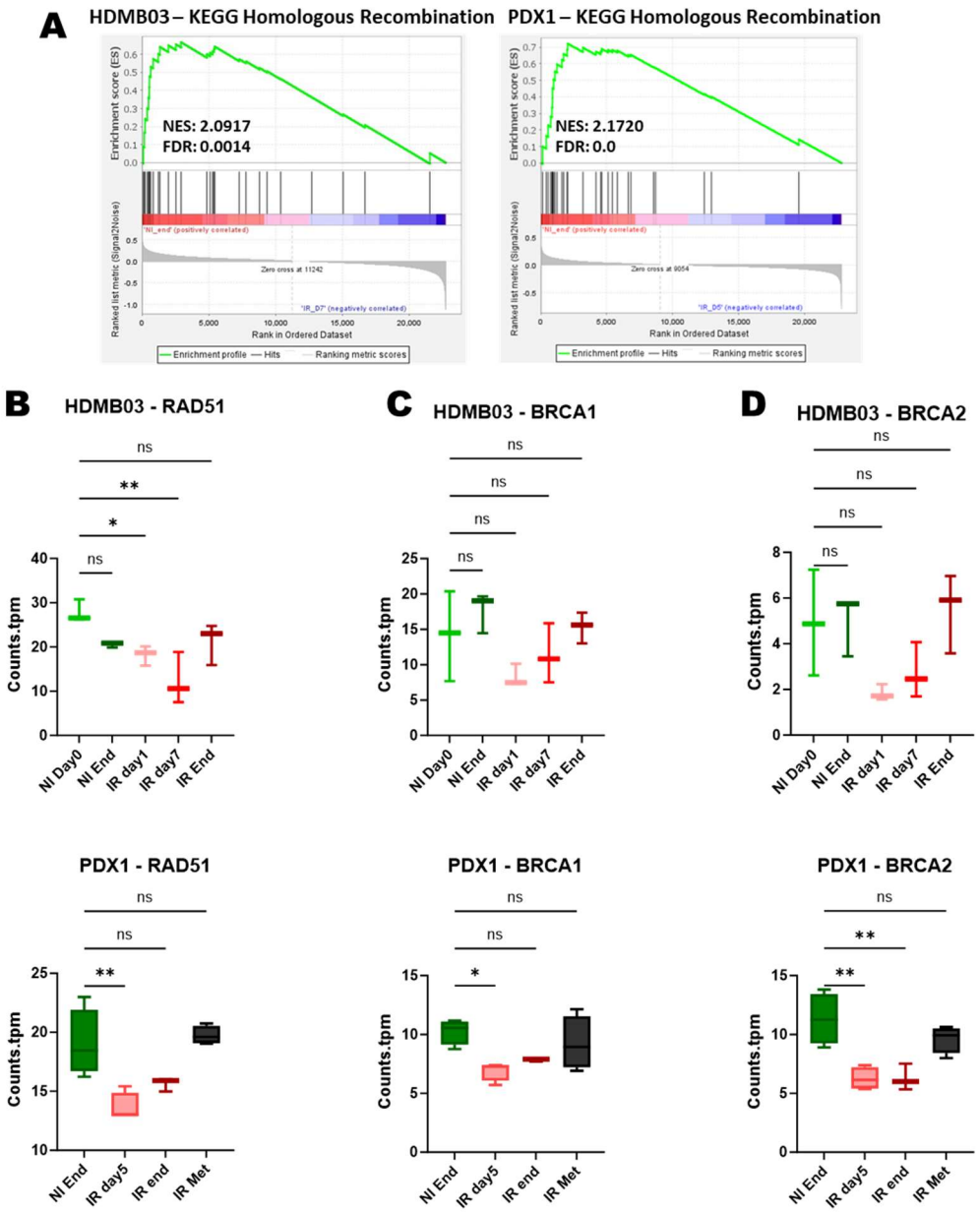

FIGURE 17 THE HOMOLOGOUS RECOMBINATION PATHWAY IS DOWNREGULATED IN IRRADIATED TUMORS.

(A) GSEA analysis of homologous recombination pathway-related genes in non-irradiated endpoint tumors and irradiated control phase tumors in HDMB03 (left panel) and PDX1 (right panel) grafted tumors. Expression plots of the genes Rad51 (B), BRCA1 (C), and BRCA2 (D) in HDMB03 (top panel) and PDX1 (bottom panel) grafted tumors. All statistical differences were assessed by one-way ANOVA. GSEA, Gene set enrichment analysis; IR Day 5/7, tumors in the control phase 5 (PDX1) or 7 (HDMB03) days post-irradiation; IR End, Irradiated tumors collected at ethical endpoint; NI day0, non-irradiated tumors collected at the start of the irradiation regimen; NI day1, non-irradiated tumors collected at the end of the irradiation regimen; NI end, non-irradiated tumors collected at ethical endpoint.

Post transcriptional regulation associated with relapse: Phosphoarray analysis

It is well known that transcriptional profiles do not always fully mirror the cellular proteomic landscape, as many changes occur post-translationally. Although transcriptomic alterations represent an important aspect of cellular adaptation, many other pathways, including cell signalling and activation of resilience pathways (e.g. DNA repair, apoptosis, cell cycle arrest, etc.) are also regulated at the post-translational level. As such, as an addendum to the RNAseq analysis, we further performed a phosphoarray analysis using the Phospho Explorer Antibody Array from FullMoon Biosciences (France) to investigate some of the post-transcriptional modifications which could be observed in irradiated tumours. This array comprises 1318 antibodies which can be used to assess activation of over 30 signalling pathways. For this analysis, we assessed stereotactically-grafted PDX1 tumours at three different timepoints: non-irradiated and irradiated primary tumours at the ethical endpoint, and irradiated tumours in the control phase (5 days post the final irradiation dose). The timecourse of the experiment is similar to those shown in Fig 9C and Fig 10B.

Unfortunately, as only one replicate of this experiment has so far been performed, no final analyses have yet been performed, and no statistical analyses could be conducted. Nevertheless, initial analyses have indicated a potential upregulation of ATM and ATR (data not shown) in relapsed irradiated endpoint tumours compared to non-irradiated endpoint tumours. This result indicates a possible increase in replication stress in relapsed tumours, which has previously been shown to be therapeutically targetable[302].

Identification of cellular drivers of relapse: scRNAseq

As mentioned in the introduction, it has been well-established that therapy resistance is often driven by the presence of cells which are intrinsically resistant, due to either genetic or non-genetic mechanisms. As previous studies have shown the importance of non-genetic resistance pathways in response to irradiation in medulloblastoma[89,370], we sought to investigate the potential role this may play in driving relapse. As such, to achieve a better understanding of the mechanisms of escape of group 3 medulloblastoma, and to identify persister cell populations which may escape from irradiation to allow relapse, we performed an scRNAseq experiment in the PDX1 in vivo model. The aim of this experiment was to track cell populations in tumours at different stages of tumour growth with and without irradiation in order to identify specific

cell populations which may drive radiation resistance and/or recurrence. The timepoints for assessment were the same as those for the bulk RNAseq experiment in PDX1 (24 hrs pre-irradiation, 24 hrs post-irradiation, control phase, and ethical endpoint for unirradiated and irradiated cerebellar tumours, as well as metastasis to the olfactory bulb). These collection points are described in detail above, and illustrated in Fig 10B. The timecourse of the experiment is similar to those shown in Fig 9C and Fig 10B.

In brief, for this experiment, we sacrificed mice at the different timepoints mentioned above, and dissected the brains under a GFP fluorescence lamp to collect tumours with as little of the mouse brain as possible (Fig 18A). These tumours were then dissociated enzymatically, as described in the methods section, and suspended in PBS + 10% FBS on ice. FACS was then performed to separate GFP+ tumour cells from contaminating mouse brain cells (Fig 18B). Immediately after sorting, cells were processed on the 10x Genomics Chromium™, Single-Cell RNA-Seq System, targeting 10,000 cells/condition.

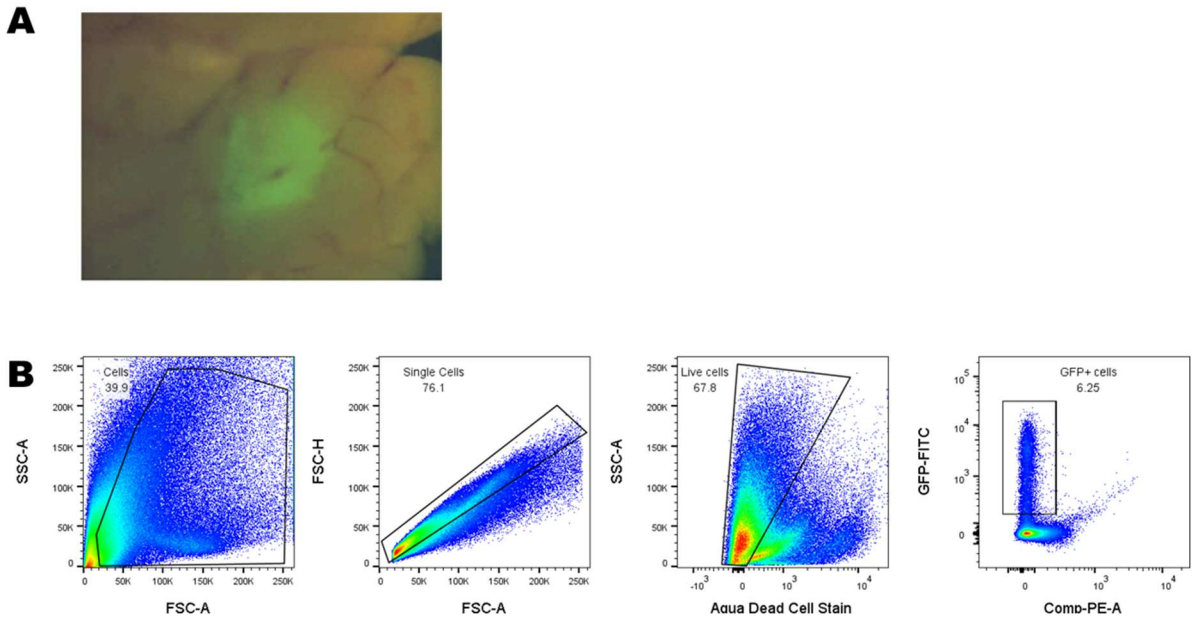

FIGURE 18 EXPERIMENTAL CONDITIONS FOR THE COLLECTION OF GFP+ TUMOUR CELLS FOR SCRNASEQ

(A) PDX1 tumours could be visualized by GFP signal to allow accurate macrodissection of the tumour. (B) Live, GFP+ tumour cells were separated from dead cells and contaminating mouse brain cells by FACS. In brief, cells were separated from debris by gating in the FSC-A and SSC-A channel. Single cells were separated from doublets by assessing the FSC-A/FSC-H profile. Live cells were separated from dead cells by gating for cells which did not uptake the aqua dead cell stain. Finally, GFP+ cells were separated from non-GFP+ cells by gating for GFP expression.
FACS, Fluorescence activated cell sorting; FSC, forward scatter; SSC, side scatter.

Currently the analysis of the scRNAseq data has not yet been performed. As such, I am unfortunately unable to comment on the results of this experiment. Nevertheless, there are

several avenues that we hope to investigate in the near future. Most importantly, we plan to investigate the potential role of CSCs in MB escape from radiotherapy. Indeed, many studies have shown a link between CSCs and radioresistance/recurrence, with research showing both that tumour irradiation drives the generation of CSCs from non-stem like radiosensitive cells in some instances[94], while in other circumstances, radiation selects for radioresistant CSCs[95,96] in other cancers. Further, several studies have shown a potential role of CSCs in MB treatment escape. Firstly, one study of patient biopsies revealed increased expression of the stem cell/glial fate marker SOX9 in relapsed tumours compared to tumours at initial treatment[98]. Another study using in vivo murine models revealed that quiescent cells expressing the multipotent stem cell marker SOX2 were more resistant to anti-mitotic chemotherapy, thereby promoting relapse in a murine model of SHH MB[99]. Regarding radiation in particular, one study showed that stem-like CD133+ DAOY cells showed a greater resistance to irradiation than corresponding CD133- cells[97]. Although research specifically investigating the role of CSCs in promoting relapse from radiotherapy in MB remains relatively underdeveloped, considering the considerable evidence supporting the role of CSCs in escape from radiotherapy in other cancers, it is likely that a similar effect may be observed in MB.

Identification of genes required for relapse: CRISPR-Cas9 screen

As prior research has identified genetic divergence between original and matched relapse tumours[80,370], we sought to further assess the roles of genetic mechanisms of radiotherapy escape in group 3 MB. To achieve this, we performed a negative CRISPR screen to identify genes which drive radiation resistance in group 3 MB. The aim of this experiment was again to gain an improved understanding of the mechanisms underlying radiotherapy escape, as well as to identify potential targets for treatment.

The first stage of this project was the construction of Cas9-expressing clones, which were produced from the cell line D425MED, as outlined in the methods. In brief, D425MED clones were infected with a Cas9-mCherry vector, after which individual cells (clones) were separated by FACS and allowed to grow. After amplification of these clones, the lines which showed the greatest similarity to non-infected cells in terms of morphology and growth characteristics were tested for Cas9 expression and efficacy. First, mCherry expression was assessed by FACS (Fig 19A), and Cas9 expression was assessed by western blot (Fig 19B). The clones with the highest Cas9 expression (clones 1, 4, and 14 in Fig 19) were then taken forwards for Cas9 activity testing. Activity testing was performed over a time course (5, 8, 10, and 12 days post-infection) to assess the timepoint with the optimal cutting efficiency. One clone (clone 14 in Fig 19)

showed the highest cutting efficiency of ~70% at 10 days post-infection. For verification, this timecourse analysis was repeated again to confirm the cutting efficiency (Fig 19C).

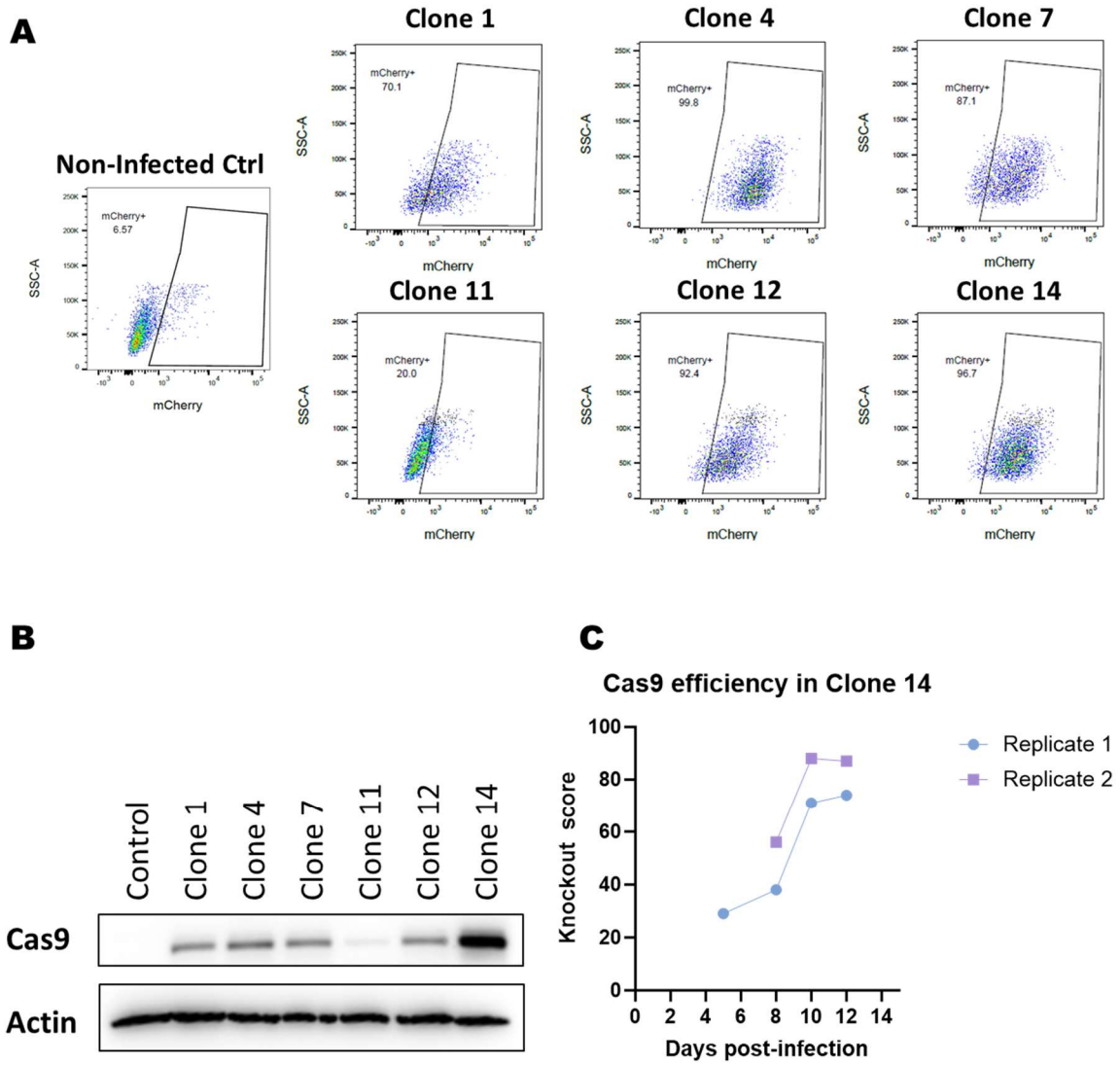

FIGURE 19 PILOT EXPERIMENTS WERE CONDUCTED TO CONSTRUCT AND VALIDATE A CAS9-COMPETENT D425MED CELL LINE.

(A) FACS for mCherry expression in different cell lines grown from Cas9-expressing D425MED clones (clones 1, 4, 7, 11, 12, and 14) compared to a non-infected control. (B) Western blots to assess Cas9 expression in Cas9-expressing D425MED clones (clones 1, 4, 7, 11, 12, and 14). (C) Graph showing the results of the Cas9 efficiency testing (shown as the knockout score, y-axis) of D425MED clone 14 at different days post-infection with an exemplar gRNA (x-axis). Two replicates are shown.
FACS, fluorescence activated cell sorting.

After verifying the efficacy of the Cas9 clone produced, the CRISPR-Cas9 screen was completed in duplicate following the schedule outlined in Figure 20, and the experimental procedures outlined in the methods section. In brief, D425MED cells were seeded, infected with the Brunello gRNA library, and maintained for 10 days to allow maximal cutting of the target genes. Cells were then split, and irradiated with a fractionated regimen of 3x2 Gy, administered

over three consecutive days. Samples of 40-50 million cells were collected under irradiated and non-irradiated conditions at each doubling time. In the final analysis, the relative abundances of gRNAs in the irradiated and unirradiated samples were compared to identify gRNAs depleted in the irradiated condition. The targets of these gRNAs could be considered as necessary for radiation resistance.

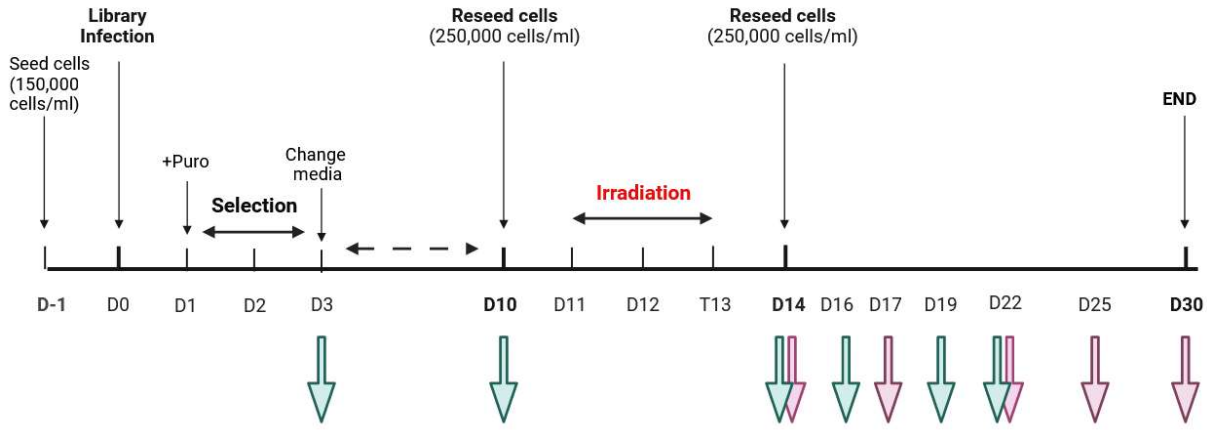

FIGURE 20 OVERVIEW OF THE SCHEDULE FOR THE CAS9 SCREEN IN D425MED

On day -1, cells were seeded in T125 flasks at a density of 150,000 cells/ml. On day 0, cells were infected with viruses expressing the Brunello library, at a concentration targeting a multiplicity of infection of 30%. On day 1, puromycin was added to cultured cells to reach a concentration of 1 µg/ml. On day 3, cells were centrifuged and resuspended in fresh media. Between days 3 and 10, cells were passaged 1 in 3 twice a week. On day 10, cells were seeded in T75 flasks at a density of 250,000 cells/ml. Cells were irradiated with 3 doses of 2 Gy on days 11, 12, and 13. On day 14, cells were reseeded at a density of 250,000 cells/ml. Green arrows represent timepoints for collected of unirradiated cells. Red arrows represent timepoints for collection of irradiated cells. At each collection, 40-50 million cells were collected and frozen to ensure complete representation of the library.

Preliminary results:

Unfortunately, analysis of the CRISPR-Cas9 screen in the D425MED screen revealed very few hits, due largely to a lack of statistical power caused by the low number of replicates (two) and high background selection caused by the long period between library infection and selection with irradiation. Nevertheless, comparison of irradiated and non-irradiated cells at the final timepoint revealed significant depletion of gRNAs targeting TLR9, ATM, WDR11, and SWSAP1 in the irradiated condition (data not shown). The presence of TLR9, a toll-like receptor which is known to induce a pro-inflammatory cytokine response following binding to DNA (largely bacterial or viral), is strange given that this receptor is primarily involved in the immune response and is most commonly expressed by immune cells[371]. However, the other hits may be more promising avenues of research. Of these, SWSAP1 is a RAD51 paralogue[372] which has been shown to drive inter-homolog homology-directed repair and sister-chromatid exchange, thereby inhibiting heterozygosity implicated in tumorigenesis[373]. Further, WDR11

has been identified as a potential driver of group 3 medulloblastoma[374], while ATM is a well-known possible target for radiosensitization in cancers[171–175]. However, it should be noted that our screen of DDR inhibitors (results chapter 1) revealed no effect of ATM inhibition in any group 3 cell lines either with or without irradiation.

7.5 Plans for Future Analyses:

The next step in this project will be to complete the bioinformatic analyses of the bulk and scRNAseq data, and to perform more replicates of the CRISPR screen in D425MED and other cell lines. Although the aforementioned preliminary analyses of this data have identified some global alterations in transcriptional profiles, much deeper investigation is required. In this section, I will discuss our plans for the immediate future.

Firstly, we plan to compare the transcriptional signatures of all of the tumor types (irradiated, non-irradiated, and metastasis) to identify differences between these tumours. The aim of this analysis is to identify the differences between relapsed and primary tumours, which would provide clues for how relapsed tumours escape irradiation to drive relapse. To achieve this, as radiotherapy is known to primarily (although certainly not exclusively) induce tumor killing via the induction of DNA damage repair pathways, we first plan to more deeply investigate the different activities of the homologous recombination (HR) and non-homologous end joining (NHEJ) pathways. Indeed, prior research has shown that the majority of double-strand breaks induced by ionizing radiation are repaired by NHEJ[158]. We therefore hope to investigate this pathway more deeply. Further, we hope to better characterize the interplay between these two repair pathways, particularly in the immediate response to irradiation. In addition, although we have already shown activation of apoptosis in irradiated tumours, we plan to investigate more deeply the importance of the extrinsic and intrinsic apoptosis pathways in the radiation response. The intrinsic apoptosis pathway is generally considered to be the primary apoptosis pathway activated by irradiation[375,376], and has been shown to induce radiation sensitivity in transgenic mouse models of SHH MB[377]. However, the extrinsic pathway is also upregulated following irradiation in some cancers due to modulation of the tumor microenvironment[378]. In addition, we will look at the activation of other cell death pathways, such as necrosis. Further, we hope to look more deeply at the cell checkpoint landscape of irradiated tumours, to better assess the cell profile in response to irradiation. These analyses would focus primarily on comparing the bulk and scRNAseq data of irradiated and non-irradiated samples collected 24 hours after the final irradiation dose. Results of these analyses should identify the entire

landscape of the mechanisms by which radiation induces cell death in group 3 medulloblastoma tumours.

Further, through better understanding of the biology of tumours in different stages of the response to irradiation, we hope to identify the mechanisms by which cells escape radiotherapy. This will be achieved through comparison of the signatures of irradiated tumours in the control/minimal residual disease phase with non-irradiated tumours at the same time-points. Although the bulk RNAseq analysis will undoubtedly be helpful for this, analysis of the scRNAseq data will be key. In brief, we aim to potentially look at signatures of cancer stem cells, which are well known to drive relapse[92,93], to identify whether a plastic stem-cell like population of cells may drive radioresistance and recurrence. Further, we will look at different metabolic pathways to identify any differences in metabolism of these cells, as metabolism is an important determinant of therapy resistance[379,380]. Specific pathways to investigate include glycolysis[381,382], which has been shown to be important for therapy resistance, and oxidative phosphorylation, which has been shown to play a role in radioresistance in some cancers[383,384]. All of these aforementioned analyses will be complemented by further investigation of the phosphoarray data, which should further identify some post-transcriptional modifications unique to irradiated tumours.

In addition to further analysis of the in vivo data, we plan to also develop the existing data obtained from the CRISPR screen. As previously discussed, the initial analyses of the CRISPR-Cas9 screening data failed to reveal many potential targets due to a lack of statistical power. As such, further replicates must be conducted in the future. Once these are completed, analysis will be performed to identify genes which are enriched or depleted in irradiated vs non-irradiated cells. The idea of this analysis is that genes enriched in the irradiation population are those which drive radioresistance; these may be potential targets for inhibition to induce radiosensitization. In the meantime, it may be interesting to investigate the roles of the genes identified in the CRISPR-Cas9 screen in the response to irradiation, of which ATM, WDR11, and SWSAP1 may be the most important.

7.6 Future directions and perspectives:

Overall, although significant experimental work has been conducted, and bioinformatics analyses have been initiated, this project remains in the nascent stages. Firstly, and most importantly, the bioinformatics analyses will need to be completed for all of the bulk and scRNAseq experiments, as outlined above. Finalized analyses of the bulk RNAseq data should

identify the overall landscape of the tumours at different stages of the response to irradiation, which should allow the identification of possible pathways that may be therapeutically targetable at this stage. However, it should be noted that both of the models used for this experiment (HDMB03 and PDX1) are relatively sensitive to irradiation. It may therefore also be interesting to repeat this bulk RNAseq experiment in a more radioresistant model, such as the D425MED cell line, for which the in vivo experimental analyses have already been set up. Furthermore, once complete, analysis of the scRNAseq data should provide interesting information regarding tumoural heterogeneity at the different stages of tumour response. Overall, this analysis should allow us to determine whether relapse is driven by a specific population of persister cells, possibly cancer stem cells, which show a greater intrinsic resistance to irradiation.

Regarding the CRISPR-Cas9 screen, there are currently plans to also perform this screen in the more radiation-sensitive cell line HDMB03. Unfortunately, this arm of the project is still in the very early stages, as production of a Cas9-expressing clone with a sufficiently high cutting efficiency remains a work in progress.

Once all of these screens have been completed, and the results have been analyzed, this work should identify a number of pathways and genes which play an important role in the escape from radiotherapy in group 3 medulloblastoma. This should allow the identification of potential therapeutic targets or drugs which may increase the sensitivity of group 3 tumours to irradiation. Thus, this project should both broaden our understanding of the mechanisms of relapse in medulloblastoma, and allow the identification of novel therapeutic strategies to decrease the rates of relapse and mortality in this vulnerable patient population.

8. Discussion

With the exception of some changes in precise timing or dosage, the therapeutic modality for medulloblastoma has remained largely static for decades, with therapy generally comprising surgical resection followed by radio and chemotherapy, among which radiotherapy is necessary to achieve cure. Despite achieving a 5-year survival rate of ~70%, post-therapy relapse of medulloblastoma remains an important cause of death among pediatric cancer patients, while the mechanisms underlying this relapse remain poorly understood. As such, the development of novel therapeutic strategies to improve response to first-line treatment, including radiotherapy, remains an important unmet need in the field. Throughout my PhD, I have conducted research to identify targeted therapies to increase the response of group 3 medulloblastoma to radiotherapy, and to understand the mechanisms by which these tumours escape radiation to relapse.

In this discussion, I will elaborate on some of the points discussed in the results sections, specifically discussing the future applications of the work investigating the mechanisms by which group 3 MB escapes radiotherapy to form relapse. Further, I will elaborate on the knowledge regarding DNA-PK in medulloblastoma and the possibility of its targeting as a radiosensitizer in the clinic.

8.1 Targeting radiation resistance mechanisms to improve therapeutic outcomes

DNA-PK in Medulloblastoma:

Although the global analyses discussed in the second results chapter of this thesis are still needed to understand the exact pathways underlying irradiation escape in group 3 MB, there are some mechanisms which are universally required to survive radiation insult. Among these, the DNA damage repair networks and cell cycle checkpoints feature heavily. While the relative importances of the exact repair pathways (SSB repair, NHEJ, and HR) and checkpoints (G1, S, and G2/M) activated by irradiation differ among different cancers and cell types, DNA repair and modulation of cell cycling on some level have been well-established as key in cellular survival of irradiation[155]. It was this knowledge that drove us to perform the targeted screen of DNA damage repair inhibitors which identified DNA-PK as a target for radiosensitization in group 3 MB.

As discussed in the introduction (sections 4.2 and 4.3), DNA-PK plays a well-established role in a variety of cancers. However, its action in medulloblastoma remains relatively poorly understood. Although a few prior studies have presented preliminary evidence to suggest an important function of DNA-PK in medulloblastoma, none have so far proposed a solid basis for therapeutic targeting as a radiosensitizer. Regarding the existing papers investigating DNA-PK, one study showed that dual inhibition of DNA-PK and telomerase was cytotoxic in the MB cell line ONS-76[350], while another showed that inhibition of DNA-PK with the inhibitor NU7441 radiosensitized the MB cell lines DAOY and D283MED to radiation[351]. Only one paper has so far investigated the potential role of DNA-PK in group 3 specifically: this study, which primarily investigated the proteomic profiles of different MB subgroups, presented in vitro results indicating an association between phosphorylated MYC and phosphorylated DNA-PK, subsequently finding that inhibition of DNA-PK sensitized the D458MED group 3 MB cell line, but not the non-group 3 DAOY cell line, to irradiation *in vitro*[352].

Although the results of these studies validate our proposition of DNA-PK as a therapeutic target in MB, particularly the observation of a radiosensitizing effect in the group 3 MB cells lines D283MED[351] and D458MED[352], my project significantly extends this preliminary work. Indeed, these abovementioned papers did not investigate the mechanisms of action of DNA-PK, nor did they deeply investigate the therapeutic possibilities of DNA-PK inhibition.

Radiosensitization through inhibition of DNA-PK in Medulloblastoma: Future perspectives

In our paper 'The DNA-PK inhibitor Peposertib as a radiosensitizer in high-risk Group 3 pediatric medulloblastoma.' (results chapter 1), we validated the drug peposertib as a radiosensitizing treatment in group 3 MB with good tolerability in pediatric models, and have begun to outline the mechanisms underlying its activity.

Although our work did begin to identify the mechanisms underlying the action of peposertib in group 3 MB, room for further research remains. In our study, apoptosis analysis revealed an increase in apoptosis with combined treatment vs irradiation alone, while cell cycle analysis revealed an increase in G2/M arrest. This latter result is consistent with the results of several prior studies, which showed that treatment of cancer cells with peposertib resulted in a G2/M arrest when combined with DNA-damage inducing agents[347,385]. The lack of any observable G1 arrest, despite the known activity of the NHEJ pathway in this stage of the cell cycle, may be due to the MYC-amplified nature of the cells, as MYC has been shown to 'push'

cells past the G1 checkpoint despite the presence of DNA damage[386]. Further, our immunofluorescence analysis for γH2AX definitively showed an increase in DNA damage in cells treated with peposertib and irradiation vs irradiation alone, while similar analysis of 53BP1 (which is known to promote NHEJ following association with DSBs[387]) foci indicated that treatment decreased the activity of the NHEJ pathway. This increase in DNA damage, as assessed by γH2AX foci, has been previously shown in several studies investigating the effects of peposertib with irradiation[358,361]. Further, as it has been shown that NHEJ is responsible for the repair of ~80% of DSB breaks induced by X-ray irradiation[158], it is likely that this increase in total DNA damage is largely due to the observed decrease in NHEJ activation. However, it would still be interesting to investigate whether peposertib treatment also influences the homologous recombination repair pathway, as prior research has shown that DNA-PK plays a modulating role in this pathway as well, primarily in decision making between the NHEJ and HR pathways[291]. This investigation could initially be performed by assessing foci of RAD51, a key player in HR repair[182]. To further assess the importance of these two repair pathways in combination with peposertib, we may also assess the killing effect of the peposertib/irradiation combination in cells knocked-down for the NHEJ factors ligase 4 or KU and the HR factors BRCA1 and BRCA2.

Finally, the results of our mechanistic analysis suggest that peposertib drives apoptosis and cell cycle arrest in group 3 MB by triggering an accumulation of DNA damage caused by the blocking of the NHEJ repair pathway. However, it should be noted that our preliminary results showing an association between expression of *MYC* and *PRKDC*, and the results of a prior study indicating an association between MYC and DNA-PKcs phosphorylation/activation[352], both indicate the potential importance of the cells' MYC status in the response to DNA-PK inhibition. As such, the interplay between MYC and DNA-PK in group 3 MB, as well as the influence of MYC status on the response of MB cells to DNA-PK inhibition, represent an important avenue for future research. The characterization of this interplay would be important in understanding both the mechanisms of action of DNA-PK inhibition, and in stratifying patients for potential treatment. For example, it is possible that group 3 MB patients with MYC amplifications (classified as group 3γ) may show a greater response to DNA-PK inhibition. Indeed, our results showed that the non-group 3 cell lines DAOY and ONS-76, as well as the non-MYC amplified cell line D283MED, were less sensitive to DNA-PK inhibition; it is possible that this may be due to the relatively decreased activity of MYC in these non-group 3 cell lines.

Indeed, in addition to the aforementioned specific medulloblastoma paper, several studies have shown a link between DNA-PK and MYC in other cancers. One study showed that MYC was directly phosphorylated by activated DNA-PKcs in Raji Burkitt's lymphoma[312], while another showed that DNA-PK drove cell proliferation and oncogenic transformation by stabilizing MYC through modulation of the Akt/GSK3 pathway[388]. Similarly, another study showed that DNA-PK drove high levels of MYC through interaction with the transcriptional activator OCT4 in small cell lung cancer[389]. Another study showed that dual inhibition of DNA-PK and KIT resulted in decreased phosphorylation of MYC in KIT-mutant acute myeloid leukemia[390]. Together, these results indicate the possibility that DNA-PK acts as an upstream regulator of MYC, potentially driving its activity or promoting its stability. This will need to be investigated in future studies.

Another axis that was beyond the scope of the current project is the potential role that DNA-PK may play in tumor metastasis. Group 3 MB, which has the highest DNA-PK expression of all the subgroups (as shown in Results chapter 1), also has the highest rate of metastasis at diagnosis[84]. Further, numerous studies have shown that DNA-PK can drive metastasis in a number of other cancers, largely via modulation of the tumor microenvironment and induction of the secretion of pro-migratory factors[327,338]. Therefore, it may also be interesting to investigate a potential association between DNA-PK and metastasis in group 3 MB. To achieve this, we could initially utilize the data obtained in our global screening experiments to answer some questions left over from this work on DNA-PK. Specifically, we could look at the bulk and scRNAseq data for the PDX1 model (for which olfactory bulb metastases were collected) to see if we could identify any possible link between DNA-PK and its downstream pathways in metastatic tumours compared to primary tumours. Further, it will be interesting to see if the finalized CRISPR-Cas9 screen identifies DNA-PK or any of the other NHEJ-related factors as important genes in the response to irradiation.

Potential clinical applications of peposertib in medulloblastoma

As mentioned in the introduction, there are currently no clinical trials investigating any targeted treatments as radiosensitizers in medulloblastoma. However, peposertib is in clinical trial as a radiosensitizer in a number of other cancers (Table 3, Introduction Section 4.5). Most importantly, one clinical trial is investigating the safety and efficacy of peposertib with standard irradiation, followed by temozolomide chemotherapy, in treating newly diagnosed MGMT unmethylated glioblastoma or gliosarcoma (ClinicalTrials.gov Identifier: NCT04555577). This trial aims to evaluate both the maximum tolerated dose of peposertib when combined with the

standard-of-care irradiation regimen (2 Gy/fraction over 6 weeks, total 60 Gy), to assess the pharmacokinetics of the drug through examination of resected tissue, and to evaluate the overall response rate, median progression free survival, and median overall survival of patients treated with the drug. In this study, patients are administered peposertib 1-2 hours prior to irradiation, which is similar to the treatment timing we used in our in vivo studies. Thus, completion of this trial should prove the possibility of using peposertib as a radiosensitizer in brain tumours, and further validates the treatment schedule we postulated in our pre-clinical study. Furthermore, prior research has proven the good tolerability of peposertib as a monotherapy in adult cancer patients[354].

Together, this clinical trial history suggests that future clinical trials to assess the efficacy of peposertib as a radiosensitizer in the first-line treatment of MYC-driven high risk group 3 medulloblastoma are eminently plausible. However, it should be noted that all previous clinical trials have been conducted in adults aged >18 years, and there is currently no data regarding administration of peposertib and fractionated radiation in pediatric patients. This is therefore a topic for future research

8.2 Understanding radiation resistance and relapse

The necessity of in vivo modelling of relapse

As was outlined extensively in the Introduction and Results chapter 2, while recent research has begun to reveal the features and characteristics of relapsed medulloblastoma tumours, knowledge is still scarce compared to our understanding of untreated tumours. The reason for this disparity is that, unlike in the initial treatment phase, resection is relatively rarely performed when treating relapsed tumours. As such, biopsies of relapse are comparatively scarce. In this context, experimental models of relapse are key in gaining an increased understanding of both the mechanism of relapse, and the features of relapsed tumours. In our study, we constructed in vitro and in vivo models which recapitulate the tumor growth observed in relapsed MB patients, with irradiation inducing a shrinkage in tumor size, resulting in a period of low tumor burden and growth, followed by rapid and aggressive relapse. We believe that the results obtained with these faithful models will allow us to obtain a clear picture of the mechanisms by which group 3 MB escapes radiotherapy to form relapse.

Preliminary results

Overall, the analyses of all of the experiments described in the second results chapter require significantly more work before they can be finalized. However, preliminary results of the bulk

RNAseq analysis have begun to show the landscape of tumours in the different phases of recurrence. Perhaps most interestingly, the intermediary results of the CRISPR Cas9 screen results identified ATM, WDR11, and SWSAP1 as potential targets to investigate. As previously discussed in the introduction, ATM is a sensor of DNA damage which plays an important role in the cellular response to irradiation, and has been investigated as a target for radiosensitization in a variety of cancers[171–175]. Although we identified no impact of transient ATM inhibition on cell survival in combination with irradiation (Results Chapter 1, Figure 1), this may nevertheless be a topic for future research. For example, it may be possible that ATM is important in the late responses to irradiation rather than the immediate response (assessed in our screen). Further, WDR11, a member of the WD repeat protein family which remains relatively poorly characterized, has previously been identified as a potential tumor suppressor in group 3 medulloblastoma, whose loss increases tumour aggressiveness in MB mouse models[374]. Further, another study showed that WDR11 loss due to chromosomal translocations is associated with glioblastoma tumorigenesis[391]. Although knowledge on the cellular functions of WDR11 is limited, the aforementioned study in medulloblastoma showed that WDR11 overexpression triggered a down-regulation in MYC expression[374]. Thus, it is possible that loss of WDR11 promotes irradiation escape by decreasing MYC-driven cell cycling, allowing more time for DNA repair – however, this hypothesis remains highly speculative. Finally, the RAD51 homologue SWSAP1 may warrant further investigation. Although knowledge of this protein is again scarce, the existing research suggests that SWSAP1 inhibits cancer development by inhibiting a loss of heterozygosity[373]. It could therefore be hypothesized that it is this pathway which underlies the importance of SWSAP1 in the radiation response.

Future applications of the work

The plan for the future analysis of the different in vivo and in vitro experiments investigating relapse has already been outlined in the Results Chapter 2. Together, the results of this study should characterize the mechanisms by which group 3 medulloblastoma escapes relapse, and identify pathways which could be targeted to promote the activity of the original treatment. Most importantly, this study should provide a strong basis for future studies investigating therapeutic strategies to improve survival in group 3 MB by improving the response to irradiation in the initial round of therapy. Indeed, most of the studies investigating radiosensitizers in the current literature have used a similar approach to ours, basing the choice of targets to investigate on existing knowledge of pan-cancer tumour biology, or specific knowledge of primary MB tumour biology. In fact, most studies investigating targets for

radiosensitization in MB have simply focused on investigating drugs targeting proteins shown to be overexpressed in primary MB tumours[265,266,271], or on repurposing strategies used to promote radiosensitization in other cancers[261,263,264]. Other studies have used a similar strategy to that used in our investigation of DNA-PK, performing screens of likely compounds to identify effective radiosensitizers[392]. Although these aforementioned studies have achieved promising results, such targeted approaches are limited, and have a high chance of missing promising targets or approaches that may be revealed in more global analyses. As such, our approach to characterize the full landscape of radiation resistance and mechanisms of relapse in group 3 medulloblastoma should identify novel treatment mechanisms that may otherwise have been missed.

9. Conclusions

Overall, the aim of this work was to identify novel treatments for group 3 medulloblastoma, with the final aim of identifying drugs which could be combined with radiotherapy to decrease the relapse and mortality rates of this high-risk pediatric cancer. We achieved this goal in the first branch of this chapter, which represents one of the most complete works identifying a potential novel therapeutic radiosensitizer in group 3 medulloblastoma. While the global investigation of the mechanisms underlying irradiation escape remain incomplete, continuation of the project outlined in chapter 2 should identify novel genes which could be targeted to promote radiosensitization in group 3 medulloblastoma. Such analyses could be applied to develop novel therapeutic strategies to enhance the therapeutic index of radiotherapy in group 3 MB. These strategies may subsequently be applied to alternatively reduce the rate of relapse, or to allow radiotherapy de-escalation to reduce side-effects and improve quality of life without comprising patient prognosis.

10. REFERENCES

1. Northcott PA, Robinson GW, Kratz CP, et al. Medulloblastoma. *Nat Rev Dis Prim*. 2019;5(1). doi:10.1038/s41572-019-0063-6

2. Wang J, Garancher A, Ramaswamy V, Wechsler-Reya RJ. Medulloblastoma: From Molecular Subgroups to Molecular Targeted Therapies. *Annu Rev Neurosci*. 2018;41(1):207-232. doi:10.1146/annurev-neuro-070815-013838

3. Juraschka K, Taylor MD. Medulloblastoma in the age of molecular subgroups: A review: JNSPG 75th Anniversary invited review article. *J Neurosurg Pediatr*. 2019;24(4):353-363. doi:10.3171/2019.5.PEDS18381

4. Smith KS, Bihannic L, Gudenas BL, et al. Unified rhombic lip origins of group 3 and group 4 medulloblastoma. *Nature*. 2022;609(7929):1012-1020. doi:10.1038/s41586-022-05208-9

5. Schüller U, Heine VM, Mao J, et al. Acquisition of Granule Neuron Precursor Identity Is a Critical Determinant of Progenitor Cell Competence to Form Shh-Induced Medulloblastoma. *Cancer Cell*. 2008;14(2):123-134. doi:10.1016/j.ccr.2008.07.005

6. Polkinghorn WR, Tarbell NJ. Medulloblastoma: Tumorigenesis, current clinical paradigm, and efforts to improve risk stratification. *Nat Clin Pract Oncol*. 2007;4(5):295-304. doi:10.1038/ncponc0794

7. Bloom HJG. Medulloblastoma in children: Increasing survival rates and further prospects. *Int J Radiat Oncol Biol Phys*. 1982;8(11):2023-2027. doi:10.1016/0360-3016(82)90466-7

8. Adan L, Trivin C, Sainte-Rose C, Zucker JM, Hartmann O, Brauner R. GH Deficiency Caused by Cranial Irradiation during Childhood: Factors and Markers in Young Adults. *J Clin Endocrinol Metab*. 2001;86(11):5245-5251. doi:10.1210/jcem.86.11.8056

9. Fossati P, Ricardi U, Orecchia R. Pediatric medulloblastoma: Toxicity of current treatment and potential role of protontherapy. *Cancer Treat Rev*. 2009;35(1):79-96. doi:10.1016/j.ctrv.2008.09.002

10. Ogilvy-Stuart AL, Clayton PE, Shalet SM. Cranial irradiation and early puberty. *J Clin*

Endocrinol Metab. 1994;78(6):1282-1286. doi:10.1210/jcem.78.6.8200926

11. Thompson MC, Fuller C, Hogg TL, et al. Genomics identifies medulloblastoma subgroups that are enriched for specific genetic alterations. *J Clin Oncol*. 2006;24(12):1924-1931. doi:10.1200/JCO.2005.04.4974

12. Northcott PA, Shih DJH, Peacock J, et al. Subgroup-specific structural variation across 1,000 medulloblastoma genomes. *Nature*. 2012;487(7409):49-56. doi:10.1038/nature11327

13. Schwalbe EC, Williamson D, Lindsey JC, et al. DNA methylation profiling of medulloblastoma allows robust subclassification and improved outcome prediction using formalin-fixed biopsies. *Acta Neuropathol*. 2013;125(3):359-371. doi:10.1007/s00401-012-1077-2

14. Cavalli FMG, Remke M, Rampasek L et al. Intertumoral Heterogeneity within Medulloblastoma Subgroups. *Cancer Cell*. 2017;31(6):737-754. doi:10.1016/j.ccell.2017.05.005

15. Clifford SC, Lusher ME, Lindsey JC, et al. Wnt/Wingless pathway activation and chromosome 6 loss characterize a distinct molecular sub-group of medulloblastomas associated with a favorable prognosis. *Cell Cycle*. 2006;5(22):2666-2670. doi:10.4161/cc.5.22.3446

16. Ellison DW, Onilude OE, Lindsey JC, et al. β-Catenin Status Predicts a Favorable Outcome in Childhood Medulloblastoma: The United Kingdom Children's Cancer Study Group Brain Tumour Committee. *J Clin Oncol*. 2005;23(31):7951-7957. doi:10.1200/JCO.2005.01.5479

17. Komiya Y, Habas R. Wnt signal transduction pathways. *Organogenesis*. 2008;4(2):68-75. doi:10.4161/org.4.2.5851

18. Phoenix TN, Patmore DM, Boop S, et al. Medulloblastoma Genotype Dictates Blood Brain Barrier Phenotype. *Cancer Cell*. 2016;29(4):508-522. doi:10.1016/j.ccell.2016.03.002

19. Liu J, Xiao Q, Xiao J, et al. Wnt/β-catenin signalling: function, biological mechanisms, and therapeutic opportunities. *Signal Transduct Target Ther*. 2022;7(1). doi:10.1038/s41392-021-00762-6

20. Thompson MC, Fuller C, Hogg TL, et al. Genomics identifies medulloblastoma subgroups that are enriched for specific genetic alterations. *J Clin Oncol*. 2006;24(12):1924-1931. doi:10.1200/JCO.2005.04.4974

21. Sursal T, Ronecker JS, Dicpinigaitis AJ, et al. Molecular Stratification of Medulloblastoma: Clinical Outcomes and Therapeutic Interventions. *Anticancer Res*. 2022;42(5):2225-2239. doi:10.21873/anticanres.15703

22. da Silva R, Marie SKN, Uno M, et al. CTNNB1, AXIN1 and APC expression analysis of different medulloblastoma variants. *Clinics*. 2013;68(2):167-172. doi:10.6061/clinics/2013(02)OA08

23. Bish R, Vogel C. RNA binding protein-mediated post-transcriptional gene regulation in medulloblastoma. *Mol Cells*. 2014;37(5):357-364. doi:10.14348/molcells.2014.0008

24. Northcott PA, Buchhalter I, Morrissy AS, et al. The whole-genome landscape of medulloblastoma subtypes. *Nature*. 2017;547(7663):311-317. doi:10.1038/nature22973

25. Zhukova N, Ramaswamy V, Remke M, et al. Subgroup-specific prognostic implications of TP53 mutation in medulloblastoma. *J Clin Oncol*. 2013;31(23):2927-2935. doi:10.1200/JCO.2012.48.5052

26. Ramaswamy V, Nör C, Taylor MD. p53 and meduloblastoma. *Cold Spring Harb Perspect Med*. 2016;6(2):a026278. doi:10.1101/cshperspect.a026278

27. Skoda AM, Simovic D, Karin V, Kardum V, Vranic S, Serman L. The role of the hedgehog signaling pathway in cancer: A comprehensive review. *Bosn J Basic Med Sci*. 2018;18(1):8-20. doi:10.17305/bjbms.2018.2756

28. Lupi O. Correlations between the Sonic Hedgehog pathway and basal cell carcinoma. *Int J Dermatol*. 2007;46(11):1113-1117. doi:10.1111/j.1365-4632.2007.03391.x

29. Lee D-H, Lee S-Y, Oh SC. Hedgehog signaling pathway as a potential target in the treatment of advanced gastric cancer. *Tumour Biol J Int Soc Oncodevelopmental Biol Med*. 2017;39(6):1010428317692266. doi:10.1177/1010428317692266

30. Menyhárt O, Győrffy B. Principles of tumorigenesis and emerging molecular drivers of SHH-activated medulloblastomas. *Ann Clin Transl Neurol*. 2019;6(5):990-1005. doi:10.1002/acn3.762

31. Kool M, Jones DTW, Jäger N, et al. Genome sequencing of SHH medulloblastoma predicts genotype-related response to smoothened inhibition. *Cancer Cell*. 2014;25(3):393-405. doi:10.1016/j.ccr.2014.02.004

32. Sarić N, Selby M, Ramaswamy V, et al. The AHR pathway represses TGFβ-SMAD3 signalling and has a potent tumour suppressive role in SHH medulloblastoma. *Sci Rep*. 2020;10(1):148. doi:10.1038/s41598-019-56876-z

33. Ray S, Chaturvedi NK, Bhakat KK, Rizzino A, Mahapatra S. Subgroup-Specific Diagnostic, Prognostic, and Predictive Markers Influencing Pediatric Medulloblastoma Treatment. *Diagnostics (Basel, Switzerland)*. 2021;12(1). doi:10.3390/diagnostics12010061

34. Archer TC, Ehrenberger T, Mundt F, et al. Proteomics, Post-translational Modifications, and Integrative Analyses Reveal Molecular Heterogeneity within Medulloblastoma Subgroups. *Cancer Cell*. 2018;34(3):396-410.e8. doi:10.1016/j.ccell.2018.08.004

35. Lu Y, Labak CM, Jain N, et al. OTX2 expression contributes to proliferation and progression in Myc-amplified medulloblastoma. *Am J Cancer Res*. 2017;7(3):647.

36. Northcott PA, Lee C, Zichner T, et al. Enhancer hijacking activates GFI1 family oncogenes in medulloblastoma. *Nature*. 2014;511(7510):428-434. doi:10.1038/nature13379

37. Garancher A, Lin CY, Morabito M, et al. NRL and CRX Define Photoreceptor Identity and Reveal Subgroup-Specific Dependencies in Medulloblastoma. *Cancer Cell*. 2018;33(3):435-449.e6. doi:10.1016/j.ccell.2018.02.006

38. Morabito M, Larcher M, Cavalli FM, et al. An autocrine ActivinB mechanism drives TGF β/Activin signaling in Group 3 medulloblastoma. *EMBO Mol Med*. 2019;11(8). doi:10.15252/emmm.201809830

39. Forget A, Martignetti L, Puget S, et al. Aberrant ERBB4-SRC Signaling as a Hallmark of Group 4 Medulloblastoma Revealed by Integrative Phosphoproteomic Profiling. *Cancer Cell*. 2018;34(3):379-395.e7. doi:10.1016/j.ccell.2018.08.002

40. Northcott PA, Korshunov A, Witt H, et al. Medulloblastoma Comprises Four Distinct Molecular Variants. *J Clin Oncol*. 2010;29(11):1408-1414.

doi:10.1200/JCO.2009.27.4324

41. Cho Y-J, Tsherniak A, Tamayo P, et al. Integrative Genomic Analysis of Medulloblastoma Identifies a Molecular Subgroup That Drives Poor Clinical Outcome. *J Clin Oncol*. 2010;29(11):1424-1430. doi:10.1200/JCO.2010.28.5148

42. Merve A, Dubuc AM, Zhang X, et al. Polycomb group gene BMI1 controls invasion of medulloblastoma cells and inhibits BMP-regulated cell adhesion. *Acta Neuropathol Commun*. 2014;2(1):10. doi:10.1186/2051-5960-2-10

43. Badodi S, Pomella N, Zhang X, et al. Inositol treatment inhibits medulloblastoma through suppression of epigenetic-driven metabolic adaptation. *Nat Commun*. 2021;12(1):2148. doi:10.1038/s41467-021-22379-7

44. Orr BA. Pathology, diagnostics, and classification of medulloblastoma. *Brain Pathol*. 2020;30(3):664-678. doi:10.1111/bpa.12837

45. Williamson D, Schwalbe EC, Hicks D, et al. Medulloblastoma group 3 and 4 tumors comprise a clinically and biologically significant expression continuum reflecting human cerebellar development. *Cell Rep*. 2022;40(5):111162. doi:10.1016/j.celrep.2022.111162

46. Hovestadt V, Smith KS, Bihannic L, et al. Resolving medulloblastoma cellular architecture by single-cell genomics. *Nature*. 2019;572(7767):74-79. doi:10.1038/s41586-019-1434-6

47. Kline CN, Packer RJ, Hwang EI, et al. Case-based review: pediatric medulloblastoma. *Neuro-Oncology Pract*. 2017;4(3):138. doi:10.1093/NOP/NPX011

48. Chang CH, Housepian EM, Herbert C. An operative staging system and a megavoltage radiotherapeutic technic for cerebellar medulloblastomas. *Radiology*. 1969;93(6):1351-1359. doi:10.1148/93.6.1351

49. Ellison DW. Childhood medulloblastoma: Novel approaches to the classification of a heterogeneous disease. *Acta Neuropathol*. 2010;120(3):305-316. doi:10.1007/s00401-010-0726-6

50. Thompson EM, Hielscher T, Bouffet E, et al. Prognostic value of medulloblastoma extent of resection after accounting for molecular subgroup: a retrospective integrated clinical and molecular analysis. *Lancet Oncol*. 2016;17(4):484-495.

doi:10.1016/S1470-2045(15)00581-1

51. Deutsch M, Thomas PRM, Krischer J, et al. Results of a prospective randomized trial comparing standard dose neuraxis irradiation (3,600 cgy/20) with reduced neuraxis irradiation (2,340 cgy/13) in patients with low-stage medulloblastoma. *Pediatr Neurosurg*. 1996;24(4):167-177. doi:10.1159/000121042

52. Gajjar A, Chintagumpala M, Ashley D, et al. Risk-adapted craniospinal radiotherapy followed by high-dose chemotherapy and stem-cell rescue in children with newly diagnosed medulloblastoma (St Jude Medulloblastoma-96): long-term results from a prospective, multicentre trial. *Lancet Oncol*. 2006;7(10):813-820. doi:10.1016/S1470-2045(06)70867-1

53. Gerber NU, Mynarek M, von Hoff K, Friedrich C, Resch A, Rutkowski S. Recent developments and current concepts in Medulloblastoma. *Cancer Treat Rev*. 2014;40(3):356-365. doi:10.1016/j.ctrv.2013.11.010

54. Ramaswamy V, Remke M, Bouffet E, et al. Risk stratification of childhood medulloblastoma in the molecular era: the current consensus. *Acta Neuropathol*. 2016;131(6):821-831. doi:10.1007/s00401-016-1569-6

55. Menyhárt O, Győrffy B. Molecular stratifications, biomarker candidates and new therapeutic options in current medulloblastoma treatment approaches. doi:10.1007/s10555-020-09854-1

56. Kortmann RD, Kühl J, Timmermann B, et al. Postoperative neoadjuvant chemotherapy before radiotherapy as compared to immediate radiotherapy followed by maintenance chemotherapy in the treatment of medulloblastoma in childhood: results of the German prospective randomized trial HIT '91. *Int J Radiat Oncol Biol Phys*. 2000;46(2):269-279. doi:10.1016/s0360-3016(99)00369-7

57. Hoff K von, Hinkes B, Gerber NU, et al. Long-term outcome and clinical prognostic factors in children with medulloblastoma treated in the prospective randomised multicentre trial HIT'91. *Eur J Cancer*. 2009;45(7):1209-1217. doi:10.1016/j.ejca.2009.01.015

58. Packer RJ, Gajjar A, Vezina G, et al. Phase III study of craniospinal radiation therapy followed by adjuvant chemotherapy for newly diagnosed average-risk medulloblastoma. *J Clin Oncol*. 2006;24(25):4202-4208.

doi:10.1200/JCO.2006.06.4980

59. Kann BH, Park HS, Lester-Coll NH, et al. Postoperative radiotherapy patterns of care and survival implications for medulloblastoma in young children. *JAMA Oncol*. 2016;2(12):1574-1581. doi:10.1001/jamaoncol.2016.2547

60. Rutkowski S, Gerber NU, von Hoff K, et al. Treatment of early childhood medulloblastoma by postoperative chemotherapy and deferred radiotherapy. *Neuro Oncol*. 2009;11(2):201-210. doi:10.1215/15228517-2008-084

61. Sung KW, Lim DH, Shin HJ. Tandem High-dose Chemotherapy and Autologous Stem Cell Transplantation in Children with Brain Tumors : Review of Single Center Experience. *J Korean Neurosurg Soc*. 2018;61(3):393-401. doi:10.3340/jkns.2018.0039

62. Mabbott DJ, Spiegler BJ, Greenberg ML, Rutka JT, Hyder DJ, Bouffet E. Serial Evaluation of Academic and Behavioral Outcome After Treatment With Cranial Radiation in Childhood. *J Clin Oncol*. 2005;23(10):2256-2263. doi:10.1200/JCO.2005.01.158

63. Palmer SL, Gajjar A, Reddick WE, et al. Predicting Intellectual Outcome among Children Treated with 35-40 Gy Craniospinal Irradiation for Medulloblastoma. *Neuropsychology*. 2003;17(4):548-555. doi:10.1037/0894-4105.17.4.548

64. Moxon-Emre I, Bouffet E, Taylor MD, et al. Impact of craniospinal dose, boost volume, and neurologic complications on intellectual outcome in patients with medulloblastoma. *J Clin Oncol*. 2014;32(17):1760-1768. doi:10.1200/JCO.2013.52.3290

65. Jenkin D, Danjoux C, Greenberg M. Subsequent quality of life for children irradiated for a brain tumor before age four years. *Med Pediatr Oncol*. 1998;31(6):506-511. doi:10.1002/(SICI)1096-911X(199812)31:6<506::AID-MPO7>3.0.CO;2-X

66. Paulino AC. Hypothyroidism in children with medulloblastoma: A comparison of 3600 and 2340 cGy craniospinal radiotherapy. *Int J Radiat Oncol Biol Phys*. 2002;53(3):543-547. doi:10.1016/S0360-3016(02)02744-X

67. Xu W, Janss A, Moshang T. Adult Height and Adult Sitting Height in Childhood Medulloblastoma Survivors. *J Clin Endocrinol Metab*. 2003;88(10):4677-4681.

doi:10.1210/jc.2003-030619

68. Moeller BJ, Chintagumpala M, Philip JJ, et al. Low early ototoxicity rates for pediatric medulloblastoma patients treated with proton radiotherapy. *Radiat Oncol*. 2011;6:58. doi:10.1186/1748-717X-6-58

69. Bouffet E, Bernard JL, Frappaz D, et al. M4 protocol for cerebellar medulloblastoma: Supratentorial radiotherapy may not be avoided. *Int J Radiat Oncol Biol Phys*. 1992;24(1):79-85. doi:10.1016/0360-3016(92)91025-I

70. Duffner PK, Horowitz ME, Krischer JP, et al. Postoperative Chemotherapy and Delayed Radiation in Children Less Than Three Years of Age with Malignant Brain Tumors. *N Engl J Med*. 1993;328(24):1725-1731. doi:10.1056/NEJM199306173282401

71. Duffner PK, Krischer JP, Horowitz ME, et al. Second malignancies in young children with primary brain tumors following treatment with prolonged postoperative chemotherapy and delayed irradiation: A pediatric oncology group study. *Ann Neurol*. 1998;44(3):313-316. doi:10.1002/ana.410440305

72. Evans AE, Jenkin RDT, Sposto R, et al. The treatment of medulloblastoma. Results of a prospective randomized trial of radiation therapy with and without CCNU, vincristine, and prednisone. *J Neurosurg*. 1990;72(4):572-582. doi:10.3171/jns.1990.72.4.0572

73. Tait DM, Thornton-Jones H, Bloom HJG, Lemerle J, Morris-Jones P. Adjuvant chemotherapy for medulloblastoma: The first multi-centre control trial of the International Society of Paediatric Oncology (SIOP I). *Eur J Cancer Clin Oncol*. 1990;26(4):463-469. doi:10.1016/0277-5379(90)90017-N

74. Taylor RE, Bailey CC, Robinson K, et al. Results of a randomized study of preradiation chemotherapy versus radiotherapy alone for nonmetastatic medulloblastoma: The International Society of Paediatric Oncology/United Kingdom Children's Cancer Study Group PNET-3 Study. *J Clin Oncol*. 2003;21(8):1581-1591. doi:10.1200/JCO.2003.05.116

75. Gentet JC, Bouffet E, Doz F, et al. Preirradiation chemotherapy including "eight drugs in 1 day" regimen and high-dose methotrexate in childhood medulloblastoma: Results of the M7 French Cooperative Study. *J Neurosurg*. 1995;82(4):608-614.

doi:10.3171/jns.1995.82.4.0608

76. Packer RJ, Goldwein J, Nicholson HS, et al. Treatment of children with medulloblastomas with reduced-dose craniospinal radiation therapy and adjuvant chemotherapy: A Children's Cancer Group study. *J Clin Oncol*. 1999;17(7):2127-2136. doi:10.1200/jco.1999.17.7.2127

77. Thompson EM, Ashley D, Landi D. Current medulloblastoma subgroup specific clinical trials. *Transl Pediatr*. 2020;9(2):157-162. doi:10.21037/tp.2020.03.03

78. Carrie C, Kieffer V, Figarella-Branger D, et al. Exclusive Hyperfractionated Radiation Therapy and Reduced Boost Volume for Standard-Risk Medulloblastoma: Pooled Analysis of the 2 French Multicentric Studies MSFOP98 and MSFOP 2007 and Correlation With Molecular Subgroups. *Int J Radiat Oncol*. 2020;108(5):1204-1217. doi:10.1016/j.ijrobp.2020.07.2324

79. Padovani L, Chapon F, Geoffray A, et al. B-47 Risk of hippocampal region metastasis in high risk medulloblastoma: sufficient rational for hippocampal sparing during craniospinal irradiation? *Neuro Oncol*. 2016;18(suppl_3):iii107-iii107. doi:10.1093/neuonc/now076.45

80. Hill RM, Kuijper S, Lindsey JC, et al. Combined MYC and P53 defects emerge at medulloblastoma relapse and define rapidly progressive, therapeutically targetable disease. *Cancer Cell*. 2015;27(1):72-84. doi:10.1016/j.ccell.2014.11.002

81. Redmond KM, Wilson TR, Johnston PG, Longley DB. Resistance mechanisms to cancer chemotherapy. *Front Biosci*. 2008;13(13):5138-5154. doi:10.2741/3070

82. Boumahdi S, de Sauvage FJ. The great escape: tumour cell plasticity in resistance to targeted therapy. *Nat Rev Drug Discov*. 2020;19(1):39-56. doi:10.1038/s41573-019-0044-1

83. Mullard A. Stemming the tide of drug resistance in cancer. *Nat Rev Drug Discov*. 2020;19(4):221-223. doi:10.1038/d41573-020-00050-y

84. Ramaswamy V, Remke M, Bouffet E, et al. Recurrence patterns across medulloblastoma subgroups: An integrated clinical and molecular analysis. *Lancet Oncol*. 2013;14(12):1200-1207. doi:10.1016/S1470-2045(13)70449-2

85. Kumar R, Smith KS, Deng M, et al. Clinical Outcomes and Patient-Matched Molecular

Composition of Relapsed Medulloblastoma. *J Clin Oncol*. 2021;39(7):807-821. doi:10.1200/JCO.20.01359

86. Morrissy AS, Garzia L, Shih DJH, et al. Divergent clonal selection dominates medulloblastoma at recurrence. *Nature*. 2016;529(7586):351-357. doi:10.1038/nature16478

87. Ocasio J, Babcock B, Malawsky D, et al. scRNA-seq in medulloblastoma shows cellular heterogeneity and lineage expansion support resistance to SHH inhibitor therapy. *Nat Commun*. 2019;10(1):1-17. doi:10.1038/s41467-019-13657-6

88. Bakhshinyan D, Adile AA, Liu J, et al. Temporal profiling of therapy resistance in human medulloblastoma identifies novel targetable drivers of recurrence. *Sci Adv*. 2021;7(50):1-14. doi:10.1126/sciadv.abi5568

89. Xu Z, Murad N, Malawsky D, et al. OLIG2 Is a Determinant for the Relapse of MYC-Amplified Medulloblastoma. *Clin Cancer Res*. 2022;28(19):4278-4291. doi:10.1158/1078-0432.CCR-22-0527

90. Morgan MA, Lawrence TS. Molecular pathways: Overcoming radiation resistance by targeting DNA damage response pathways. *Clin Cancer Res*. 2015;21(13):2898-2904. doi:10.1158/1078-0432.CCR-13-3229

91. Kim, Lee, Seo, et al. Cellular Stress Responses in Radiotherapy. *Cells*. 2019;8(9):1105. doi:10.3390/cells8091105

92. Ayob AZ, Ramasamy TS. Cancer stem cells as key drivers of tumour progression. *J Biomed Sci*. 2018;25(1):1-18. doi:10.1186/s12929-018-0426-4

93. Reya T, Morrison SJ, Clarke MF, Weissman IL. Stem cells, cancer, and cancer stem cells. *Nature*. 2001;414(6859):105-111. doi:10.1038/35102167

94. Li F, Zhou K, Gao L, et al. Radiation induces the generation of cancer stem cells: A novel mechanism for cancer radioresistance. *Oncol Lett*. 2016;12(5):3059-3065. doi:10.3892/ol.2016.5124

95. Olivares-Urbano MA, Griñán-Lisón C, Marchal JA, Núñez MI. CSC Radioresistance: A Therapeutic Challenge to Improve Radiotherapy Effectiveness in Cancer. *Cells*. 2020;9(7). doi:10.3390/cells9071651

96. Arnold CR, Mangesius J, Skvortsova II, Ganswindt U. The Role of Cancer Stem Cells in Radiation Resistance. *Front Oncol*. 2020;10(February):1-12. doi:10.3389/fonc.2020.00164

97. Blazek ER, Foutch JL, Maki G. Daoy medulloblastoma cells that express CD133 are radioresistant relative to CD133- cells, and the CD133+ sector is enlarged by hypoxia. *Int J Radiat Oncol Biol Phys*. 2007;67(1):1-5. doi:10.1016/j.ijrobp.2006.09.037

98. Borgenvik A, Holmberg KO, Bolin S, et al. Dormant SOX9-Positive Cells Facilitate MYC-Driven Recurrence of Medulloblastoma. *Cancer Res*. 2022;82(24):4586-4603. doi:10.1158/0008-5472.CAN-22-2108

99. Vanner RJ, Remke M, Gallo M, et al. Quiescent sox2(+) cells drive hierarchical growth and relapse in sonic hedgehog subgroup medulloblastoma. *Cancer Cell*. 2014;26(1):33-47. doi:10.1016/j.ccr.2014.05.005

100. Douyère M, Gong C, Richard M, et al. NRP1 inhibition modulates radiosensitivity of medulloblastoma by targeting cancer stem cells. *Cancer Cell Int*. 2022;22(1):377. doi:10.1186/s12935-022-02796-4

101. Elbadawy M, Usui T, Yamawaki H, Sasaki K. Emerging Roles of C-Myc in Cancer Stem Cell-Related Signaling and Resistance to Cancer Chemotherapy: A Potential Therapeutic Target Against Colorectal Cancer. *Int J Mol Sci*. 2019;20(9). doi:10.3390/ijms20092340

102. Liu Y, Zhu C, Tang L, et al. MYC dysfunction modulates stemness and tumorigenesis in breast cancer. *Int J Biol Sci*. 2021;17(1):178-187. doi:10.7150/ijbs.51458

103. Wang J, Wang H, Li Z, et al. c-Myc Is Required for Maintenance of Glioma Cancer Stem Cells. doi:10.1371/journal.pone.0003769

104. Venkataraman S, Alimova I, Balakrishnan I, et al. Inhibition of BRD4 attenuates tumor cell self-renewal and suppresses stem cell signaling in MYC driven medulloblastoma. *Oncotarget*. 2014;5(9):2355-2371. doi:10.18632/oncotarget.1659

105. Hambardzumyan D, Becher OJ, Rosenblum MK, Pandolfi PP, Manova-Todorova K, Holland EC. PI3K pathway regulates survival of cancer stem cells residing in the perivascular niche following radiation in medulloblastoma in vivo. *Genes Dev*. 2008;22(4):436-448. doi:10.1101/gad.1627008

106. Frasson C, Rampazzo E, Accordi B, et al. Inhibition of PI3K Signalling Selectively Affects Medulloblastoma Cancer Stem Cells. 2015. doi:10.1155/2015/973912

107. Fan X, Matsui W, Khaki L, et al. Notch Pathway Inhibition Depletes Stem-like Cells and Blocks Engraftment in Embryonal Brain Tumors. *Cancer Res*. 2006;66(15):7445-7452. doi:10.1158/0008-5472.CAN-06-0858

108. Tanno B, Leonardi S, Babini G, et al. Nanog-driven cell-reprogramming and self-renewal maintenance in Ptch1+/− granule cell precursors after radiation injury. *Sci Rep*. 2017;7(1):14238. doi:10.1038/s41598-017-14506-6

109. Kostaras X, Easaw JC. Management of recurrent medulloblastoma in adult patients: A systematic review and recommendations. *J Neurooncol*. 2013;115(1):1-8. doi:10.1007/s11060-013-1206-3

110. Sabel M, Fleischhack G, Tippelt S, et al. Relapse patterns and outcome after relapse in standard risk medulloblastoma: a report from the HIT-SIOP-PNET4 study. *J Neurooncol*. 2016;129(3):515-524. doi:10.1007/s11060-016-2202-1

111. Nadi M, Malbari F, Dunkel IJ. Treatment approach for recurrent medulloblastoma. In: *Clinical Insights: Optimal Therapy of Pediatric Medulloblastoma*. Future Medicine Ltd; 2015:59-73. doi:10.2217/ebo.13.450

112. Bakst RL, Dunkel IJ, Gilheeney S, et al. Reirradiation for recurrent medulloblastoma. *Cancer*. 2011;117(21):4977-4982. doi:10.1002/cncr.26148

113. Tokuuye K, Akine Y, Sumi M, et al. Reirradiation of brain and skull base tumors with fractionated stereotactic radiotherapy. *Int J Radiat Oncol Biol Phys*. 1998;40(5):1151-1155. doi:10.1016/S0360-3016(97)00954-1

114. Bauman GS, Sneed PK, Wara WM, et al. Reirradiation of primary CNS tumors. *Int J Radiat Oncol Biol Phys*. 1996;36(2):433-441. doi:10.1016/S0360-3016(96)00315-X

115. Tsang DS, Sarhan N, Ramaswamy V, et al. Re-irradiation for children with recurrent medulloblastoma in Toronto, Canada: a 20-year experience. *J Neurooncol*. 2019;145(1):107-114. doi:10.1007/s11060-019-03272-2

116. Wetmore C, Herington D, Lin T, Onar-Thomas A, Gajjar A, Merchant TE. Reirradiation of recurrent medulloblastoma: Does clinical benefit outweigh risk for toxicity? *Cancer*. 2014;120(23):3731-3737. doi:10.1002/cncr.28907

117. Hill RM, Richardson S, Schwalbe EC, et al. Time, pattern, and outcome of medulloblastoma relapse and their association with tumour biology at diagnosis and therapy: a multicentre cohort study. *Lancet Child Adolesc Heal*. 2020;4(12):865-874. doi:10.1016/S2352-4642(20)30246-7

118. Pajtler KW, Hill RM, Plasschaert SLA, et al. Relapsed Medulloblastoma in Pre-Irradiated Patients: Current Practice for Diagnostics and Treatment. *Cancers (Basel)*. 2021;2022:126. doi:10.3390/cancers14010126

119. Barton MB, Jacob S, Shafiq J, et al. Estimating the demand for radiotherapy from the evidence: A review of changes from 2003 to 2012. *Radiother Oncol*. 2014;112(1):140-144. doi:10.1016/j.radonc.2014.03.024

120. Mehta SR, Suhag V, Semwal M, Sharma N. Radiotherapy: Basic concepts and recent advances. *Med J Armed Forces India*. 2010;66(2):158-162. doi:10.1016/S0377-1237(10)80132-7

121. Wang J song, Wang H juan, Qian H li. Biological effects of radiation on cancer cells. *Mil Med Res*. 2018;5(1). doi:10.1186/s40779-018-0167-4

122. Guo S, Yao Y, Tang Y, et al. Radiation-induced tumor immune microenvironments and potential targets for combination therapy. *Signal Transduct Target Ther*. 2023;8(1):205. doi:10.1038/s41392-023-01462-z

123. Daguenet E, Louati S, Wozny A-S, et al. Radiation-induced bystander and abscopal effects: important lessons from preclinical models. *Br J Cancer*. 2020;123(3):339-348. doi:10.1038/s41416-020-0942-3

124. Wanebo HJ, Glicksman AS, Vezeridis MP, et al. Preoperative chemotherapy, radiotherapy, and surgical resection of locally advanced pancreatic cancer. *Arch Surg*. 2000;135(1):81-87. doi:10.1001/archsurg.135.1.81

125. Abraha I, Aristei C, Palumbo I, et al. Preoperative radiotherapy and curative surgery for the management of localised rectal carcinoma. *Cochrane Database Syst Rev*. 2018;2018(10). doi:10.1002/14651858.CD002102.pub3

126. Brunner TB. The rationale of combined radiotherapy and chemotherapy – Joint action of Castor and Pollux. *Best Pract Res Clin Gastroenterol*. 2016;30(4):515-528. doi:10.1016/j.bpg.2016.07.002

127. Bernier J, Bentzen SM. Altered fractionation and combined radio-chemotherapy approaches: Pioneering new opportunities in head and neck oncology. *Eur J Cancer*. 2003;39(5):560-571. doi:10.1016/S0959-8049(02)00838-9

128. Rambow F, Rogiers A, Marin-Bejar O, et al. Toward Minimal Residual Disease-Directed Therapy in Melanoma. *Cell*. 2018;174(4):843-855.e19. doi:10.1016/j.cell.2018.06.025

129. Rallis KS, Yau THL, Sideris M. Chemoradiotherapy in cancer treatment: Rationale and clinical applications. *Anticancer Res*. 2021;41(1):1-7. doi:10.21873/anticanres.14746

130. Kim JH, Jenrow KA, Brown SL. Mechanisms of radiation-induced normal tissue toxicity and implications for future clinical trials. *Radiat Oncol J*. 2014;32(3):103-115. doi:10.3857/roj.2014.32.3.103

131. Benson R, Mallick S. Therapeutic Index and Its Clinical Significance. In: *Practical Radiation Oncology*. Springer Singapore; 2020:191-192. doi:10.1007/978-981-15-0073-2_31

132. Bucci MK, Bevan A, Roach M. Advances in Radiation Therapy: Conventional to 3D, to IMRT, to 4D, and Beyond. *CA Cancer J Clin*. 2005;55(2):117-134. doi:10.3322/canjclin.55.2.117

133. Cho B. Intensity-modulated radiation therapy: A review with a physics perspective. *Radiat Oncol J*. 2018;36(1):1-10. doi:10.3857/roj.2018.00122

134. Rana S. Intensity modulated radiation therapy versus volumetric intensity modulated arc therapy. *J Med Radiat Sci*. 2013;60(3):81-83. doi:10.1002/jmrs.19

135. Li G, Citrin D, Camphausen K, et al. Advances in 4D medical imaging and 4D radiation therapy. *Technol Cancer Res Treat*. 2008;7(1):67-81. doi:10.1177/153303460800700109

136. Prezado Y, Fois GR. Proton-minibeam radiation therapy: A proof of concept. *Med Phys*. 2013;40(3). doi:10.1118/1.4791648

137. Symonds P, Jones GDD. FLASH Radiotherapy: The Next Technological Advance in Radiation Therapy? *Clin Oncol*. 2019;31(7):405-406. doi:10.1016/j.clon.2019.05.011

138. Hughes JR, Parsons JL. Flash radiotherapy: Current knowledge and future insights

using proton-beam therapy. *Int J Mol Sci*. 2020;21(18):1-14. doi:10.3390/ijms21186492

139. Vozenin M-C, Bourhis J, Durante M. Towards clinical translation of FLASH radiotherapy. *Nat Rev Clin Oncol*. 2022;19(12):791-803. doi:10.1038/s41571-022-00697-z

140. Kurup G. CyberKnife: A new paradigm in radiotherapy. *J Med Phys*. 2010;35(2):63-64. doi:10.4103/0971-6203.62194

141. Augustin M, Wilhelm M, Reichert B, et al. Radiochemotherapy with gemcitabine as radiosensitizer in patients with soft tissue sarcoma. *J Clin Oncol*. 2020;38(15_suppl):e23559-e23559. doi:10.1200/JCO.2020.38.15_suppl.e23559

142. Mornex F, Girard N. Gemcitabine and radiation therapy in non-small cell lung cancer: state of the art. *Ann Oncol*. 2006;17(12):1743-1747. doi:https://doi.org/10.1093/annonc/mdl117

143. Harrabi SB, Adeberg S, Winter M, Haberer T, Debus J, Weber K-J. S-phase-specific radiosensitization by gemcitabine for therapeutic carbon ion exposure in vitro. *J Radiat Res*. 2016;57(2):110-114. doi:10.1093/jrr/rrv097

144. Boeckman HJ, Trego KS, Turchi JJ. Cisplatin sensitizes cancer cells to ionizing radiation via inhibition of nonhomologous end joining. *Mol Cancer Res*. 2005;3(5):277-285. doi:10.1158/1541-7786.MCR-04-0032

145. Leary SES, Packer RJ, Li Y, et al. Efficacy of Carboplatin and Isotretinoin in Children With High-risk Medulloblastoma A Randomized Clinical Trial From the Children's Oncology Group Supplemental content. *JAMA Oncol*. 2021;7(9):1313-1321. doi:10.1001/jamaoncol.2021.2224

146. Jakacki RI, Burger PC, Zhou T, et al. Outcome of children with metastatic medulloblastoma treated with carboplatin during craniospinal radiotherapy: a Children's Oncology Group Phase I/II study. *J Clin Oncol* . 2012;30(21):2648-2653. doi:10.1200/JCO.2011.40.2792

147. Zhang Z, Liu X, Chen D, Yu J. Radiotherapy combined with immunotherapy: the dawn of cancer treatment. *Signal Transduct Target Ther*. 2022;7(1):258. doi:10.1038/s41392-022-01102-y

148. Voskamp MJ, Li S, van Daalen KR, Crnko S, Ten Broeke T, Bovenschen N. Immunotherapy in Medulloblastoma: Current State of Research, Challenges, and Future Perspectives. *Cancers (Basel)*. 2021;13(21). doi:10.3390/cancers13215387

149. Schakelaar MY, Monnikhof M, Crnko S, et al. Cellular immunotherapy for medulloblastoma. *Neuro Oncol*. 2023;25(4):617-627. doi:10.1093/neuonc/noac236

150. Bockmayr M, Mohme M, Klauschen F, et al. Subgroup-specific immune and stromal microenvironment in medulloblastoma. *Oncoimmunology*. 2018;7(9):e1462430. doi:10.1080/2162402X.2018.1462430

151. Pouessel D, Mervoyer A, Larrieu-Ciron D, et al. Hypofractionnated stereotactic radiotherapy and anti-PDL1 durvalumab combination in recurrent glioblastoma: Results of the phase I part of the phase I/II STERIMGLI trial. *J Clin Oncol*. 2018;36(15_suppl):2046. doi:10.1200/JCO.2018.36.15_suppl.2046

152. Dehais C, Ducray F, Belin L, et al. Revolumab: A phase II trial of nivolumab in recurrent IDH-mutant high-grade gliomas. *J Clin Oncol*. 2022;40(16_suppl):2048. doi:10.1200/JCO.2022.40.16_suppl.2048

153. Farmer H, McCabe H, Lord CJ, et al. Targeting the DNA repair defect in BRCA mutant cells as a therapeutic strategy. *Nature*. 2005;434(7035):917-921. doi:10.1038/nature03445

154. Sishc BJ, Davis AJ. The role of the core non-homologous end joining factors in carcinogenesis and cancer. *Cancers (Basel)*. 2017;9(7). doi:10.3390/cancers9070081

155. Huang R-X, Zhou P-K. DNA damage response signaling pathways and targets for radiotherapy sensitization in cancer. *Signal Transduct Target Ther*. 2020;5(1):60. doi:10.1038/s41392-020-0150-x

156. Davis AJ, Chen DJ. DNA double strand break repair via non-homologous end-joining. *Transl Cancer Res*. 2013;2(3):130-143. doi:10.3978/j.issn.2218-676X.2013.04.02

157. Li X, Heyer WD. Homologous recombination in DNA repair and DNA damage tolerance. *Cell Res*. 2008;18(1):99-113. doi:10.1038/cr.2008.1

158. Kakarougkas A, Jeggo PA. DNA DSB repair pathway choice: an orchestrated handover mechanism. *Br J Radiol*. 2014;87(1035):20130685. doi:10.1259/bjr.20130685

159. Helleday T. The underlying mechanism for the PARP and BRCA synthetic lethality: clearing up the misunderstandings. *Mol Oncol*. 2011;5(4):387-393. doi:10.1016/j.molonc.2011.07.001

160. Powell C, Mikropoulos C, Kaye SB, et al. Pre-clinical and clinical evaluation of PARP inhibitors as tumour-specific radiosensitisers. *Cancer Treat Rev*. 2010;36(7):566-575. doi:10.1016/j.ctrv.2010.03.003

161. Biau J, Chautard E, Verrelle P, Dutreix M. Altering DNA repair to improve radiation therapy: Specific and multiple pathway targeting. *Front Oncol*. 2019;9(SEP):1-10. doi:10.3389/fonc.2019.01009

162. Wang L, Liang C, Li F, et al. PARP1 in carcinomas and PARP1 inhibitors as antineoplastic drugs. *Int J Mol Sci*. 2017;18(10). doi:10.3390/ijms18102111

163. Rose M, Burgess JT, O'Byrne K, Richard DJ, Bolderson E. PARP Inhibitors: Clinical Relevance, Mechanisms of Action and Tumor Resistance. *Front cell Dev Biol*. 2020;8:564601. doi:10.3389/fcell.2020.564601

164. Wu Y, Xu S, Cheng S, Yang J, Wang Y. Clinical application of PARP inhibitors in ovarian cancer: from molecular mechanisms to the current status. *J Ovarian Res*. 2023;16(1):1-15. doi:10.1186/s13048-023-01094-5

165. Chow JPH, Man WY, Mao M, et al. PARP1 Is overexpressed in nasopharyngeal carcinoma and its inhibition enhances radiotherapy. *Mol Cancer Ther*. 2013;12(11):2517-2528. doi:10.1158/1535-7163.MCT-13-0010

166. Jannetti SA, Carlucci G, Carney B, et al. PARP-1-targeted radiotherapy in mouse models of glioblastoma. *J Nucl Med*. 2018;59(8):1225-1233. doi:10.2967/jnumed.117.205054

167. Soni A, Li F, Wang Y, et al. Inhibition of PARP1 by BMN673 effectively sensitizes cells to radiotherapy by upsetting the balance of repair pathways processing DNA double-strand breaks. *Mol Cancer Ther*. 2018;17(10):2206-2216. doi:10.1158/1535-7163.MCT-17-0836

168. Michmerhuizen AR, Pesch AM, Moubadder L, et al. PARP1 Inhibition Radiosensitizes Models of Inflammatory Breast Cancer to Ionizing Radiation. *Mol Cancer Ther*. 2019;18(11):2063-2073. doi:10.1158/1535-7163.MCT-19-0520

169. Barcellini A, Loap P, Murata K, et al. PARP Inhibitors in Combination with Radiotherapy: To Do or Not to Do? *Cancers (Basel)*. 2021;13(21). doi:10.3390/cancers13215380

170. Maréchal A, Zou L. DNA damage sensing by the ATM and ATR kinases. *Cold Spring Harb Perspect Biol*. 2013;5(9). doi:10.1101/cshperspect.a012716

171. Dosani M, Schrader KA, Nichol A, et al. Severe Late Toxicity After Adjuvant Breast Radiotherapy in a Patient with a Germline Ataxia Telangiectasia Mutated Gene: Future Treatment Decisions. *Cureus*. 2017;9(7). doi:10.7759/cureus.1458

172. Hickson I, Zhao Y, Richardson CJ, et al. Identification and characterization of a novel and specific inhibitor of the ataxia-telangiectasia mutated kinase ATM. *Cancer Res*. 2004;64(24):9152-9159. doi:10.1158/0008-5472.CAN-04-2727

173. Carruthers R, Ahmed SU, Strathdee K, et al. Abrogation of radioresistance in glioblastoma stem-like cells by inhibition of ATM kinase. *Mol Oncol*. 2015;9(1):192-203. doi:10.1016/j.molonc.2014.08.003

174. Batey MA, Zhao Y, Kyle S, et al. Preclinical evaluation of a novel ATM inhibitor, KU59403, In Vitro and In Vivo in p53 functional and dysfunctional models of human cancer. *Mol Cancer Ther*. 2013;12(6):959-967. doi:10.1158/1535-7163.MCT-12-0707

175. Karlin J, Allen J, Ahmad SF, et al. Orally bioavailable and blood–brain barrier-penetrating ATM inhibitor (AZ32) radiosensitizes intracranial gliomas in mice. *Mol Cancer Ther*. 2018;17(8):1637-1647. doi:10.1158/1535-7163.MCT-17-0975

176. Waqar SN, Robinson C, Olszanski AJ, et al. Phase I trial of ATM inhibitor M3541 in combination with palliative radiotherapy in patients with solid tumors. *Invest New Drugs*. 2022;40(3):596-605. doi:10.1007/s10637-022-01216-8

177. Dillon MT, Barker HE, Pedersen M, et al. Radiosensitization by the ATR inhibitor AZD6738 through generation of acentric micronuclei. *Mol Cancer Ther*. 2017;16(1):25-34. doi:10.1158/1535-7163.MCT-16-0239

178. García MEG, Kirsch DG, Reitman ZJ. Targeting the ATM Kinase to Enhance the Efficacy of Radiotherapy and Outcomes for Cancer Patients. *Semin Radiat Oncol*. 2022;32(1):3-14. doi:10.1016/j.semradonc.2021.09.008

179. Hosoya N, Miyagawa K. Targeting DNA damage response in cancer therapy. *Cancer*

Sci. 2014;105(4):370-388. doi:https://doi.org/10.1111/cas.12366

180. Chernikova SB, Game JC, Brown JM. Inhibiting homologous recombination for cancer therapy. *Cancer Biol Ther*. 2012;13(2):61-68. doi:10.4161/cbt.13.2.18872

181. Gu P, Xue L, Zhao C, et al. Targeting the Homologous Recombination Pathway in Cancer With a Novel Class of RAD51 Inhibitors. *Front Oncol*. 2022;12:885186. doi:10.3389/fonc.2022.885186

182. Chen Q, Cai D, Li M, Wu X. The homologous recombination protein RAD51 is a promising therapeutic target for cervical carcinoma. *Oncol Rep*. 2017;38(2):767-774. doi:10.3892/or.2017.5724

183. Huang F, Mazin A V. A small molecule inhibitor of human RAD51 potentiates breast cancer cell killing by therapeutic agents in mouse xenografts. *PLoS One*. 2014;9(6). doi:10.1371/journal.pone.0100993

184. Shkundina IS, Gall AA, Dick A, Cocklin S, Mazin A V. New RAD51 Inhibitors to Target Homologous Recombination in Human Cells. *Genes (Basel)*. 2021;12(6). doi:10.3390/genes12060920

185. Glanzer JG, Liu S, Wang L, Mosel A, Peng A, Oakley GG. RPA inhibition increases replication stress and suppresses tumor growth. *Cancer Res*. 2014;74(18):5165-5172. doi:10.1158/0008-5472.CAN-14-0306

186. Trenner A, Sartori AA. Harnessing DNA Double-Strand Break Repair for Cancer Treatment. *Front Oncol*. 2019;9:1388. doi:10.3389/fonc.2019.01388

187. Chang HHY, Pannunzio NR, Adachi N, Lieber MR. Non-homologous DNA end joining and alternative pathways to double-strand break repair. *Nat Rev Mol Cell Biol*. 2017;18(8):495-506. doi:10.1038/nrm.2017.48

188. Drouet J, Frit P, Delteil C, De Villartay JP, Salles B, Calsou P. Interplay between Ku, artemis, and the DNA-dependent protein kinase catalytic subunit at DNA ends. *J Biol Chem*. 2006;281(38):27784-27793. doi:10.1074/jbc.M603047200

189. Yoo S, Dynan WS. Geometry of a complex formed by double strand break repair proteins at a single DNA end: Recruitment of DNA-PKcs induces inward translocation of Ku protein. *Nucleic Acids Res*. 1999;27(24):4679-4686. doi:10.1093/nar/27.24.4679

190. Cui X, Yu Y, Gupta S, Cho Y-M, Lees-Miller SP, Meek K. Autophosphorylation of DNA-Dependent Protein Kinase Regulates DNA End Processing and May Also Alter Double-Strand Break Repair Pathway Choice. *Mol Cell Biol*. 2005;25(24):10842-10852. doi:10.1128/mcb.25.24.10842-10852.2005

191. Ebert D, Greenberg ME. Beyond DNA repair: DNA-PK function in cancer. *Bone*. 2013;23(1):237-337. doi:10.1158/2159-8290.CD-14-0358.Beyond

192. Chang HHY, Watanabe G, Lieber MR. Unifying the DNA end-processing roles of the artemis nuclease: Ku-dependent artemis resection at blunt DNA ends. *J Biol Chem*. 2015;290(40):24036-24050. doi:10.1074/jbc.M115.680900

193. Ramsden DA. Polymerases in nonhomologous end joining: building a bridge over broken chromosomes. *Antioxid Redox Signal*. 2011;14(12):2509-2519. doi:10.1089/ars.2010.3429

194. Conlin MP, Reid DA, Small GW, et al. DNA Ligase IV Guides End-Processing Choice during Nonhomologous End Joining. *Cell Rep*. 2017;20(12):2810-2819. doi:10.1016/j.celrep.2017.08.091

195. Brouwer I, Sitters G, Candelli A, et al. Sliding sleeves of XRCC4-XLF bridge DNA and connect fragments of broken DNA. *Nature*. 2016;535(7613):566-569. doi:10.1038/nature18643

196. Mukherjee B, Choy H, Nirodi C, Burma S. Targeting nonhomologous end-joining through epidermal growth factor receptor inhibition: Rationale and strategies for radiosensitization. *Semin Radiat Oncol*. 2010;20(4):250-257. doi:10.1016/j.semradonc.2010.05.002

197. Srivastava M, Nambiar M, Sharma S, et al. An inhibitor of nonhomologous end-joining abrogates double-strand break repair and impedes cancer progression. *Cell*. 2012;151(7):1474-1487. doi:10.1016/j.cell.2012.11.054

198. Gopalakrishnan V, Sharma S, Ray U, et al. SCR7, an inhibitor of NHEJ can sensitize tumor cells to ionization radiation. *Mol Carcinog*. 2021;60(9):627-643. doi:10.1002/mc.23329

199. Greco GE, Matsumoto Y, Brooks RC, Lu Z, Lieber MR, Tomkinson AE. SCR7 is neither a selective nor a potent inhibitor of human DNA ligase IV. *DNA Repair (Amst)*.

2016;43:18-23. doi:10.1016/j.dnarep.2016.04.004

200. Zhu C, Wang X, Li P, et al. Developing a Peptide That Inhibits DNA Repair by Blocking the Binding of Artemis and DNA Ligase IV to Enhance Tumor Radiosensitivity. *Int J Radiat Oncol Biol Phys*. 2021;111(2):515-527. doi:10.1016/j.ijrobp.2021.05.120

201. Liu H, Sun X, Zhang S, et al. The dominant negative mutant Artemis enhances tumor cell radiosensitivity. *Radiother Oncol*. 2011;101(1):66-72. doi:10.1016/j.radonc.2011.05.034

202. Wen Y, Dai G, Wang L, Fu K, Zuo S. Silencing of XRCC4 increases radiosensitivity of triple-negative breast cancer cells. *Biosci Rep*. 2019;39(3). doi:10.1042/BSR20180893

203. Jones KR, Gewirtz DA, Yannone SM, et al. Radiosensitization of MDA-MB-231 breast tumor cells by adenovirus-mediated overexpression of a fragment of the XRCC4 protein. 2005;4(October):1541-1547. doi:10.1158/1535-7163.MCT-05-0193

204. Visconti R, Della Monica R, Grieco D. Cell cycle checkpoint in cancer: A therapeutically targetable double-edged sword. *J Exp Clin Cancer Res*. 2016;35(1):153. doi:10.1186/s13046-016-0433-9

205. Donzelli M, Draetta GF. Regulating mammalian checkpoints through Cdc25 inactivation. *EMBO Rep*. 2003;4(7):671-677. doi:https://doi.org/10.1038/sj.embor.embor887

206. Barnum KJ, O'Connell MJ. Cell cycle regulation by checkpoints. *Methods Mol Biol*. 2014;1170:29-40. doi:10.1007/978-1-4939-0888-2_2

207. Bertoli C, Skotheim JM, De Bruin RAM. Control of cell cycle transcription during G1 and S phases. *Nat Rev Mol Cell Biol*. 2013;14(8):518-528. doi:10.1038/nrm3629

208. Vitale I, Galluzzi L, Castedo M, Kroemer G. Mitotic catastrophe: a mechanism for avoiding genomic instability. *Nat Rev Mol Cell Biol*. 2011;12(6):385-392. doi:10.1038/nrm3115

209. Vlatkovic T, Veldwijk MR, Giordano FA, Herskind C. Targeting Cell Cycle Checkpoint Kinases to Overcome Intrinsic Radioresistance in Brain Tumor Cells. *Cancers (Basel)*. 2022;14(3). doi:10.3390/cancers14030701

210. Sørensen CS, Syljuåsen RG, Falck J, et al. Chk1 regulates the S phase checkpoint by coupling the physiological turnover and ionizing radiation-induced accelerated proteolysis of Cdc25A. *Cancer Cell*. 2003;3(3):247-258. doi:10.1016/s1535-6108(03)00048-5

211. de Gooijer MC, van den Top A, Bockaj I, Beijnen JH, Würdinger T, van Tellingen O. The G2 checkpoint-a node-based molecular switch. *FEBS Open Bio*. 2017;7(4):439-455. doi:10.1002/2211-5463.12206

212. Zhang Y, Hunter T. Roles of Chk1 in cell biology and cancer therapy. *Int J cancer*. 2014;134(5):1013-1023. doi:10.1002/ijc.28226

213. Borst GR, McLaughlin M, Kyula JN, et al. Targeted radiosensitization by the Chk1 inhibitor SAR-020106. *Int J Radiat Oncol Biol Phys*. 2013;85(4):1110-1118. doi:10.1016/j.ijrobp.2012.08.006

214. Barker HE, Patel R, McLaughlin M, et al. CHK1 Inhibition Radiosensitizes Head and Neck Cancers to Paclitaxel-Based Chemoradiotherapy. *Mol Cancer Ther*. 2016;15(9):2042-2054. doi:10.1158/1535-7163.MCT-15-0998

215. Morgan MA, Parsels LA, Zhao L, et al. Mechanism of radiosensitization by the Chk1/2 inhibitor AZD7762 involves abrogation of the G2 checkpoint and inhibition of homologous recombinational DNA repair. *Cancer Res*. 2010;70(12):4972-4981. doi:10.1158/0008-5472.CAN-09-3573

216. Zannini L, Delia D, Buscemi G. CHK2 kinase in the DNA damage response and beyond. *J Mol Cell Biol*. 2014;6(6):442-457. doi:10.1093/jmcb/mju045

217. Gogineni VR, Nalla AK, Gupta R, Dinh DH, Klopfenstein JD, Rao JS. Chk2-mediated G2/M cell cycle arrest maintains radiation resistance in malignant meningioma cells. *Cancer Lett*. 2011;313(1):64-75. doi:10.1016/j.canlet.2011.08.022

218. Jobson AG, Lountos GT, Lorenzi PL, et al. Cellular inhibition of checkpoint kinase 2 (Chk2) and potentiation of camptothecins and radiation by the novel Chk2 inhibitor PV1019 [7-nitro-1H-indole-2-carboxylic acid {4-[1-(guanidinohydrazone)-ethyl]-phenyl}- amide]. *J Pharmacol Exp Ther*. 2009;331(3):816-826. doi:10.1124/jpet.109.154997

219. ClinicalTrials.gov. A Study of Prexasertib (LY2606368) in Platinum-Resistant or

Refractory Recurrent Ovarian Cancer - Full Text View - ClinicalTrials.gov. https://clinicaltrials.gov/ct2/show/NCT03414047. Published 2018. Accessed March 26, 2020.

220. Endersby R, Hii H, Strowger B, et al. MBRS-35. COMBINING Chk1/2 INHIBITION WITH RADIATION ENHANCES IN VITRO AND IN VIVO CYTOTOXICITY IN MEDULLOBLASTOMA. *Neuro Oncol*. 2018;20(suppl_2):i135-i136. doi:10.1093/neuonc/noy059.480

221. Zeng L, Beggs RR, Cooper TS, Weaver AN, Yang ES. Combining Chk1/2 inhibition with cetuximab and radiation enhances in vitro and in vivo cytotoxicity in head and neck squamous cell carcinoma. *Mol Cancer Ther*. 2017;16(4):591-600. doi:10.1158/1535-7163.MCT-16-0352

222. Ghelli Luserna di Rorà A, Cerchione C, Martinelli G, Simonetti G. A WEE1 family business: regulation of mitosis, cancer progression, and therapeutic target. *J Hematol Oncol*. 2020;13(1):126. doi:10.1186/s13045-020-00959-2

223. Lee Y-Y, Cho Y-J, Shin S, et al. Anti-Tumor Effects of Wee1 Kinase Inhibitor with Radiotherapy in Human Cervical Cancer. *Sci Rep*. 2019;9(1):15394. doi:10.1038/s41598-019-51959-3

224. Caretti V, Hiddingh L, Lagerweij T, et al. WEE1 kinase inhibition enhances the radiation response of diffuse intrinsic pontine gliomas. *Mol Cancer Ther*. 2013;12(2):141-150. doi:10.1158/1535-7163.MCT-12-0735

225. PosthumaDeBoer J, Würdinger T, Graat HCA, et al. WEE1 inhibition sensitizes osteosarcoma to radiotherapy. *BMC Cancer*. 2011;11(1):156. doi:10.1186/1471-2407-11-156

226. Cuneo KC, Morgan MA, Davis MA, et al. Wee1 Kinase Inhibitor AZD1775 Radiosensitizes Hepatocellular Carcinoma Regardless of TP53 Mutational Status Through Induction of Replication Stress. *Int J Radiat Oncol Biol Phys*. 2016;95(2):782-790. doi:10.1016/j.ijrobp.2016.01.028

227. Lee YY, Cho YJ, Shin S won, et al. Anti-Tumor Effects of Wee1 Kinase Inhibitor with Radiotherapy in Human Cervical Cancer. *Sci Rep*. 2019;9(1):1-11. doi:10.1038/s41598-019-51959-3

228. Bukhari AB, Chan GK, Gamper AM. Targeting the DNA Damage Response for Cancer Therapy by Inhibiting the Kinase Wee1. *Front Oncol*. 2022;12(February):1-13. doi:10.3389/fonc.2022.828684

229. Shah M, Nunes MR, Stearns V. CDK4/6 inhibitors: Game changers in the management of hormone receptor– positive advanced breast cancer? *Oncol (United States)*. 2018;32(5):216-222.

230. Salvador-Barbero B, Álvarez-Fernández M, Zapatero-Solana E, et al. CDK4/6 Inhibitors Impair Recovery from Cytotoxic Chemotherapy in Pancreatic Adenocarcinoma. *Cancer Cell*. 2020;37(3):340-353.e6. doi:10.1016/j.ccell.2020.01.007

231. Yang Y, Luo J, Chen X, et al. CDK4/6 inhibitors: a novel strategy for tumor radiosensitization. doi:10.1186/s13046-020-01693-w

232. Hashizume R, Zhang A, Mueller S, et al. Inhibition of DNA damage repair by the CDK4/6 inhibitor palbociclib delays irradiated intracranial atypical teratoid rhabdoid tumor and glioblastoma xenograft regrowth. *Neuro Oncol*. 2016;18(11):1519-1528. doi:10.1093/neuonc/now106

233. Meattini I, Desideri I, Scotti V, Simontacchi G, Livi L. Ribociclib plus letrozole and concomitant palliative radiotherapy for metastatic breast cancer. *Breast*. 2018;42:1-2. doi:10.1016/j.breast.2018.08.096

234. Ippolito E, Greco C, Silipigni S, et al. Concurrent radiotherapy with palbociclib or ribociclib for metastatic breast cancer patients: Preliminary assessment of toxicity. *Breast*. 2019;46:70-74. doi:10.1016/j.breast.2019.05.001

235. Kalapurakal JA, Wang Y, Ghoreishi-Haack N, et al. CDK 4/6 Inhibitors are Potent Radiosensitizers in Retinoblastoma Protein Positive Meningiomas. *Int J Radiat Oncol*. 2022;114(3, Supplement):S63-S64. doi:https://doi.org/10.1016/j.ijrobp.2022.07.450

236. Farnebo M, Bykov VJN, Wiman KG. The p53 tumor suppressor: A master regulator of diverse cellular processes and therapeutic target in cancer. *Biochem Biophys Res Commun*. 2010;396(1):85-89. doi:10.1016/j.bbrc.2010.02.152

237. Robles AI, Jen J, Harris CC. Clinical outcomes of TP53 mutations in cancers. *Cold Spring Harb Perspect Med*. 2016;6(9). doi:10.1101/cshperspect.a026294

238. Lee JM, Bernstein A. p53 Mutations increase resistance to ionizing radiation. *Proc Natl Acad Sci U S A*. 1993;90(12):5742-5746. doi:10.1073/pnas.90.12.5742

239. Akiyama A, Minaguchi T, Fujieda K, et al. Abnormal accumulation of p53 predicts radioresistance leading to poor survival in patients with endometrial carcinoma. *Oncol Lett*. 2019;18(6):5952-5958. doi:10.3892/ol.2019.10940

240. Tisato V, Voltan R, Gonelli A, Secchiero P, Zauli G. MDM2/X inhibitors under clinical evaluation: Perspectives for the management of hematological malignancies and pediatric cancer. *J Hematol Oncol*. 2017;10(1). doi:10.1186/s13045-017-0500-5

241. Konopleva MY, Röllig C, Cavenagh J, et al. Idasanutlin plus cytarabine in relapsed or refractory acute myeloid leukemia: results of the MIRROS trial. *Blood Adv*. 2022;6(14):4147-4156. doi:10.1182/bloodadvances.2021006303

242. Alimova I, Wang D, Danis E, et al. Targeting the TP53/MDM2 axis enhances radiation sensitivity in atypical teratoid rhabdoid tumors. *Int J Oncol*. 2022;60(3). doi:10.3892/ijo.2022.5322

243. Phelps D, Bondra K, Seum S, et al. Inhibition of MDM2 by RG7388 confers hypersensitivity to X-radiation in xenograft models of childhood sarcoma. *Pediatr Blood Cancer*. 2015;62(8):1345-1352. doi:10.1002/pbc.25465

244. Lambert JMR, Gorzov P, Veprintsev DB, et al. PRIMA-1 Reactivates Mutant p53 by Covalent Binding to the Core Domain. *Cancer Cell*. 2009;15(5):376-388. doi:10.1016/j.ccr.2009.03.003

245. Hyder. PRIMA-1 inhibits growth of breast cancer cells by re-activating mutant p53 protein. *Int J Oncol*. 2009;35(05):1015-1023. doi:10.3892/ijo_00000416

246. Zache N, Lambert JMR, Wiman KG, Bykov VJN. PRIMA-1MET inhibits growth of mouse tumors carrying mutant p53. *Cell Oncol*. 2008;30(5):411-418. doi:10.3233/CLO-2008-0440

247. Shi H, Lambert JMR, Hautefeuille A, et al. In vitro and in vivo cytotoxic effects of PRIMA-1 on hepatocellular carcinoma cells expressing mutant p53ser249. *Carcinogenesis*. 2008;29(7):1428-1434. doi:10.1093/carcin/bgm266

248. Overgaard J, Hansen HS, Overgaard M, et al. A randomized double-blind phase III study of nimorazole as a hypoxic radiosensitizer of primary radiotherapy in supraglottic

larynx and pharynx carcinoma. Results of the Danish Head and Neck Cancer Study (DAHANCA) Protocol 5-85. *Radiother Oncol*. 1998;46(2):135-146. doi:10.1016/s0167-8140(97)00220-x

249. Telarovic I, Wenger RH, Pruschy M. Interfering with Tumor Hypoxia for Radiotherapy Optimization. *J Exp Clin Cancer Res*. 2021;40(1):197. doi:10.1186/s13046-021-02000-x

250. Loap P, Loirat D, Berger F, et al. Combination of Olaparib and Radiation Therapy for Triple Negative Breast Cancer: Preliminary Results of the RADIOPARP Phase 1 Trial. *Int J Radiat Oncol*. 2021;109(2):436-440. doi:10.1016/J.IJROBP.2020.09.032

251. Jagsi R, Griffith KA, Bellon JR, et al. Concurrent Veliparib With Chest Wall and Nodal Radiotherapy in Patients With Inflammatory or Locoregionally Recurrent Breast Cancer: The TBCRC 024 Phase I Multicenter Study. *J Clin Oncol*. 2018;36(13):1317-1322. doi:10.1200/JCO.2017.77.2665

252. Cuneo KC, Morgan MA, Sahai V, et al. Dose Escalation Trial of the Wee1 Inhibitor Adavosertib (AZD1775) in Combination With Gemcitabine and Radiation for Patients With Locally Advanced Pancreatic Cancer. *J Clin Oncol*. 2019;37(29):2643-2650. doi:10.1200/JCO.19.00730

253. Elbanna M, Chowdhury NN, Rhome R, Fishel ML. Clinical and Preclinical Outcomes of Combining Targeted Therapy With Radiotherapy. *Front Oncol*. 2021;11. doi:10.3389/fonc.2021.749496

254. Cuneo KC, Nyati MK, Ray D, Lawrence TS. EGFR targeted therapies and radiation: Optimizing efficacy by appropriate drug scheduling and patient selection. *Pharmacol Ther*. 2015;154:67-77. doi:10.1016/j.pharmthera.2015.07.002

255. Bonner JA, Harari PM, Giralt J, et al. Radiotherapy plus cetuximab for squamous-cell carcinoma of the head and neck. *N Engl J Med*. 2006;354(6):567-578. doi:10.1056/NEJMoa053422

256. Bradley JD, Paulus R, Komaki R, et al. Standard-dose versus high-dose conformal radiotherapy with concurrent and consolidation carboplatin plus paclitaxel with or without cetuximab for patients with stage IIIA or IIIB non-small-cell lung cancer (RTOG 0617): a randomised, two-by-two factorial . *Lancet Oncol*. 2015;16(2):187-199. doi:10.1016/S1470-2045(14)71207-0

257. Sparano JA, Lee JY, Palefsky J, et al. Cetuximab Plus Chemoradiotherapy for HIV-Associated Anal Carcinoma: A Phase II AIDS Malignancy Consortium Trial. *J Clin Oncol* . 2017;35(7):727-733. doi:10.1200/JCO.2016.69.1642

258. Zaidi S, Huddart R, Harrington K. Novel Targeted Radiosensitisers in Cancer Treatment. *Curr Drug Discov Technol*. 2009;6(2):103-134. doi:10.2174/157016309788488348

259. Bailey S, André N, Gandola L, Massimino M, Rutkowski S, Clifford SC. Clinical Trials in High-Risk Medulloblastoma: Evolution of the SIOP-Europe HR-MB Trial. *Cancers (Basel)*. 2022;14(2):1-21. doi:10.3390/cancers14020374

260. Padovani L, Andre N, Gentet JC, et al. Reirradiation and concomitant metronomic temozolomide: an efficient combination for local control in medulloblastoma disease? *J Pediatr Hematol Oncol*. 2011;33(8):600-604. doi:10.1097/MPH.0b013e3182331eaf

261. Buck J, Dyer PJC, Hii H, et al. Veliparib Is an Effective Radiosensitizing Agent in a Preclinical Model of Medulloblastoma. *Front Mol Biosci*. 2021;8(April):1-11. doi:10.3389/fmolb.2021.633344

262. Pezuk J, Valera E, Delsin L, Scrideli C, Tone L, Brassesco M. The Antiproliferative and Pro-apoptotic Effects of Methoxyamine on Pediatric Medulloblastoma Cell Lines Exposed to Ionizing Radiation and Chemotherapy. *Cent Nerv Syst Agents Med Chem*. 2015;16(1):67-72. doi:10.2174/1871524915666150817112946

263. Ferreira S, Foray C, Gatto A, et al. AsiDNA Is a radiosensitizer with no added toxicity in medulloblastoma pediatric models. *Clin Cancer Res*. 2021;26(21):5735-5746. doi:10.1158/1078-0432.CCR-20-1729

264. Chetty C, Dontula R, Gujrati M, Dinh DH, Lakka SS. Blockade of SOX4 mediated DNA repair by SPARC enhances radioresponse in medulloblastoma. *Cancer Lett*. 2012;323(2):188-198. doi:10.1016/j.canlet.2012.04.014

265. Whiteway SL, Harris PS, Venkataraman S, et al. Inhibition of cyclin-dependent kinase 6 suppresses cell proliferation and enhances radiation sensitivity in medulloblastoma cells. *J Neurooncol*. 2013;111(2):113-121. doi:10.1007/s11060-012-1000-7

266. Wang D, Veo B, Pierce A, et al. A novel PLK1 inhibitor onvansertib effectively sensitizes MYC-driven medulloblastoma to radiotherapy. *Neuro Oncol*.

2022;24(3):414-426. doi:10.1093/neuonc/noab207

267. Ramos PMM, Pezuk JA, Castro-Gamero AM, et al. Antineoplastic Effects of NF-κB Inhibition by DHMEQ (Dehydroxymethylepoxyquinomicin) Alone and in Co-treatment with Radio-and Chemotherapy in Medulloblastoma Cell Lines. *Anticancer Agents Med Chem*. 2018;18(4):541-549. doi:10.2174/1871520617666171113151335

268. Markowitz D, Powell C, Tran NL, et al. Pharmacological Inhibition of the Protein Kinase MRK/ZAK Radiosensitizes Medulloblastoma. *Mol Cancer Ther*. 15(8). doi:10.1158/1535-7163.MCT-15-0849

269. Meister N, Shalaby T, von Bueren AO, et al. Interferon-γ mediated up-regulation of caspase-8 sensitises medulloblastoma cells to radio- and chemotherapy. *Eur J Cancer*. 2007;43(12):1833-1841. doi:10.1016/j.ejca.2007.05.028

270. Dritschilo A, Scifoni E, Mansour WY, et al. The Combination of Particle Irradiation With the Hedgehog Inhibitor GANT61 Differently Modulates the Radiosensitivity and Migration of Cancer Cells Compared to X-Ray Irradiation. *Front Oncol | www.frontiersin.org*. 2019;1:391. doi:10.3389/fonc.2019.00391

271. Bhatia S, Baig NA, Timofeeva O, et al. Knockdown of ephb1 receptor decreases medulloblastoma cell growth and migration and increases cellular radiosensitization. *Oncotarget*. 2015;6(11):8929-8946. doi:10.18632/oncotarget.3369

272. Song H, Xi S, Chen Y, et al. Histone chaperone FACT complex inhibitor CBL0137 interferes with DNA damage repair and enhances sensitivity of medulloblastoma to chemotherapy and radiation. *Cancer Lett*. 2021;520(June):201-212. doi:10.1016/j.canlet.2021.07.020

273. Sonnemann J, Kumar KS, Heesch S, et al. Histone deacetylase inhibitors induce cell death and enhance the susceptibility to ionizing radiation, etoposide, and TRAIL in medulloblastoma cells. *Int J Oncol*. 2006;28(3):755-766. doi:10.3892/ijo.28.3.755

274. Asuthkar S, Kumar Nalla A, Gondi CS, et al. Gadd45a sensitizes medulloblastoma cells to irradiation and suppresses MMP-9-mediated EMT. *Neuro Oncol*. 2011;13(10):1059-1073. doi:10.1093/neuonc/nor109

275. Oehler C, von Bueren AO, Furmanova P, et al. The microtubule stabilizer patupilone (epothilone B) is a potent radiosensitizer in medulloblastoma cells.

doi:10.1093/neuonc/nor069

276. Henrique P, Klinger S, Elis L, et al. Arsenic trioxide exerts cytotoxic and radiosensitizing effects in pediatric Medulloblastoma cell lines of SHH Subgroup. doi:10.1038/s41598-020-63808-9

277. Rossi M, Talbot J, Piris P, et al. Beta-blockers disrupt mitochondrial bioenergetics and increase radiotherapy efficacy independently of beta-adrenergic receptors in medulloblastoma. *eBioMedicine*. 2022;82:104149. doi:https://doi.org/10.1016/j.ebiom.2022.104149

278. Chang C-J, Chiang C-H, Song W-S, et al. Inhibition of phosphorylated STAT3 by cucurbitacin I enhances chemoradiosensitivity in medulloblastoma-derived cancer stem cells. *Childs Nerv Syst*. 2012;28:363-373. doi:10.1007/s00381-011-1672-x

279. Yang M-Y, Lee H-T, Chen C-M, Shen C-C, Ma H-I. Celecoxib Suppresses the Phosphorylation of STAT3 Protein and Can Enhance the Radiosensitivity of Medulloblastoma-Derived Cancer Stem-Like Cells. *Int J Mol Sci*. 2014;15:11013-11029. doi:10.3390/ijms150611013

280. Endersby R, Whitehouse J, Pribnow A, et al. Small-molecule screen reveals synergy of cell cycle checkpoint kinase inhibitors with DNA-damaging chemotherapies in medulloblastoma. *Sci Transl Med*. 2021;13(577). doi:10.1126/scitranslmed.aba7401

281. Prince EW, Balakrishnan I, Shah M, et al. Checkpoint kinase 1 expression is an adverse prognostic marker and therapeutic target in MYC-driven medulloblastoma. *Oncotarget*. 2016;7(33):53881-53894. doi:10.18632/oncotarget.10692

282. Krüger K, Geist K, Stuhldreier F, et al. Multiple DNA damage-dependent and DNA damage-independent stress responses define the outcome of ATR/Chk1 targeting in medulloblastoma cells. *Cancer Lett*. 2018;430:34-46. doi:10.1016/j.canlet.2018.05.011

283. Di Giulio S, Colicchia V, Pastorino F, et al. A combination of PARP and CHK1 inhibitors efficiently antagonizes MYCN-driven tumors. *Oncogene*. 2021;40(43):6143-6152. doi:10.1038/s41388-021-02003-0

284. Matheson CJ, Venkataraman S, Amani V, et al. A WEE1 Inhibitor Analog of AZD1775 Maintains Synergy with Cisplatin and Demonstrates Reduced Single-Agent Cytotoxicity in Medulloblastoma Cells. *ACS Chem Biol*. 2016;11(4):921-930.

doi:10.1021/acschembio.5b00725

285. Moreira DC, Venkataraman S, Subramanian A, et al. Targeting MYC-driven replication stress in medulloblastoma with AZD1775 and gemcitabine. *J Neurooncol*. 2020;147(3):531-545. doi:10.1007/s11060-020-03457-0

286. Harris PS, Venkataraman S, Alimova I, et al. Integrated genomic analysis identifies the mitotic checkpoint kinase WEE1 as a novel therapeutic target in medulloblastoma. *Mol Cancer*. 2014;13:72. doi:10.1186/1476-4598-13-72

287. Cole KA, Ijaz H, Surrey LF, et al. Pediatric phase 2 trial of a WEE1 inhibitor, adavosertib (AZD1775), and irinotecan for relapsed neuroblastoma, medulloblastoma, and rhabdomyosarcoma. *Cancer*. April 2023. doi:10.1002/cncr.34786

288. Walker AI, Hunt T, Jackson RJ, Anderson CW. Double-stranded DNA induces the phosphorylation of several proteins including the 90 000 mol. wt. heat-shock protein in animal cell extracts. 1985;4(I):139-145.

289. Shrivastav M, De Haro LP, Nickoloff JA. Regulation of DNA double-strand break repair pathway choice. *Cell Res*. 2008;18(1):134-147. doi:10.1038/CR.2007.111

290. Sallmyr A, Tomkinson AE. Repair of DNA double-strand breaks by mammalian alternative end-joining pathways. *J Biol Chem*. 2018;293(27):10536-10549. doi:10.1074/jbc.TM117.000375

291. Neal JA, Dang V, Douglas P, Wold MS, Lees-Miller SP, Meek K. Inhibition of Homologous Recombination by DNA-Dependent Protein Kinase Requires Kinase Activity, Is Titratable, and Is Modulated by Autophosphorylation. *Mol Cell Biol*. 2011;31(8):1719-1733. doi:10.1128/mcb.01298-10

292. Shibata A, Conrad S, Birraux J, et al. Factors determining DNA double-strand break repair pathway choice in G2 phase. *EMBO J*. 2011;30(6):1079-1092. doi:10.1038/emboj.2011.27

293. Zhao F, Kim W, Kloeber JA, Lou Z. DNA end resection and its role in DNA replication and DSB repair choice in mammalian cells. *Exp Mol Med*. 2020;52(10):1705-1714. doi:10.1038/s12276-020-00519-1

294. Katsuki Y, Jeggo PA, Uchihara Y, Takata M, Shibata A. DNA double-strand break end resection: a critical relay point for determining the pathway of repair and signaling.

Genome Instab Dis. 2020;1(4):155-171. doi:10.1007/s42764-020-00017-8

295. Davis AJ, Chi L, So S, et al. BRCA1 modulates the autophosphorylation status of DNA-PKcs in S phase of the cell cycle. *Nucleic Acids Res*. 2014;42(18):11487-11501. doi:10.1093/nar/gku824

296. Zhou Y, Lee JH, Jiang W, Crowe JL, Zha S, Paull TT. Regulation of the DNA Damage Response by DNA-PKcs Inhibitory Phosphorylation of ATM. *Mol Cell*. 2017;65(1):91-104. doi:10.1016/j.molcel.2016.11.004

297. Obeng E. Apoptosis (programmed cell death) and its signals - A review. *Braz J Biol*. 2021;81(4):1133-1143. doi:10.1590/1519-6984.228437

298. Tomita M. Involvement of DNA-PK and ATM in radiation- and heat-induced DNA damage recognition and apoptotic cell death. *J Radiat Res*. 2010;51(5):493-501. doi:10.1269/jrr.10039

299. Gurley KE, Moser R, Gu Y, Hasty P, Kemp CJ. DNA-PK suppresses a p53-independent apoptotic response to DNA damage. *EMBO Rep*. 2009;10(1):87-93. doi:10.1038/embor.2008.214

300. Bozulic L, Surucu B, Hynx D, Hemmings BA. PKBα/Akt1 Acts Downstream of DNA-PK in the DNA Double-Strand Break Response and Promotes Survival. *Mol Cell*. 2008;30(2):203-213. doi:10.1016/J.MOLCEL.2008.02.024

301. Zhang Q, Steinle JJ. DNA-PK phosphorylation of IGFBP-3 is required to prevent apoptosis in retinal endothelial cells cultured in high glucose. *Investig Ophthalmol Vis Sci*. 2013;54(4):3052-3057. doi:10.1167/iovs.12-11533

302. da Costa AABA, Chowdhury D, Shapiro GI, D'Andrea AD, Konstantinopoulos PA. Targeting replication stress in cancer therapy. *Nat Rev Drug Discov*. 2023;22(1):38-58. doi:10.1038/s41573-022-00558-5

303. Lin Y-F, Shih H-Y, Shang Z-F, et al. PIDD mediates the association of DNA-PKcs and ATR at stalled replication forks to facilitate the ATR signaling pathway. *Nucleic Acids Res*. 2018;46(4):1847-1859. doi:10.1093/nar/gkx1298

304. Yajima H, Lee K-J, Chen BPC. ATR-dependent phosphorylation of DNA-dependent protein kinase catalytic subunit in response to UV-induced replication stress. *Mol Cell Biol*. 2006;26(20):7520-7528. doi:10.1128/MCB.00048-06

305. Dibitetto D, Marshall S, Sanchi A, et al. DNA-PKcs promotes fork reversal and chemoresistance. *Mol Cell*. 2022;82(20):3932-3942.e6. doi:10.1016/j.molcel.2022.08.028

306. Zhang J, Chen M, Pang Y, et al. Flap endonuclease 1 and DNA-PKcs synergistically participate in stabilizing replication fork to encounter replication stress in glioma cells. *J Exp Clin Cancer Res*. 2022;41(1):140. doi:10.1186/s13046-022-02334-0

307. Ashley AK, Shrivastav M, Nie J, et al. DNA-PK phosphorylation of RPA32 Ser4/Ser8 regulates replication stress checkpoint activation, fork restart, homologous recombination and mitotic catastrophe. *DNA Repair (Amst)*. 2014;21:131-139. doi:10.1016/j.dnarep.2014.04.008

308. Chibazakura T, Watanabe F, Kitajima S, Tsukada K, Yasukochi Y, Teraoka H. Phosphorylation of human general transcription factors TATA-binding protein and transcription factor IIB by DNA-dependent protein kinase--synergistic stimulation of RNA polymerase II basal transcription in vitro. *Eur J Biochem*. 1997;247(3):1166-1173. doi:10.1111/j.1432-1033.1997.01166.x

309. Mohiuddin IS, Kang MH. DNA-PK as an Emerging Therapeutic Target in Cancer. *Front Oncol*. 2019;9:635. doi:10.3389/fonc.2019.00635

310. Medunjanin S, Weinert S, Schmeisser A, Mayer D, Braun-Dullaeus RC. Interaction of the double-strand break repair kinase DNA-PK and estrogen receptor-alpha. *Mol Biol Cell*. 2010;21(9):1620-1628. doi:10.1091/mbc.e09-08-0724

311. Goodwin JF, Kothari V, Drake JM, et al. DNA-PKcs-Mediated Transcriptional Regulation Drives Prostate Cancer Progression and Metastasis. *Cancer Cell*. 2015;28(1):97-113. doi:10.1016/j.ccell.2015.06.004

312. Iijima S, Teraoka H, Date T, Tsukada K. DNA-activated protein kinase in Raji Burkitt's lymphoma cells. Phosphorylation of c-Myc oncoprotein. *Eur J Biochem*. 1992;206(2):595-603. doi:10.1111/j.1432-1033.1992.tb16964.x

313. Roth DB. V(D)J Recombination: Mechanism, Errors, and Fidelity. *Microbiol Spectr*. 2014;2(6). doi:10.1128/MICROBIOLSPEC.MDNA3-0041-2014

314. Björkman A, Du L, Felgentreff K, et al. DNA-PKcs Is Involved in Ig Class Switch Recombination in Human B Cells. *J Immunol*. 2015;195(12):5608-5615.

doi:10.4049/jimmunol.1501633

315. Azevedo-Pouly AC, Appell LE, Burdine L, et al. Inhibition of DNA-PKcs impairs the activation and cytotoxicity of CD4+ helper and CD8+ effector T cells. *bioRxiv*. 2022:2022.06.23.497236. doi:10.1101/2022.06.23.497236

316. Waldrip ZJ, Burdine L, Harrison DK, et al. DNA-PKcs kinase activity stabilizes the transcription factor Egr1 in activated immune cells. *J Biol Chem*. 2021;297(4):101209. doi:10.1016/j.jbc.2021.101209

317. Shao L, Goronzy JJ, Weyand CM. DNA-dependent protein kinase catalytic subunit mediates T-cell loss in rheumatoid arthritis. *EMBO Mol Med*. 2010;2(10):415-427. doi:10.1002/emmm.201000096

318. Terstege DJ, Addo-Osafo K, Campbell Teskey G, Epp JR. New neurons in old brains: implications of age in the analysis of neurogenesis in post-mortem tissue. *Mol Brain*. 2022;15(1):38. doi:10.1186/s13041-022-00926-7

319. Sorrells SF, Paredes MF, Cebrian-Silla A, et al. Human hippocampal neurogenesis drops sharply in children to undetectable levels in adults. *Nature*. 2018;555(7696):377-381. doi:10.1038/nature25975

320. Enriquez-Rios V, Dumitrache LC, Downing SM, et al. DNA-PKcs, ATM, and ATR Interplay Maintains Genome Integrity during Neurogenesis. *J Neurosci*. 2017;37(4):893-905. doi:10.1523/JNEUROSCI.4213-15.2016

321. Baleriola J, Suárez T, De La Rosa EJ. DNA-PK promotes the survival of young neurons in the embryonic mouse retina. *Cell Death Differ*. 2010;17(11):1697-1706. doi:10.1038/cdd.2010.46

322. Gu Y, Sekiguchi J, Gao Y, et al. Defective embryonic neurogenesis in Ku-deficient but not DNA-dependent protein kinase catalytic subunit-deficient mice. *Proc Natl Acad Sci U S A*. 2000;97(6):2668-2673. doi:10.1073/pnas.97.6.2668

323. Vemuri MC, Schiller E, Naegele JR. Elevated DNA double strand breaks and apoptosis in the CNS of scid mutant mice. *Cell Death Differ*. 2001;8(3):245-255. doi:10.1038/sj.cdd.4400806

324. Chechlacz M, Vemuri MC, Naegele JR. Role of DNA-dependent protein kinase in neuronal survival. *J Neurochem*. 2001;78(1):141-154. doi:10.1046/j.1471-

4159.2001.00380.x

325. Frank KM, Sharpless NE, Gao Y, et al. DNA ligase IV deficiency in mice leads to defective neurogenesis and embryonic lethality via the p53 pathway. *Mol Cell*. 2000;5(6):993-1002. doi:10.1016/S1097-2765(00)80264-6

326. Roch B, Abramowski V, Etienne O, et al. An XRCC4 mutant mouse, a model for human X4 syndrome, reveals interplays with Xlf, PAXX, and ATM in lymphoid development. *Elife*. 2021;10. doi:10.7554/eLife.69353

327. Kotula E, Berthault N, Agrario C, et al. DNA-PKcs plays role in cancer metastasis through regulation of secreted proteins involved in migration and invasion. *Cell Cycle*. 2015;14(12):1961-1972. doi:10.1080/15384101.2015.1026522

328. Dylgjeri E, Kothari V, Shafi AA, et al. A Novel Role for DNA-PK in Metabolism by Regulating Glycolysis in Castration-Resistant Prostate Cancer. *Clin Cancer Res*. 2022;28(7):1446-1459. doi:10.1158/1078-0432.CCR-21-1846

329. Chen Y, Li Y, Guan Y, et al. Prevalence of PRKDC mutations and association with response to immune checkpoint inhibitors in solid tumors. *Mol Oncol*. 2020;14(9):2096-2110. doi:10.1002/1878-0261.12739

330. Xing J, Wu X, Vaporciyan AA, Spitz MR, Gu J. Prognostic significance of ataxia-telangiectasia mutated, DNA-dependent protein kinase catalytic subunit, and Ku heterodimeric regulatory complex 86-kD subunit expression in patients with nonsmall cell lung cancer. *Cancer*. 2008;112(12):2756-2764. doi:10.1002/cncr.23533

331. Zhang Y, Wen G-M, Wu C-A, et al. PRKDC is a prognostic marker for poor survival in gastric cancer patients and regulates DNA damage response. *Pathol Res Pract*. 2019;215(8):152509. doi:10.1016/j.prp.2019.152509

332. Zhang Y, Yang W-K, Wen G-M, et al. High expression of PRKDC promotes breast cancer cell growth via p38 MAPK signaling and is associated with poor survival. *Mol Genet genomic Med*. 2019;7(11):e908. doi:10.1002/mgg3.908

333. Zhu L, Ni Z, Luo X, Wang X. Aberrant DNA-PKcs and ERGIC1 expression may be involved in initiation of gastric cancer. *World J Gastroenterol*. 2017;7(1):17-28.

334. Chen Y, Li Y, Xiong J, et al. Role of PRKDC in cancer initiation, progression, and treatment. *Cancer Cell Int*. 2021;21(1):563. doi:10.1186/s12935-021-02229-8

335. Zheng B, Mao J-H, Li X-Q, et al. Over-expression of DNA-PKcs in renal cell carcinoma regulates mTORC2 activation, HIF-2α expression and cell proliferation. *Sci Rep*. 2016;6(1):29415. doi:10.1038/srep29415

336. Stronach EA, Chen M, Maginn EN, et al. DNA-PK mediates AKT activation and apoptosis inhibition in clinically acquired platinum resistance. *Neoplasia*. 2011;13(11):1069-1080. doi:10.1593/neo.111032

337. Liu Y, Zhang L, Liu Y, et al. DNA-PKcs deficiency inhibits glioblastoma cell-derived angiogenesis after ionizing radiation. *J Cell Physiol*. 2015;230(5):1094-1103. doi:10.1002/jcp.24841

338. Yang H, Yao F, Marti TM, Schmid RA, Peng RW. Beyond DNA repair: DNA-PKcs in tumor metastasis, metabolism and immunity. *Cancers (Basel)*. 2020;12(11):1-19. doi:10.3390/cancers12113389

339. Dylgjeri E, McNair C, Goodwin JF, et al. Pleiotropic impact of DNA-PK in cancer and implications for therapeutic strategies. *Clin Cancer Res*. 2019;25(18):5623-5638. doi:10.1158/1078-0432.CCR-18-2207

340. Shimura T, Kakuda S, Ochiai Y, et al. Acquired radioresistance of human tumor cells by DNA-PK/AKT/GSK3b-mediated cyclin D1 overexpression. *Oncogene*. 2010;29:4826-4837. doi:10.1038/onc.2010.238

341. Yu Y, Liu T, Yu G, et al. PRDM15 interacts with DNA-PK-Ku complex to promote radioresistance in rectal cancer by facilitating DNA damage repair. *Cell Death Dis*. 2022;13(11). doi:10.1038/s41419-022-05402-7

342. Kienker LJ, Shin EK, Meek K. Both V(D)J recombination and radioresistance require DNA-PK kinase activity, though minimal levels suffice for V(D)J recombination. *Nucleic Acids Res*. 2000;28(14):2752-2761. doi:10.1093/nar/28.14.2752

343. Ciszewski WM, Tavecchio M, Dastych J, Curtin NJ. DNA-PK inhibition by NU7441 sensitizes breast cancer cells to ionizing radiation and doxorubicin. *Breast Cancer Res Treat*. 2014;143(1):47-55. doi:10.1007/s10549-013-2785-6

344. Fang X, Huang Z, Zhai K, et al. Inhibiting DNA-PK induces glioma stem cell differentiation and sensitizes glioblastoma to radiation in mice. *Sci Transl Med*. 2021;13(600). doi:10.1126/scitranslmed.abc7275

345. Timme CR, Rath BH, O'Neill JW, Camphausen K, Tofilon PJ. The DNA-PK Inhibitor VX-984 Enhances the Radiosensitivity of Glioblastoma Cells Grown In Vitro and as Orthotopic Xenografts. *Mol Cancer Ther*. 2018;17(6):1207-1216. doi:10.1158/1535-7163.MCT-17-1267

346. Wang W, McMillan MT, Zhao X, et al. DNA-PK Inhibition and Radiation Promote Antitumoral Immunity through RNA Polymerase III in Pancreatic Cancer. *Mol Cancer Res*. 2022;20(7):1137-1150. doi:10.1158/1541-7786.MCR-21-0725

347. Wang M, Chen S, Wei Y, Wei X. DNA-PK inhibition by M3814 enhances chemosensitivity in non-small cell lung cancer. *Acta Pharm Sin B*. 2021;11(12):3935-3949. doi:10.1016/j.apsb.2021.07.029

348. Damia G. Targeting DNA-PK in cancer. *Mutat Res Mol Mech Mutagen*. 2020;821:111692. doi:10.1016/J.MRFMMM.2020.111692

349. Vlahos CJ, Matter WF, Hui KY, Brown RF. A specific inhibitor of phosphatidylinositol 3-kinase, 2-(4-morpholinyl)- 8-phenyl-4H-1-benzopyran-4-one (LY294002). *J Biol Chem*. 1994;269(7):5241-5248. doi:10.1016/s0021-9258(17)37680-9

350. Gurung RL, Lim HK, Venkatesan S, Lee PSW, Hande MP. Targeting DNA-PKcs and telomerase in brain tumour cells. *Mol Cancer*. 2014;13:232. doi:10.1186/1476-4598-13-232

351. Tanori M, Pannicelli A, Pasquali E, et al. Cancer risk from low dose radiation in Ptch1(+)(/)(-) mice with inactive DNA repair systems: Therapeutic implications for medulloblastoma. *DNA Repair (Amst)*. 2019;74:70-79. doi:10.1016/j.dnarep.2018.12.003

352. Archer TC, Ehrenberger T, Mundt F, et al. Proteomics, Post-translational Modifications, and Integrative Analyses Reveal Molecular Heterogeneity within Medulloblastoma Subgroups. *Cancer Cell*. 2018;34(3):396-410.e8. doi:10.1016/j.ccell.2018.08.004

353. Liang S, Thomas SE, Chaplin AK, Hardwick SW, Chirgadze DY, Blundell TL. Structural insights into inhibitor regulation of the DNA repair protein DNA-PKcs. *Nature*. 2022;601(7894):643-648. doi:10.1038/s41586-021-04274-9

354. van Bussel MTJ, Awada A, de Jonge MJA, et al. A first-in-man phase 1 study of the DNA-dependent protein kinase inhibitor peposertib (formerly M3814) in patients with advanced solid tumours. *Br J Cancer*. 2021;124(4):728-735. doi:10.1038/s41416-020-01151-6

355. Van Triest B, Damstrup L, Falkenius J, et al. A phase Ia/Ib trial of the DNA-dependent protein kinase inhibitor (DNA-PKi) M3814 in combination with radiotherapy in patients with advanced solid tumors. *J Clin Oncol*. 2017;35(15_suppl):e14048-e14048. doi:10.1200/JCO.2017.35.15_suppl.e14048

356. Talele S, Zhang W, Oh JH, et al. Central Nervous System Delivery of the Catalytic Subunit of DNA-Dependent Protein Kinase Inhibitor Peposertib as Radiosensitizer for Brain Metastases. *J Pharmacol Exp Ther*. 2022;381(3):217-228. doi:10.1124/jpet.121.001069

357. Smithson M, Irwin RK, Williams G, et al. Inhibition of DNA-PK may improve response to neoadjuvant chemoradiotherapy in rectal cancer. *Neoplasia*. 2022;25:53-61. doi:10.1016/J.NEO.2022.01.004

358. Gordhandas SB, Manning-Geist B, Henson C, et al. Pre-clinical activity of the oral DNA-PK inhibitor, peposertib (M3814), combined with radiation in xenograft models of cervical cancer. *Sci Rep*. 2022;12(1). doi:10.1038/s41598-021-04618-5

359. Carr MI, Chiu L-Y, Guo Y, et al. DNA-PK Inhibitor Peposertib Amplifies Radiation-Induced Inflammatory Micronucleation and Enhances TGFβ/PD-L1 Targeted Cancer Immunotherapy. *Mol Cancer Res*. 2022;20(4):568-582. doi:10.1158/1541-7786.MCR-21-0612

360. Haines E, Nishida Y, Carr MI, et al. DNA-PK inhibitor peposertib enhances p53-dependent cytotoxicity of DNA double-strand break inducing therapy in acute leukemia. *Sci Rep*. 2021;11(1):12148. doi:10.1038/s41598-021-90500-3

361. Zenke FT, Zimmermann A, Sirrenberg C, et al. Pharmacologic Inhibitor of DNA-PK, M3814, Potentiates Radiotherapy and Regresses Human Tumors in Mouse Models. *Mol Cancer Ther*. 2020;19(5):1091-1101. doi:10.1158/1535-7163.MCT-19-0734

362. Sun Q, Guo Y, Liu X, et al. Therapeutic implications of p53 status on cancer cell fate following exposure to ionizing radiation and the DNA-PK inhibitor M3814. *Mol Cancer Res*. 2019;17(12):2457-2468. doi:10.1158/1541-7786.MCR-19-0362

363. Klein C, Dokic I, Mairani A, et al. Overcoming hypoxia-induced tumor radioresistance in non-small cell lung cancer by targeting DNA-dependent protein kinase in combination with carbon ion irradiation. *Radiat Oncol*. 2017;12(1). doi:10.1186/s13014-017-0939-0

364. Massimino M, Vennarini S, Ferroli P, et al. Medulloblastoma at relapse : for which patients and which tumors reirradiation is the better choice. *J Neuro oncol*. (Preprint). doi:10.21203/rs.3.rs-2899535/v1

365. Rolland A, Aquilina K. Surgery for recurrent medulloblastoma: A review. *Neurochirurgie*. 2021;67(1):69-75. doi:10.1016/j.neuchi.2019.06.008

366. Balter-Seri J, Mor C, Shuper A, Zaizov R, Cohen IJ. Cure of recurrent medulloblastoma: the contribution of surgical resection at relapse. *Cancer*. 1997;79(6):1241-1247. doi:10.1002/(sici)1097-0142(19970315)79:6<1241::aid-cncr25>3.0.co;2-z

367. Gupta T, Maitre M, Sastri GJ, et al. Outcomes of salvage re-irradiation in recurrent medulloblastoma correlate with age at initial diagnosis, primary risk-stratification, and molecular subgrouping. *J Neurooncol*. 2019;144(2):283-291. doi:10.1007/s11060-019-03225-9

368. Gaab C, Adolph JE, Tippelt S, et al. Local and Systemic Therapy of Recurrent Medulloblastomas in Children and Adolescents: Results of the P-HIT-REZ 2005 Study. *Cancers (Basel)*. 2022;2022:471. doi:10.3390/cancers14030471

369. Sanson KR, Hanna RE, Hegde M, et al. Optimized libraries for CRISPR-Cas9 genetic screens with multiple modalities. *Nat Commun*. 2018;9(1). doi:10.1038/s41467-018-07901-8

370. Richardson S, Hill RM, Kui C, et al. Emergence and maintenance of actionable genetic drivers at medulloblastoma relapse. *Neuro Oncol*. 2022;24(1):153-165. doi:10.1093/neuonc/noab178

371. Leifer CA, Kennedy MN, Mazzoni A, Lee C, Kruhlak MJ, Segal DM. TLR9 is localized in the endoplasmic reticulum prior to stimulation. *J Immunol*. 2004;173(2):1179-1183. doi:10.4049/jimmunol.173.2.1179

372. Matsuzaki K, Kondo S, Ishikawa T, Shinohara A. Human RAD51 paralogue SWSAP1

fosters RAD51 filament by regulating the anti-recombinase FIGNL1 AAA+ ATPase. *Nat Commun*. 2019;10(1):1407. doi:10.1038/s41467-019-09190-1

373. Prakash R, Sandoval T, Morati F, et al. Distinct pathways of homologous recombination controlled by the SWS1–SWSAP1–SPIDR complex. *Nat Commun*. 2021;12(1):4255. doi:10.1038/s41467-021-24205-6

374. Wei L, Murphy BL, Wu G, et al. Exome sequencing analysis of murine medulloblastoma models identifies WDR11 as a potential tumor suppressor in Group 3 tumors. *Oncotarget*. 2017;8(39):64685-64697. doi:10.18632/oncotarget.19642

375. Panganiban RAM, Snow AL, Day RM. Mechanisms of radiation toxicity in transformed and non-transformed cells. *Int J Mol Sci*. 2013;14(8):15931-15958. doi:10.3390/IJMS140815931

376. Cao X, Wen P, Fu Y, et al. Radiation induces apoptosis primarily through the intrinsic pathway in mammalian cells. *Cell Signal*. 2019;62:109337. doi:10.1016/j.cellsig.2019.06.002

377. Crowther AJ, Ocasio JK, Fang F, et al. Radiation sensitivity in a preclinical mouse model of medulloblastoma relies on the function of the intrinsic apoptotic pathway. *Cancer Res*. 2016;76(11):3211-3223. doi:10.1158/0008-5472.CAN-15-0025

378. Jiao Y, Cao F, Liu H. Radiation-induced Cell Death and Its Mechanisms. *Health Phys*. 2022;123(5):376-386. doi:10.1097/HP.0000000000001601

379. Gonçalves AC, Richiardone E, Jorge J, et al. Impact of cancer metabolism on therapy resistance - Clinical implications. *Drug Resist Updat Rev Comment Antimicrob Anticancer Chemother*. 2021;59:100797. doi:10.1016/j.drup.2021.100797

380. Stine ZE, Schug ZT, Salvino JM, Dang C V. Targeting cancer metabolism in the era of precision oncology. *Nat Rev Drug Discov*. 2022;21(2):141-162. doi:10.1038/s41573-021-00339-6

381. Radic Shechter K, Kafkia E, Zirngibl K, et al. Metabolic memory underlying minimal residual disease in breast cancer. *Mol Syst Biol*. 2021;17(10):e10141. doi:https://doi.org/10.15252/msb.202010141

382. Peng J, Cui Y, Xu S, et al. Altered glycolysis results in drug-resistant in clinical tumor therapy. *Oncol Lett*. 2021;21(5):369. doi:10.3892/ol.2021.12630

383. Le M, McNeill FE, Seymour CB, et al. Modulation of oxidative phosphorylation (OXPHOS) by radiation- induced biophotons. *Environ Res*. 2018;163:80-87. doi:10.1016/j.envres.2018.01.027

384. Lu C-L, Qin L, Liu H-C, Candas D, Fan M, Li JJ. Tumor Cells Switch to Mitochondrial Oxidative Phosphorylation under Radiation via mTOR-Mediated Hexokinase II Inhibition - A Warburg-Reversing Effect. *PLoS One*. 2015;10(3):e0121046.

385. Carr MI, Zimmermann A, Chiu L-Y, Zenke FT, Blaukat A, Vassilev LT. DNA-PK Inhibitor, M3814, as a New Combination Partner of Mylotarg in the Treatment of Acute Myeloid Leukemia. *Front Oncol*. 2020;10:127. doi:10.3389/fonc.2020.00127

386. García-Gutiérrez L, Delgado MD, León J. Myc oncogene contributions to release of cell cycle brakes. *Genes (Basel)*. 2019;10(3). doi:10.3390/genes10030244

387. Gupta A, Hunt CR, Chakraborty S, et al. Role of 53BP1 in the regulation of DNA double-strand break repair pathway choice. *Radiat Res*. 2014;181(1):1-8. doi:10.1667/RR13572.1

388. An J, Yang DY, Xu QZ, et al. DNA-dependent protein kinase catalytic subunit modulates the stability of c-Myc oncoprotein. *Mol Cancer*. 2008;7. doi:10.1186/1476-4598-7-32

389. Wei S-J, Yang I-H, Mohiuddin IS, et al. DNA-PKcs as an upstream mediator of OCT4-induced MYC activation in small cell lung cancer. *Biochim Biophys acta Gene Regul Mech*. 2023;1866(2):194939. doi:10.1016/j.bbagrm.2023.194939

390. Murray HC, Miller K, Brzozowski JS, et al. Synergistic Targeting of DNA-PK and KIT Signaling Pathways in KIT Mutant Acute Myeloid Leukemia. *Mol Cell Proteomics*. 2023;22(3). doi:10.1016/j.mcpro.2023.100503

391. Chernova OB, Hunyadi A, Malaj E, et al. A novel member of the WD-repeat gene family, WDR11, maps to the 10q26 region and is disrupted by a chromosome translocation in human glioblastoma cells. *Oncogene*. 2001;20(38):5378-5392. doi:10.1038/sj.onc.1204694

392. Lagerweij T, Hiddingh L, Biesmans D, et al. A chemical screen for medulloblastoma identifies quercetin as a putative radiosensitizer. *Oncotarget*. 2016;7(24):35776-35788.

doi:10.18632/oncotarget.7980

11. ANNEX – Second author publications

"Epigenetic upregulation of Schlafen11 renders WNT- and SHH-activated medulloblastomas sensitive to cisplatin"

Nakate et al., Neuro Oncol

Contribution Statement:

In this publication, I and other members of the lab aided in the completion of revision experiments assessing the impact of SLFN11 knockdown in DAOY cells.

Neuro-Oncology

XX(XX), 1–14, 2022 | https://doi.org/10.1093/neuonc/noac243 | Advance Access date 23 October 2022

Epigenetic upregulation of Schlafen11 renders WNT- and SHH-activated medulloblastomas sensitive to cisplatin

Satoshi Nakata, Junko Murai, Masayasu Okada, Haruhiko Takahashi, Tyler H. Findlay, Kristen Malebranche, Akhila Parthasarathy, Satoshi Miyashita, Ramil Gabdulkhaev, Ilan Benkimoun, Sabine Druillennec, Sara Chabi, Eleanor Hawkins, Hiroaki Miyahara, Kensuke Tateishi, Shinji Yamashita; Shiori Yamada, Taiki Saito, Jotaro On, Jun Watanabe, Yoshihiro Tsukamoto, Junichi Yoshimura, Makoto Oishi, Toshimichi Nakano, Masaru Imamura, Chihaya Imai, Tetsuya Yamamoto, Hideo Takeshima; Atsuo T. Sasaki, Fausto J Rodriguez, Sumihito Nobusawa, Pascale Varlet, Celio Pouponnot, Satoru Osuka, Yves Pommier, Akiyoshi Kakita, Yukihiko Fujii, Eric H. Raabe, Charles G Eberhart, and Manabu Natsumeda

Department of Pathology, Johns Hopkins University School of Medicine, Baltimore, Maryland, USA (Sa.N., T.H.F., K.M., A.P., F.J.R., C.G.E., M.N.); Department of Neurosurgery, Gunma University, Maebashi, Japan (Sa.N.); Institute for Advanced Biosciences, Keio University, Tsuruoka, Japan (J.M., A.T.S.); Department of Neurosurgery, Brain Research Institute, Niigata University, Niigata, Japan (M.Ok., H.T., Shio.Y., T.S., J.O., J.W., Y.T., J.Y., M.Oi., Y.F., M.N.); Department of System Pathology for Neurological Disorders, Brain Research Institute, Niigata University, Niigata, Japan (S.M.); Department of Pathology, Brain Research Institute Niigata University, Niigata, Japan (R.G., A.K.); Department of Neuropathology, GHU Paris-Psychiatrie Et Neurosciences, Sainte-Anne Hospital, Paris, France (I.B., P.V.); Institut Curie, Centre de Recherche, F-91405, Orsay, France (S.D., S.C., E.H., C.P.); INSERM U1021, Centre Universitaire, F-91405, Orsay, France (S.D., S.C., E.H., C.P.); CNRS UMR 3347, Centre Universitaire, F-91405, Orsay, France (S.D., S.C., E.H., C.P.); Université Paris-Saclay, F-91405, Orsay, France (S.D., S.C., E.H., C.P.); Equipe Labellisée Ligue Nationale Contre le Cancer, F-91405, Orsay, France (S.D., S.C., E.H., C.P.); Department of Neuropathology, Institute for Medical Science of Aging, Aichi Medical University, Nagakute, Japan (H.M.); Department of Neurosurgery, Yokohama City University, Yokohama, Japan (T.K., T.Y.); Division of Neurosurgery, Department of Clinical Neuroscience, Faculty of Medicine University of Miyazaki, Miyazaki, Japan (Shin.Y., H.T.); Department of Radiology and Radiation Oncology Niigata University Medical and Dental Hospital, Niigata, Japan (T.N.); Department of Pediatrics, Niigata University Medical and Dental Hospital, Niigata, Japan (M.I., C.I.); Department of Internal Medicine, Department of Cancer Biology, University of Cincinnati College of Medicine, Columbus, Ohio, USA (A.T.S.); Department of Neurosurgery, Brain Tumor Center at UC Gardner Neuroscience Institute, Cincinnati, Ohio, USA (A.T.S.); Department of Pathology, Gunma University, Maebashi, Japan (Su.N.); Department of Neurosurgery, School of Medicine and O'Neal Comprehensive Cancer Center, University of Alabama at Birmingham, Alabama, USA (S.O.); Developmental Therapeutics Branch, Center for Cancer Research, National Cancer Institute, NIH, Bethesda, USA (Y.P.); Department of Pediatric Oncology, Johns Hopkins University School of Medicine, Baltimore, Maryland, USA (E.H.R.)

Corresponding Author: Manabu Natsumeda, MD, PhD, Department of Neurosurgery, Brain Research Institute, Niigata University, Niigata, Japan (natsumeda@bri.niigata-u.ac.jp).

Abstract

Background. Intensive chemotherapeutic regimens with craniospinal irradiation have greatly improved survival in medulloblastoma patients. However, survival markedly differs among molecular subgroups and their biomarkers are unknown. Through unbiased screening, we found Schlafen family member 11 (SLFN11), which is known to improve response to DNA damaging agents in various cancers, to be one of the top prognostic markers in medulloblastomas. Hence, we explored the expression and functions of SLFN11 in medulloblastoma.

Methods. SLFN11 expression for each subgroup was assessed by immunohistochemistry in 98 medulloblastoma patient samples and by analyzing transcriptomic databases. We genetically or epigenetically modulated SLFN11 expression in medulloblastoma cell lines and determined cytotoxic response to the DNA damaging agents cisplatin and topoisomerase I inhibitor SN-38 in vitro and in vivo.

Results. High SLFN11 expressing cases exhibited significantly longer survival than low expressing cases. SLFN11 was highly expressed in the WNT-activated subgroup and in a proportion of the SHH-activated subgroup. While WNT activation was not a direct cause of the high expression of SLFN11, a specific hypomethylation locus on the *SLFN11* promoter was significantly correlated with high SLFN11 expression. Overexpression or deletion of *SLFN11* made medulloblastoma cells sensitive and resistant to cisplatin and SN-38, respectively. Pharmacological upregulation of SLFN11 by the brain-penetrant histone deacetylase-inhibitor RG2833 markedly increased sensitivity to cisplatin and SN-38 in SLFN11-negative medulloblastoma cells. Intracranial xenograft studies also showed marked sensitivity to cisplatin by SLFN11-overexpression in medulloblastoma cells.

Conclusions. High SLFN11 expression is one factor which renders favorable outcomes in WNT-activated and a subset of SHH-activated medulloblastoma possibly through enhancing response to cisplatin.

Key Points

- SLFN11 is expressed in WNT-activated and a subset of SHH-activated medulloblastomas and is prognostic.
- SLFN11 expression correlates with hypomethylation of *SLFN11* promoter; upregulation using HDAC inhibitors sensitizes medulloblastomas to cisplatin.

Importance of the Study

Intensive treatment strategies including chemotherapy and craniospinal irradiation have greatly improved overall survival in medulloblastoma. However, treatment response and thus prognosis, vary significantly among the four molecular subgroups, with WNT-activated and SHH-activated subgroups showing better prognosis, and Group 3 the poorest. So far, very little is known regarding the molecular bases of this high heterogeneity in terms of prognosis. The present study shows that SLFN11, a novel sensitizer to DNA damaging agents, is highly expressed in WNT-activated and a subset of SHH-activated medulloblastomas, and that its expression is significantly correlated with the better prognosis of these subtypes. Mechanistically, SLFN11 overexpression enhanced sensitivity to the DNA damaging agents cisplatin and SN-38 while knockout of SLFN11 attenuated cytotoxicity. Additionally, we provide preliminary evidence that activation of SLFN11 in medulloblastoma cells with low SLFN11 expression can sensitize cells to DNA damaging agents, providing a potential new avenue in the treatment of medulloblastomas.

Medulloblastomas are among the most common malignant brain tumors in the pediatric and young adult populations, although high-grade gliomas are more common. Intensive regimens including DNA damaging agents such as cisplatin and cyclophosphamide and non-DNA damaging agents such as vincristine, combined with craniospinal irradiation (CSI) have led to a drastic improvement in survival, with a 5-year overall survival rate of more than 80% for average-risk disease.[1,2] Medulloblastoma can be classified into four molecular subgroups according to genetic signatures, WNT-activated, SHH-activated, Group 3, and Group 4, with different clinical outcomes.[3,4] The WNT-activated subgroup, which accounts for 10–15% of all medulloblastoma, is known to have the best prognosis with a 5-year overall survival as high as 97–100%.[4] This group harbors activating mutations in beta-catenin (*CTNNB1*). An important study indicated that WNT-activated medulloblastomas have aberrant fenestrated vasculature, possibly allowing for better penetration of chemotherapy to the tumor.[5] However, it remains unclear whether the favorable outcome of WNT-activated group is linked to an increased response to chemoradiotherapy via *CTNNB1* mutations.[6] SHH-activated medulloblastoma, characterized by frequent desmoplastic/nodular morphology, accounts for about 30% of all medulloblastoma and has the second-best prognosis.[4] Several markers in medulloblastomas have been proposed to be either prognostic or subgroup-specific.[4,7–11] However, the exact mechanisms determining therapeutic response in these subgroups remain to be elucidated.

Schlafen11 (*SLFN11*), a putative DNA/RNA helicase, has garnered attention as an enhancer of sensitivity to various DNA damaging agents.[12] The history of SLFN11 in oncology is still short, starting in 2012 when drug screening of multiple cancer cell lines (NCI-60) revealed its high correlation with sensitivity to DNA damaging agents including platinum-derivatives (cisplatin, carboplatin), topoisomerase I inhibitors (irinotecan, topotecan), topoisomerase II

inhibitors (etoposide, doxorubicin) and DNA synthesis inhibitors (gemcitabine, cytarabine).[13] An independent drug screening study using the Cancer Cell Line Encyclopedia (CCLE), published in the same year, confirmed the highly significant correlation between *SLFN11* expression and sensitivity to irinotecan.[14] The causality between high SLFN11 expression and high sensitivity to DNA damaging agents including poly (ADP-ribose) polymerase (PARP) inhibitors was subsequently validated through genetic approaches with various cell systems from laboratories around the world.[15–20] Moreover, implications of SLFN11 in the clinic as a predictive biomarker for platinum- or topoisomerase I inhibitor-or γ-irradiation sensitivity have been reported with patient samples in ovarian, colorectal, breast, and small cell lung cancer,[13,15,16,21–23] as well as Ewing's sarcoma,[24] but has hardly been studied in brain tumors,[25] and its role in medulloblastomas is unknown.

Mechanistically, we have shown that SLFN11 is recruited onto replication forks under excessive replication stress where it induces lethal replication block[12,26–28] when cells are exposed to DNA damaging agents.[12,26] Because these functions presumably occur regardless of cell or tissue types, we speculated that the favorable response to chemoradiotherapy in WNT-activated or SHH-activated medulloblastoma could be linked to SLFN11 activation. The present study shows that SLFN11 is one of the top prognostic markers in medulloblastomas through unbiased screening. We examine for the first time SLFN11 expression levels in medulloblastoma patient samples as well as public databases. Additionally, we identify the specific methylated CpG locus in the *SLFN11* promoter that potentially mediates SLFN11 inactivation in medulloblastoma. We perform in vitro and in vivo functional analyses of SLFN11 using medulloblastoma cells and provide a novel strategy to enhance SLFN11 expression and reverse resistance to chemotherapy.

Methods

Gene Expression and Survival Analyses Using Public Databases

Cavalli (763 cases)[4] and Pfister (223 cases) databases were assessed by R2 analysis and visualization platform (https://hgserver1.amc.nl/cgi-bin/r2/main.cgi) to assess the expression of SLFN11 in the four molecular subgroups and the Kool (62 cases)[7] and Fattet databases were analyzed in Oncomine (https://www.oncomine.org) to assess SLFN11 expression in *CTNNB1*-mutant and wildtype medulloblastoma. Additionally, we used RegParallel and survival packages in R to carry out univariate Cox regression analysis. Survival and mRNA expressions of 612 medulloblastoma patients in the Cavalli study[4] were examined. Expression of 21637 genes was used as input after basic filtering. *P*-values were obtained from univariate Cox proportional-hazard regression models for the entire list of genes. All Kaplan–Meier survival curves were constructed using survival and ggplots2 packages. The difference in survival between high SLFN11-expressing cases (top 15%), intermediate expressing cases (middle 70%), and low SLFN11-expressing cases (bottom 15%) of medulloblastoma subgroups were assessed using normalized data obtained through the Gene Expression Omnibus (GEO) with the GEO accession code GSE85217.[4]

Patients and Cell Lines

Twenty-five WNT-activated, 27 SHH-activated, and 46 non-WNT/non-SHH medulloblastoma tissues, including cases represented on tissue microarrays (TMAs) sent from Johns Hopkins University, were examined after obtaining approval from the institutional review board of Niigata University (#2019-0386). DAOY and D425 lines were purchased from American Type Culture Collection (ATCC; Manassas, VA, USA) and ONS-76 from RIKEN Cell Bank (Tsukuba, Japan). DU145, CCRF-CEM, and MOLT4 lines were obtained from the Division of Cancer Treatment (DCTD), Developmental Therapeutics Program (DTP, NCI), and EW8 is a kind gift from Dr. Lee Helman (NCI/NIH). D425 cells were cultured in minimum essential medium (Thermo Fisher Scientific, Waltham, MA, USA) containing 10% fetal bovine serum (FBS; Thermo Fisher Scientific), penicillin (100 U/mL), streptomycin (100 μg/mL), and non-essential amino acids (Thermo Fisher Scientific). DAOY, UW228, and ONS-76 lines were cultured in Dulbecco's modified Eagle's medium (DMEM; Thermo Fisher Scientific) containing 10% FBS, penicillin, and streptomycin. DU145, CCRF-CEM, and MOLT4 cells were grown in RPMI medium containing 10% FBS, penicillin, and streptomycin.

Immunohistochemical Analysis

Surgical specimens were fixed with 10% buffered formalin and embedded in paraffin. Histological examination was performed with sections stained with hematoxylin-eosin staining and the following antibodies as previously published[29]: SLFN11 (sc-515071X, particular order 2 mg/mL, Santa Cruz Biotechnology, 1:500), GAB1 (ab133486, Abcam, 1:100), YAP1 (sc-011199, Santa Cruz Biotechnology, 1:200), and β-catenin/CTNNB1 (ab610154, BD Transduction Laboratories, San Diego, CA, USA, 1:100). Presence of intranuclear β-catenin, GAB1 and YAP1 staining, Nanostring analysis, and/or *CTNNB1* mutation was used to determine WNT-type medulloblastoma (Supplementary Table S2). Intranuclear staining, but not cytoplasmic staining of SLFN11 was considered positive. TMAs containing primary medulloblastoma obtained from the Department of Pathology, Johns Hopkins University School of Medicine were created by the Johns Hopkins microarray core facility (core diameter 0.6 mm).[29] These TMAs, which had previously been molecularly subtyped into four groups by integrative molecular analysis[8] and three groups (WNT, SHH, and non-WNT/SHH) by immunohistochemistry of GAB1, YAP1, and b-catenin, were stained for SLFN11. Nuclear staining of SLFN11 was considered positive, and immunoreactivity was assessed by using *H*-scores (H) (0–200) which were obtained by multiplying the intensity of stain (0: no stain, 1: weak stain, 2: strong stain) by percentage (0–100) of neoplastic cells showing the staining intensity.

Generation of SLFN11-Knockout Cells

To disrupt the SLFN11 gene, we utilized the CRISPR/Cas9 method. Details are as reported previously.[19] In brief, each guide RNA (5′-gcgttccatggactcaagag-3′ or 5′-gttgagcatcccgtggagat-3′) was inserted into the pX330 plasmid (pX330-SLFN11). The gene-targeting constructs harboring homology arms and a puromycin-resistance cassette were prepared. The targeting construct and pX330-SLFN11 were co-transfected into DAOY cells by electroporation. After transfection, cells were released into drug-free medium for 48 h followed by puromycin selection until single colonies were formed. Single clones were expanded, and gene-deletion was confirmed by Western blotting.

Generation of SLFN11-Overexpressing Cells

The doxycycline-inducible SLFN11 expression vector (pPCTetOn-SLFN11) and the modified expression vector of hyperactive PB transposase under CAG promoter (pCAG2-hyPB) were generated previously.[18] The two plasmids were co-transfected into D425 or ONS-76 cells. One week after the transfection, the cells were incubated in puromycin (0.2 μg/mL) containing medium for another 2 weeks.

Methylation Profiling of SLFN11 Promoter Region and Correlation with SLFN11 Expression in Medulloblastomas

For analysis of DNA methylation pattern in *SLFN11* promoter by methylation array among eight control cerebella and 276 medulloblastoma cases including 33 WNT-activated medulloblastoma, the b value [methylated/(methylated + unmethylated)] from 18 probes across the promoter region of *SLFN11* was obtained from the dataset GSE54880.[30] The Spotfire software package was used to generate a heatmap with sample values. For correlation of DNA methylation of *SLFN11* promoter and expression of *SLFN11*, gene expression value from RNA-seq dataset (PMID 28726821) and b value from DNA methylation dataset[30] were used. The methylation pattern from CpG islands on chromosome 17 (33701776-33738370), encompassing the *SLFN11* gene, was shown in 5 normal cerebella and 169 MB samples. Location of the array probes was compared the location of H3K4me3 and H3K27Ac marks in 1 medulloblastoma cell line and seven other cancer cell lines using UCSD Genome Browser (https://genome.ucsc.edu).

Statistical Analysis

Differences between three or more groups were determined using a one-way ANOVA test with post hoc Tukey's multiple comparison test. Multiple *t*-tests were corrected using the Holm-Sidak method. Association between *SLFN11* expression and methylation β-value was determined by Pearson's correlation. The median overall survival time was estimated by the Kaplan–Meier method, and differences in the survival were analyzed by log-rank test (Mantel-cox test) or by log-rank test for trend. Statistical tests were performed using the GraphPad Prism 9 software (GraphPad Software, La Jolla, CA, USA). $P < .05$ was considered statistically significant.

Please refer to Supplementary Materials for further details about methods.

Results

Unbiased and Biased Screenings Reveal SLFN11 as a Robust Prognostic Factor in Medulloblastomas

Univariate Cox regression analysis of a public dataset with information on survival[4] was used to determine prognostic markers from 21 637 genes in 612 medulloblastoma patients. A total of 2281 genes were associated with overall survival (log-rank $P < .01$; Supplementary Table S1). *SLFN11* was the 151 highest (within the top 1%) prognostic gene. Additionally, 34 genes, including *SLFN11*, known to be prognostic or over-expressed in a subgroup-specific manner in medulloblastomas, were assessed in detail. Patients across the subgroups were divided into three groups (top 15% expressing, intermediate 70% expressing, and bottom 15% expressing) based on gene expression and compared for survival. For only three genes, *SLFN11*, *EYS* (*EGFL11*), and *GABRA5*, the log-rank *P*-value was less than .0001, with *SLFN11* having the best separation; high *SLFN11* expression being associated with significantly longer survival and low *SLFN11* expression with poor prognosis (Figures 1A–C, Supplementary Figure S1A–C).

Medulloblastomas with High Expression of SLFN11 have Good Prognosis

We next sought to find whether high expression of *SLFN11* is a favorable signature in the subgroups. WNT-activated medulloblastomas, having the best prognosis of all medulloblastoma subgroups (Figure 1D)[3,4] had universally high *SLFN11* expression (Figure 1E). We found that high (top 15%) *SLFN11*-expressing cases had a significantly better prognosis compared to intermediate (middle 70%) and low (bottom 15%) *SLFN11*-expressing cases ($P < .0001$, log-rank for trend, Figure 1A). The same was true for SHH-activated ($P = .0059$, Supplementary Figure S2C, D) and Group 3 ($P = .0199$, Supplementary Figure S2E, F) subgroups, and Group 4α subtype ($P = .0405$, Supplementary Figure S2G, H). Multivariate analysis taking into account molecular subgroups revealed that *SLFN11* was an independent, positive prognostic factor ($P = .035$, Cox proportional hazards analysis). Additionally, we found that in cases aged ≤3, many of which had deferred radiation during initial treatment, high SLFN11 expressing cases tended to have better survival, although not significant due to the small number of cases ($P = .083$, Supplementary Figure S2B). These results suggest that high *SLFN11* expression is associated with the good prognosis of all molecular subgroups possibly through enhancing response to chemotherapy, although high *SLFN11* cases are largely restricted to WNT-activated and a subset of SHH-activated medulloblastomas.

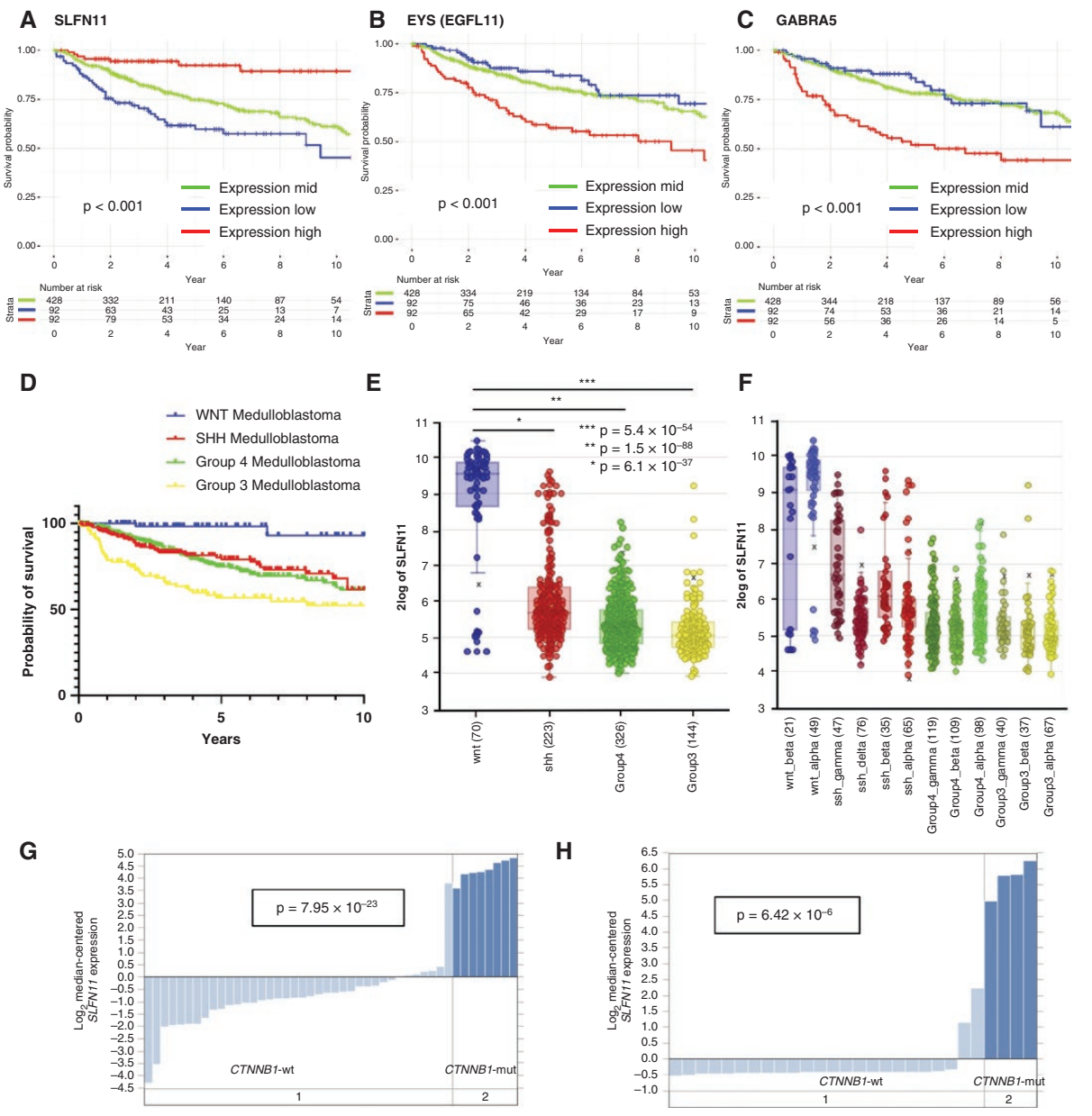

Figure 1. *SLFN11* mRNA is highly expressed in WNT-activated and subset of SHH-activated medulloblastoma and confers a favorable prognosis. Kaplan-Meier analysis comparing the top 15%, intermediate, and bottom 15% *SLFN11* (A), *EYS (EGFL11)* (B) and *GABRA5* (C). (D) Kaplan–Meier analysis of 612 cases with available survival data. (E) *SLFN11* mRNA expression was almost universally high in the WNT-activated subgroup and a proportion of SHH-activated subgroup. (F) Subtype analysis showed that SLFN11 high cases were distributed between SHH-α, -β, -γ subtypes but not -δ subtype. Analysis of Kool (G) and Fattet (H) datasets in Oncomine.

SLFN11 is Highly Expressed in WNT-Activated and a Subset of SHH-Activated Medulloblastoma Subgroups

Having shown that *SLFN11* is a powerful prognostic marker in medulloblastomas, we next sought to compare *SLFN11* mRNA expression in the four molecular subgroups. Analysis of the Cavalli (Figure 1E) and Pfister databases (Supplementary Figure S2A) on R2 platform showed almost universally high expression of *SLFN11* in the WNT-activated subgroup and a portion of the SHH-activated subgroup. Cases showing high *SLFN11* expression were scattered in the SHH-α, β, and γ subtypes but not δ subtype (Figure 1F). Somewhat surprisingly, SLFN11 expression was high in only half of the SHH-γ cases, which are known to be highly curable by chemotherapy alone. Analysis of Kool (Figure 1G) and Fattet (Figure 1H) datasets in Oncomine yielded similar results; cases harboring *CTNNB1* mutations, belonging to the WNT-activated subgroup, had high expression of

SLFN11, whereas cases lacking *CTNNB1* mutation generally did not.

We next set out to look at SLFN11 expression at the protein level. Twenty-five WNT-activated, 27 SHH-activated, and 46 non-WNT/SHH medulloblastomas were stained for SLFN11. WNT-activated cases were defined by intranuclear staining of β-catenin, Nanostring analysis,[29] or presence of *CTNNB1* mutations (Supplementary Figure S3, Supplementary Table S2). Several WNT-activated cases were highly positive for SLFN11 (Figure 2A–C), and a subset of SHH-activated cases was also positive (Figure 2D–F). By contrast, non-WNT, and non-SHH cases were either negative or only slightly positive for SLFN11 (Figure 2G–I). The mean *H*-score of SLFN11 expression was significantly higher in WNT-activated medulloblastomas (67.58) compared to SHH-activated (12.56) and Group 3/4 medulloblastomas (1.31, both $P < .0001$, Figure 2J). Notably, SLFN11 was highly expressed in the desmoplastic area of a desmoplastic/nodular type medulloblastoma belonging to the SHH-activated subgroup (Figure 2F).

Additionally, we looked at SLFN11 expression in a WNT-activated, patient-derived xenograft model. The Ymed4 xenograft, established from a WNT-activated medulloblastoma, produced intracranial tumors that also showed strong nuclear staining of SLFN11 (Figure 2K) and intranuclear staining of β-catenin (Figure 2L), whereas an intracranial xenograft produced from a high-MYC (Group 3) medulloblastoma cell line D425 did not express SLFN11 (Figure 2M).

Activation of the WNT/β-Catenin Pathway is not a Direct Cause of High SLFN11 Expression

Having found that SLFN11 expression is generally high in the WNT-activated subgroup, we tested whether aberrant activation of the WNT/β-catenin pathway upregulates SLFN11 expression in medulloblastoma cell lines. First, we overexpressed wildtype (*CTNNB1-WT*) or constitutively active β-catenin (*CTNNB1-S33Y*) in ONS-76 medulloblastoma cells expressing low SLFN11 or CTNNB1. However, the transient or stable overexpression of either CTNNB1-WT or CTNNB1-S33Y failed to induce SLFN11 expression (Supplementary Figure 4A, B). As expected, the S33Y mutant was more stable than the wildtype β-catenin.

RUNX2 expression is dominantly regulated by β-catenin signals,[31] and *RUNX2* hypomethylation and its high expression are specific to the WNT-activated group.[30] Analyses of the Kool Brain dataset[8] also revealed that *RUNX2* is the most highly correlated gene with the WNT-activated group, and *SLFN11* follows as 11th most correlated (Supplementary Figure 4C). Next, we utilized several *SLFN11*-expressing cell lines (leukemia CCRF-CEM, leukemia MOLT4, and prostate cancer DU145) and attempted to inhibit β-catenin signals using a small compound FH535, a β-catenin inhibitor.[32] As expected, the treatment of FH535 for 24 h reduced RUNX2 expression in CCRF-CEM and DU145 cells. MOLT4 cells had less RUNX2 expression at baseline. Expression levels of SLFN11 were not affected by FH535 treatment (Supplementary Figure 4D). To further examine the link between *SLFN11* and *CTNNB1* expression, we generated CTNNB1 knockout cells in DU145 or Ewing's sarcoma cell line EW8. However, expression levels of SLFN11 were not changed by the knockout of *CTNNB1* in either cell line (Supplementary Figure 4E). These results suggest that SLFN11 expression is not directly regulated by β-catenin signals.

Additionally, we examined nine non-medulloblastoma cell lines harboring constitutive active mutations in the *CTNNB1* gene found through the CCLE database (https://depmap.org/portal/). Only three (NCI-H1092, SW1573, and LXF-289) out of nine lines expressed *SLFN11* at high levels (Supplementary Figure 4F). Taken together, the constitutive active mutation of *CTNNB1* in medulloblastoma coincides with high *SLFN11* expression for unknown reasons while constitutive WNT/β-catenin signaling itself is not the cause of high *SLFN11* expression.

SLFN11 Increases Sensitivity to DNA Damaging Agents in SHH-Activated Medulloblastoma Cell Lines

Having found that high SLFN11 expression is associated with good prognosis in medulloblastoma, we attempted to examine its causality. Unfortunately, WNT-activated cell lines were not available,[33] so we decided to check the SHH-activated cell lines DAOY, UW228, and ONS-76,[34] as well as the Group 3 cell line D425 with *MYC* amplification.[35] Baseline SLFN11 expression was detected in DAOY and UW228 but not in ONS-76 and D425 (Figure 3A). DAOY and UW228 were more sensitive to cisplatin compared to ONS-76 and D425 (Figure 3B), consistent with a previous report[36] and data obtained from the Genomics of Drug Sensitivity in Cancer (GDSC) database (https://www.cancerrxgene.org; Supplementary Figure S5) for DAOY versus ONS-76. Cells taken from Ymed4, a WNT-activated medulloblastoma, were more sensitive to cisplatin, a topoisomerase inhibitor camptothecin (CPT) and a PARP inhibitor talazoparib compared to Ymed6, belonging to Group 4 (Supplementary Figure S6A–D).

We next generated *SLFN11*-knockout (SLFN11-KO) DAOY cells using CRISPR/Cas9 system. SLFN11-KO cells showed markedly reduced sensitivity to CPT (Figure 3C), cisplatin (Figure 3D) and talazoparib (Supplementary Figure S6E). Drastic reduction of cleaved-PARP (C-PARP) (Figure 3E) and an approximately four-fold induction in the percentage of Annexin-positive cells (Supplementary Figure S6F) were also observed in SLFN11-KO cells compared to parent cells after cisplatin treatment. In contrast, *SLFN11* overexpression in D425 cells using doxycycline (DOX)-inducible constructs increased cytotoxicity of cisplatin and SN-38, the active metabolite of irinotecan, which was evidenced by increased C-PARP (Figure 3F) and decreased cell viability (Figure 3G, H). Similarly, SLFN11 over-expression markedly sensitized ONS-76 cells to SN-38 (Figure 3I) and cisplatin (Figure 3J). Interestingly, SLFN11 overexpression alone was sufficient to induce apoptosis in D425 cells (Figure 3F), suggesting that in highly proliferative tumors such as medulloblastoma with intrinsic replication stress, ectopic SLFN11 expression alone can cause cell death.

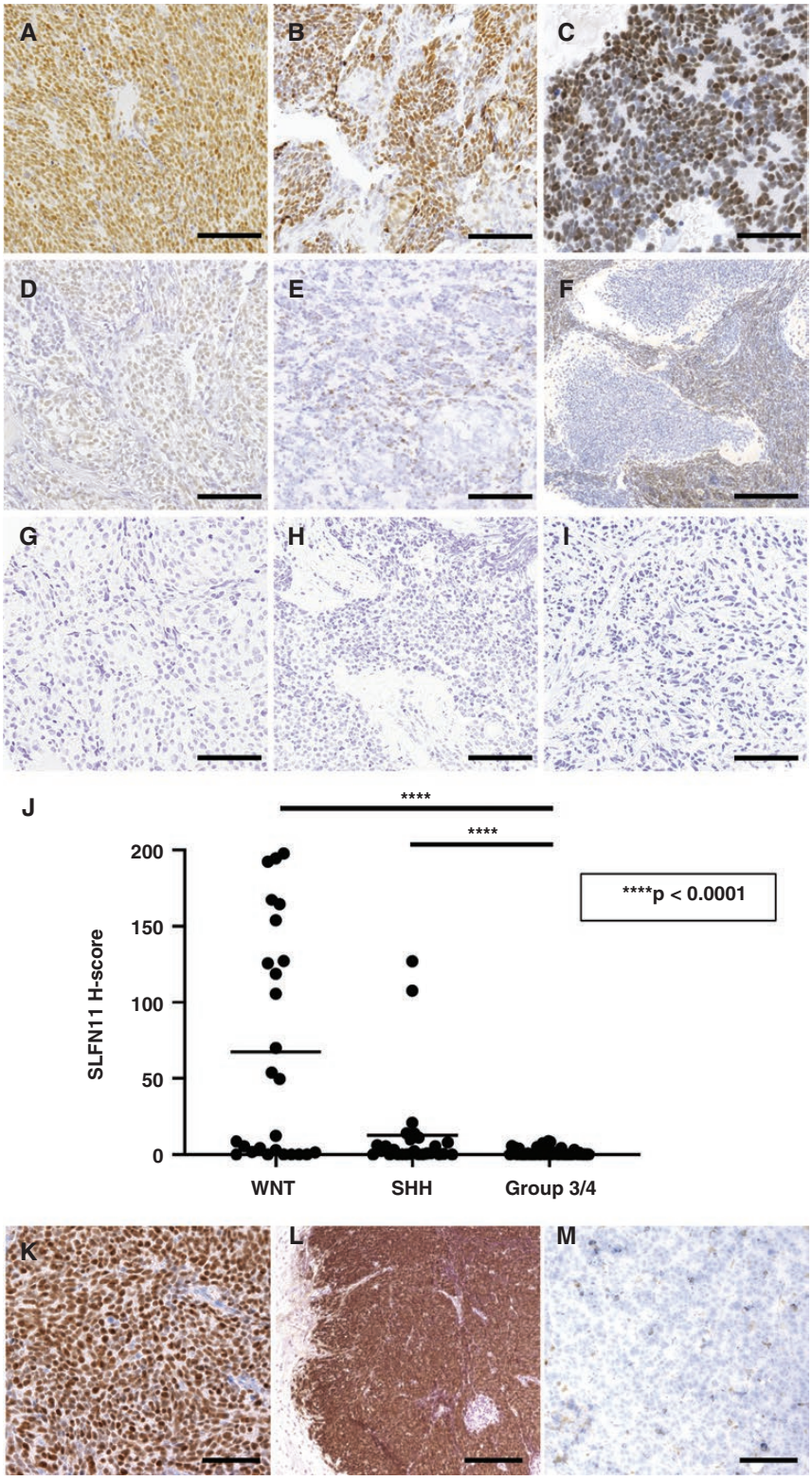

Figure 2. SLFN11 is highly expressed in WNT-activated medulloblastoma samples. (A–C) WNT-activated medulloblastoma with high expression of SLFN11. (D–F) SHH-activated medulloblastoma with moderate expression of SLFN11. (G–I) Non-WNT/non-SHH cases with negative or low expression of SLFN11. (J) SLFN11 H-scores in WNT-activated, SHH-activated and Group 3/4. (K) SLFN11 is highly expressed in the nuclei of tumor cells in the Ymed4sc xenograft established from a WNT-activated medulloblastoma. (L) Intranuclear β-catenin staining found in the same xenograft. (M) Weak SLFN11 expression in D425 intracranial xenograft. Scale bars: (A, B, D, E, H, I, M) = 100 μm; (C, G, K) = 200 μm; (F, L) = 50 μm.

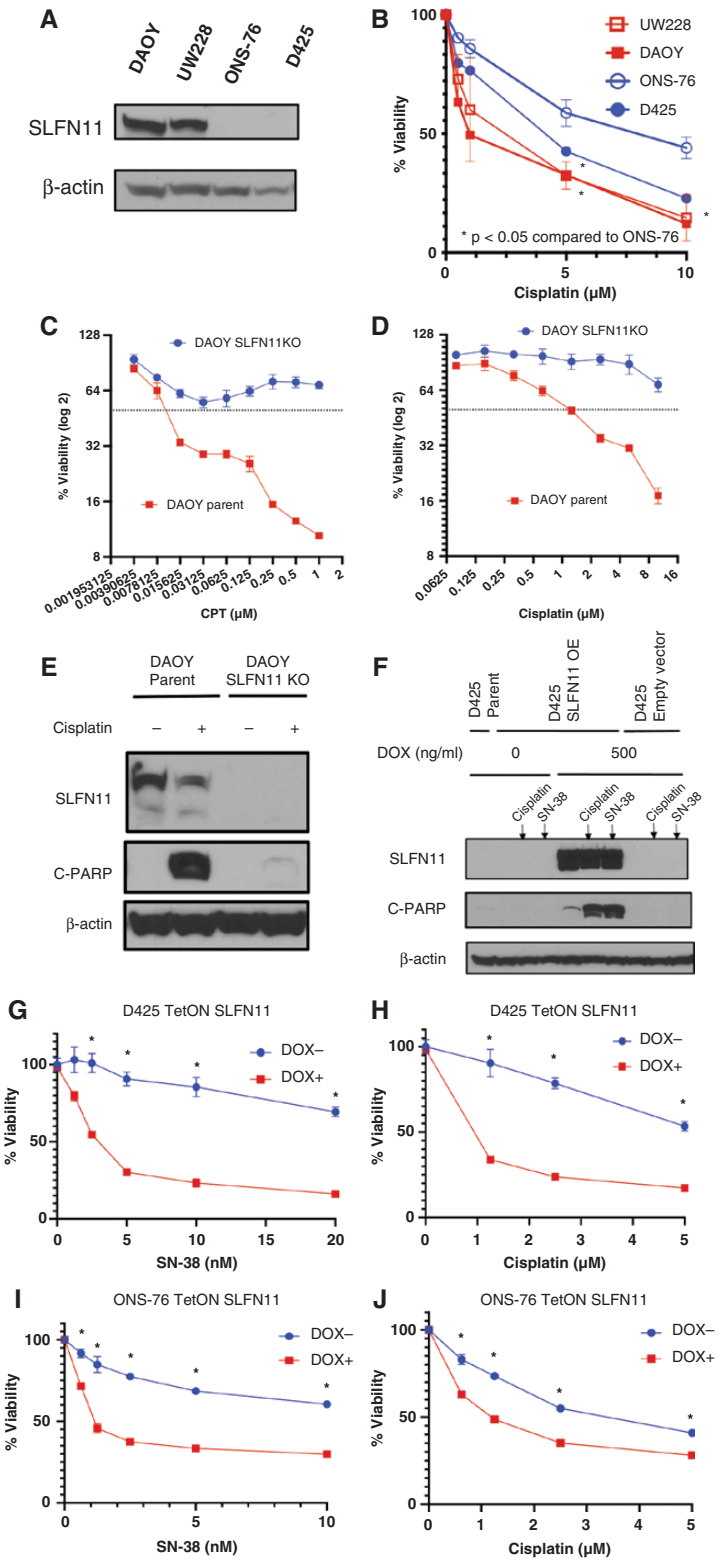

Figure 3. SLFN11 sensitizes medulloblastoma cells to DNA damaging agents. (A) Western blot analysis of SLFN11 in medulloblastoma cell lines (DAOY, UW228, ONS-76, and D425). (B) Sensitivity curves of SLFN11 expressing (red) and non-SLFN11 expressing (blue) medulloblastoma cell lines to cisplatin. (C, D) SLFN11-KO cells displayed markedly reduced sensitivity to DNA damaging agents CPT or cisplatin (D). (E) Western blot analysis of the indicated proteins in cells treated with vehicle or 5 μM cisplatin for 48 h. Cleaved-PARP is a marker of apoptosis. (F) Western blot analysis of the indicated proteins after treatment with 5 μM cisplatin or 10 nM SN-38 for 48 h. (G–J) Viability curves were of the indicated cells after treatment with SN-38 or cisplatin for 72 h.

SLFN11 Overexpression Sensitizes Medulloblastoma to Cisplatin In Vivo

Having confirmed sensitization to DNA damaging agents by over-expression of SLFN11 in medulloblastoma cells, we set out to confirm whether SLFN11 expression sensitizes cells to cisplatin in vivo. SLFN11-TetON D425 and ONS-76 cells were intracranially implanted into mice and treated with cisplatin ± DOX. Over-expression of SLFN11 (+DOX) in D425 sensitized these tumors to cisplatin, prolonging survival (Figure 4A, $P < .0001$, Mantel-Cox test) and reducing tumor volume (Figures 4B, C, $P = .0005$ cisplatin vs cisplatin + DOX at week 3, *t*-test with Holm-Sidak correction). Over-expression of SLFN11 alone was sufficient to reduce tumor volume (Figure 4B) and prolong survival compared to the vehicle group (Figure 4A). Similar effects on survival were observed in a small number of mice injected with ONS-76 cells, although results were affected by the need to discontinue cisplatin in all treatment groups due to suspected toxicity after 10 weeks (Figure 4D, $P = .0006$ Mantel-Cox test). As we know from previous experience that establishing DAOY and UW228 xenografts is difficult,[35] we did not conduct in vivo experiments with these cells. Protein expression of SLFN11 was confirmed in DOX treated SLFN11-TetON D425 xenografts (Figure 4E).

SLFN11 Expression Correlates with SLFN11 Promoter Hypomethylation and is Epigenetically Upregulated by the HDAC Inhibitor RG2833

A significant association between *SLFN11* CpG island promoter hypermethylation and low *SLFN11* mRNA levels in cancer cells has been established in the National Cancer Institute Human Tumor Cell Line Screen (NCI-60 and SCLC)[16,37,38] and CCLE.[17] To determine whether this association is also observed in medulloblastoma tissues, methylation (β-value) of 18 probes on chromosome 17, encompassing the *SLFN11* gene, was broadly assessed. Methylation was not different among the four subgroups and normal cerebella (Figure 5A), except for the area 33701776–33704725, which was hypomethylated in most WNT-activated cases and some SHH-activated cases (Figure 5A). This region overlapped with the *SLFN11* promoter in the medulloblastoma cell line D341 and seven other cancer cell lines (Figure 5B). A moderate, negative correlation ($r = -0.376$) between DNA methylation (β-value) and *SLFN11* mRNA expression was observed (Figure 5C, D). A similar negative correlation between *SLFN11* mRNA expression and hypomethylation of a specific area (cg0080081, Supplementary Figure S7A) of the *SLFN11* promoter was obtained from the Cavalli database (Supplementary Figure S7B), specifically in the WNT-activated, SHH-activated and Group 3 subgroups (Supplementary Figure S7C). Furthermore, by methylation-specific high resolution melting analysis, we found that *SLFN11* promoter was hypomethylated in WNT-activated medulloblastoma samples with high (>150) SLFN11 *H*-scores (Supplementary Figure S7D). These results suggest that hypomethylation of the *SLFN11* promoter is responsible for the high SLFN11 expression in medulloblastomas. We next tested whether the brain-penetrant HDAC inhibitor RG2833, EZH2 inhibitors (EPZ6438 and GSK343), and/or the DNA demethylating agent 5-AZA could induce SLFN11 in D425 and DAOY cells. We found that RG2833 was most effective in robustly increasing SLFN11 protein and mRNA expression in these cell lines (Figure 5E, F).

The Brain-Penetrant HDAC Inhibitor RG2833 Synergizes with Cisplatin and SN-38 in Medulloblastoma

We observed synergistic effects between cisplatin and RG2833 in D425 and ONS-76 cell lines. High HSA synergy scores of 11.71 (Figure 6A, >10 is considered synergistic) and 20.95 (Figure 6B) were observed, respectively. Additionally, synergistic (11.25) and partially synergistic (7.66) effects between SN-38 and RG2833 were found in D425 and ONS-76 cells, respectively (Supplementary Figure S8A, B). Interestingly, synergistic effects of cisplatin and RG2833 (14.18) and partially synergistic effects of SN-38 and RG2833 (9.48) were also observed in DAOY (Supplementary Figure S8C, D). Results of HSA synergy score of DNA damaging agents and RG2833 are summarized in Figure 6C. These results suggest that increased expression of SLFN11 effectively reverses resistance of SLFN11-negative and drives sensitivity to cisplatin and SN-38 in both SLFN11-negative and -positive cells.

Discussion

This is the first study examining SLFN11 protein expression in medulloblastoma patient samples. It demonstrates that most WNT-activated and a proportion of SHH-activated medulloblastomas have high SLFN11 expression, which was extended from RNA levels using transcriptome-based datasets. Our study also establishes that SLFN11 expression level critically determines the drug sensitivity of medulloblastoma cells in vitro and in vivo, which is possibly relevant to favorable response to chemotherapy and good survival in WNT- and SHH-activated subgroups. Notably, overexpression of SLFN11 using constructs not only sensitized medulloblastoma cells to DNA damaging agents, but induction of SLFN11 alone was sufficient in inducing apoptosis in vitro as well as in vivo.

While CSI and intensive chemotherapy regimens have markedly improved survival for average-risk medulloblastoma,[1,2] we still seek ways to reduce treatment intensity to avoid late adverse effects by selecting well-responsive patients to treatments. A recently published phase 3 trial has shown that reducing CSI dosage from 23.4 to 18 Gy decreased 5-year event-free survival from 82.9 to 71.4% in average-risk young, medulloblastoma patients aged 3–7 years.[39] Interestingly, subgroup analysis revealed that event-free survival was significantly reduced in low-dose CSI patients compared to standard dose in Group 4, but not in WNT-activated and SHH-activated subgroups.[39] These results suggest that reducing CSI dosage should be reserved for those patients which are expected to respond to chemotherapy.

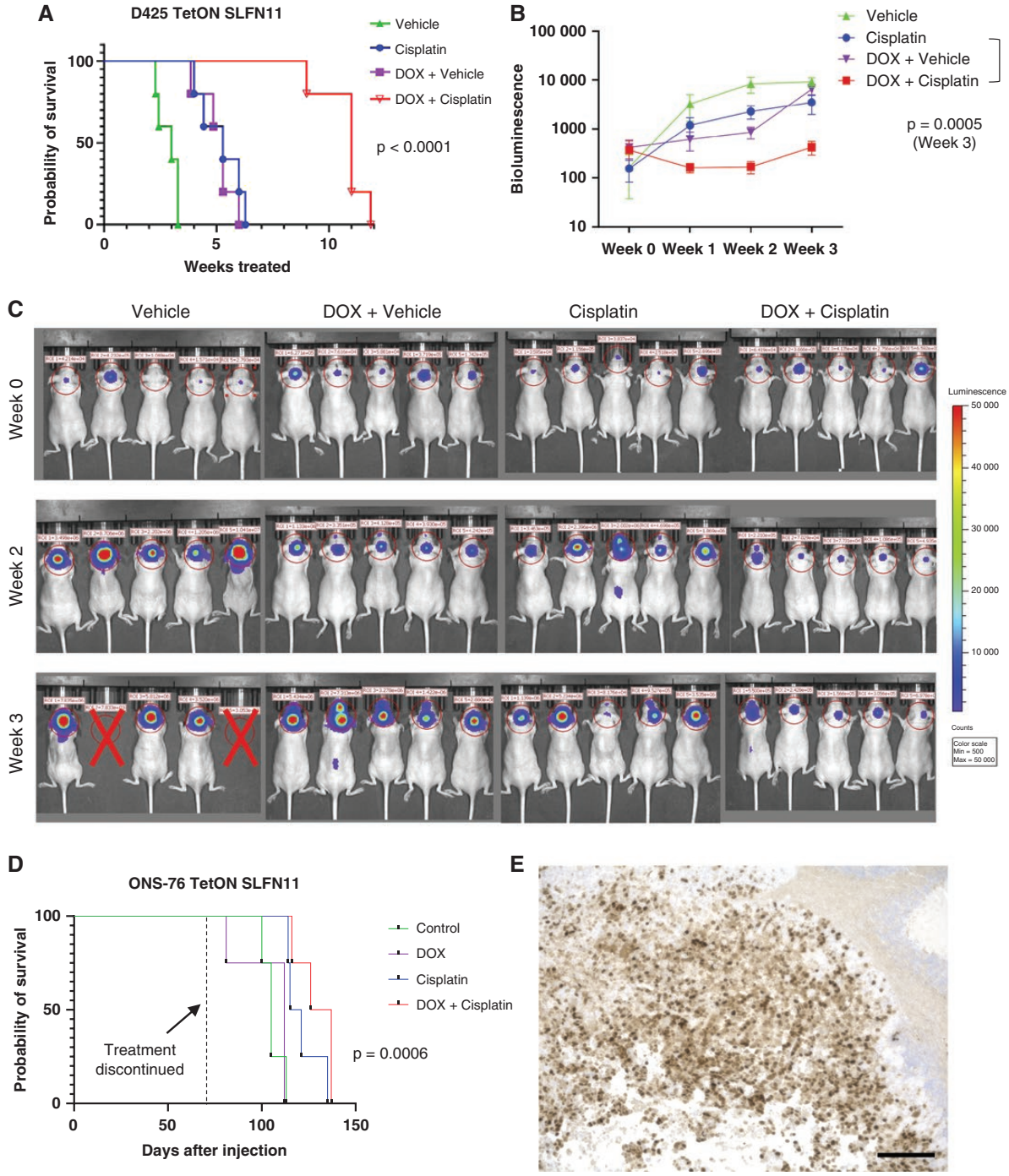

Figure 4. SLFN11 overexpression sensitizes D425 cells to cisplatin treatment in intracranial xenografts. Kaplan–Meier survival curves are plotted for D425 intracranial xenografts and show prolonged survival in DOX + cisplatin group ($P < .0001$, Mantel-Cox test) (A). Bioluminescence studies show increased sensitivity to cisplatin treatment by induction of SLFN11 ($P = .0005$, *t*-test, cisplatin vs DOX + cisplatin) after 3 weeks of treatment (B). (C) Representative IVIS images of D425 xenografts. (D) Kaplan–Meier analysis of ONS-76 cisplatin ± DOX treatment, in which treatment was discontinued after 10 weeks because of toxicity ($P = .0006$). (E) SLFN11 immunohistochemistry showing increased SLFN11 expression in DOX-induced D425 xenografts.

Based on the current study, we propose that one such biomarker for predicting response to chemotherapy for medulloblastoma is SLFN11. SLFN11 can be assessed by IHC, adding to its clinical usefulness through rapid and low-cost detection. As shown in this study and others,[18,22,28,40,41] SLFN11 is exclusively stained in the nucleus regardless of

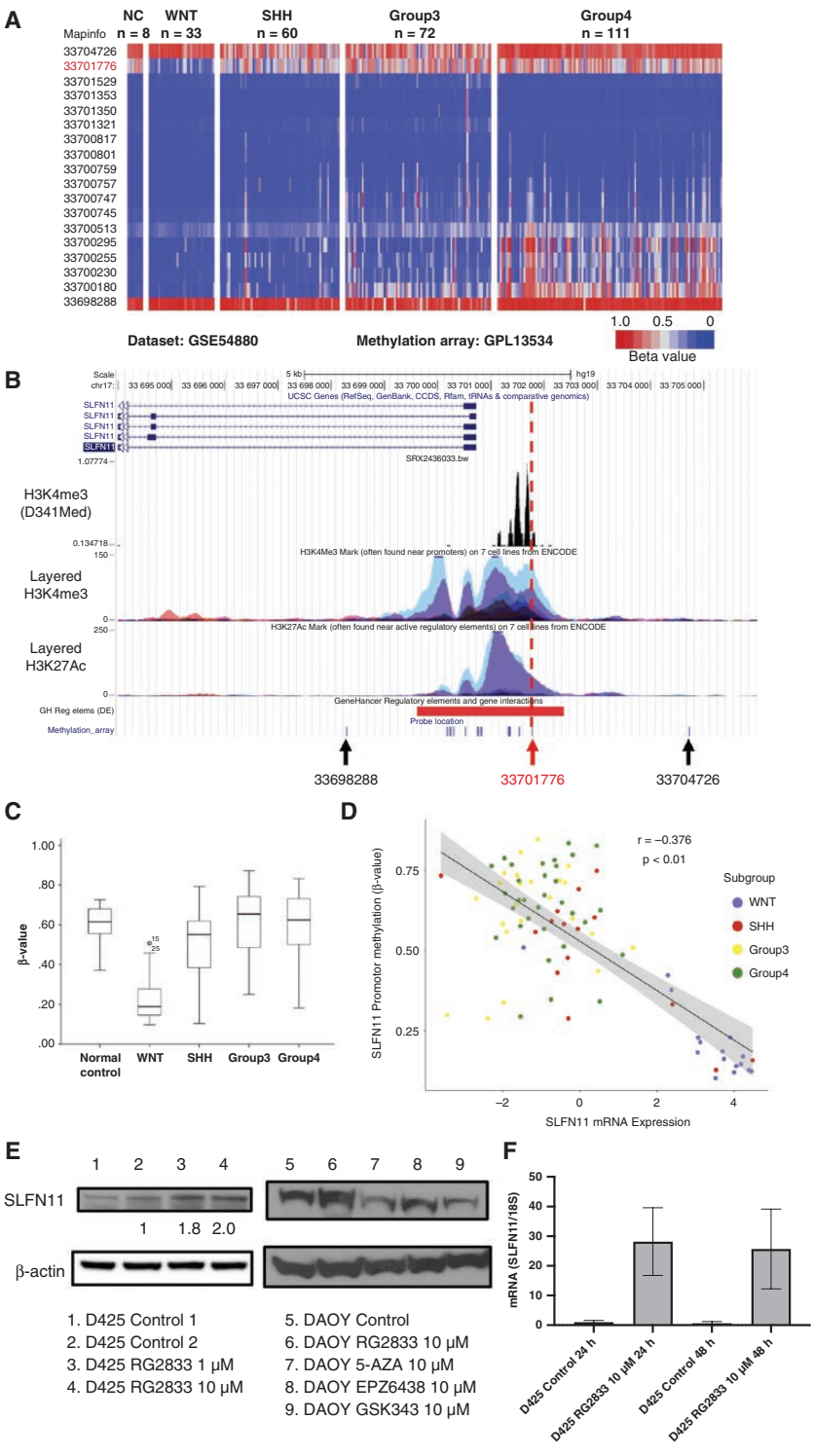

Figure 5. Expression of *SLFN11* correlates with *SLFN11* promoter hypomethylation and is activated by Class I HDAC inhibitor RG2833. Methylation (β-value) of 18 probes on chromosome 17, encompassing the *SLFN11* gene, was assessed in normal cerebella and medulloblastomas samples of the four molecular subgroups. These showed similar methylation patterns (A), except for the area 33701776–33704725, located at the *SLFN11* promoter and H3K4me3 mark in the SHH-activated medulloblastoma cell line D341-Med and 7 other cancer cell lines (B), which was hypomethylated in most WNT-activated cases and some SHH-activated cases (A, C). (D) Correlation ($r = -0.376$) between DNA methylation (β-value) and *SLFN11* mRNA expression. (E) Western blots show a dose-dependent increase in SLFN11 expression after treatment with RG2833, but not 5-AZA EPZ6438 or GSK343 in low SLFN11 expressing cells. (F) Real-time qPCR analysis of *SLFN11* mRNA expression after 24- and 48-h treatment with RG2833.

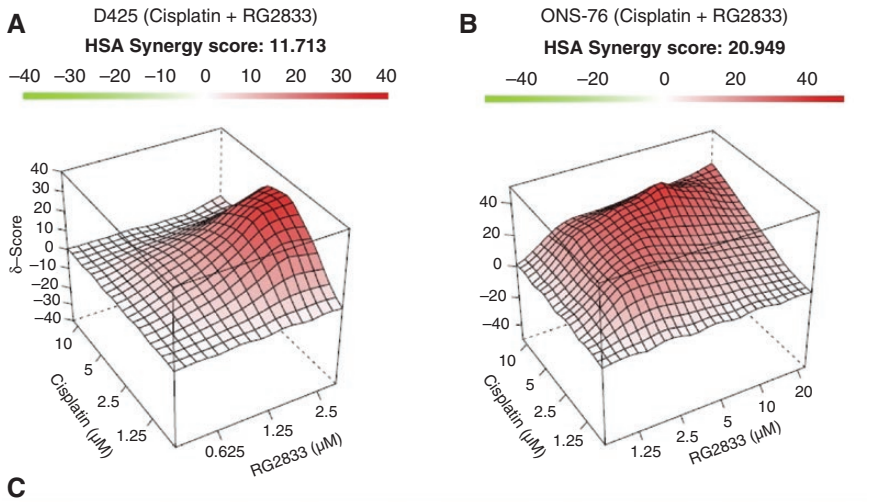

C

Drug combination	Cell line	SLFN11 Expression	HSA Synergy score	Interpretation
Cisplatin + RG2833	D425	–	11.71	Synergistic
	ONS76	–	20.95	Synergistic
	DAOY	+	14.18	Synergistic
SN-38 + RG2833	D425	–	11.25	Synergistic
	ONS76	–	7.66	Partially synergistic
	DAOY	+	9.48	Partially synergistic

Figure 6. Brain-penetrant Class I HDAC inhibitor RG2833 synergizes with cisplatin. Synergistic effects are observed with combined cisplatin and RG2833 treatment in D425 (HSA synergy score 11.713) (A) and ONS-76 (20.949) (B). (C) A summary of the HSA synergy scores.

tissue types. Lymphocytes, macrophages, and vascular endothelial cells can be used for positive internal control. A couple of commercial antibodies are available. Thus, SLFN11 is readily available as a tool for companion diagnostics. Nevertheless, further patient data including prospective clinical studies are warranted to establish SLFN11 expression as a predictive biomarker for chemotherapy.

It is not biologically established whether SLFN11 can also contribute to the response to γ-irradiation therapy. However, we have previously shown that SLFN11 is recruited to replication forks and generates focus formation in response to replication stress, which is caused by DNA damaging agents.[26] Replication stress is hallmarked by an accumulation of replication protein A (RPA) on DNA, which recruits SLFN11 to DNA. As γ-irradiation is known to exert replication stress and generates RPA foci,[42] SLFN11 could also be involved in response to γ-irradiation. Besides SLFN11 inducing lethal replication blocks under replication stress,[26] recent studies have revealed actions for SLFN11 including tRNA-cleavage leading to insufficient ATR synthesis,[43] chromatin opening, degradation of the replication initiation factor CDT1 and degradation of reversed replication forks.[26,27,44] A recent study showed that CD47-induced SLFN11 expression is associated with sensitivity to ionizing radiation in prostate cancer.[45] Hence, non-WNT medulloblastomas with low expression of SLFN11 may be relatively resistant to γ-irradiation. This may partially explain the results of a clinical trial with average-risk medulloblastoma showing that reduction of CSI doses lead to poorer outcomes.[39] Yet, radiation therapy induces a wide range of additional cellular lesions other than replication stress and elucidating the relevance of SLFN11 expression will be required to test clinical usefulness of SLFN11 as a prognostic marker for γ-irradiation.

In the present study, we found that SLFN11 is highly expressed in a majority of WNT-activated medulloblastomas. Deleterious mutations of *SLFN11* have until now been rarely found, and expression levels of *SLFN11* are mainly regulated by epigenetic modification on the *SLFN11* promoter and gene body.[15,16] The present study looking at CpG island methylation in medulloblastoma tissues also detected hypomethylation of the *SLFN11* promoter in most WNT-activated cases. Moreover, DNA methylation (β-value) inversely correlated with *SLFN11* mRNA expression (Figure 5D). Although we identified the specific hypomethylated sites that activate *SLFN11* expression in medulloblastoma, the process of hypomethylation during tumor development is unclear. While mechanisms of SLFN11 regulation other than epigenetic regulation are poorly understood, studies have shown that an ETS transcription family member FLI1 acts as a transcriptional activator at *SLFN11* promoter,[24] and that JAK signal activates SLFN11 expression via elevating FLI1 expression.[46] We predicted that activated WNT-signal is responsible for the high SLFN11 expression, yet various genetic experiments failed to prove this (Supplementary Figure S4). While crosstalk between WNT and JAK signaling is implied,[47] we have not found clear evidence showing that WNT-activated medulloblastomas are prone to act on JAK signaling. In the present study, we found that a specific

CpG locus of *SLFN11* promoter was hypermethylated in normal cerebella (Figure 5A). Whether or not the relevant area is hypomethylated in lower rhombic lip progenitors, the proposed origin of WNT-activated medulloblastomas,[11] remains to be elucidated.

For cases of diminished SLFN11 expression, activation of SLFN11 using histone deacetylase (HDAC) inhibitors,[17] EZH2 inhibitors,[15] and DNA demethylating agent 5-azacytidine (5-AZA),[16] has been proposed as a strategy to sensitize resistant cells to DNA damaging agents. In the present study, sensitization of medulloblastoma cell lines to cisplatin and SN-38 was found by combination treatment with the brain-penetrant HDAC inhibitor RG2833 in vitro. Further studies of combinatorial effects are warranted as a potential strategy to treat resistant, low SLFN11 expressing medulloblastomas.

In conclusion, we discovered high expression of SLFN11 in WNT-activated medulloblastoma and a subset of SHH-activated medulloblastomas, regulated by *SLFN11* promoter hypomethylation. These medulloblastomas are thought to be sensitive to cisplatin and have good prognoses. Activation of SLFN11 in cases with low SLFN11 using HDAC inhibitors is a potential new therapeutic option for treatment-resistant medulloblastomas and warrants further investigation.

Supplementary material

Supplementary material is available online at *Neuro-Oncology* (http://neuro-oncology.oxfordjournals.org/).

Keywords

DNA damaging agent | medulloblastoma | SLFN11

Acknowledgements

The authors would like to acknowledge Dr. Akihiko Yokoyama for advice on methylation analysis and Akiko Yoshii for technical assistance.

Funding

This study was partially funded by Alex Lemonade Stand, 2019 Young Investigators Award to S.N., Japanese Society for Promotion of Science (JSPS) grants to M.N. (17K16632, 19K09476, 21KK0156), Y.T. (22K16679), M.Ok. (17K17739, 20K17955), J.W. (19K18418) and J.M. (JP19H03505), NIH grant to A.T.S. (R01CA255331), research funds from the Yamagata prefectural government and the City of Tsuruoka to J.M., Center for Cancer Research, the Intramural Program of the National Cancer Institute (Z01-BC-006150), NIH, Bethesda, Maryland, DHHS to Y.P. and Niigata University Brain Research Institute Global Collaborative Project to C.G.E., F.J.R., E.H.R., A.T.S., J.M. and S.O.

Conflict of interest statement: The authors declare no conflicts of interest.

Authorship statement

Conceptualization: J.M. and M.N. Supervision: C.G.E., Y.P. and Y.F. Data analysis and interpretation: Sa.N., J.M., M.Ok., S.M., C.P., S.O., A.K., E.H.R., C.G.E., and M.N. Investigation: Sa.N., J.M., M.Ok., H.T., T.H.F., K.M., A.P., S.M., R.G., I.B., S.D., S.C., E.H., K.T., Shin.Y., Shio.Y., T.S., J.O., J.W., S.No., C.P., S.O., and M.N. Resources: Sa.N., J.M., Y.T., J.Y., H.M., K.T., M.Oi., T.N., M.I., C.I., T.Y., H.T., A.T.S., F.J.R., Su.N., P.V., C.G.E., A.K., and M.N. Writing-original draft: Sa.N., J.M., and M.N. Writing- review and editing: Sa.N., J.M., H.M., K.T., A.T.S., C.P., S.O., Y.P., A.K., C.G.E. and M.N. All authors approved the final manuscript.

References

1. Gajjar A, Chintagumpala M, Ashley D, et al. Risk-adapted craniospinal radiotherapy followed by high-dose chemotherapy and stem-cell rescue in children with newly diagnosed medulloblastoma (St Jude Medulloblastoma-96): long-term results from a prospective, multicentre trial. *Lancet Oncol.* 2006;7(10):813–820.
2. Packer RJ, Gajjar A, Vezina G, et al. Phase III study of craniospinal radiation therapy followed by adjuvant chemotherapy for newly diagnosed average-risk medulloblastoma. *J Clin Oncol.* 2006;24(25):4202–4208.
3. Northcott PA, Korshunov A, Witt H, et al. Medulloblastoma comprises four distinct molecular variants. *J Clin Oncol.* 2011;29(11):1408–1414.
4. Cavalli FMG, Remke M, Rampasek L, et al. Intertumoral heterogeneity within medulloblastoma subgroups. *Cancer Cell.* 2017;31(6):737–754.e6.
5. Phoenix TN, Patmore DM, Boop S, et al. Medulloblastoma genotype dictates blood brain barrier phenotype. *Cancer Cell.* 2016;29(4):508–522.
6. Northcott PA, Jones DT, Kool M, et al. Medulloblastomics: the end of the beginning. *Nat Rev Cancer.* 2012;12(12):818–834.
7. Kool M, Koster J, Bunt J, et al. Integrated genomics identifies five medulloblastoma subtypes with distinct genetic profiles, pathway signatures and clinicopathological features. *PLoS One.* 2008;3(8):e3088.
8. Kool M, Korshunov A, Remke M, et al. Molecular subgroups of medulloblastoma: an international meta-analysis of transcriptome, genetic aberrations, and clinical data of WNT, SHH, Group 3, and Group 4 medulloblastomas. *Acta Neuropathol.* 2012;123(4):473–484.
9. Ramaswamy V, Remke M, Bouffet E, et al. Risk stratification of childhood medulloblastoma in the molecular era: the current consensus. *Acta Neuropathol.* 2016;131(6):821–831.
10. Northcott PA, Shih DJ, Remke M, et al. Rapid, reliable, and reproducible molecular sub-grouping of clinical medulloblastoma samples. *Acta Neuropathol.* 2012;123(4):615–626.
11. Gibson P, Tong Y, Robinson G, et al. Subtypes of medulloblastoma have distinct developmental origins. *Nature.* 2010;468(7327):1095–1099.
12. Murai J, Thomas A, Miettinen M, Pommier Y. Schlafen 11 (SLFN11), a restriction factor for replicative stress induced by DNA-targeting anticancer therapies. *Pharmacol Ther.* 2019;201:94–102.

13. Zoppoli G, Regairaz M, Leo E, et al. Putative DNA/RNA helicase Schlafen-11 (SLFN11) sensitizes cancer cells to DNA-damaging agents. *Proc Natl Acad Sci USA.* 2012;109(37):15030–15035.
14. Barretina J, Caponigro G, Stransky N, et al. The Cancer Cell Line Encyclopedia enables predictive modelling of anticancer drug sensitivity. *Nature.* 2012;483(7391):603–607.
15. Gardner EE, Lok BH, Schneeberger VE, et al. Chemosensitive relapse in small cell lung cancer proceeds through an EZH2-SLFN11 axis. *Cancer Cell.* 2017;31(2):286–299.
16. Nogales V, Reinhold WC, Varma S, et al. Epigenetic inactivation of the putative DNA:RNA helicase SLFN11 in human cancer confers resistance to platinum drugs . *Oncotarget.* 2016;7(3):3084–3097.
17. Tang SW, Thomas A, Murai J, et al. Overcoming resistance to DNA-targeted agents by epigenetic activation of Schlafen 11 (SLFN11) expression with class I histone deacetylase inhibitors. *Clin Cancer Res.* 2018;24(8):1944–1953.
18. Moribe F, Nishikori M, Takashima T, et al. Epigenetic suppression of SLFN11 in germinal center B-cells during B-cell development. *PLoS One.* 2021;16(1):e0237554.
19. Murai J, Feng Y, Yu GK, et al. Resistance to PARP inhibitors by SLFN11 inactivation can be overcome by ATR inhibition. *Oncotarget.* 2016;7(47):76534–76550.
20. Uhler JP, Falkenberg M. Primer removal during mammalian mitochondrial DNA replication. *DNA Repair (Amst).* 2015;34:28–38.
21. Deng Y, Cai Y, Huang Y, et al. High SLFN11 expression predicts better survival for patients with KRAS exon 2 wild type colorectal cancer after treated with adjuvant oxaliplatin-based treatment. *BMC Cancer.* 2015;15:833.
22. Coussy F, El-Botty R, Chateau-Joubert S, et al. BRCAness, SLFN11, and RB1 loss predict response to topoisomerase I inhibitors in triple-negative breast cancers. *Sci Transl Med.* 2020;12(531):eaax2625.
23. Winkler C, King M, Berthe J, et al. SLFN11 captures cancer-immunity interactions associated with platinum sensitivity in high-grade serous ovarian cancer. *JCI Insight.* 2021;6(18):e146098.
24. Tang SW, Bilke S, Cao L, et al. SLFN11 is a transcriptional target of EWS-FLI1 and a determinant of drug response in Ewing sarcoma. *Clin Cancer Res.* 2015;21(18):4184–4193.
25. Sen A, Prager BC, Zhong C, et al. Leveraging allele-specific expression for therapeutic response gene discovery in glioblastoma. *Cancer Res.* 2022;82(3):377–390.
26. Murai J, Tang SW, Leo E, et al. SLFN11 blocks stressed replication forks independently of ATR. *Mol Cell.* 2018;69(3):371–384.e6.
27. Jo U, Murai Y, Chakka S, et al. SLFN11 promotes CDT1 degradation by CUL4 in response to replicative DNA damage, while its absence leads to synthetic lethality with ATR/CHK1 inhibitors. *Proc Natl Acad Sci USA.* 2021;118(6):e2015654118.
28. Jo U, Murai Y, Takebe N, Thomas A, Pommier Y. Precision oncology with drugs targeting the replication stress, ATR, and Schlafen 11. *Cancers (Basel).* 2021;13(18):4601.
29. Natsumeda M, Miyahara H, Yoshimura J, et al. GLI3 is associated with neuronal differentiation in SHH-activated and WNT-activated medulloblastoma. *J Neuropathol Exp Neurol.* 2021;80(2):129–136.
30. Hovestadt V, Jones DT, Picelli S, et al. Decoding the regulatory landscape of medulloblastoma using DNA methylation sequencing. *Nature.* 2014;510(7506):537–541.
31. Hamidouche Z, Hay E, Vaudin P, et al. FHL2 mediates dexamethasone-induced mesenchymal cell differentiation into osteoblasts by activating Wnt/beta-catenin signaling-dependent Runx2 expression. *FASEB J.* 2008;22(11):3813–3822.
32. Tanaka S, Terada K, Nohno T. Canonical Wnt signaling is involved in switching from cell proliferation to myogenic differentiation of mouse myoblast cells. *J Mol Signal.* 2011;6:12.
33. Geron L, Salomao KB, Borges KS, et al. Molecular characterization of Wnt pathway and function of beta-catenin overexpression in medulloblastoma cell lines. *Cytotechnology.* 2018;70(6):1713–1722.
34. Ivanov DP, Coyle B, Walker DA, Grabowska AM. In vitro models of medulloblastoma: choosing the right tool for the job. *J Biotechnol.* 2016;236:10–25.
35. Stearns D, Chaudhry A, Abel TW, et al. c-myc Overexpression causes anaplasia in medulloblastoma. *Cancer Res.* 2006;66(2):673–681.
36. Pezuk JA, Valera ET, Delsin LE, et al. The antiproliferative and pro-apoptotic effects of methoxyamine on pediatric medulloblastoma cell lines exposed to ionizing radiation and chemotherapy. *CNS Agents Med Chem.* 2016;16(1):67–72.
37. Krushkal J, Silvers T, Reinhold WC, et al. Epigenome-wide DNA methylation analysis of small cell lung cancer cell lines suggests potential chemotherapy targets. *Clin Epigenet.* 2020;12(1):93.
38. Tlemsani C, Pongor L, Elloumi F, et al. SCLC-CellMiner: a resource for small cell lung cancer cell line genomics and pharmacology based on genomic signatures. *Cell Rep.* 2020;33(3):108296.
39. Michalski JM, Janss AJ, Vezina LG, et al. Children's oncology group phase III trial of reduced-dose and reduced-volume radiotherapy with chemotherapy for newly diagnosed average-risk medulloblastoma. *J Clin Oncol.* 2021;39(24):2685–2697.
40. Takashima T, Sakamoto N, Murai J, et al. Immunohistochemical analysis of SLFN11 expression uncovers potential non-responders to DNA-damaging agents overlooked by tissue RNA-seq. *Virchows Arch.* 2020;478(3):569-579.
41. Kagami T, Yamade M, Suzuki T, et al. The first evidence for SLFN11 expression as an independent prognostic factor for patients with esophageal cancer after chemoradiotherapy. *BMC Cancer.* 2020;20(1):1123.
42. Allen C, Ashley AK, Hromas R, Nickoloff JA. More forks on the road to replication stress recovery. *J Mol Cell Biol.* 2011;3(1):4–12.
43. Li M, Kao E, Malone D, et al. DNA damage-induced cell death relies on SLFN11-dependent cleavage of distinct type II tRNAs. *Nat Struct Mol Biol.* 2018;25(11):1047–1058.
44. Murai J, Zhang H, Pongor L, et al. Chromatin remodeling and immediate early gene activation by SLFN11 in response to replication stress. *Cell Rep.* 2020;30(12):4137–4151.e6.
45. Kaur S, Schwartz AL, Jordan DG, et al. Identification of Schlafen-11 as a target of CD47 signaling that regulates sensitivity to ionizing radiation and topoisomerase inhibitors. *Front Oncol.* 2019;9:994.
46. Murai Y, Jo U, Murai J, et al. Schlafen 11 expression in human acute leukemia cells with gain-of-function mutations in the interferon-JAK signaling pathway. *iScience.* 2021;24(10):103173.
47. Fragoso MA, Patel AK, Nakamura RE, et al. The Wnt/beta-catenin pathway cross-talks with STAT3 signaling to regulate survival of retinal pigment epithelium cells. *PLoS One.* 2012;7(10):e46892.

ABSTRACT (Français)

Le médulloblastome (MB) est la tumeur cérébrale maligne la plus fréquente chez l'enfant qui est traitée par un schéma multimodal de résection chirurgicale, de chimiothérapie et de radiothérapie. Le MB est classé en quatre groupes moléculaires, dont le groupe 3 (G3), caractérisé par la surexpression de MYC, qui a le plus mauvais pronostic. Un traitement agressif, dans lequel la radiothérapie est essentielle, permet un taux de survie d'environ 50 %, mais induit des effets secondaires importants. En outre, les rechutes sont fréquentes. La rechute du MB représente ~10% de tous les décès liés au cancer chez les enfants. Mon projet a deux axes principaux: dans le premier, j'ai utilisé des approches ciblées pour valider le peposertib, un inhibiteur de la DNA-PK, en tant que radiosensibilisateur dans la MB de G3, et dans le second, j'ai utilisé des approches non biaisées pour tenter d'élucider les mécanismes par lesquels le MB de G3 échappe à l'irradiation pour aboutir à une rechute.

Projet 1: Nous avons identifié DNA-PK comme une cible potentielle pour la radiosensibilisation des cellules tumorales dans le traitement initial de MB de G3 afin de prévenir les rechutes. DNA-PK a été identifiée dans un criblage in vitro, où son inhibition s'est avérée significativement efficace pour radiosensibler les cellules de MB de G3 en comparaison à d'autres composés ciblant les dommages à l'ADN. Une analyse de bases de données publiques a révélé une forte expression de DNA-PK dans les MB de G3, ainsi qu'une forte corrélation avec l'expression de MYC. L'inhibition pharmacologique avec le peposertib, un inhibiteur spécifique de DNA-PK, ou le knockdown (KD) de DNA-PK par shRNA in vitro ont augmenté la radiosensibilité des cellules G3 en induisant l'apoptose. En outre, des analyses mécanistiques ont révélé que l'inhibition pharmacologique de DNA-PK associée à l'irradiation induisait un puissant arrêt du cycle cellulaire en phase G2/M et une augmentation significative des lésions de l'ADN, mesurées par les foyers positifs pour la protéine γH2AX. Les analyses des foyers positifs pour 53BP1 suggèrent que cet effet est dû à une diminution de l'activité de la voie de réparation de l'ADN par NHEJ. L'intérêt d'une combinaison de l'inhibition de DNA-PK avec l'irradiation a été validé in vivo sur des souris greffées en orthotopique avec des lignées de G3 et des modèles très pertinents de PDX de MB de G3 (xénogreffes dérivées de patients). Cette combinaison n'a pas montré de toxicité majeure (tests de poids et sanguins) dans les modèles murins pédiatriques. Dans l'ensemble, nos résultats identifient le peposertib comme un radiosensibilisant dans le traitement de MB à haut risque de G3. [Le peposertib a été fourni par Merck (CrossRef Funder ID: 10.13039/100009945)].
Projet 2 : Dans ce projet, nous avons généré des modèles murins in vivo de MB par greffe orthotopique qui récapitulent le processus de rechute observée chez les patients après thérapie. Ainsi, après une croissance initiale, les tumeurs sont irradiées en fractionné ce qui conduit à une diminution du volume tumoral correspondant à la maladie résiduelle suivie par une reprise de la croissance tumorale et à une rechute. Nous avons utilisé ces modèles pour effectuer des analyses de séquençage d'ARN (RNAseq) par "bulk" et sur cellules uniques ainsi que de "phosphoarray" sur des tumeurs avant irradiation, immédiatement après irradiation, au moment de la maladie résiduelle et après reprise de croissance/rechute. Nous avons également réalisé un criblage CRISPR-Cas9 in vitro, afin d'identifier les gènes qui permettent aux cellules MB de G3 de survivre à l'irradiation. Les résultats obtenus ont révélé une reprogrammation significative des tumeurs après l'irradiation.
Globalement, l'objectif de ces travaux était de mieux comprendre la manière dont les cellules de MB de G3 répondent à l'irradiation, afin d'identifier de nouveaux mécanismes et cibles thérapeutiques dans le but de diminuer le taux de rechute.

KEYWORDS

Radiorésistance, Médulloblastome, Radiothérapie, Radiosensibilisation, DNA-PK

ABSTRACT (English)

Medulloblastoma (MB) is the most common malignant pediatric brain tumour, and is treated with a multimodal regimen of surgical resection, chemotherapy, and radiotherapy. Transcriptomic analysis has allowed the categorization of these tumours into four molecular subtypes, of which Group 3 (G3), characterized by MYC overexpression, has the worst prognosis. Aggressive treatment, in which radiotherapy is essential, allows a ~50% survival rate, but induces strong side effects. Further, relapse is common and almost always fatal, with relapsed MB accounting for ~10% of all cancer-related deaths in children. My project had two primary branches: in the first I used targeted approaches to validate peposertib, an inhibitor of DNA-PK, as an effective radiosensitizer in G3 MB; and in the second, I used unbiased approaches to attempt to elucidate the mechanisms by which G3 MB escapes irradiation to result in relapse.

Project 1: Herein, I identified DNA-PK as a target for radiosensitization in the initial treatment of G3-MB to prevent relapse. DNA-PK was identified as a target in an in vitro screen, where its inhibition was shown to significantly radiosensitive G3-MB compared with other DNA damage targeting compounds. Subsequent database analysis revealed high expression of DNA-PK in G3-MB, as well as a strong correlation with MYC expression. Pharmacological inhibition by peposertib or shRNA-mediated knockdown (KD) of DNA-PK in vitro increased the radiosensitivity of G3 cells by inducing apoptosis. Furthermore, mechanistic analyses revealed that pharmacological inhibition of DNA-PK together with irradiation induced a potent G2/M arrest, and a significant increase in DNA damage, measured as γH2AX foci. Analyses of 53BP1 foci suggested that this effect was driven by a decrease in activity of the non-homologous end joining (NHEJ) DNA repair pathway. In vivo treatment of orthotopic tumor-bearing mouse models of G3-MB, including G3-PDX, with a combination of the DNA-PK inhibitor peposertib and irradiation sensitized tumours compared to irradiation alone, inducing a significant survival benefit. This combination showed no major toxicity (weight and blood testing) in pediatric mouse models. Overall, our results identify the specific DNA-PK inhibitor peposertib as a potential radiosensitizer in high-risk group 3 MB. [Peposertib was provided by Merck (CrossRef Funder ID: 10.13039/100009945)].

Project 2: In this project, I constructed in vivo models to model the process of relapse following therapy observed in patients, involving initial tumor growth, tumor shrinkage and minimal residual disease following fractionated irradiation, and eventually aggressive relapse. These models were then used to perform bulk RNAseq, single-cell RNAseq, and phosphoarray analysis of tumours at different timepoints (pre-irradiation, immediately post-irradiation, minimal residual disease, and relapse/endpoint), in order to compare the activity of tumours at different timepoints with/without irradiation. We further performed a negative CRISPR-Cas9 screen in vitro, to identify genes which allow G3 MB cells to survive irradiation. Our results have revealed significant reprogramming of tumours following irradiation.

Overall, the aim of this work was to gain a better understanding of the manner in which G3 MB responds to irradiation, in order to identify novel therapeutic mechanisms, to decrease the rate the relapse by promoting the efficacy of the initial therapy.

KEYWORDS

Radioresistance, Medulloblastoma, Radiotherapy, Radiosensitization, DNA-PK